DRAFT FINAL REPORT

EXPERIMENTAL AND ANALYTICAL EVALUATION OF FLEXIBLE PIPES FOR CULVERTS AND STORM SEWERS

VOLUME II - LABORATORY WORK

Submitted to:

Director, Research Center

Florida Department of Transportation

605 Suwannee St., MS 30

Tallahassee, Florida 32399-0450

CONTRACT No. BC-775

By

Dr. M. Arockiasamy

Principal Investigator

Professor: and Director

Center for Infrastructure and Constructed Facilities

Department of Civil: Engineering

Florida Atlantic University

Boca Raton, FL 33431

Dr. O. Chaallal

Co-Principal Investigator

Professor and Director

Dev. & Research for Str. and Rehab. (DRSR)

Department of Construction Engineering

University of Quebec/

Ecole de Technologie superieure

Montreal, Quebec, Canada H3ClK3

August 2002

DISCLAIMER

The report is prepared in cooperation with the Florida Department of Transportation and the Federal Highway Administration.

ACKNOWLEDGEMENTS

Most of the laboratory work was performed in the FDOT Structures Research Center in Tallahassee, Florida. The technical staff including the technicians Steve, Tony, Frank, Paul, and Dave, as well as the engineers Adnan and Tom, are gratefully acknowledged for their effective contribution to the different aspects of the laboratory testing. Special thanks are due to Adnan Al-Saad, P.E., former project manager. His dedication and hard work to the project are gratefully acknowledged.

SUMMARY

This volume is the second of the four-volume-report on the study entitled, "Experimental and Analytical Evaluation of Flexible Pipes for Culverts and Storm Sewers". It describes the laboratory work performed and presents results for ten different tests carried out in this study. The main objective of the laboratory work was to evaluate .and characterize, under laboratory conditions, the performance and properties of the different plastic and metal pipes considered in the study.

Visual Inspections of the different pipes indicated that HDPE, PVC, and metal pipes generally meet the requirements of AASHTO-M294, ASTM F949, and ASSHTO-T249. However, visible creasing at the surface of inside and outside walls, as well as irregular surface, at certain locations around, the circumference of the bell and spigot joint, were observed in ADS 48. Also the contact length of the seam lap in the case of, aluminum and its distance from the adjacent ribs for both types of metal pipes do not conform to AASHTO T249 requirements. These irregularities, even though they seem not to have an apparent incidence on structural performance, may require improvement.

Beam Test results show that for the plastic pipes the valley longitudinal bending strains were greater than the crown longitudinal bending strains. For the metal pipes, the longitudinal bending strains in the ribs were greater than the longitudinal bending strains in the wall (valley) between the ribs.

Parallel Plate. Test results indicated that for 5% vertical deflection and a loading rate of 0.5 in./min., all the pipes achieved a pipe stiffness, PS, greater than the minimum specified by the Standards. They also revealed no sign of distress or buckling in the pipes for vertical deflections less than 15%. For a given vertical deflection, the HDPE pipe stiffness (PS) substantially decreased as the loading rate decreased and vice-versa.

Flattening Test results indicated that all the HDPE pipes passed the test, since no splitting, cracking, breaking, or separation of ribs or seams, or both, were observed under normal light with unaided eyes. The PVC specimens that could be flattened up to 60% vertical deflection without failure also passed the flattening test. However, a number of PVC pipe specimens ruptured before reaching the 60% limit.

Curved Beam Test results indicated that time-independent pipe stiffness is 2 to 3 times greater than the PS values determined by the parallel plate test for all the pipes and increase with the loading rate for HDPE pipes.

Joint Integrity Test results indicated that all the pipes exhibited no sign of cracks or excessive gaps up to 10% vertical deflection. The presence of a joint generally modified the PS of the pipe.

Type C tension tests (small dog bone with no welds) indicated that he tensile properties of the pipes, the modulus of elasticity and the tensile strength, are within the range of values specified by the AASHTO code. Type A tension tests (double wall Dumbbell shape), performed on ADS 48 only, underestimated the tensile strength of the D-wall-type pipes such as ADS 48. Type B tension tests (single wall Dumbbell shape) indicated that the seam behavior of the D-wall-type pipe under tensile stresses is satisfactory given the maximum strength achieved. Type D tension tests (split disk test) performed on all the pipes indicated that the apparent tensile properties under split disk tests are lower than those under Type G tension tests on small dog bone specimen with no weld, but greater than those achieved on dumbbell shape specimens with welds for ADS 48.

ESCR Tests performed on HDPE pipes indicated that the 36 inch-diameter HDPE pipes behaved satisfactorily under ESCR tests. For the 48 in-diameter HDPE pipe however, one of the two specimens failed the ESCR test under the conditions described in this study.

TABLE OF CONTENTS

ACKNOWLEDGEMENTS

SUMMARY ....

LIST OF TABLES ....

LIST OF FIGURES ....

TABLE OF CONVERSION ....

1 INTRODUCTION
- 1.1 General 1-1
- 1.2 Objective 1-1
- 1.3 Organization of Volume II 1-1

2 VISUAL INSPECTION AND MEASUREMENTS
- 2.1 Objectives 2-1
- 2.2 Geometry of Pipes 2-1
- 2.3 Visual Inspection 2-1
- 2.4 Conclusions 2-2

3 SIMPLE BEAM TESTS
- 3.1 Objectives 3-1
- 3.2 Experimental Program 3-1
- 3.3 Results 3-2
- 3.4 Observations and Discussions 3-3

4 PARALLEL PLATE LOADING TESTS
- 4.1 Objectives 4-1
- 4.2 Experimental Program 4-1
- 4.3 Description of Significant Pipe Events 4-2
- 4.4 Calculations 4-2
- 4.5 Results and Discussions 4-3
- 4.6 Conclusions 4-4

5 FLATTENING TESTS
- 5.1 Objectives 5-1
- 5.2 Apparatus, Test Specimens and Procedure 5-1
- 5.3 Observations on Behavior of Pipes Flattened According to Standards 5-1
- 5.4 Observations on Behavior of Pipes Flattened up to 60% 5-3
- 5.5 Conclusions 5-4

6.0 CURVED BEAM STIFFNESS TEST
- 6.1 Scope and Objectives 6-1
- 6.2 Experimental Program 6-1
- 6.3 Time-Independent Pipe Stiffness, K(0) 6-2
- 6.4 Presentation and Discussion of Results 6-3
- 6.5 Conclusions 6-5

7 JOINT INTEGRITY TEST
7.1 Objectives 7-1
7.2 Experimental Program 7-1
7.3 Observations and Discussions....................7-2
7.4 Conclusions....................7-5

8 TENSILE TESTS ON DUMBELL-SHAPED SPECIMENS
8.1 Scope and Objectives....................8-1
8.2 Experimental Program 8-1
8.3 Calculations 8-2
8.4 Results and Observations....................8-3
8.5 Conclusions....................8-4

9 TENSILE TESTS ON FULL RING SPECIMENS
9.1 Scope and Objectives....................9-1
9.2 Experimental Program 9-1
9.3 Calculations 9-2
9.4 Test Results and Observations....................9-3
9.5 Conclusions....................9-4

10 TENSILE TESTS ON 10 INCH - DOG BONE SPECIMENS
10.1 Objectives 10-1
10.2 Experimental Program 10-1
10.3 Calculations 10-2
10.4 Results and Observations....................10-3
10.5 Conclusions....................10-4

11 ENVIRONMENTAL STRESS CRACKING TEST
11.1 Scope and Objectives....................11-1
11.2 Experimental Program 11-1
11.3 Calculations 11-2
11.4 Results and Observations....................11-3
11.5 Conclusions....................11-3

12 CONCLUSIONS

REFERENCES

LIST OF TABLES

CHAPTER 2
2.1- Geometry of ADS 48" Pipe 2-3
2.2- Geometry of ADS 36" Pipe 2-4
2.3- Geometry of HANCOR 36" Pipe 2-5
2.4- Geometry of PVC 36" Pipe 2-6
2.5- Geometry of Aluminum 36" Pipe 2-7
2.6- Geometry of steel 36" Pipe 2-8
2.7- Visual Inspection and Material Characterization for ADS 48" 2-9
2.8- Visual Inspection and Material Characterization for ADS 36 2-10
2.9- Visual Inspection and Material Characterization for Hancor 36 2-11
2.10- Visual Inspection and Material Characterization for PVC 36 2-12
2.11-Visual Inspection and Material Characterization for Aluminum 36 2-13
2.12- Visual Inspection and Material Characterization for Steel 36 2-13

CHAPTER 3
3.1- Experimental Stiffness of Pipes in Bending 3-5
3.2- Longitudinal Bending Strains for Deflections of 1% and 2% Beam Span 3-5

CHAPTER 4
4.1- Geometry (Average values) and Minimum Specified PS of Specimens 406
4.2- Parallel Plate Test Program 4-6
4.3- Summary of Experimental Results 4-7
4.4- Measured PS and SF of HDPE ADS 48" pipes 4-8
4.5- Measured PS and SF of HDPE ADS 36" pipes 4-9
4.6- Measured PS and SF of HDPE Hancor 36" pipes 4-9
4.7- Measured PS and SF of PVC 36" pipes 4-10
4.8- Measured PS and SF of Steel 36" pipes 4-10
4.9- Measured PS and SF of Aluminum 36" pipes 4-11

CHAPTER 6
6.1- Geometric Properties of Arch Specimens 6-6
6.2- Curved-Beam Test Program 6-6
6.3- Summary of Experimental Results 6-7
6.4- Strain Readings for 5% and 10% Vertical Deflection (Load Rate = 0.5 in./min) 6-8
6.5- Time-Independent Pipe Stiffness K (0) 6-9

CHAPTER 7
7.1- Joint Integrity Test Program 7-6
7.2- Experimental Pipe stiffness 7-6
7.3- radial gap at Joint versus Vertical Deflection for ADS 48 7-6
7.4a- Radial Gap at Joint versus Vertical Deflection for ADS 36 7-7
7.4b- Joint Opening versus Vertical Deflection for ADS 36 7-7
7.5a- Radial Gaps at Joint versus Vertical Deflection for Hancor 36 7-7
7.5b- Joint Opening versus Vertical Deflection for Hancor 36 7-7
7.6- Radial Gap at Joint versus Vertical Deflection for PVC 36 7-8

CHAPTER 8

8.1- Type A and B Test Program 8-5
8.2- Summary of Results for Tests Type A 8-5
8.3- Summary of Results for Tests Type B 8-5

CHAPTER 9

9.1- Experimental Program for Split Disk Tests 9-5
9.2- Summary of Results for Split Disk Tests 9-5
9.3a- Calculations for Apparent Modulus of Elasticity for HDPE Pipes 9-6
9.3b- Calculations for PVC and Metal Pipes 9-7

CHAPTER 10

10.1- Dogbone Tension Test Type C Program 10-5
10.2a- Experimental Results for Plastic Pipes 10-6
10.2b- Experimental Results for Metal Pipes 10-7
10.3a- Experimental Average Results for Plastic Pipes 10-8
10.3b- Experimental Average Results for Metal Pipes 10-8

CHAPTER 11

11.1- ESCR Test Program 11-5
11.2- Environmental Test Measurements for ADS 48 11-5
11.3- Environmental Test Length Measurements for ADS 36 11-6
11.4- Environmental Test Length Measurements for HANCOR 36 11-6
11.5- Observations 11-7

LIST OF FIGURES

CHAPTER 2
2.1- Bell and Spigot Geometry of ADS 48 (Average Values) 2-14
2.2- Bell and Spigot Geometry of ADS 36 (Average Values) 2-15
2.3- Bell and Spigot Geometry of Hancor 36 (Average Values) 2-16
2.4- Bell and Spigot Geometry of PVC 36 (Average Values) 2-17
2.5- Inside and Outside Wall Surfaces of ADS 48 2-18
2.6- Wall Section of ADS 48 2-19
2.7- Bell and Spigot Joint of ADS 48 2-20
2.8- Wall Section of ADS 36 2-20
2.9- Inside and Outside Wall Surfaces of ADS 36 2-21
2.10- Inside and Outside Wall Surfaces of Hancor 36 2-22
2.11- Wall Section of Hancor 36 2-23
2.12- Wall Section of PVC 36 2-23
2.13- Inside and Outside Wall Surfaces of Hancor 36 2-24
2.14- Lock-Seam Section of Aluminum 36 2-25
2.15- Lock-Seam Section of Steel 36 2-25

CHAPTER 3
3.1- View of Pipes Under Beam Test Setup 3-6
3.2a- Location of Deflection and Transverse Strain Gages on ADS 48 Pipe Specimen 3-7
3.2b- Location of Longitudinal Strain Gages on ADS 48 Pipe Specimen 3-8
3.3a- Location of Deflection and Transverse Strain Gages on 36in. Diameter Plastic Pipes 3-9
3.3b- Location of Longitudinal Strain Gages on 36in. Diameter Plastic Pipes 3-10
3.4a- Location of Deflection and Transverse Strain Gages on Metal Pipes 3-11
3.4b- Location of Longitudinal Strain Gages on Metal Pipes 3-12
3.5- Typical Transverse and Longitudinal Strain Gages Inside Specimen 3-13
3.6- Load vs Deflection Measured Along Top and Bottom of ADS 48 Test Specimen 3-13
3.7- Measured Top and Bottom Deflection at Sections Along ADS 48 Specimen 3-14
3.8- Measured Top and Bottom Outer Surface Strains at Sections Along ADS 48 Specimen 3-14
3.9- Measured Top and Bottom Inner Surface Strains at Sections Along ADS 48 Specimen 3-15
3.10- Bottom Deflection and Load versus Longitudinal Strains at Centerline for ADS 48 3-15
3.11- Slope of Load versus Bottom Deflection for ADS 48 Specimen at Centerline 3-16
3.12- Load vs Deflection Measured Along Top and Bottom of ADS 36 Test Specimen 3-16
3.13- Measured Top and Bottom Deflection at Sections Along ADS 36 Specimen 3-17
3.14- Measured Top and Bottom Outer Surface Strains at Sections Along ADS 36 Specimen 3-17
3.15- Measured Top and Bottom Inner Surface Strains at Sections Along ADS 36 Specimen 3-18
3.16- Bottom Deflection and Load vs Longitudinal Strains at Centerline for ADS 36 3-18
3.17- Slope of Load vs Bottom Deflection for ADS 36 Specimen at Centerline 3-19
3.18- Load versus Valley Longitudinal and Transverse Strain Readings for ADS 36 3-20
3.19- Load vs Deflection Measured Along Top and Bottom of Hancor 36 Specimen 3-21
3.20- Measured Top and Bottom Deflection at Sections Along Hancor 36 Specimen 3-21
3.21- Measured Top and Bottom Outer Surface Strains at Sections Along Hancor 36 3-22
3.22- Measured Top and Bottom Inner Surface Strains at Sections Along Hancor 36 3-22
3.23- Bottom Deflection and Load versus Longitudinal Strains at Centerline for Hancor 36 3-23
3.24- Slope of Load vs Bottom Deflection at Centerline for Hancor 36 3-23
3.25- Load vs Valley Longitudinal and Transverse Strain Readings for Hancor 36 3-24
3.26- Load vs Deflection Measured Along Top and Bottom of PVC 36 Test Specimen 3-25
3.27- Measured Top and Bottom Deflection at Sections Along PVC 36 Specimen 3-25
3.28- Measured Top and Bottom Outer Surface Strains at Sections Along PVC 36 Specimen 3-26

3.29- Measured Top and Bottom Inner Surface Strains at Sections Along PVC 36 Specimen 3-26
3.30- Bottom Deflection and Load vs Longitudinal Strains at Centerline for PVC 36.................... 3-27
3.31- Slope of Load vs Bottom Deflection for PVC 36 Specimen at Centerline 3-27
3.32- Load vs Valley Longitudinal and Transverse Strain Readings for PVC 36............................ 3-28
3.33- Load vs Deflection Measured Along Top and Bottom of Steel 36 Test Specimen 3-29
3.34 Measured Top and Bottom Deflection at Sections Along Steel 36 Specimen 3-29
3.35- Measured Top and Bottom Outer Surface Strains at Sections Along Steel 36 Specimen 3-30
3.36- Bottom Deflection and Load versus Longitudinal Strains at Centerline for Steel 36............. 3-30
3.37- Slope of Load versus Bottom Deflection for Steel 36 Specimen at Centerline 3-31
3.38- Load versus Valley Longitudinal and Transverse Strain Readings for Steel 36...................... 3-31
3.39- Lock Seam Sections of Steel Specimen near Support.. 3-31
3.40- Load vs Deflection Measured Along Top and Bottom of Aluminum 36 Test Specimen 3-32
3.41- Measured Top and Bottom Deflection at Sections Along Aluminum 36 Specimen................ 3-32
3.42- Measured Top and Bottom Outer Surface Strains at Sections Along Aluminum 36 Specimen.. 3-33
3.43- Bottom Deflection and Load vs Longitudinal Strains at Centerline of Aluminum 36 3-33
3.44- Slope of Load vs Bottom Deflection for Aluminum 36 Specimen at Centerline..................... 3-34
3.45- Load versus Valley Longitudinal and Transverse Strains for Aluminum 36.......................... 3-34
3.46- Lock Seam Sections of Aluminum Specimen 3-34

CHAPTER 4

4.1- LVDT Experimental Set-up 4-12
4.2- Test Specimen 4-12
4.3- Views of ADS 48 Pipe Specimen During Parallel Plate Test.. 4-13
4.4- Views of ADS 36 Pipe Specimen During Parallel Plate Test.. 4-13
4.5- Views of Hancor 36 Pipe Specimen During Parallel Plate Test 4-13
4.6- Views of PVC Pipe Specimen During Parallel Plate Test... 4-14
4.7- Views of Steel Pipe Specimen During Parallel Plate Test.. 4-14
4.8- Views of Aluminum Pipe Specimen During Parallel Plate Test.. 4-14
4.9- Load vs Vertical and Horizontal Deflections for ADS 48 Under Parallel Plate Test................ 4-15
4.10- Load vs Vertical and Horizontal Deflections for ADS 36 Under Parallel Plate Test.............. 4-16
4.11- Load vs Vertical and Horizontal Deflections for Hancor 36 Under Parallel Plate Test 4-17
4.12- Load vs Vertical and Horizontal Deflections for PVC 36 Steel and Aluminum 4-18
4.13- Comparison of Measured PS Values at 5% Deflection for HDPE Pipes................................ 4-19
4.14- Comparison of Measured PS Values at 5% Deflection for PVC and Metal Pipes. 4-19
4.15- Comparison of Measured PS Values at 10% Deflection for HDPE Pipes.............................. 4-20
4.16- Comparison of Measured PS Values at 10% Deflection for PVC and Metal Pipes. 4-20

CHAPTER 5

5.1- Wall Buckling on the Outside of Hancor 36 Pipe at Vertical Deflection of 15% 5-6
5.2a- Deformed Shape of ADS 48" Pipe at Vertical Deflection of 20% Diameter........................... 5-6
5.2b- Scattered Wall local Buckling at Vertical Deflection of 20% Diameter 5-6
5.3- Deformed Elliptical Shape of PVC 36" Pipe at the Vertical Deflection of 20%....................... 5-7
5.4a- Failure of PVC Due to Wall Rupture 5-7
5.4b- Close up View of invert Rupture of PVC 36 at 30% Deflection 5-7
5.5a- Deformed Elliptical Shape of PVC 36 at 36% Deflection 5-8
5.5b- Close up View of Crown of PVC 36 at 36% Deflection.. 5-8
5.5c- Wall Buckling at Springline of PVC 36 at 36% Deflection... 5-8
5.6- Deformed Shapes of ADS 48 Under Parallel Plates 5-9
5.7- Wall Local Buckling and Cracking at 30% Deflection... 5-10
5.8- Part Edge Area Bulging at Vertical Deflection of 30% Diameter 5-10

5.9- Wide-Spread Wall Buckling at Vertical Deflection of 42% Diameter 5-10
5.10- Deformed Shapes of ADS 36 Under Parallel Plates 5-11
5.11- Inside Wall Deformation at 20% Deflection 5-12
5.12- Wide Spread Wall Buckling Forming at Springline at 30% Deflection 5-12
5.13- Outside Wall Buckling at Deflection of 30% Diameter.. 5-12
5.14- Wide Spread Inside Wall Buckling at Deflection of 36% Diameter....................................... 5-12
5.15- Deformation of the Outside Surface at Springline at 59% Deflection.................................... 5-13
5.16- Lightly Reversed Curvature of Invert Region at Deflection of 59% Diameter........................ 5-13
5.17- Deformed Shapes of Hancor 36 at Different Deflections 5-14
5.18- Inside Wall Buckling at Springline of Hancor 36 at Deflection of 30%................................. 5-15
5.19- Deformation of the Invert Region of Hancor 36 at Deflection of 36%................................... 5-15
5.20- Extensive Wall Buckling on the Exterior of Hancor 36 at Deflection of 59% 5-15
5.21- Breaking of Rib of Hancor 36 at Deflection of 59%... 5-15
5.22- Deformed Shapes of PVC 36 Under Parallel Plates 5-16
5.23- The Rupture Shape of PVC 36 Specimen 5-17
5.23- Deformed Shapes of Aluminum 36 at Different Vertical Deflections.................................... 5-17
5.24- Deformed Shapes of Steel 36 at Different Vertical Deflections 5-18

CHAPTER 6

6.1- Schematic of Locations of Vertical and Horizontal Deflectometers 6-10
6.2- Schematic of Locations of Strain Gages on the Inner and Outer Pipe Walls 6-10
6.3- Pipe Ring Cut Into 4 Test Specimens 6-10
6.4- Views of ADS 48 Specimen at Different Deformed Shapes During Curved-Beam Tests 6-11
6.5- Views of ADS 36 Specimen at Different Deformed Shapes During Curved-Beam Tests 6-12
6.6- Views of Hancor 36 Specimen at Different Deformed Shapes During Curved-Beam Tests..... 6-13
6.7- Views of PVC 36 Specimen at Different Deformed Shapes During Curved-Beam Tests......... 6-14
6.8- Views of Steel36 Specimen at Different Deformed Shapes During Curved-Beam Tests 6-15
6.9- Views of Aluminum 36 Specimen at Different Deformed Shapes 6-16
6.10- Load vs Vertical and Horizontal Deflections for ADS 48 6-17
6.11- Load vs Vertical and Horizontal Deflections for ADS 36 6-18
6.12- Load vs Vertical and Horizontal Deflections for Hancor 36 6-19
6.13- Load vs Vertical and Horizontal Deflections for PVC 36 6-20
6.14- Load vs Vertical and Horizontal Deflections for Steel 36 6-21
6.15- Load vs Vertical and Horizontal Deflections for Aluminum 36 6-21
6.16- Load and Vertical Deflection vs Strains for ADS 48.. 6-22
6.17- Load and Vertical Deflection vs Strains for ADS 36.. 6-23
6.18- Load and Vertical Deflection vs Strains for Hancor 36 6-24
6.19- Load and Vertical Deflection vs Strains for PVC 36.. 6-25
6.20- Load and Vertical Deflection vs Strains for Steel 36.. 6-26
6.21- Load and Vertical Deflection vs Strains for Aluminum 36 6-27
6.22- Typical Curve Fitting for K(0) 6-28

CHAPTER 7

7.1- LVDT Experimental Set-up 7-9
7.2- Test Specimen 7-9
7.3- Load vs Vertical and Horizontal Deflections for ADS 48 7-10
7.4- Load vs Vertical and Horizontal Deflections for ADS 36 7-10
7.5- Load vs Vertical and Horizontal Deflections for Hancor 36 7-11
7.6- Load vs Vertical and Horizontal Deflections for PVC 36 7-11

7.7- Joint integrity test setup for ADS 48" Pipe 7-12
7.8- Exterior View of Joint of ADS 48 Specimen Prior to Testing 7-12
7.9- Behavior of Joint of ADS 48 Specimen at 20% Vertical Deflection 7-12
7.10- Behavior of Joint of ADS 48 Specimen at 30% Vertical Deflection 7-13
7.11- Joint Integrity Test Setup for ADS 36" Pipe 7-13
7.12- Exterior and Interior Views of ADS 36 Specimen Prior to Testing 7-14
7.13- Behavior of Joint of ADS 36 Specimen at 10% and 20% Vertical Deflection 7-14
7.14- Behavior of Joint of ADS 48 Specimen at 30% Vertical Deflection 7-15
7.15- Joint integrity test setup for Hancor 36" Pipe 7-16
7.16- Exterior view of joint of Hancor 36" Pipe 7-16
7.17- Behavior of Joint of ADS 36 Specimen at 15% and 20% Vertical Deflection 7-17
7.18- Behavior of Joint of Hancor 36 Specimen at 30% and 33% vertical Deflection 7-18
7.19- Joint integrity test setup for PVC 36" Pipe 7-19
7.20- Behavior of Joint of Hancor 36 Specimen at 30% Deflection 7-20
7.21- Failure of PVC 36" pipe at 12 in. Vertical Deflection 7-20

CHAPTER 8

8.1- Double wall type specimen (Type A) 8-6
8.2- Single wall type specimen (Type B) 8-7
8.3- Typical test setup 8-7
8.4- Specimen Cut in the Form of Longitudinal Strip from the Pipe 8-8
8.5- Specimen Cut Into Dumbbell-Shape (Dogbone Shape) 8-8
8.6- Load vs. Axial and Transverse Strain for Type A Specimen 8-10
8.7- Typical Curve Fittings for Modulus and Poisson's Ratio for Type A 8-11
8.8- Typical Views of Specimens Type A at Failure 8-12
8.9- Load vs. Axial and Transverse Strain for Type B Specimen 8-14
8.10- Typical Curve Fittings for Modulus and Poisson's Ratio for Type B 8-15
8.11- Typical Views of Specimens Type B at Failure 8-16

CHAPTER 9

9.1- Test Fixture for the 36" Diameter Pipe 9-8
9.2- Test Fixture for the 48" diameter pipe 9-8
9.3- Overall Configuration of the Test Fixture for Testing the 36" Diameter Pipe 9-9
9.4- HDPE 36" Diameter Specimen Configurations 9-9
9.5- HDPE 48" Diameter Specimen Configurations 9-9
9.6- Deformation of ADS 48 Specimen Under Tensile Load 9-10
9.7- Deformation of ADS 36 Specimen Under Tensile Load 9-10
9.8- Deformation of Hancor 36 Specimen Under Tensile Load 9-11
9.9- Deformation of PVC Specimen Under Tensile Load 9-11
9.10- External Cracking of Steel Specimen 9-12
9.11- External Cracking of Aluminum Specimen 9-12
9.12- Load vs Vertical Diametral Change for ADS 48 Specimen 9-13
9.13- Load vs Vertical Diametral Change for ADS 36 Specimen 9-13
9.14- Load vs Vertical Diametral Change for Hancor 36 Specimen 9-14
9.15- Load vs Vertical Diametral Change for PVC 36 Specimen 9-14
9.16- Load vs Vertical Diametral Change for Steel 36 Specimen 9-15
9.17- Load vs Vertical Diametral Change for Aluminum 36 Specimen 9-15

CHAPTER 10

10.1- Details of Specimens 10-9
10.2- ADS 48 Specimen During Resting 10-10
10.3- ADS 48 Specimen Prior to Failure 10-10
10.4- ADS 36 Specimen During Testing 10-11
10.5- ADS 36 Specimen at Failure 10-11
10.6- Hancor 36 Specimen During Testing 10-12
10.7- Hancor 36 Specimen at Failure 10-12
10.8- PVC 36 Specimen During Testing 10-13
10.9- PVC 36 Specimen at Failure 10-13
10.1- Steel 30 Specimen at Failure 10-14
10.11- Aluminum Specimen During Testing 10-14
10.12- Aluminum Seam Specimen During Testing 10-15
10.13- Aluminum Seam Specimen at Failure 10-15
10.14- Experimental Stress vs Strain Curves for ADS 48 10-16
10.15- Experimental Stress vs Strain Curves ADS 36 10-18
10-16- Experimental Stress vs Strain Curves Hancor 36 10-20
10-17- Experimental Stress vs Strain Curves for PVC 36 10-22
10-18- Experimental Stress vs Strain Curves Steel 36 and Aluminum 36 10-24
10-19- Experimental Stress vs Strain Curves for Seam-Steel 36 and Aluminum 36 10-25

CHAPTER 11

11.1- Configuration of the Holding Device. 11-8
11.2- Specimen After Exposure to the Active Agent 11-8
11.3- Specimen Configuration and Dimension for ADS 48 Pipe 11-9
11.4- Location of the Notch on the Specimen Crown. 11-9
11.5- Measurement of a Notch Length by the Digital Caliper 11-10
11.6- Measurement of Cord Length 11-10
11.7- Preparation of Notch for ADS 48 Specimen 11-11
11.8- Close-up of Notch Before Test for ADS 48 Specimen 11-11
11.9- Measurement of Notch Length Before Test 11-12
11.10- Preparation of Notch for ADS 48 Specimen 11-12
11.11- View of Notch after Test Under Igepal for Bound ADS 48 Specimen 11-13
11.12- View of Notch after Test Under Igepal for Unbound ADS 48 Specimen 11-14
11.13- Close-up of Notch before Test for ADS 48 Specimen 11-14
11.14- View of Notch after Test under 24 H Igepal for Bound ADS 36 Specimen 11-15
11.15- View of Notch after Test Under 24 H Air for Bound ADS 36 Specimen 11-15
11.16- Close-up of Notch before Test for Hancor 36 Specimen 11-16
11.17- View of Notch after Test Under 24 H Igepal for Bound Hancor 36 11-16
11.18- View of Notch after Test Under 24 H Igepal for Bound Hancor 36 11-17
11.19- Close-up View of Notch after Test Under 24 H Igepal for Bound Hancor 36 11-17

TABLE OF CONVERSIONS

To convert from	To	Multiply by
Length		
Inch (in.)	Millimeter (mm)	25.4
Foot (ft)	Meter (m)	0.3048
Area		
Square inch (sq. in.)	Square millimeter (sq. mm)	645.2
Square foot (sq. ft.)	Square meter (sq. m)	0.0926
Volume		
Cubic inch (cu. in.)	Cubic meter (cu. m)	0.00001639
Cubic foot (cu. ft.)	Cubic meter (cu. m)	0.02832
Cubic yard (cu. yd.)	Cubic meter (cu. m)	0.7646
Gallon (gal)	Liter	3.785
Force		
Kip	Kilogram (kgf)	453.6
Kip	Newton (N)	4448.0
Pound (lb)	Newton (N)	4.448
Pressure or Stress		
Kip/square inch (ksi)	Megapascal (MPa)**	6.895
Pound/square inch (psi)	Megapascal (MPa)**	0.006895
**One Pascal equals one newton/square meter		
Mass		
Pound	Kilogram (kg)	0.4536
Ton (short, 2000 lb)	Kilogram (kg)	907.2
Mass (weight per length)		
Kip/linear foot (klf)	Kilogram/meter (kg/m)	0.001488
Pound/linear foot (plf)	Kilogram/meter (kg/m)	1.488
Pound/linear foot (plf)	Newton/meter (N/m)	4.593

Chapter 1: Introduction

1.1 General

This volume is the second of a four-volume-report on an extensive experimental and analytical investigation of flexible pipes entitled: Experimental and Analytical Evaluation of Flexible Pipes for Culverts and Storm Sewers. This Volume II, presents results of the laboratory work carried out in this study on the six different types of pipe considered. It also describes the experimental results for the ten different tests carried out in this study. The related specimen preparations, testing procedures, and relevant ASTM and AASHTO Standards, are also presented.

1.2 Objective

The main objective of this part of the research study was to evaluate and characterize under laboratory conditions the performance and properties of the different plastic and metal pipes considered in the study.

1.3 Organization of Volume II

This report contains eleven chapters, in addition to the introductory chapter. Chapter 2 presents results of the visual inspection and measurements of the different pipes. Chapter 3 presents results of the simple beam tests performed on the pipes. Chapter 4 is dedicated to the parallel plate loading tests, while Chapter 5 presents results of flattening tests. The curved beam tests are presented in Chapter 6 and the joint integrity tests in Chapter 7. Results of tension tests are presented in Chapters 8, 9, and 10, respectively, for the dumbbell shape 28 inch-specimens with welds, for the 48 inch diameter D-wall-type full ring pipe specimens, and for the 10 inch-dog bone-shaped-specimens with no welds. Chapter 11 presents results of the environmental stress cracking tests performed on HDPE pipes. Concluding remarks related to the laboratory work undertaken in this part of the study are provided in Chapter 12.

Chapter 2: Visual Inspection and Measurements

2.1 Objectives

The objectives of this chapter are: (a) to present the measurements and geometry of the different pipes considered in this study, and: (b) to presents the results of visual inspections carried out on the pipes and the joints according to relevant AASHTO and ASTM Standards.

2.2 Geometry of pipes

The measurements of the different; pipes used in this project are presented in Table 2.1 to Table 2.6 as follows:

ADS 48" (HDPE)	Table 2.1
ADS 36" (HDPE)	Table 2.2
HANCOR 36" (HDPE)	Table 2.3
PVC 36" (PVC)	Table 2.4
ALUMINUM 36"	Table 2.5
STEEL 36"	Table 2.6

In particular, the following dimensions are provided: the inside diameter (ID), the outer diameter (OD), the thickness of the walls, and the dimensions and thickness of the corrugations. For each dimension, the average of eight readings is given. In addition, for PVC and HDPE pipes the geometry of the joint (i.e. the bell and the spigot) is also provided in Fig 2.1 (ADS 48), Fig. 2.2 (ADS 36), Fig. 2.3 (RANCOR 36) and Fig. 2.4. (PVC 36).

2.3 Visual Inspection

Visual inspections were carried out on the different pipes according to the following AASHTO and ASTM standards as follows:

- AASHTO M294 for HDPE pipes (ADS 48, ADS 36 and RANCOR 36)
- ASTM F 949 for PVC pipes
- AASHTO T 249 for steel and aluminum pipes

Results of these visual inspections and observations are presented in Tables 2.7 to 2.12 and Figs. 2.5 to 2.15 as follows:

ADS 48" (HDPE)	Table 2.7 and Figs. 2.5 to 2.7
ADS 36" (HDPE)	Table 2.8 and Figs. 2.8 to 2.9
HANCOR 36" (HDPE)	Table 2.9 and Figs. 2.10 to 2.11
PVC 36" (PVC)	Table 2.10 and Figs. 2.12 to 2.13
ALUNQNUM 36"	Table 2.11 and Fig. 2.14
STEEL 36"	Table 2.12 and Fig. 2.15

2.4 Conclusions

Visual inspections of the different pipes indicated the followings

(a) *HDPE ADS* 48: Generally, the pipe meets the AASHTO-M294 requirements for visual inspection. However, the surfaces of the inside and the outside walls revealed visible creasing. Also, the bell and spigot joint showed irregular surfaces at certain locations around the circumference.

(b) *HDPE ADS* 36: The pipe meets the AASHTO-M294 requirements for visual inspection.

(c) *HDPE HANCOR* 36: The pipe meets the AASHTO-M294 requirements for visual inspection.

(d) PVC 36: The pipe meets the ASTM F949 requirements for visual inspection.

(e) Aluminum 36: Generally the pipe meets the requirements of the ASSHTO-T249 for visual inspection. However, the seam lap is smaller than the minimum required length and is not equidistant from adjacent ribs as required. m addition, the lapped surfaces are not quite in tight contact as required.

(f) Steel 36: Generally the pipe meets the requirements of the AASHTO T249 for visual inspection. However, the seam lap is not equidistant from adjacent ribs as required.

Table 2.1 - Geometry of ADS 48" Pipe

Test No.	OD (in)	ID (in)	t_a (in)	t_{in} (in)	t_{out} (in)	d_i (in)	t_b (in)	t_c (in)	t_d (in)
1	52 ¼	47 1/8	2.6515	0.1430	0.1050	2.4420	0.1290	0.0930	0.3140
2	52	47	2.6670	0.1435	0.1260	2.5285	0.1345	0.0945	0.3090
3	52 7/16	47	2.6800	0.1250	0.1665	2.5120	0.1265	0.1025	0.3075
4	52 3/16	47	2.6535	0.1395	0.1495	2.4750	0.1105	0.0845	0.3040
5	52 3/8	47 3/16	2.6375	0.1395	0.1005	2.5365	0.1130	0.0970	0.2995
6	52 1/2	47 15/16	2.6765	0.1315	0.1065	2.4460	0.1380	0.0865	0.3025
7	52 7/16	46 15/16	2.6475	0.1345	0.0980	2.5375	0.1335	0.0965	0.3090
8	52 3/8	46 15/16	2.6685	0.1245	0.1050	2.5380	0.1045	0.0810	0.2975
Average	52.32	47.016	2.6603	0.1351	0.1196	2.5019	0.1237	0.0919	0.3054

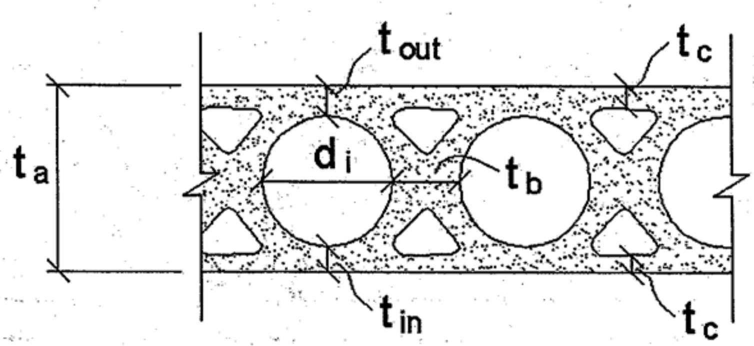

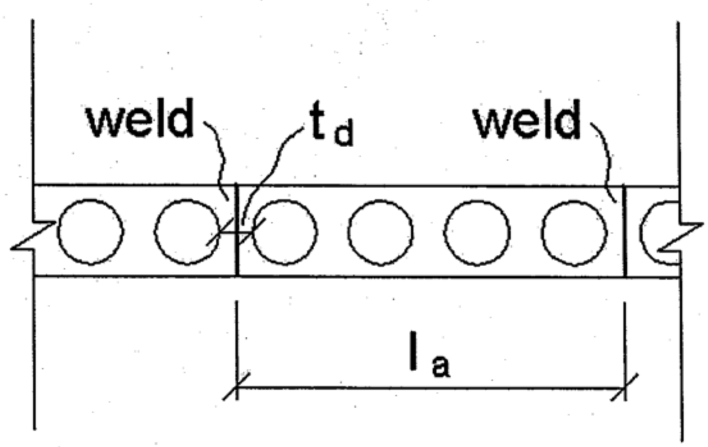

Table 2.2 - Geometry of ADS 36" Pipe

Test No.	ID (in)	OD (in)	t_a (in)	t_{in} (in)	t_{out} (in)	t_b (in)	t_c (in)	d_1 (in)	d_2 (in)
1	35.813	41.375	2.6895	0.1245	0.1650	0.2265	0.2525	2.5175	2.2835
2	36.0	41.563	2.6980	0.1220	0.1760	0.2065	0.2560	2.5070	2.2280
3	36.125	41.688	2.6845	0.1265	0.1760	0.2125	0.2585	2.4860	2.1830
4	36.0	41.688	2.6950	0.1225	0.1760	0.2050	0.2605	2.4750	2.2460
5	35.875	41.5	2.6705	0.1230	0.1780	0.2165	0.2440	2.5020	2.2105
6	35.938	41.375	2.6690	0.1285	0.1755	0.2090	0.2635	2.5500	2.2400
7	36.063	41.625	2.6575	0.1205	0.1780	0.2155	0.2570	2.4800	2.1995
8	36.188	41.75	2.6570	0.1325	0.1730	0.2070	0.2630	2.5015	2.2455
Average	36.00	41.5703	2.6776	0.1250	0.1744	0.2123	0.2569	2.5024	2.2285

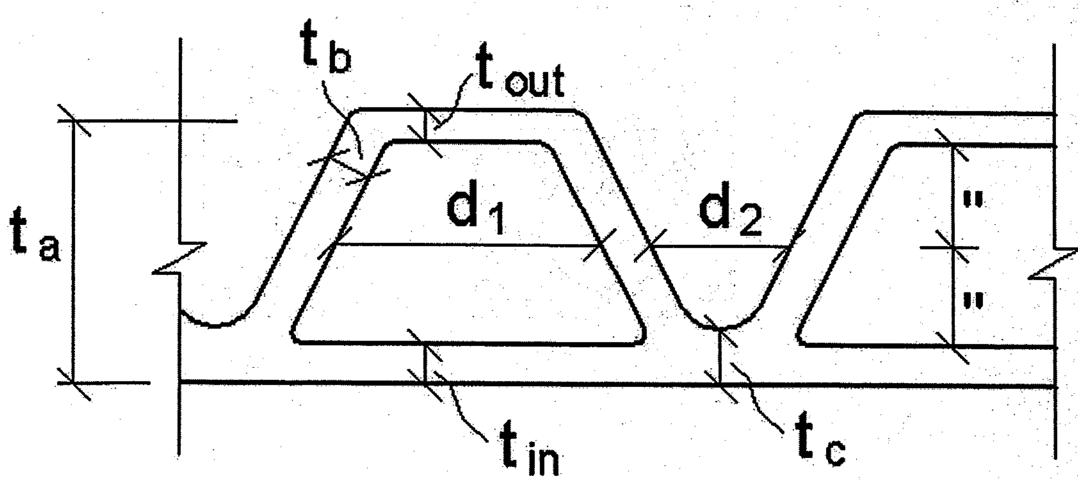

Table 2.3 - Geometry of HANCOR 36" Pipe

Test No.	OD (in)	ID (in)	t_a (in)	t_a' (in)	t_b (in)	t_c (in)	t_{in} (in)	t_{out} (in)	d_1 (in)	d_2 (in)
1	41.5	36.063	2.6430	2.4815	0.1575	0.2685	0.1215	0.0905	2.3165	2.1860
2	41.375	35.875	2.6405	2.5035	0.1520	0.2635	0.1190	0.1165	2.3505	2.1505
3	41.375	35.938	2.6225	2.5040	0.1695	0.3030	0.1145	0.0945	2.3270	2.1855
4	41.5	36.063	2.6630	2.5060	0.1475	0.3080	0.1395	0.1010	2.2675	2.1705
5	41.563	36.063	2.6655	2.5370	0.1690	0.2590	0.1230	0.0900	2.3135	2.1425
6	41.625	36.0	2.6935	2.5210	0.1760	0.2560	0.1205	0.0985	2.2835	2.1465
7	41.438	35.938	2.6475	2.5320	0.1660	0.2350	0.1175	0.1080	2.2965	2.1565
8	41.438	35.875	2.6140	2.5440	0.1560	0.2420	0.1150	0.0905	2.3060	2.2065
Average	41.477	35.852	2.6487	2.5161	0.1614	0.2669	0.1213	0.0987	2.3076	2.1681

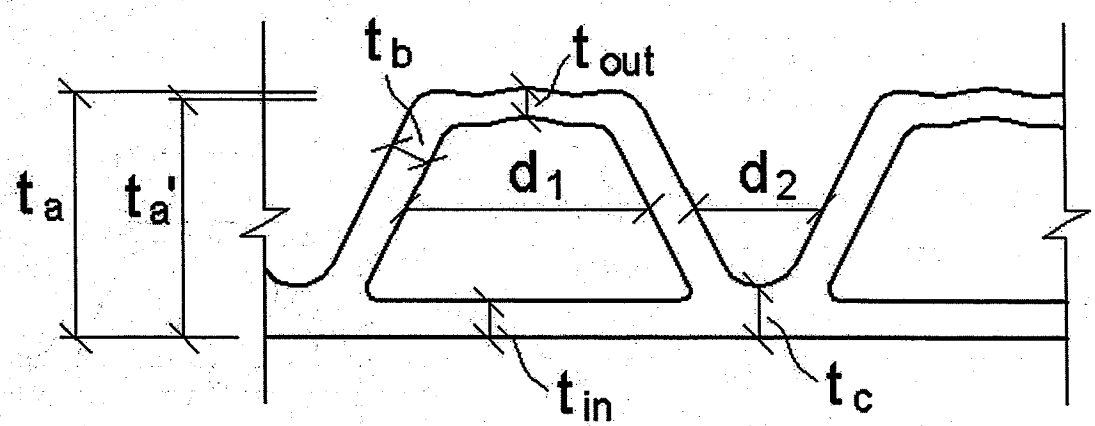

Table 2.4 (a) - Geometry of PVC 36" Pipe

Test No.	OD (in)	ID (in)	t_a (in)	t_b (in)	t_c (in)	t_{in} (in)	t_{out} (in)	d_1 (in)	d_2 (in)
1	38.813	35.5	1.6320	0.1770	0.2385	0.1900	0.1415	1.8010	1.6755
2	38.813	35.5	1.6255	0.1585	0.2380	0.2010	0.1390	1.7895	1.6685
3	38.813	35.438	1.6390	0.1660	0.2435	0.1975	0.1325	1.7880	1.6630
4	38.813	35.438	1.6230	0.1635	0.2370	0.1890	0.1370	1.7735	1.6765
5	38.75	35.5	1.6260	0.1695	0.2340	0.1960	0.1395	1.8160	1.6755
6	38.813	35.563	1.6240	0.1830	0.2350	0.1930	0.1360	1.7850	1.6760
7	38.688	35.5	1.6245	0.1615	0.2335	0.1905	0.1370	1.7850	1.6740
8	38.75	35.438	1.6225	0.1725	0.2370	0.1900	0.1385	1.7970	1.6975
Average	38.7734	35.5078	1.6271	0.1689	0.2371	0.1934	0.1376	0.1719	1.6758

Table 2.4 (b) - Inside and Outer Diameters Using Perimeter Measurements

Test No.	Perimeter P (in)	OD (in) (OD = P/π)	ID (in) (ID = OD – 2 t_a)
1	122.25	38.9134	35.6494
2	122.50	38.9930	35.7420
3	122.50	38.9930	35.7150
4	122.50	38.9930	35.7470
5	122.25	38.9134	35.6614
6	122.25	38.9134	35.6654
7	122.125	38.8736	35.6644
8	122.25	38.9134	35.6684
Average	122.3281	38.9383	35.6841

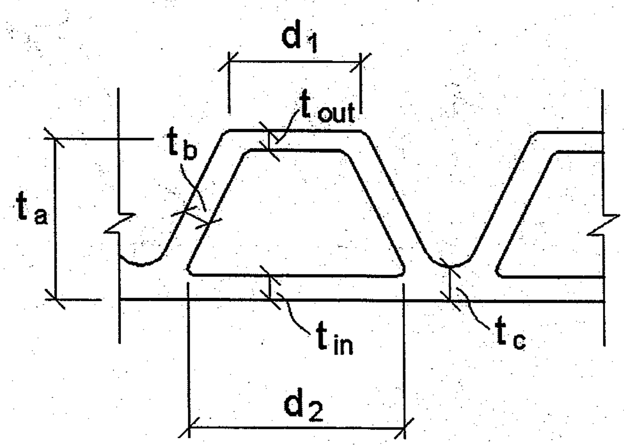

Table 2.5 - Geometry of Aluminum 36" Pipe

Test No.	OD (in)	ID (in)	t (in)	d_1 (in)	d_2 (in)	d_3 (in)	d_4 (in)	d_s (in)	d_a (in)	d_l (in)	d_{tap} (in)	t_{tap} (in)	α
1	37 1/4	35 7/16	0.0865	0.9395	0.7625	6 7/16	22 15/16	4 3/8	5 1/8	8 7/8	0.6885	0.1875	
2	37 1/2	35 7/8	0.0835	0.9470	0.7935	6 3/8	23 1/16	4 5/16	5 5/32	8 29/32	0.7155	0.2205	
3	37	35 7/8	0.0820	0.9545	0.7825	6 3/8	23	4 7/16	5 3/16	8 7/8	0.6790	0.1830	
4	37	35 11/16	0.0830	0.9440	0.7570	6 3/8	23 1/16	4 1/2	5 1/8	8 7/8	0.6980	---	
5	37 3/8	35 3/8	0.0865	0.9490	0.7805	6 3/8	23 1/16	4 1/2	5 1/8	8 7/8	0.6965	---	
6	37 3/8	35 7/8	0.0850	0.9475	0.7500	6 3/8	23 15/16	4 7/16	5 5/32	8 7/8	0.6805	---	
7	37 1/2	35 7/8	0.0815	0.9445	0.8105	6 3/8	23	4 7/16	5 5/32	8 13/16	0.6855	---	
8	37 1/4	35 11/16	0.0895	0.9410	0.7790	6 3/8	23 1/16	4 1/2	5 5/32	8 29/32	0.6905	---	
Average	37.281	35.711	0.0847	0.9459	0.7769	6.383	23.016	4.4375	5.1484	8.875	0.6918	0.1970	78.5°

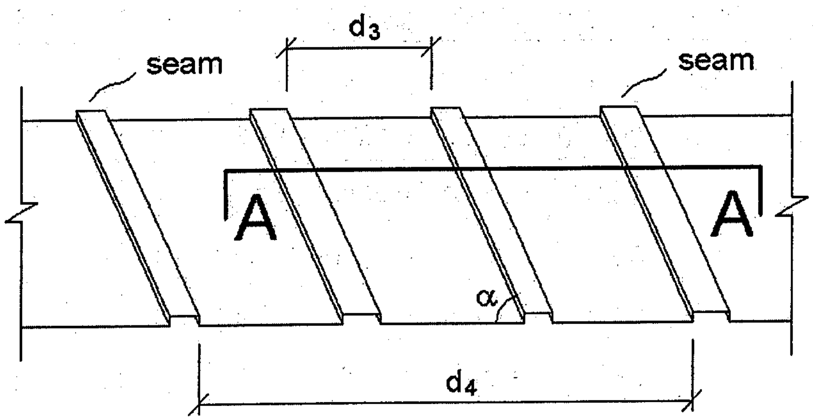

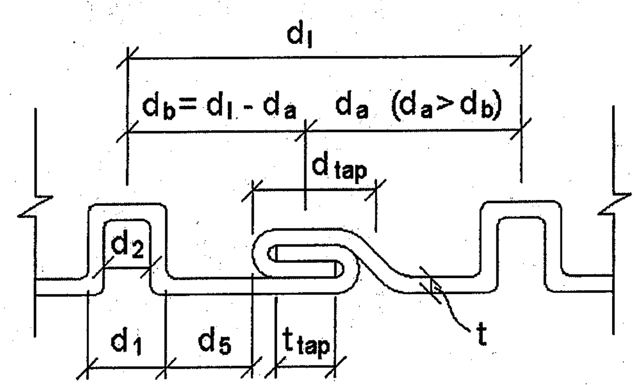

A - A

Table 2.6 - Geometry of steel 36" Pipe

Test No.	OD (in)	ID (in)	t (in)	d_1 (in)	d_2 (in)	d_3 (in)	d_4 (in)	d_5 (in)	d_a (in)	d_l (in)	d_{tap} (in)	t_{tap} (in)	α
1	36	34 11/16	0.0865	0.9395	0.7625	6 7/16	22 15/16	4 3/8	5 1/8	8 7/8	0.6885	0.3510	
2	36 3/8	34 7/8	0.0835	0.9470	0.7935	6 3/8	23 1/16	4 5/16	5 5/32	8 29/32	0.7155	0.3495	
3	36 7/16	34 7/8	0.0820	0.9545	0.7825	6 3/8	23	4 7/16	5 3/16	8 7/8	0.6790	0.3295	
4	36 7/16	34 15/16	0.0830	0.9440	0.7570	6 3/8	23 1/16	4 1/2	5 1/8	8 7/8	0.6980	---	
5	36 1/8	34 3/4	0.0865	0.9490	0.7805	6 3/8	23 1/16	4 1/2	5 1/8	8 7/8	0.6965	---	
6	36 3/8	34 7/8	0.0850	0.9475	0.7500	6 3/8	23 15/16	4 7/16	5 5/32	8 7/8	0.6805	---	
7	36 7/16	34 15/16	0.0815	0.9445	0.8105	6 3/8	23	4 7/16	5 5/32	8 13/16	0.6855	---	
8	36 5/16	35	0.0895	0.9410	0.7790	6 3/8	23 1/16	4 1/2	5 5/32	8 29/32	0.6905	---	
Average	36.313	35.836	0.0847	0.9459	0.7769	6.383	23.016	4.4375	5.1484	8.875	0.6918	0.3433	78.5°

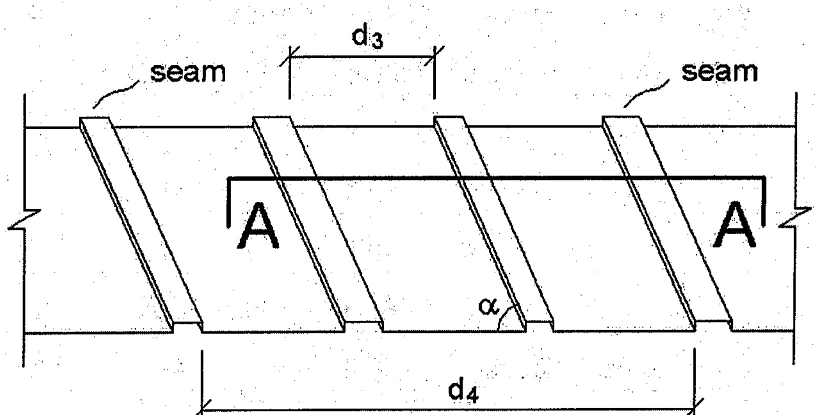

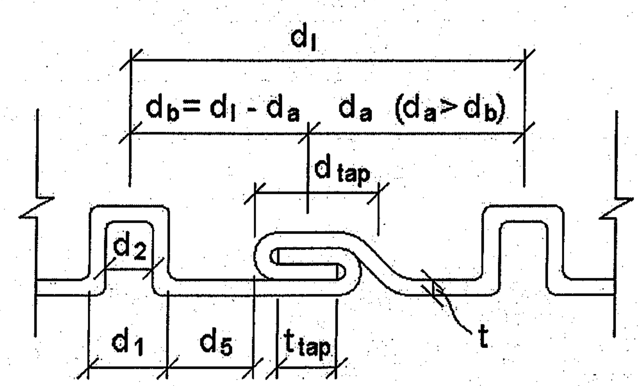

A - A

Table 2.7

Visual Inspection and Material Characterization: AASHTO : M 294M-98 for HDPE Pipe ADS 48"

Article	Details and observations
Article 6.1 (MP7 or M294) Pipes & fittings shall be made of virgin PE compounds, which conforms with the requirements of cell class 335420C.	Manufacturer's description: Letter of certification from ADS of Dec. 21, 2000 indicates compliance of the resin cell classification of 335420C and the resin meets the requirements of AASHTO M294-01. (Letter provided in appendix).
Article 4.5 (MP7 or Article 4.1.3 M294-98) The prevailing specification requires that the inner and outer surfaces be essentially smooth.	The surfaces of the interior and exterior walls are rough and irregular (see photographs, Figs. 2.5 and 2.6).
Article 7.1 (MP7 or M294-98) The prevailing specification requires that the pipe be free of visible defects, defined as: cracks, creases, unpigmented or non uniformly pigmented pipes.	The pipes' surface inside and outside walls, reveal visible deep creasing (see photographs, Figs. 2.5 and 2.6).
Article 7.8.1 (MP7 or M294-98) Requires that the fittings not impair the overall integrity or function of the pipeline.	The bell and spigot joint shows irregular surfaces at certain locations around the circumference (see photograph, Fig. 2.7).
Article 7.2.2 (MP7 for $\phi \geq 1350$ mm and M294-98 for $\phi \leq 1200$ mm) The prevailing specification requires a minimum wall thickness of 1.8 mm for pipe diameter greater than 900 mm and 1.7 mm for 900 mm diameter pipe.	The minimum measured wall thickness is 2.06 mm (0.08 in), which is greater than the minimum required wall thickness of 1.8 mm.
Article 7.2.3 Inside Diameter Tolerances (MP7 and M294-98). The tolerance on the specified ID shall be 4.5% oversize and 1.5% undersize, but not more than 30 mm oversize.	The average measured inside diameter is 1194 mm (47.02 in.); which represents 2.04% undersize based on the nominal diameter of 1219.2 mm (48 in). This undersize is smaller than 30 mm specified in MP7 and M294-98.

Table 2.8

Visual Inspection and Material Characterization: AASHTO : M 294M-98 for HDPE Pipe ADS 36

Article	Details and observations
Article 6.1 (MP7 or M294) Pipes & fittings shall be made of virgin PE compounds, which conforms with the requirements of cell class 335420C.	Manufacturer's description: As per letter (not dated) from ADS (Mr. James Park), pipes and fittings are manufactured according to AASHTO : M294M-98) with specified cell class 335420C.
Article 4.5 (MP7 or Article 4.1.3 M294-98) The prevailing specification requires that the inner and outer surfaces be essentially smooth.	The inner surface is smooth with waviness in the longitudinal direction. The rise in the waviness is in the valley and the depressions in the corrugations (see photographs, Figs. 2.8 and 2.9).
Article 7.1 (MP7 or M294-98) The prevailing specification requires that the pipe be free of visible defects, defined as: cracks, creases, unpigmented or non uniformly pigmented pipes.	No visible defects or creases were observed in the interior surface.
Article 7.8.1 (MP7 or M294-98) Requires that the fittings not impair the overall integrity or function of the pipeline.	The bell and spigot show no irregularities.
Article 7.2.2 (MP7 for $\phi \geq 1350$ mm and M294-98 for $\phi \leq 1200$ mm) The prevailing specification requires a minimum wall thickness of 1.8 mm for pipe diameter greater than 900 mm and 1.7 mm for 900 mm diameter pipe.	The minimum measured wall thickness is 3.06 mm (0.125 in), which is greater than the minimum required wall thickness of 1.7 mm.
Article 7.2.3 Inside Diameter Tolerances (MP7 and M294-98). The tolerance on the specified ID shall be 4.5% oversize and 1.5% undersize, but not more than 30 mm oversize.	The average measured inside diameter is 914 mm (36.0 in), which equals the nominal diameter.

Table 2.9

Visual Inspection and Material Characterization: AASHTO : M 294M-98 for HDPE Pipe HANCOR 36

Article	Details and observations
Article 6.1 (MP7 or M294) Pipes & fittings shall be made of virgin PE compounds, which conforms with the requirements of cell class 335420C.	Manufacturer's description: As per letter dated December 4, 2000, the pipes and fittings are manufactured according to AASHTO : M294M-98 with specified cell class 335500C
Article 4.5 (MP7 or Article 4.1.3 M294-98) The prevailing specification requires that the inner and outer surfaces be essentially smooth.	The inner surface is smooth with waviness in the longitudinal direction. The rise in the waviness is in the valley and the depressions in the corrugations (see photographs, Figs. 2.10 and 2.11).
Article 7.1 (MP7 or M294-98) The prevailing specification requires that the pipe be free of visible defects, defined as: cracks, creases, unpigmented or non uniformly pigmented pipes.	No visible defects or creases were observed in the interior surface.
Article 7.8.1 (MP7 or M294-98) Requires that the fittings not impair the overall integrity or function of the pipeline.	The bell and spigot show no irregularities.
Article 7.2.2 (MP7 for $\phi \geq 1350$ mm and M294-98 for $\phi \leq 1200$ mm) The prevailing specification requires a minimum wall thickness of 1.8 mm for pipe diameter greater than 900 mm and 1.7 mm for 900 mm diameter pipe.	The minimum measured wall thickness is 2.91 mm (0.1145 in), which is greater than the minimum required wall thickness of 1.7 mm.
Article 7.2.3 Inside diameter Tolerances (MP7 and M294-98). The tolerance on the specified ID shall be 4.5% oversize and 1.5% undersize, but not more than 30 mm oversize.	The average measured inside diameter is 910.6 mm (35.852 in), which is smaller than the nominal diameter. This represents 0.4% undersize, which is smaller than 1.5% undersize specified by the code.

Table 2.10

Visual Inspection and Material Characterization: ASTM F949-00 for PVC Pipe

Article	Details and observations
Article 4.1 The pipe shall be made of PVC compound having a minimum cell classification of 12454B or 12454C in accordance with specification ASTM D 1784. The fittings shall be made of PVC compound having a cell classification of 12454B, 12454C or 13343C.	Manufacturer's description: As per letter dated January 17, 2001 from Contech, PVC A-2000 Pipe is manufactured as detailed in Article 4.1 of ASTM F 949-00.
Article 4.3 Pipe shall be manufactured by simultaneous extrusion of the smooth inner wall fused to the outer corrugated wall.	Manufacturer's description: As per letter dated January 17, 2001 from Contech, PVC A-2000 Pipe is manufactured as detailed in Article 4.3 of ASTM F 949-00.
Article 5.1 The pipe and fittings shall be homogeneous throughout and free from visible cracks, holes, foreign inclusions or other injurious defects.	The pipe and fittings are homogeneous. No visible cracks, holes or foreign inclusions are evident (see photographs, Figs. 2.12 and 2.13). .
Article 7.3.1 Measure the average outside diameter of the pipe in accordance with test method ASTM D 2122 using a circumferential wrap tape accurate to ± 0.001 in. (± 0.02 mm). The average inside diameter may be calculated from the average outside diameter and wall thickness measurements in accordance with test method ASTM D 2122.	Average outside diameter of the pipe = 38.938 in. Average inside diameter of the pipe = 35.684 in.

Table 2.11

Visual Inspection and Material Characterization: AASHTO : T249-93 for Aluminum Pipe

Article	Details and observations
2. Lock seam quality (see Fig. below) • Seam lap • Contact of lapped surfaces • Interior angularity and roller indentation 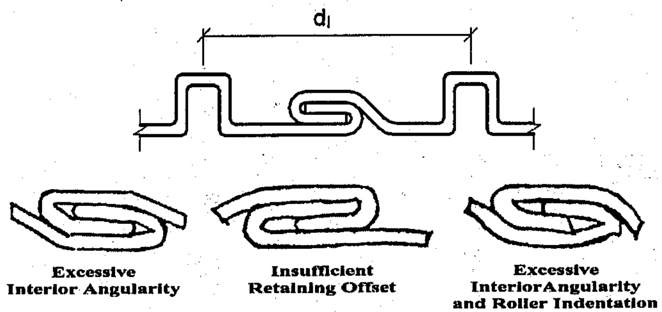	• Seam lap is smaller than the code specification average value of seam lap, which is 7.9 mm (0.311 in.). The seam lap is not equidistant from the two adjacent ribs, as required in the code. (Distance of seam lap from left rib = 99 mm (3.89 in.), distance from right rib = 132 mm (5.18 in)). • The lapped surfaces are not in tight contact as required by the code. The physical separation between the lapped surfaces is quite evident (see photograph, Fig. 2.14). • The roller indentation seems to be satisfactory, whereas the interior angularity is excessive.

Table 2.12

Visual Inspection and Material Characterization: AASHTO : T249-93 for Steel Pipe

Article	Details and observations
2. Lock seam quality (see Fig. below) • Seam lap • Contact of lapped surfaces • Interior angularity and roller indentation 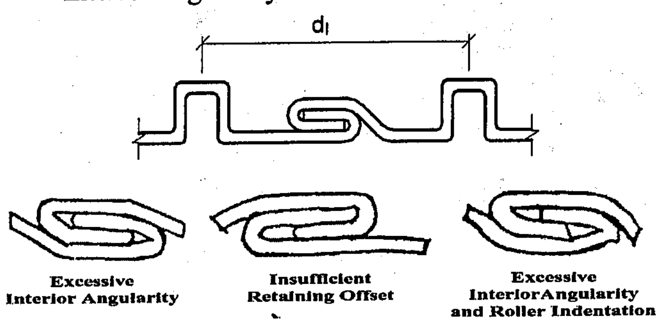	• Seam lap, which is 8.72 mm (0.343 in), is greater than the code specification minimum value of seam lap, which is 7.9 mm (0.311 in.). The seam lap is not equidistant from the two adjacent ribs as required in the code. (Distance of seam lap from left rib = 99 mm (3.89 in.), distance from right rib = 132 mm (5.18 in)). • There is no apparent physical separation between the lapped surfaces (see photograph, Fig. 2.15). • The roller indentation seems to be satisfactory. Although the interior angularity is better than that observed in the aluminum pipe, it does not comply fully with the code specifications.

(a) Bell

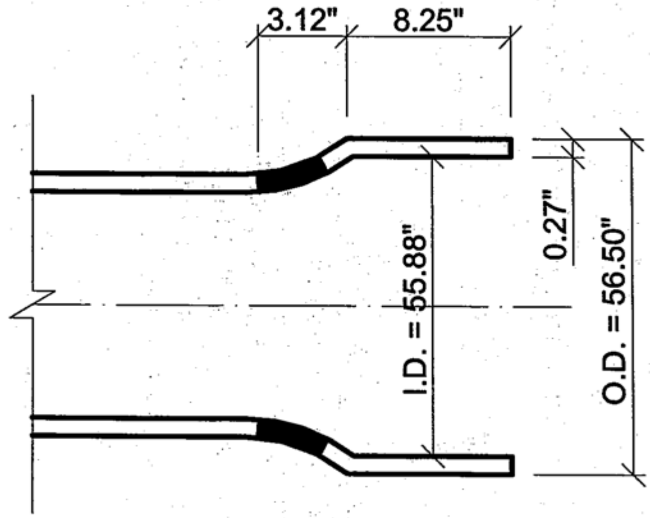

(b) Spigot

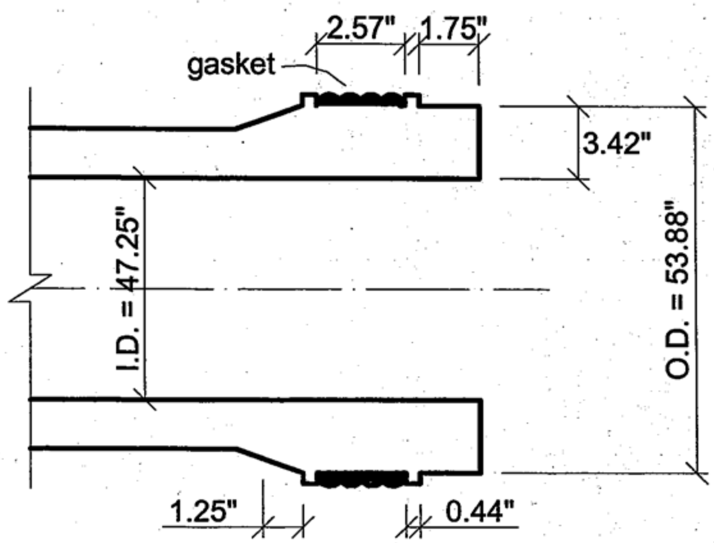

Fig. 2.1 - Bell and Spigot Geometry of ADS 48 (Average Values)

(a) Bell

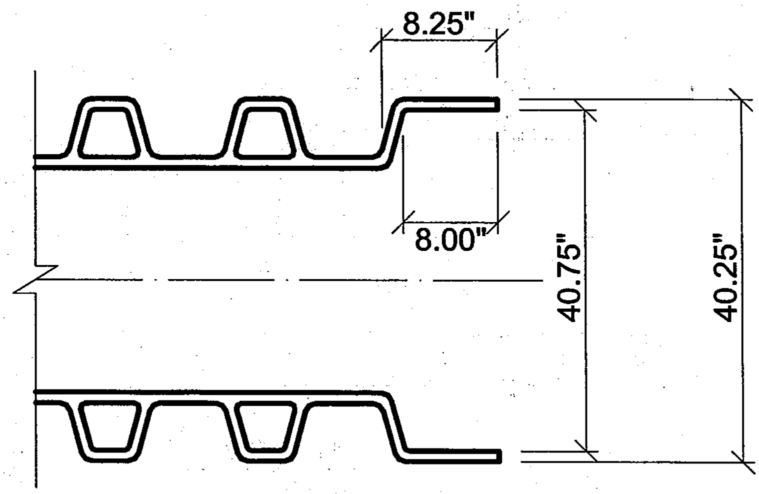

(b) Spigot

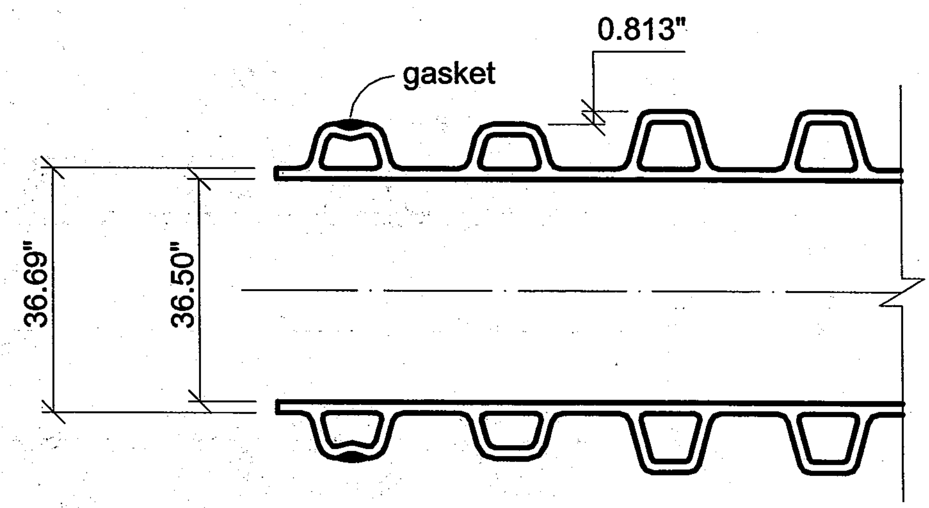

Fig. 2.2 - Bell and Spigot Geometry of ADS 36 (Average Values)

(a) Bell

(b) Spigot

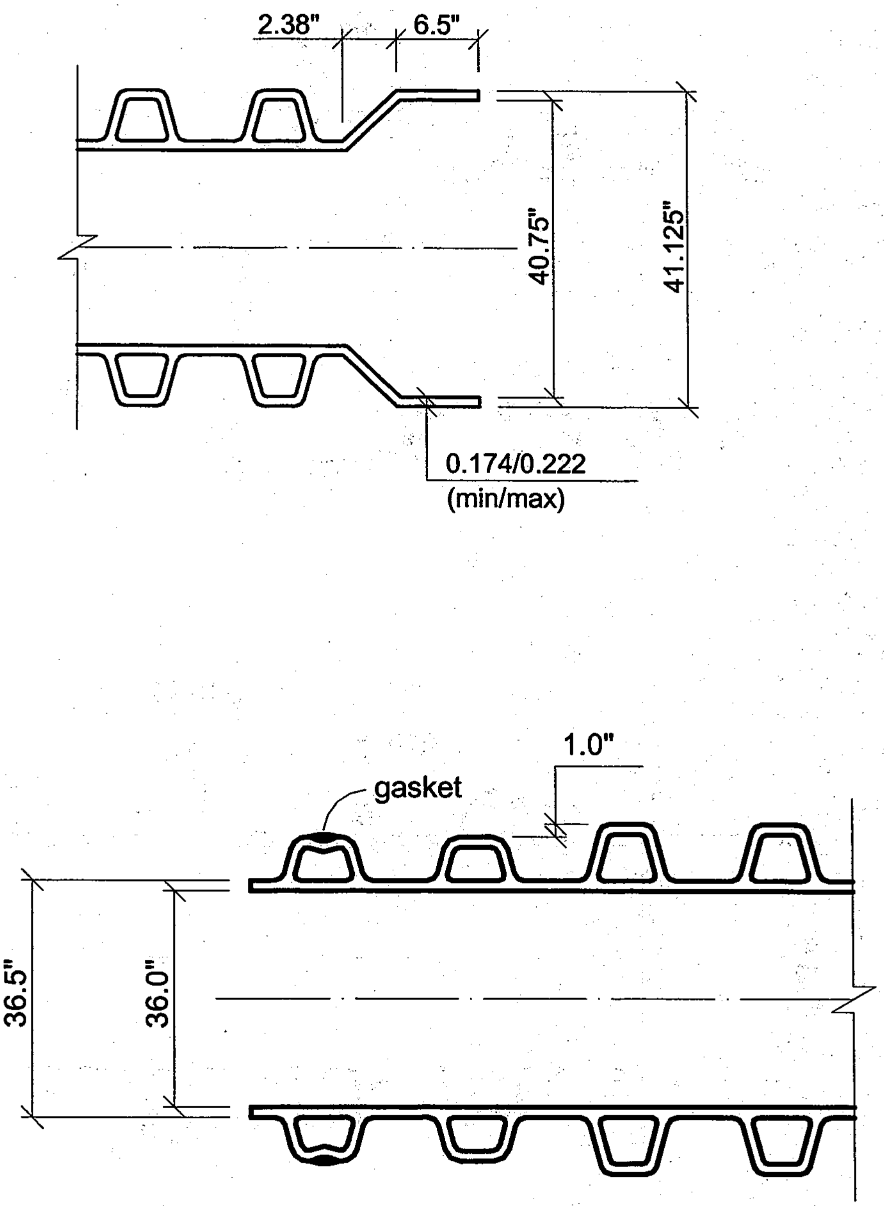

Fig. 2.3 - Bell and Spigot Geometry of Hancor 36 (Average Values)

(a) Bell

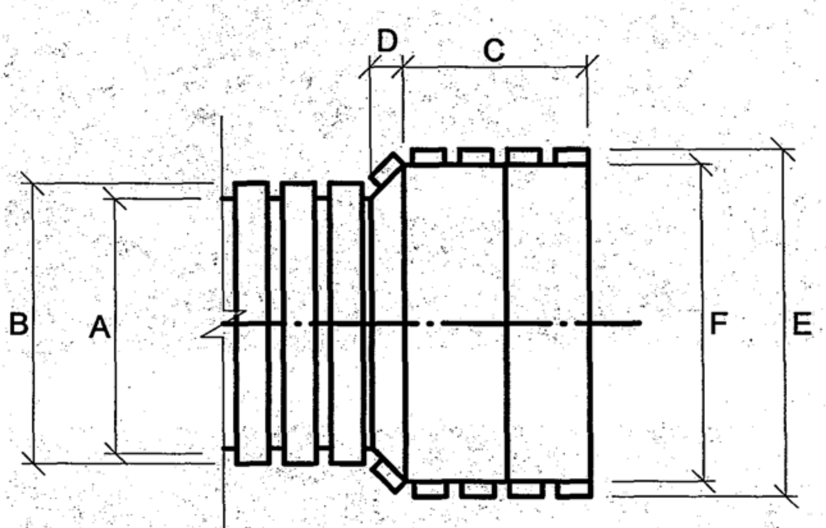

A = 35.50 in

B = 38.75 in

C = 10.75 in

D = 2.25 in

E = 42.75 in

F = 39.50 in

(b) Spigot

Spigot have the same dimensions as A and B above

Fig. 2.4 - Bell and Spigot Geometry of PVC 36 (Average Values)

(a) Inside View

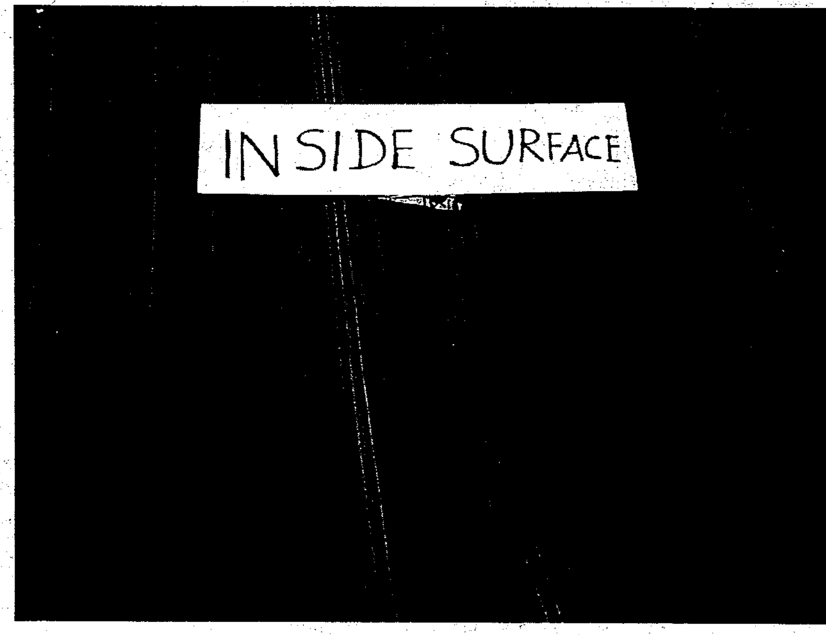

(b) Outside View

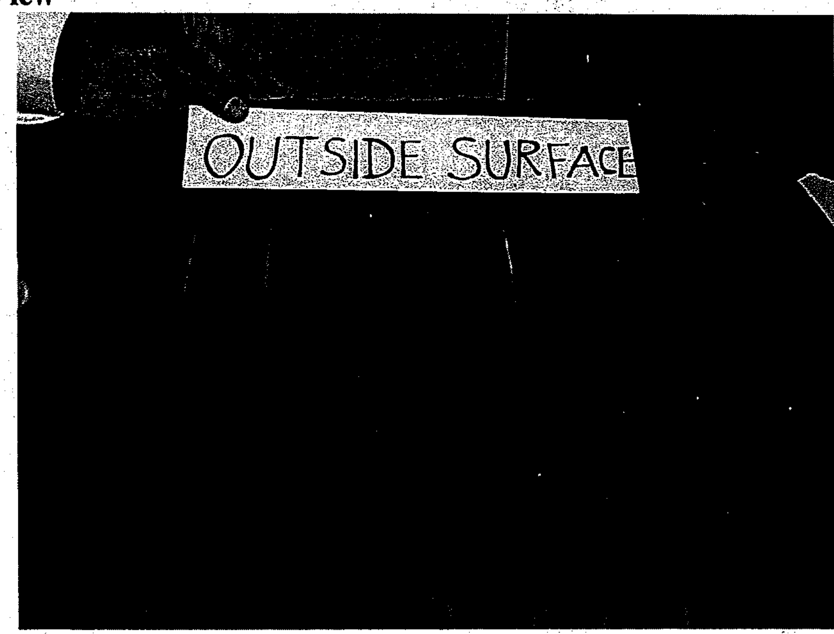

Fig. 2.5 - Inside and Outside Wall Surfaces of ADS 48

(a) Wall Section

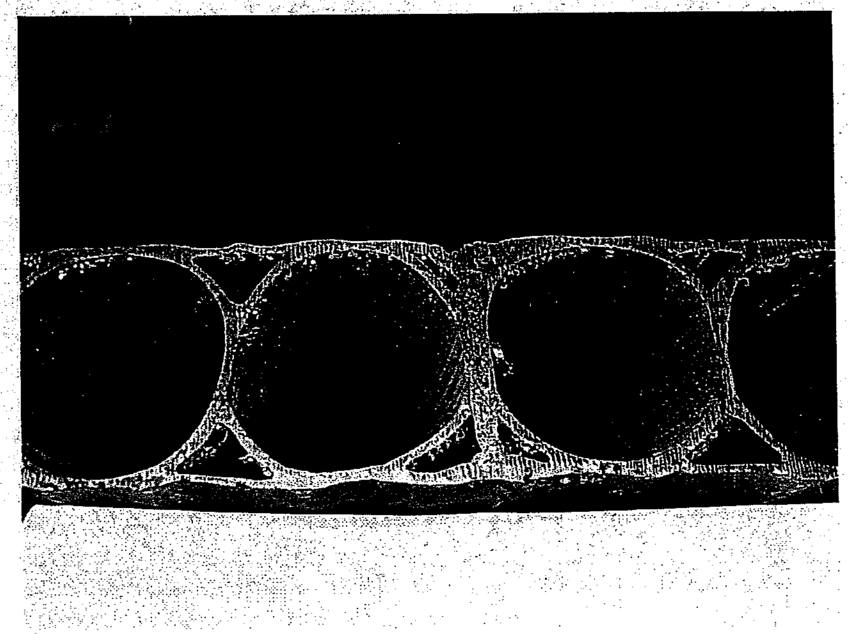

(b) Close-up View of Wall Section

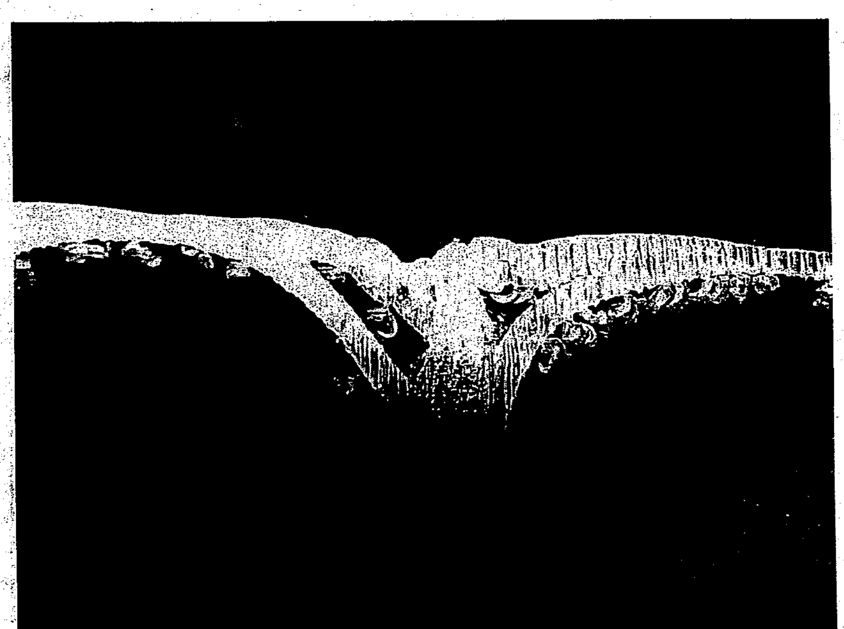

Fig. 2.6 - Wall Section of ADS 48

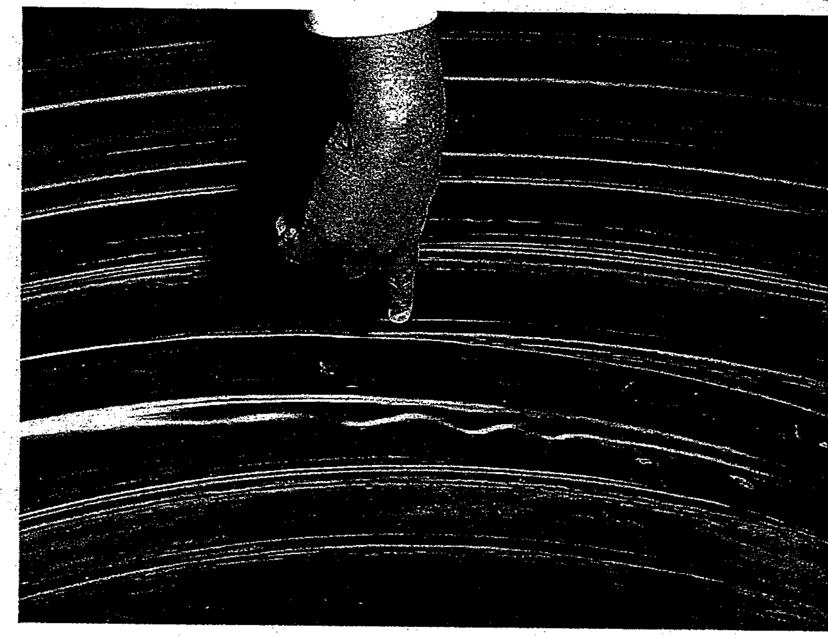

Fig. 2.7 - Bell and Spigot Joint of ADS 48

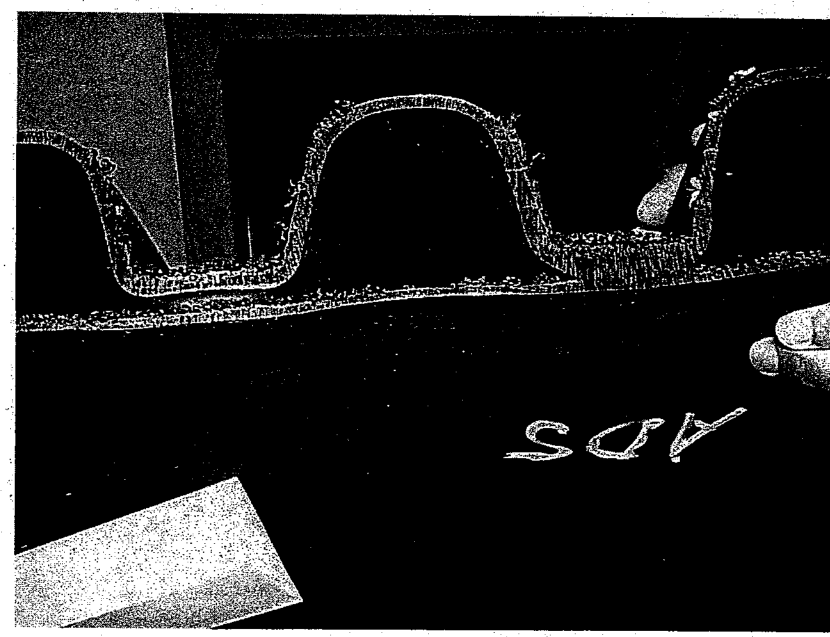

Fig. 2.8 - Wall Section of ADS 36

(a) Inside View

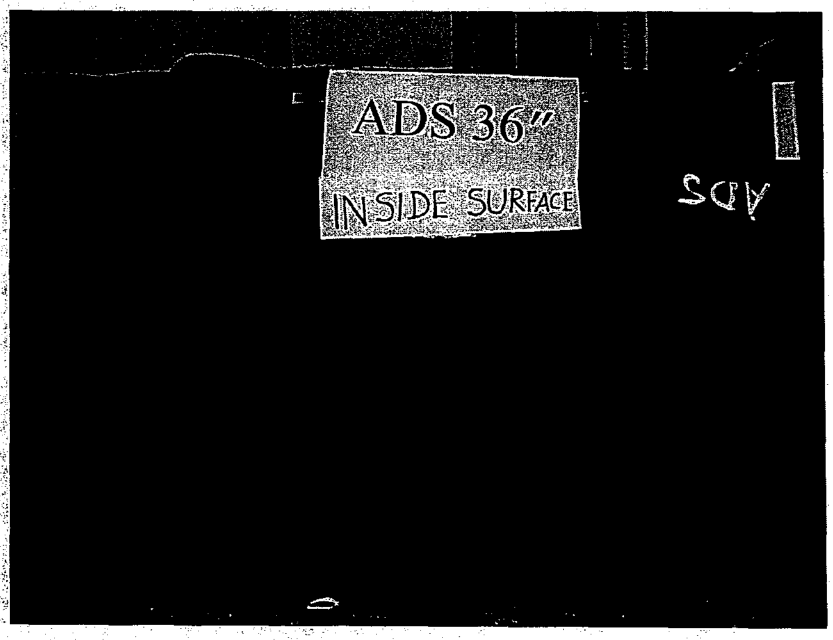

(b) Outside View

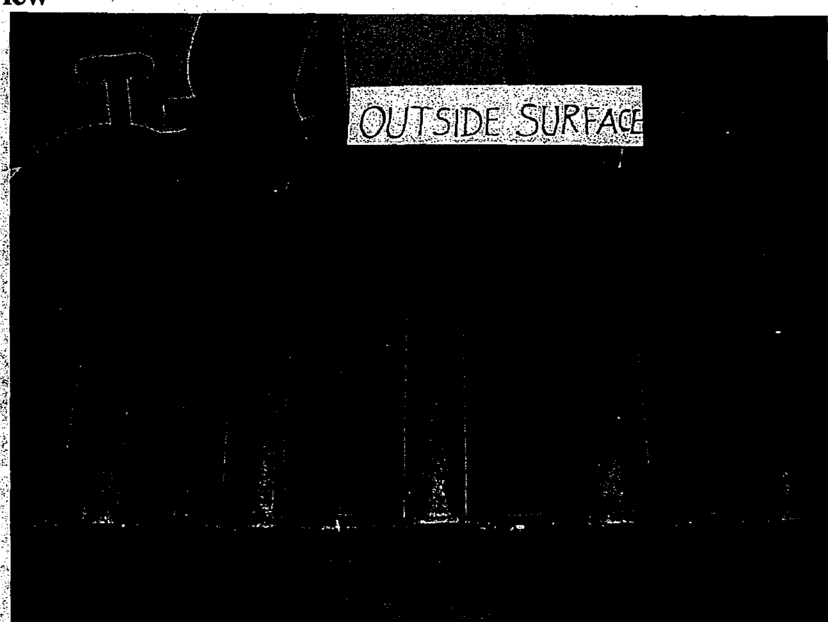

Fig. 2.9 - Inside and Outside Wall Surfaces of ADS 36

(a) Inside View

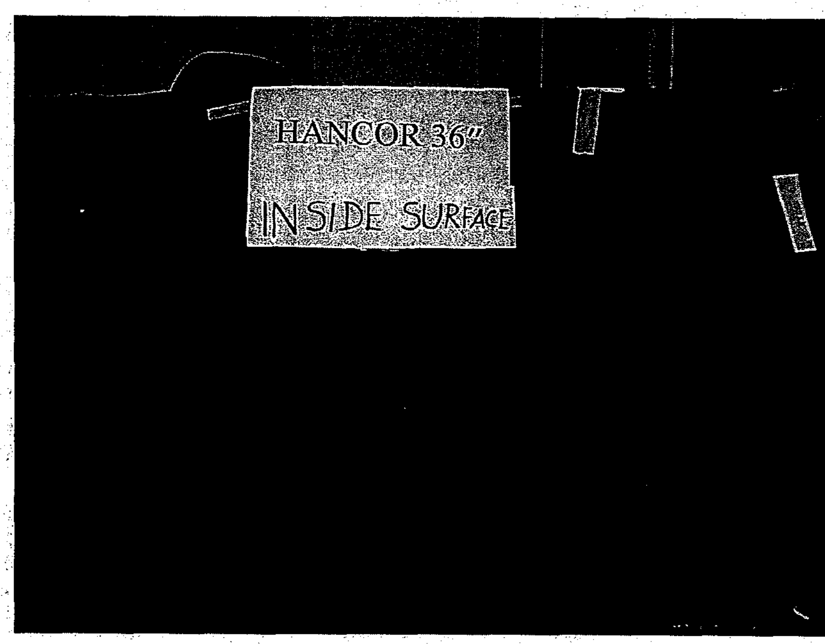

(b) Outside View

Fig. 2.10 - Inside and Outside Wall Surfaces of Hancor 36

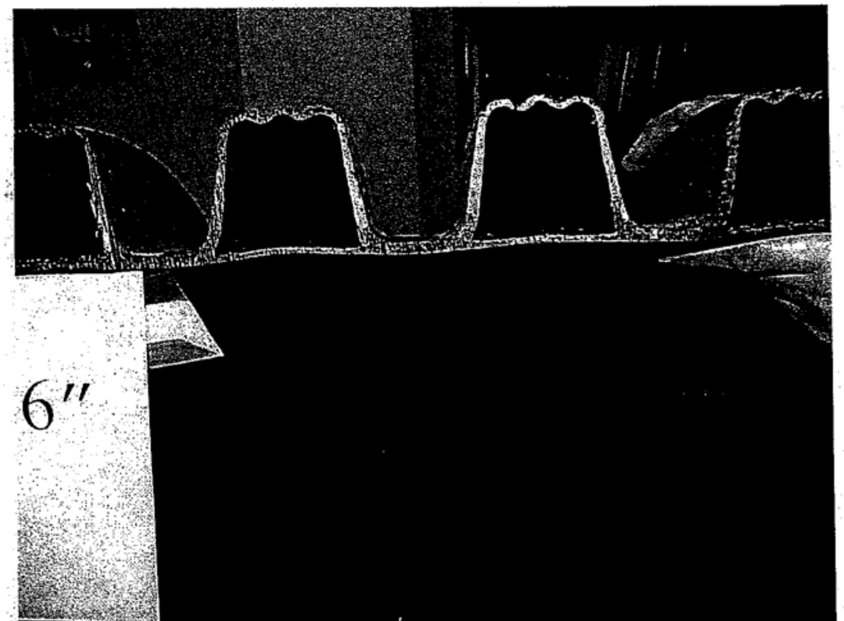

Fig. 2.11 - Wall Section of Hancor 36

Fig. 2.12 - Wall Section of PVC 36

(a) Inside View

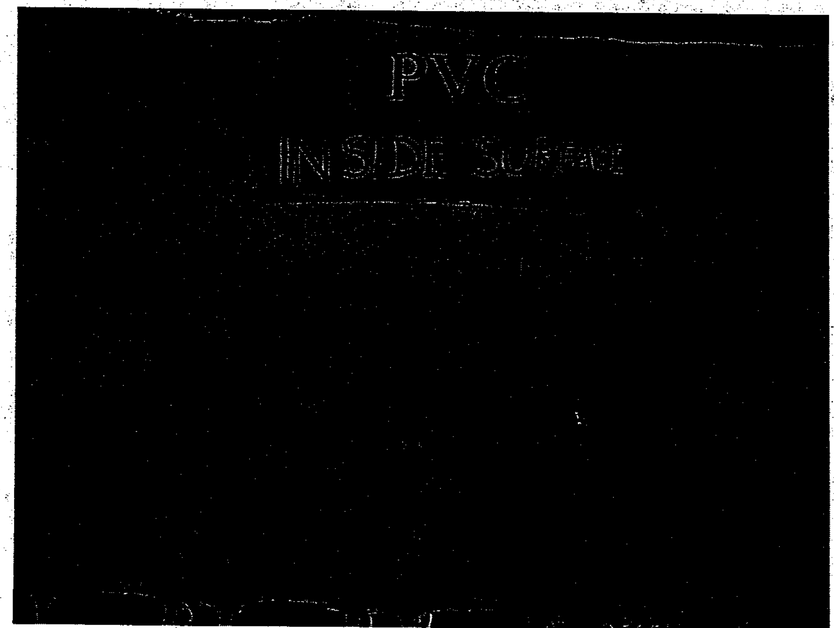

(b) Outside View

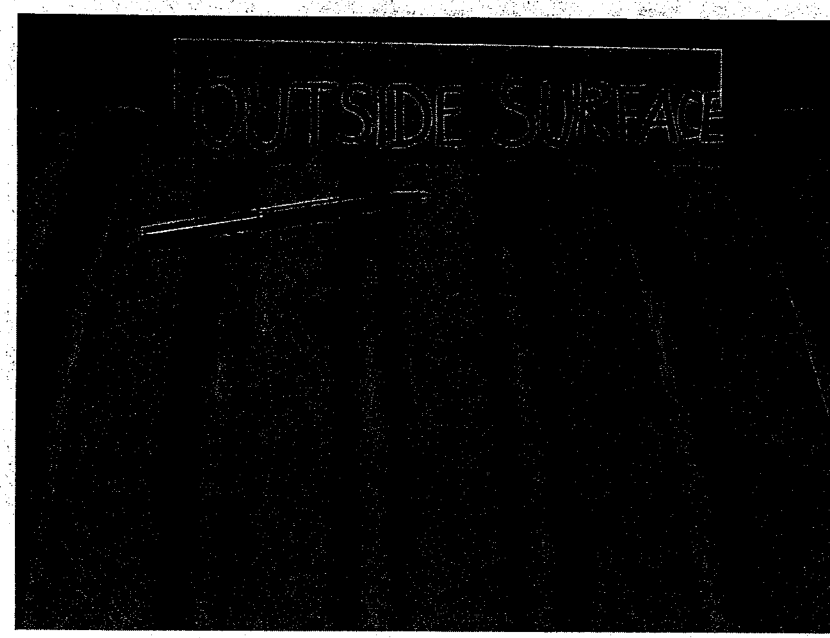

Fig. 2.13 - Inside and Outside Wall Surfaces of PVC 36

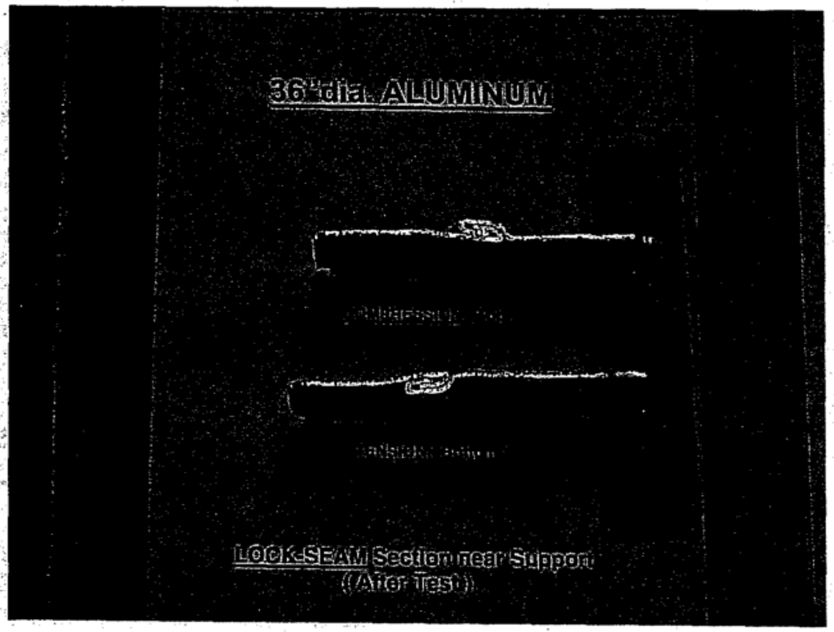

Fig. 2.14 - Lock-Seam Section of Aluminum 36

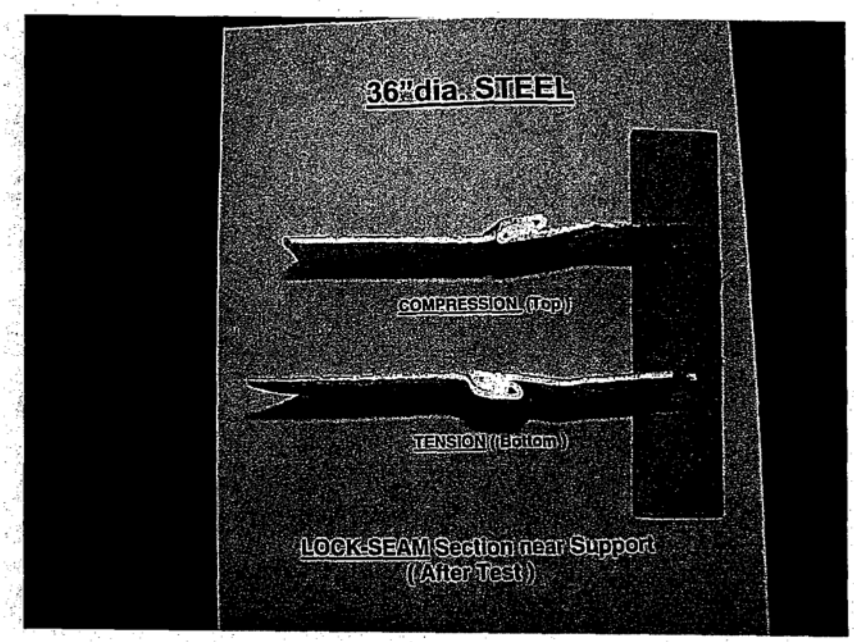

Fig. 2.15 - Lock-Seam Section of Steel 36

Chapter 3: Simple Beam Tests

3.0 Objectives

The objective of this test is to evaluate the pipe performance when subjected to longitudinal bending. The strains experienced on outside walls versus inside walls as well as the longitudinal strains and stresses in relation to vertical deflections are of particular interest.

3.1 Experimental Program

Specimens

Six test pipe specimens having approximately 20 feet in length (full length of pipe) were selected, one for each of the pipe types considered: HDPE ADS 48, HDPE ADS 36, HDPE HANCOR 36, PVC 36, Aluminum 36, and Steel 36.

Test Setup

The test specimens were simply supported and subjected to four point bending. Fig. 3.1 presents photographs of typical setups for beam tests at the Structures Research Center, FDOT, Tallahassee. The widths of the end supports were made sufficiently large to prevent local failure and to permit end rotation (see Figs. 3.2 to 3.4).

Instrumentation and Test Procedure

The test program included application of loads in predetermined increments until failure of the specimens. Each test specimen was instrumented with electrical resistance strain gages in the longitudinal and transverse directions, deflection gages, and crack gages (Figs. 3.2 to 3.4). The pipe response was. monitored and recorded after each load increment with a computer-controlled data acquisition system. Longitudinal strain gages were installed at the outer and inner surfaces at the top and bottom of the pipe at three transverse sections in one-half of the pipe specimen's span (see Fig. 3.5b). The transverse strain gages were installed (see Fig. 3.5b) at the third section around the circumference (Figs. 3.2a, 3.3a and 3.4a) to measure hoop strains. Vertical deflections were measured at the top and bottom of the specimens at 3-ft (914.4 mm) sections along the specimen's span (Figs. 3.2 to 3.4).

3.3 Presentation of Results

The experimental results are presented as follows:

- *For ADS 48 (Figs. 3.6 to 3.11)*
  - Load versus deflections along the pipe in Fig. 3.6,
  - Deflection versus distance along pipe in Fig. 3.7,
  - Top and bottom outer strains versus distance along pipe in Fig. 3.8,
  - Top and bottom inner strains versus distance along pipe in Fig. 3.9,
  - Bottom deflection and load versus longitudinal strains at centerline in Fig. 3.10,
  - Slope of load versus bottom deflection at centerline in Fig. 3.11.

- *For ADS 36 (Figs. 3.12 to 3.18)*
  - Load versus deflection along the `top and bottom of the specimen in Fig. 3.12,
  - Top and bottom deflection at sections along the specimen in Fig. 3.13,
  - Top and bottom outer surface strains at sections along the specimen in Fig. 3.14,
  - Top and bottom inner surface strains at sections along the specimen in Fig. 3.15,
  - Bottom deflection and load versus longitudinal strains at centerline in Fig. 3.16,
  - Slope of load versus bottom deflection at centerline in Fig. 3.17,
  - Load versus valley longitudinal and transverse strains in Fig. 3.18.

- *For HANCOR 36 (Fig. 3.19 to 3.25)*
  - Load versus deflections along, the top and bottom of the specimen in Fig. 3.19,
  - Top and bottom deflections at 3-ft sections along the specimen in Fig. 3.20,
  - Top and bottom outer surface strains at sections along the specimen in Fig. 3.21,
  - Top and bottom inner surface strains at sections along the specimen in Fig. 3.22,
  - Bottom deflection and load versus longitudinal strains at centerline in Fig. 3.23,
  - Slope of load versus bottom deflection at centerline in Fig. 3.24,
  - Load versus valley longitudinal and transverse strains in Fig. 3.25.

- *For PVC 36 (Figs. 3.26 to 3.32)*
  - Load versus deflections along the top and bottom of the specimen in Fig. 3.26,
  - Top and bottom deflections at 3-ft sections along the specimen in Fig. 3.27,

- Top and bottom outer surface strains at sections along the specimen in Fig. 3.28,
- TOP and bottom inner surface strains at sections along the specimen in Fig. 3.29,
- Bottom deflection and load versus longitudinal strains at centerline in Fig. 3.30,
- Slope of load versus bottom deflection at centerline in Fig. 3.31,
- Load versus valley longitudinal and transverse strains in Fig. 3.32.

- For Steel 36 (Figs. 3.33 to 3.39)
  - Load versus deflections along the top and bottom of the specimen in Fig. 3.33,
  - Top and bottom deflections at 3-ft sections along the specimen in Fig. 3.34,
  - Top and bottom outer surface strains at sections along the specimen in Fig. 3.35,
  - Bottom deflection and load versus longitudinal strains at centerline in Fig. 3.36,
  - Slope of load versus bottom deflection at centerline in Fig. 3.37,
  - Load versus valley longitudinal strains in Fig. 3.38,
  - View of lock seam lap near support and at centerline in Fig. 3.39.
- For Aluminum 36 (Figs. 3.40 to 3.46)
  - Load versus deflections along the top and bottom of the specimen in Fig. 3.40,
  - Top and bottom deflections at 3-ft sections along the specimen in Fig. 3.41,
  - Top and bottom outer surface strains at sections along the specimen in Fig. 3.42,
  - Bottom deflections and load versus longitudinal strains at centerline in Fig. 3.43,
  - Slope of load versus bottom deflection at centerline in Fig. 3.44,
  - Load versus valley longitudinal strains in Fig. 3.45,
  - View of lock seam lap near support and at centerline in Fig. 3.46.

3 4 Observations and Discussions

(a) ADS 36 and Hancor 36 achieved a similar bending stiffness (approximately 1100 Lbs/in j and properties (Table 3 1). The bending stiffness of PVC 36 is almost 3 times greater than that of ADS 36 or Hancor 36. This is mainly due to the higher modulus of elasticity of PVC compared to HDPE pipes. The aluminum pipe achieved the lowest bending stiffness (638 Lbs/in.), while ADS 48 achieved the highest bending stiffness (5213 Lbs/in.).

(b) Given the load. and the section along the pipe, the bottom deflections (invert) are generally smaller than the top deflections. This is due to the ring and wall deflections which add up to the top deflection.

(c) For ADS 48, the inner wall longitudinal strains were compressive and outer wall strains tensile at both invert and crown.

(d) For ADS 36, both the top and bottom inner walls were in tension, whereas the top outer wall was in compression. The top inner wall experienced practically no strain (Fig. 3:16).

(e) For Hancor 36, the bottom inner and outer walls were in tension. (small-strains were recorded for the outer wall) , while the top outer and inner walls were in compression (small strains were recorded for the inner wall); see. Fig. 3.23.

(f) For PVC 36, the top: and bottom outer wall strains were negligible. The top inner wall was in compression, whereas the bottom inner wall was in tension (see Fig. 3.30).

(g) For the steel and aluminum pipes, the top wall was in compression, while the bottom wall was in tension (Figs. 3.36 and 3.45).

(h) For the plastic pipes, the valley longitudinal bending strains were greater, than the crown longitudinal bending strains (Fig. 3.18, Fig. 3.32).. For the metal, pipes, the longitudinal bending, strains in the ribs were greater than the longitudinal bending strains in the wall (valley) between the ribs (Fig. 3.38: and-Fig. 3.45).

(i) The lock seams behaved satisfactorily. No separation or, loss of contact between seam laps was observed (see Figs. 3.39 and 3.46).

(j) For the aluminum pipe, the wall (valley) between the ribs experienced practically no longitudinal bending strains. The latter were concentrated in the ribs (Fig. 345).

(k) For a vertical bottom deflection of 1 % and 2% of the span, the obtained maximum longitudinal tensile strains are as given in Table 3.2. It can be observed that for l% deflection, which can be seen as the maximum grade slope during installation, the longitudinal bending strain ranged from 114με (i.e., 12.5 psi) (ADS 36) to 1000με(i.e., 110 psi) (Rancor 36) for HDRE, it reached 600με (i.e., 240, psi) for PVC and 200με (i.e., 5800 psi for steel and 2000 psi for aluminum) for metal pipes.

Table 3.1 - Experimental Stiffness of Pipes in Bending

Series	Stiffness, K[(a)] (Lbs/in.)	EI[(b)] (kip-in.^{2})	I[(c)] (in.^{4})
ADS 48	5213	931 497	8468
ADS 36	1061	189 536	1723
HANCOR 36	1221	218 103	1983
PVC 36	3291	588 010	1470
Steel 36	1311	234 256	8.08
Aluminum 36	638	113 999	11.40

Notes: (a) K = Force/displacement; see curve fittings on Figs. 3.16, 3.22, 3.29, 3.36, 3.42 and 3.49 for ADS 48, ADS 36, HANCOR 36, PVC 36, Steel 36 and Aluminum 36, respectively. $K = F\Delta$
(b) For 4 point loading, from beam theory $K = 56.4\ EI/L^3$, then $EI = KL^3/56.4$, with L =18' =216 in.
(c) Assuming E = 29 000 ksi for Steel, E = 10 000 ksi for aluminum, E = 110 ksi for HDPE and E = 400 ksi for PVC.

Table 3.2 - Longitudinal Bending Strains for Deflections of 1% and 2% Beam Span

Series	Strains at 1% ($\mu\varepsilon$)	Strains at 2% ($\mu\varepsilon$)
ADS 48[(a)]	672	1290
ADS 36[(b)]	114	221
HANCOR 36[(c)]	1000	2200
PVC 36[(d)]	600	1100
Steel 36[(e)]	186 (-185)	350 (-350)
Aluminum 36[(f)]	28 (-200)	55 (-400)

Notes: (a) Gage L34; (b) Gage VL34; (c) Gage L21; (d) Gage L33;
(e) Gages RL34 (-) and RL31 (+); (f) Gages L24 (+) and RL34(-)


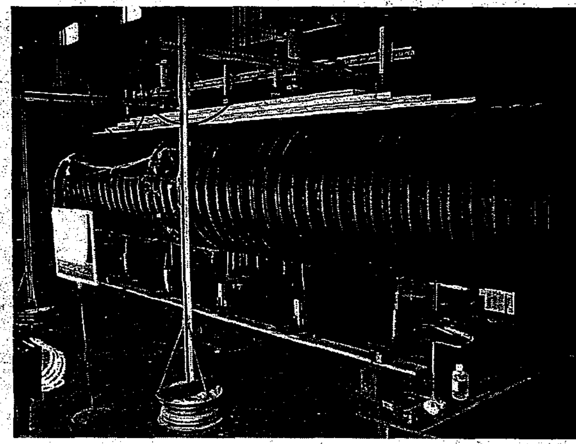

(a) ADS48 under Beam Test (b) ADS36 under Beam Test

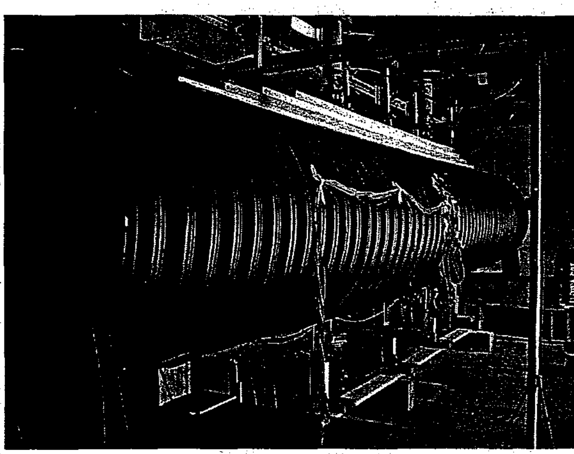
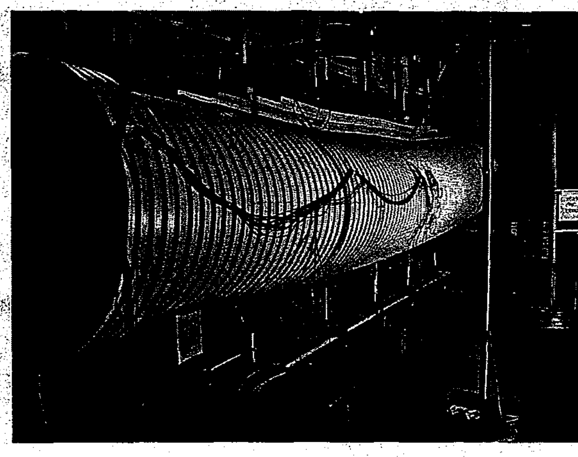

(a) Hancor36 under Beam Test (b) PVC36 under Beam Test

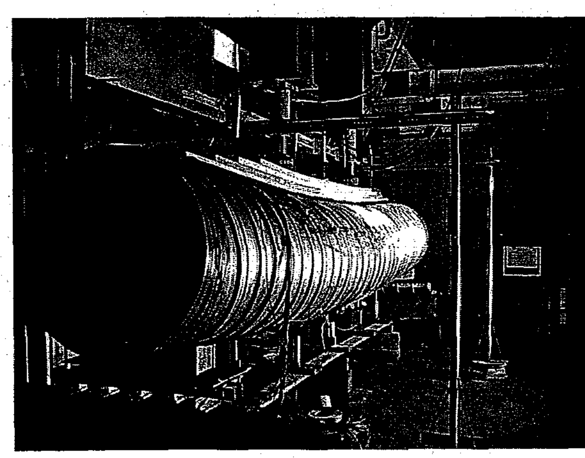
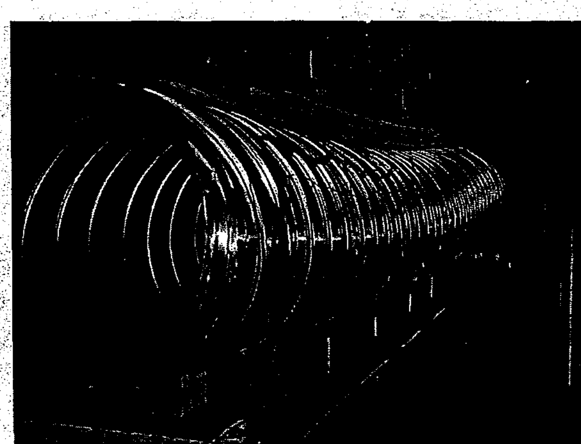

(a) Steel36 under Beam Test (b) Aluminum36 under Beam Test

Fig. 3.1 - Views of Pipes under Beam Test Setup

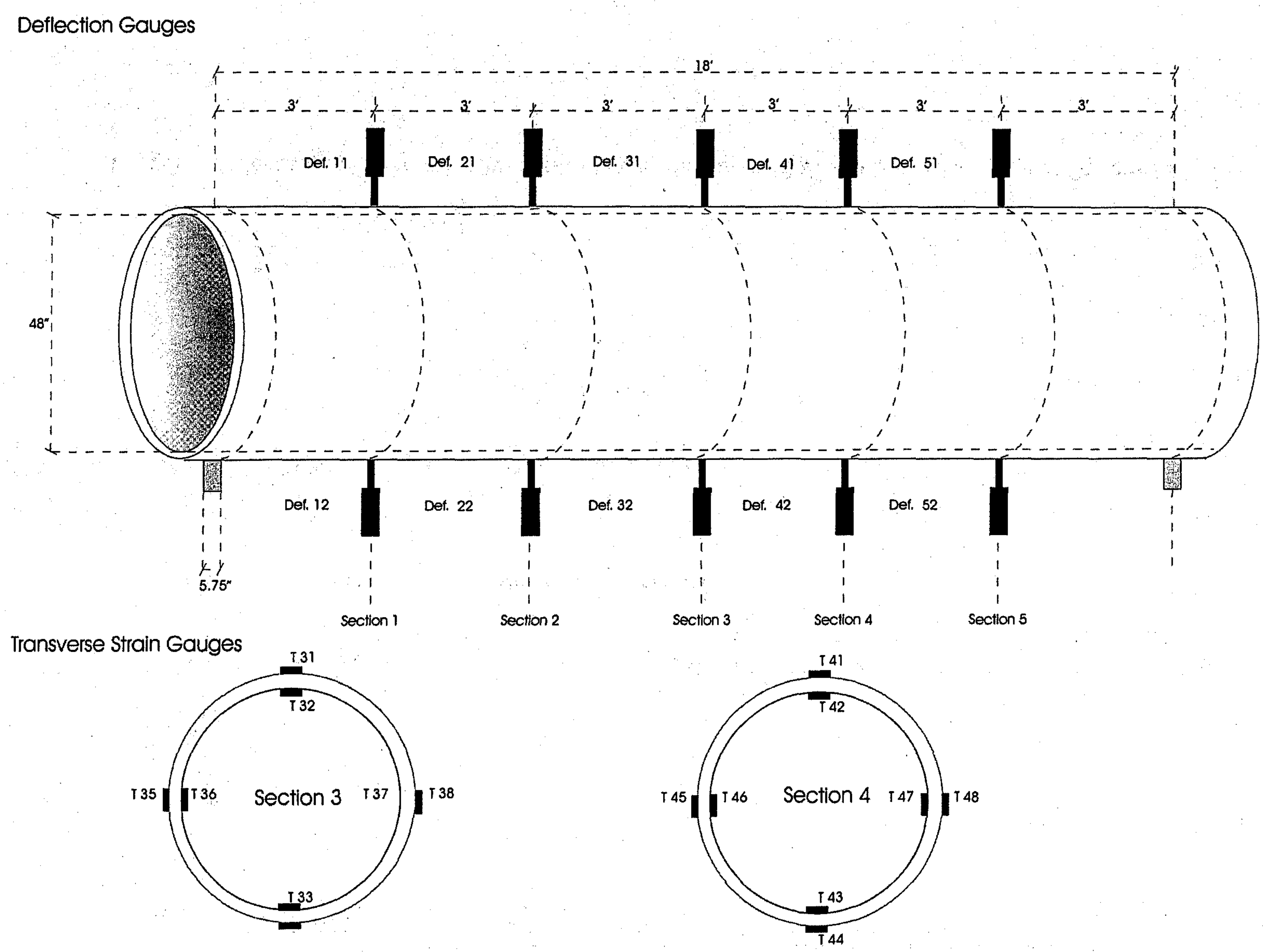

Fig 3.2a - Location of Deflection and Transverse Strain Gages at Section 3 Around Circumference of ADS 48 Pipe Specimen

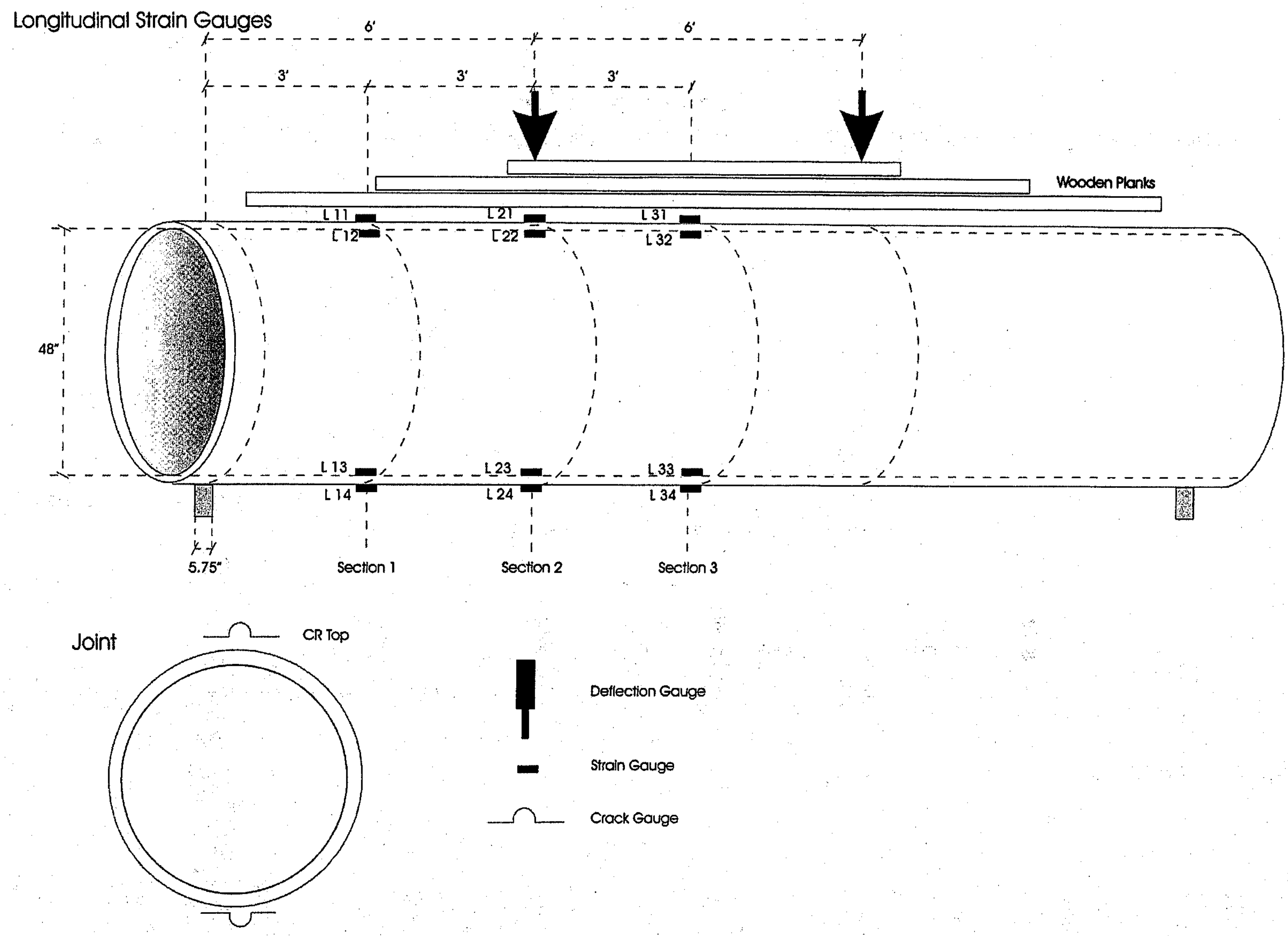

Fig 3.2b - Location of Longitudinal Strain Gages on Top and Bottom of ADS 48 Pipe Specimen

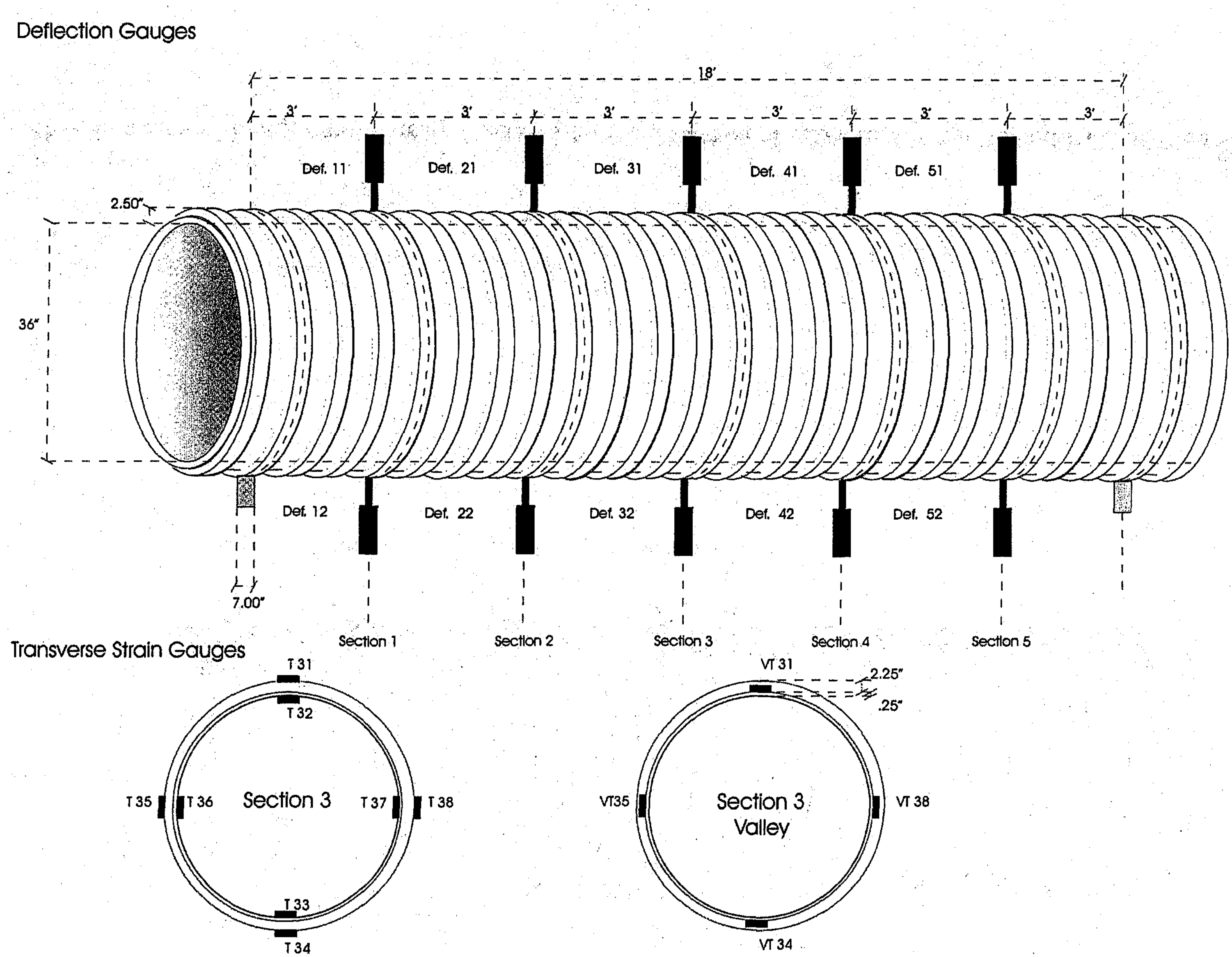

Fig 3.3a - Location of Deflection and Transverse Strain Gages at Section 3 Around Circumference of ADS 36, Hancor 36 and PVC 36 Pipe Specimens

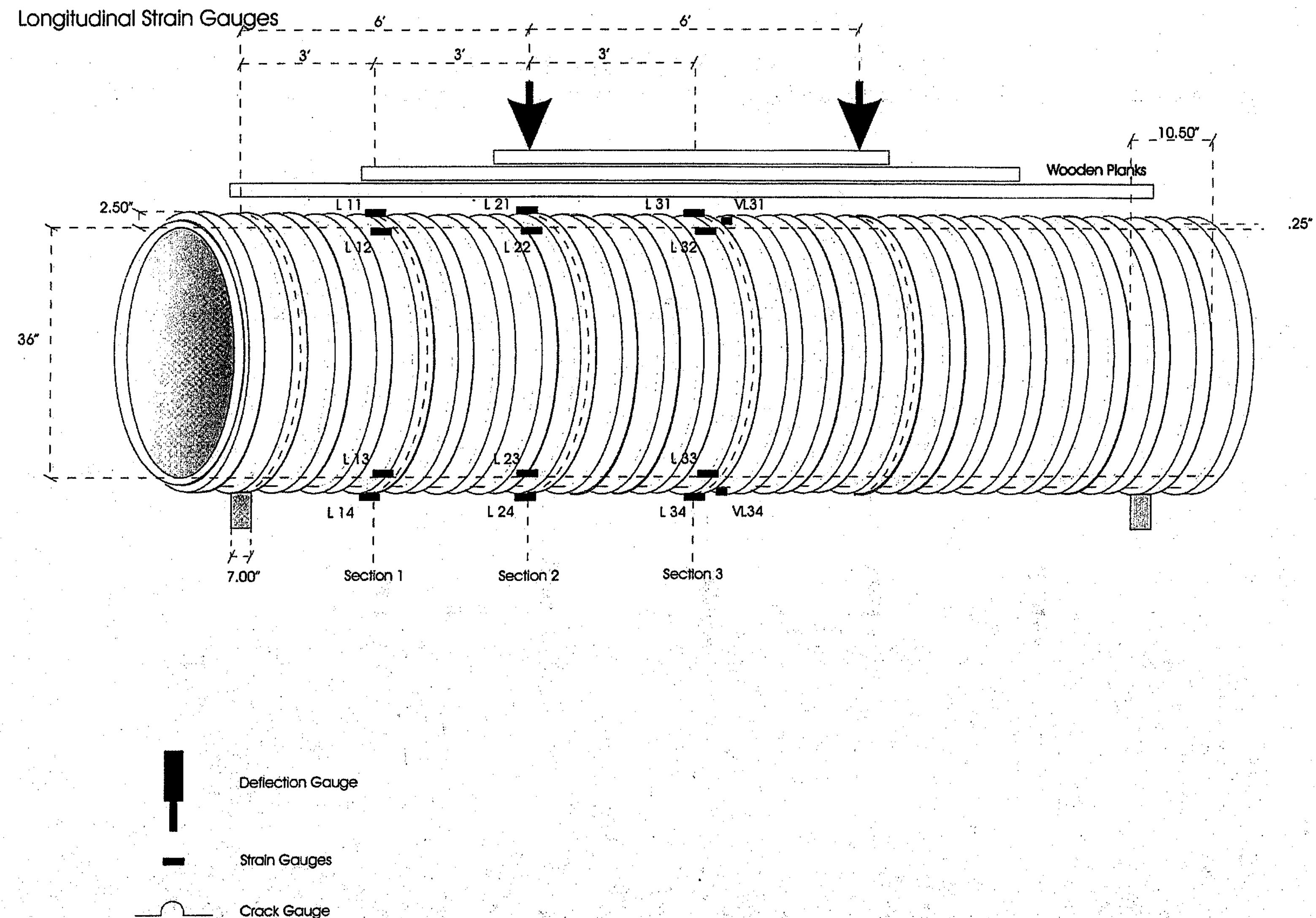

Fig 3.3b - Location of Longitudinal Strain Gages on Top and Bottom of ADS 36, Hancor 36 and PVC 36 Pipe Specimens

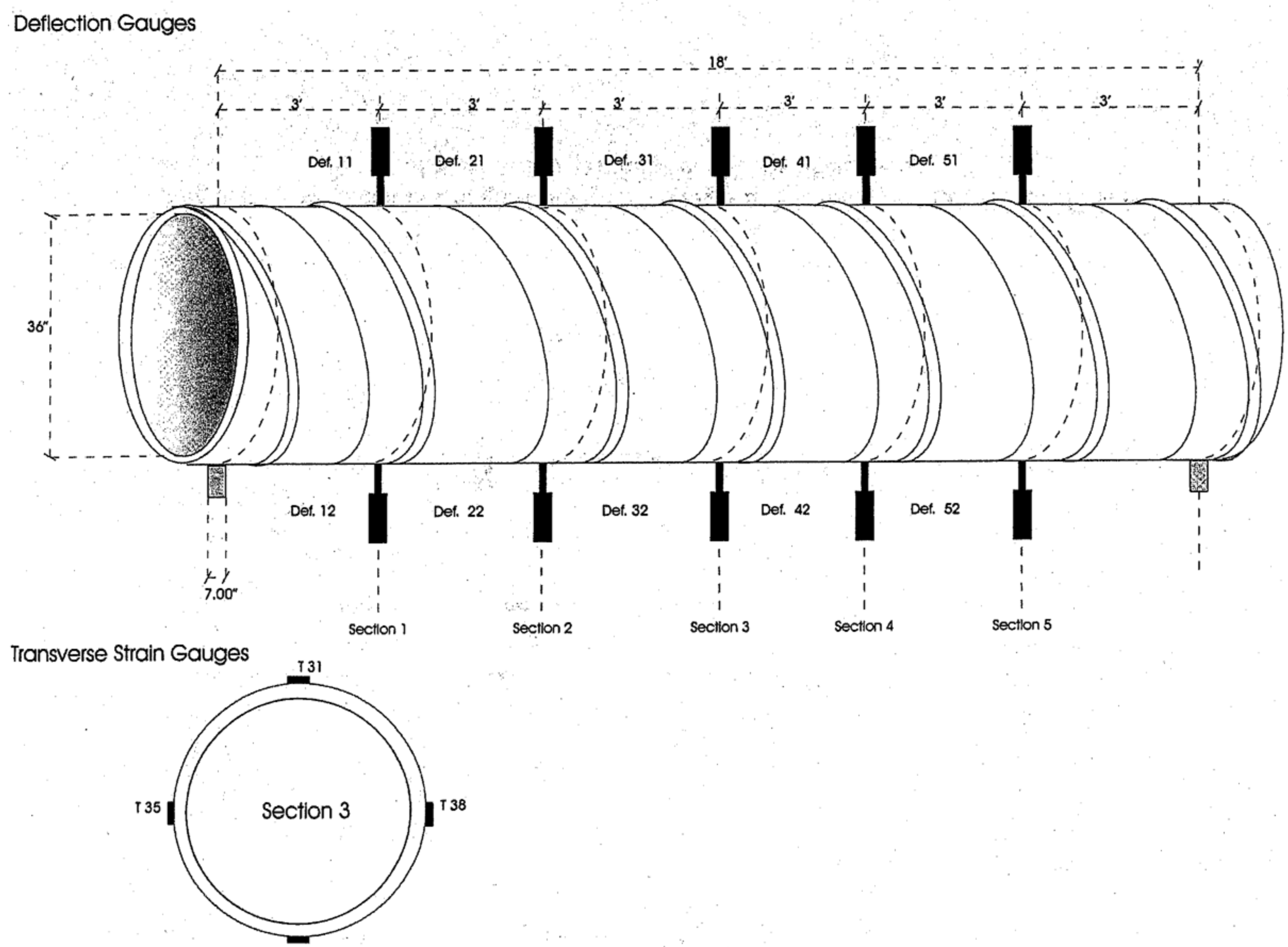

Fig 3.4a - Location of Deflection and Transverse Strain Gages at Section 3 Around Circumference of Steel 36 and Aluminum 36 Pipe Specimens

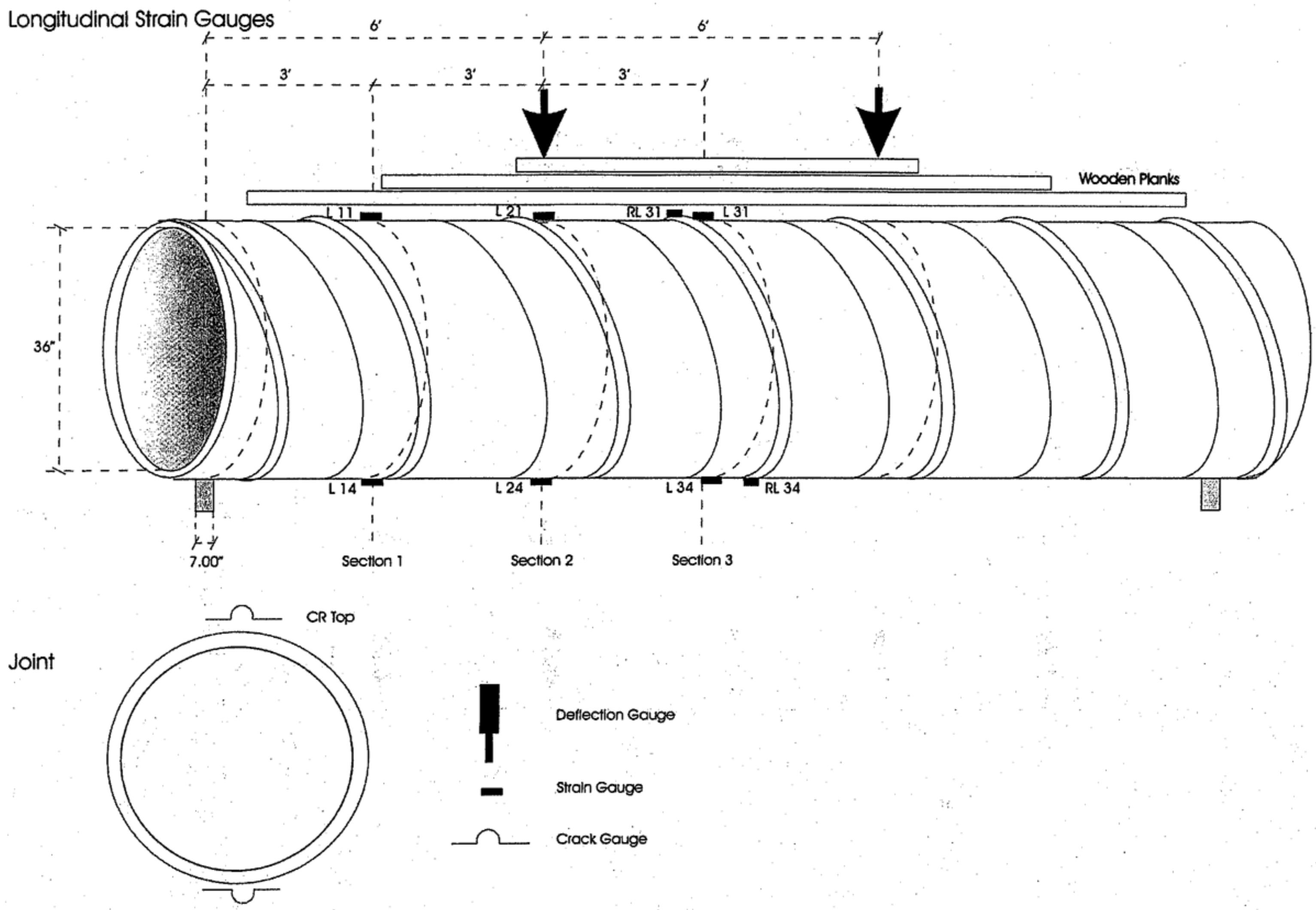

Fig 3.4b - Location of Longitudinal Strain Gages at Section 3 Around Circumference of Steel 36 and Aluminum 36 Pipe Specimens

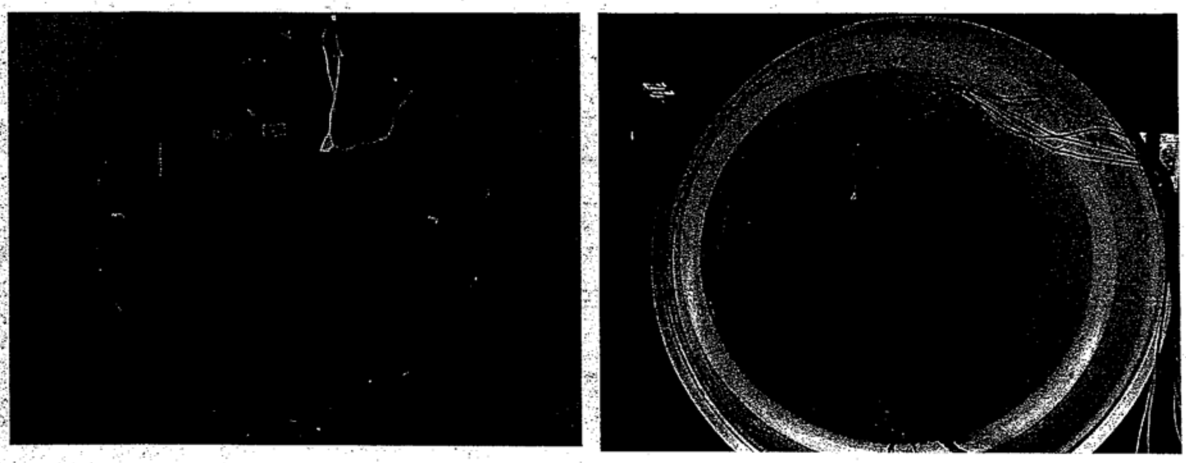

(a) Transverse Strain Gages Inside Specimen (b) Longitudinal Strain Gages Inside Specimen

Fig. 3.5 - Typical Transverse and Longitudinal Strain Gages Inside Specimen

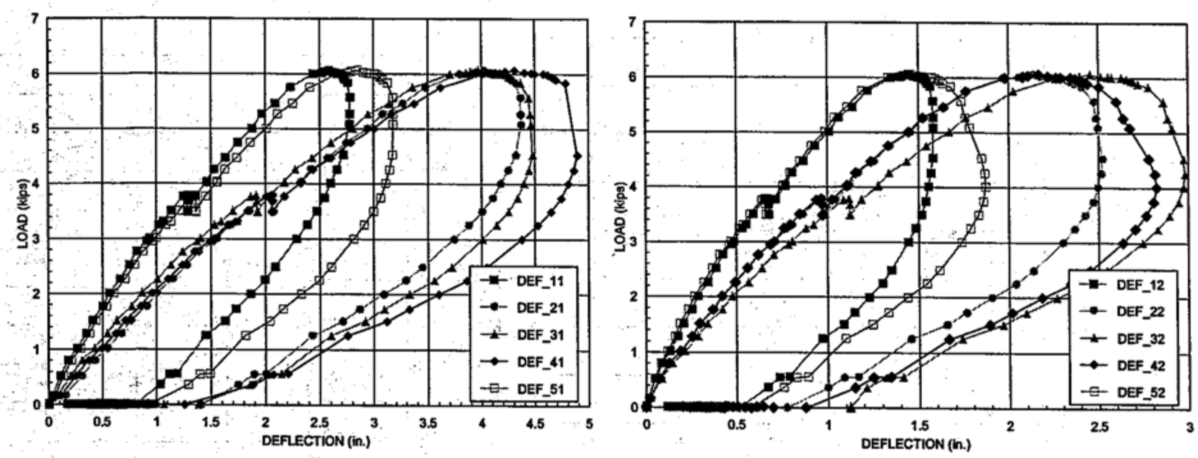

(a) Top (b) Bottom

Fig. 3.6 - Load vs Deflection Measured Along Top and Bottom of ADS 48 Specimen

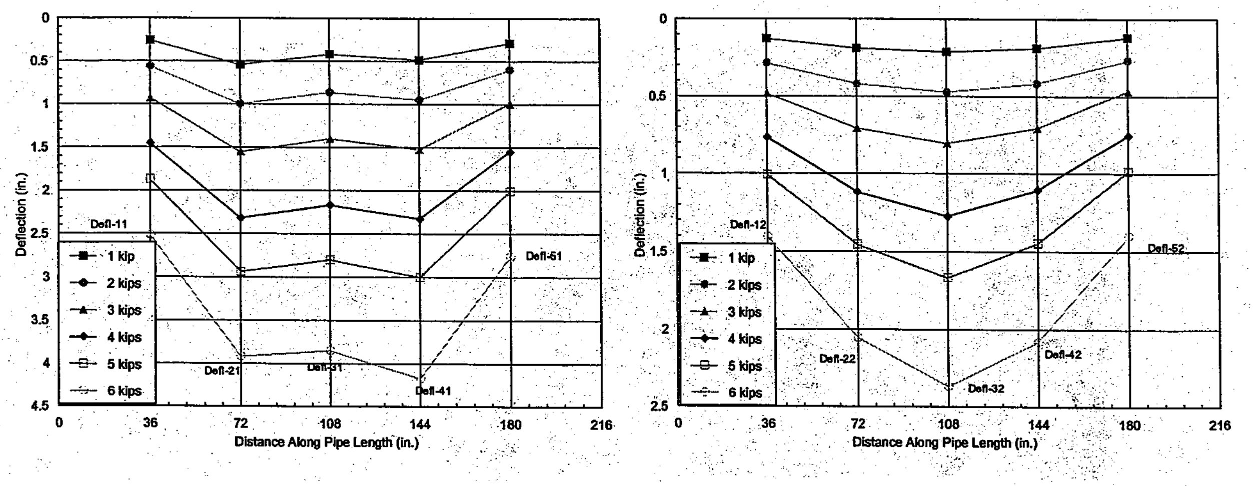

(a) Top (b) Bottom

Fig. 3.7 - Measured Top and Bottom Deflections at Sections Along ADS 48 Specimen

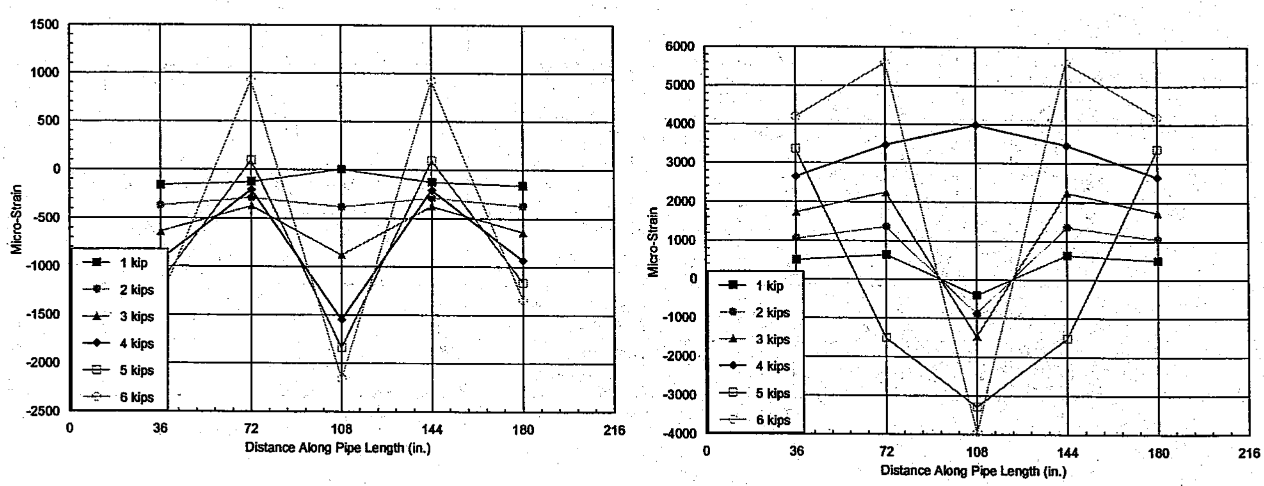

(a) Top Outer (b) Bottom Outer

Fig. 3.8 - Measured Top and Bottom Outer Surface Strains at Sections Along ADS 48

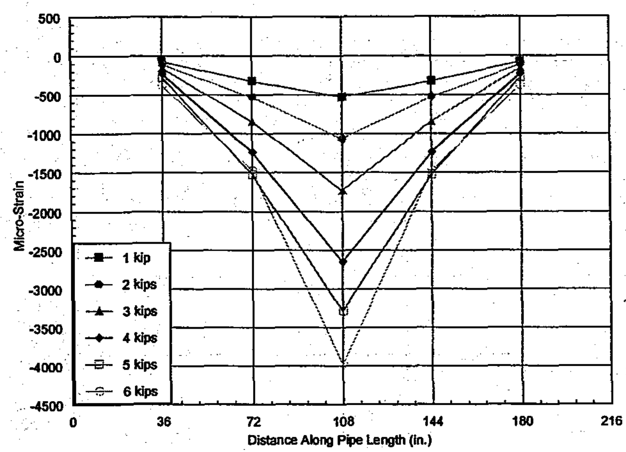

(a) Top Inner

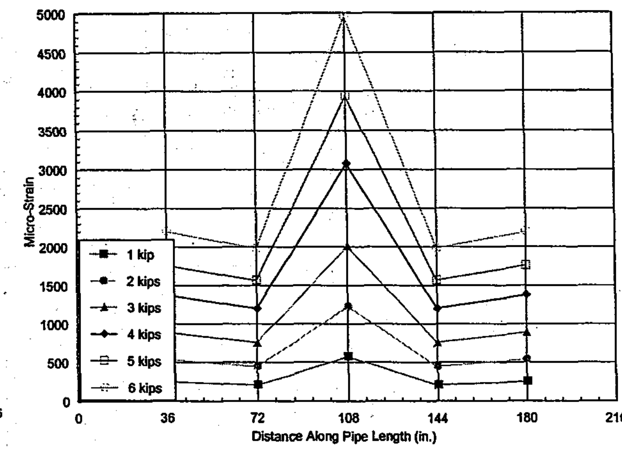

(b) Bottom Inner

Fig. 3.9 - Measured Top and Bottom Inner Surface Strains at Sections Along ADS 48

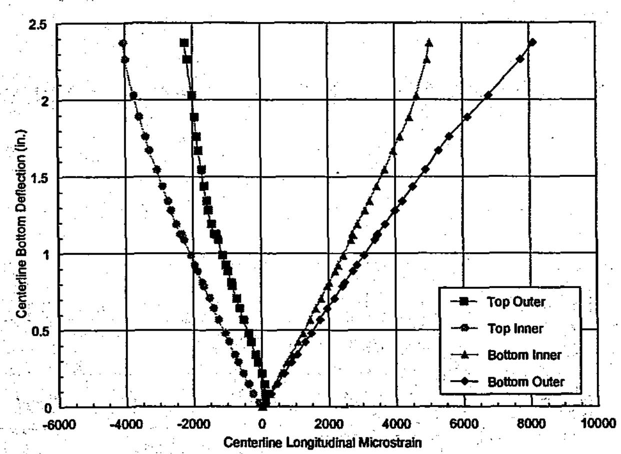

(a) Bottom Deflection

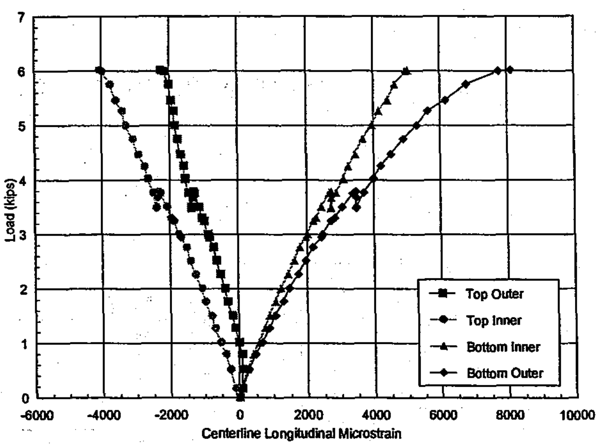

(b) Load

Fig. 3.10 Bottom Deflection and Load versus Longitudinal Strains at Centerline for ADS 48 Specimen

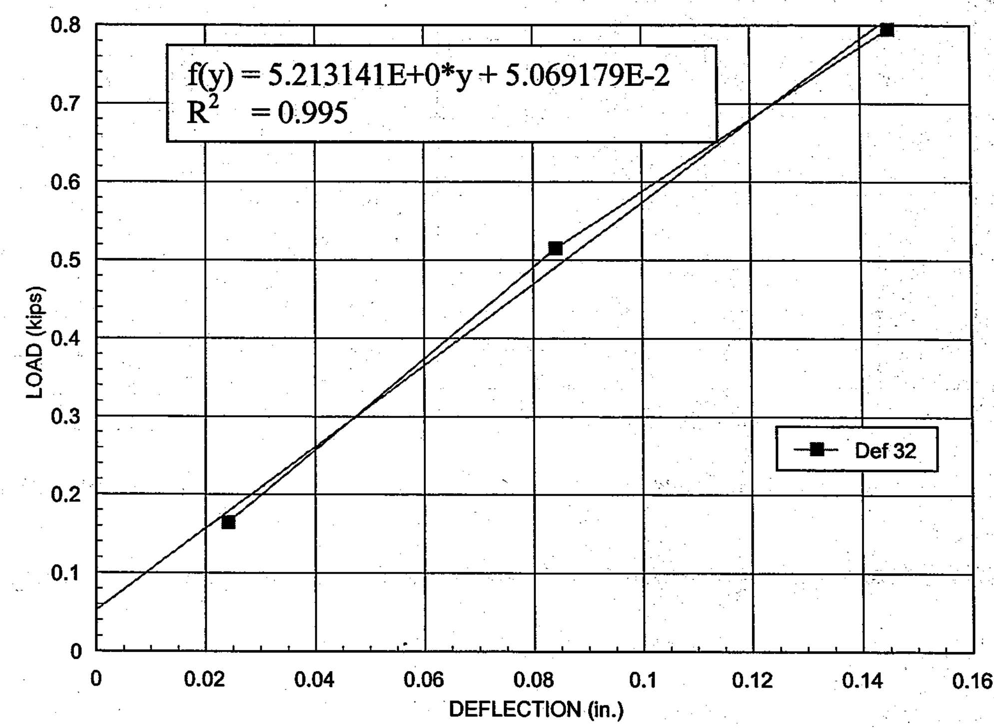

Fig. 3.11 - Slope of Load versus Bottom Deflection for ADS 48 Specimen at Centerline

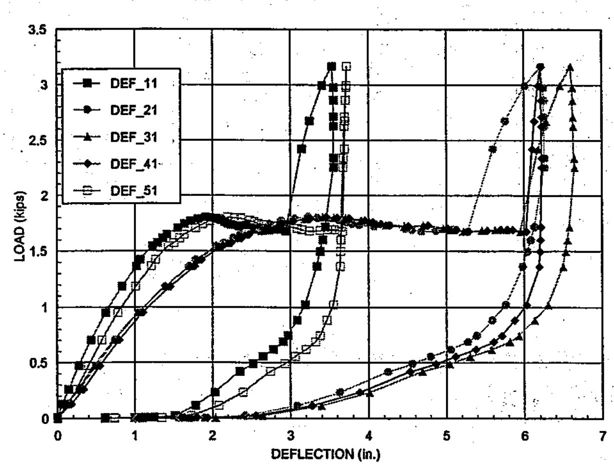

(a) Top

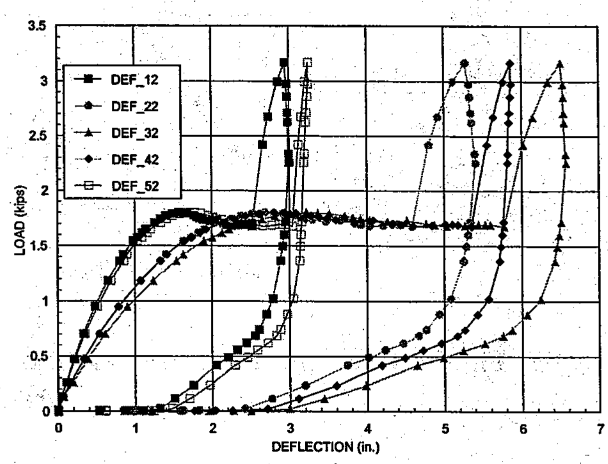

(b) Bottom

Fig. 3.12 - Load vs Deflection Measured Along Top and Bottom of ADS 36 Specimen

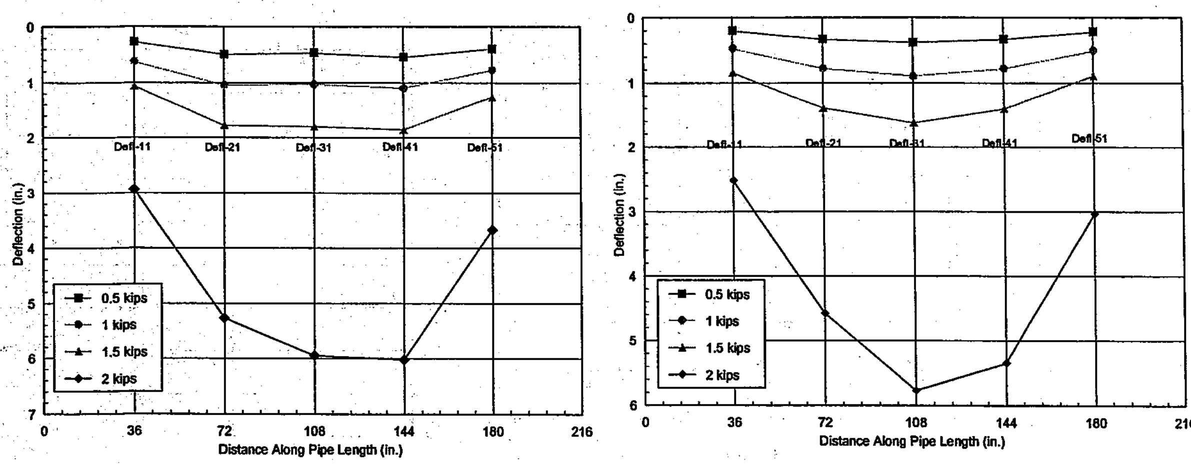

(a) Top

(b) Bottom

Fig. 3.13 - Measured Top and Bottom Deflections at Sections Along ADS 36 Specimen

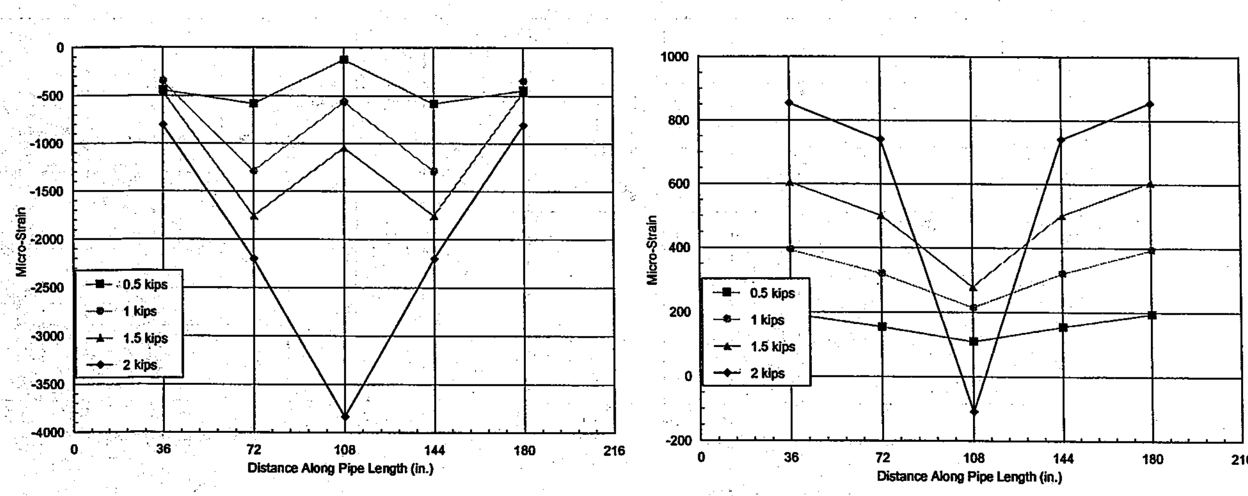

(a) Top Outer

(b) Bottom Outer

Fig. 3.14 - Measured Top and Bottom Outer Surface Strains at Sections Along ADS 36

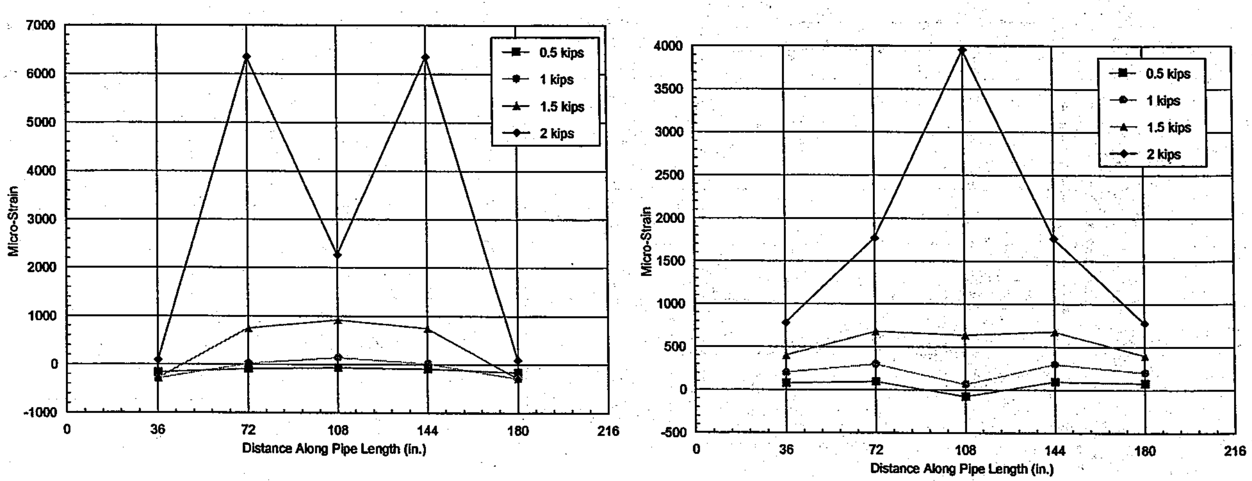

(a) Top Inner

(b) Bottom Inner

Fig. 3.15 - Measured Top and Bottom Inner Surface Strains at Sections Along ADS 36

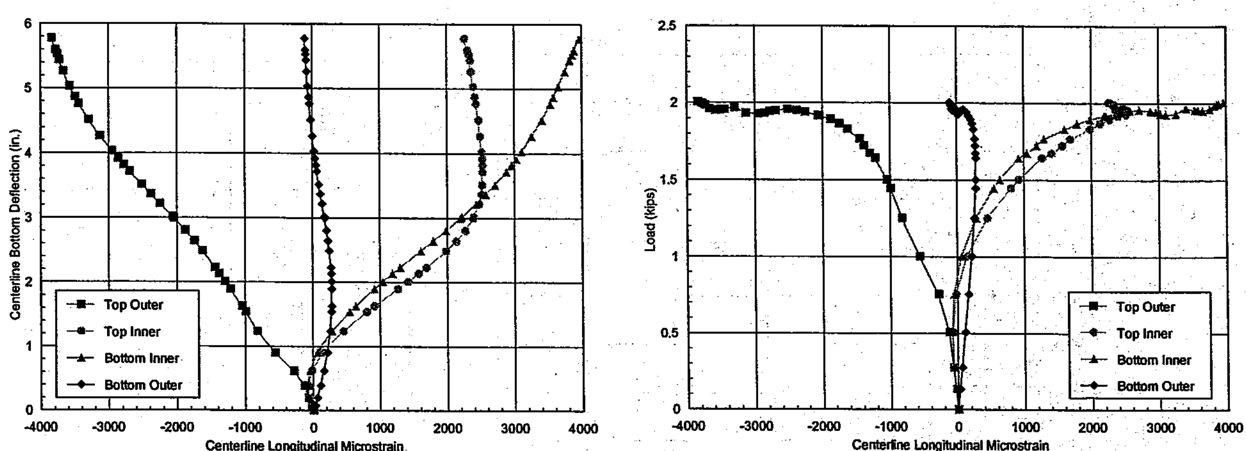

(a) Bottom Deflection

(b) Load

Fig. 3.16 - Bottom Deflection and Load versus Longitudinal Strains at Centerline for ADS 36 Specimen

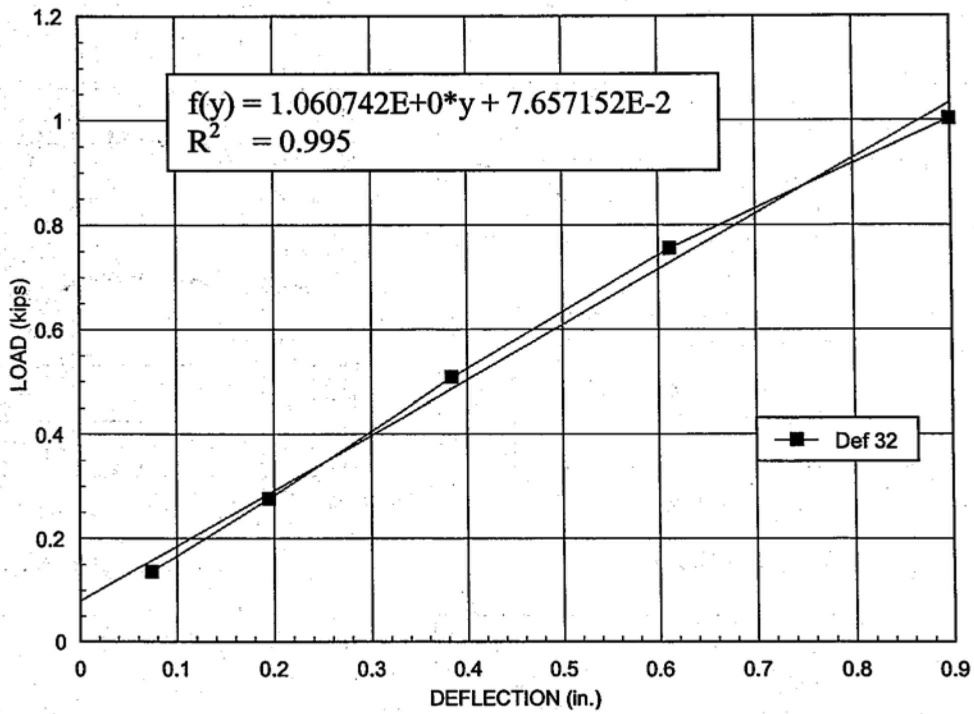

Fig. 3.17 - Slope of Load versus Bottom Deflection for ADS 36 Specimen at Centerline

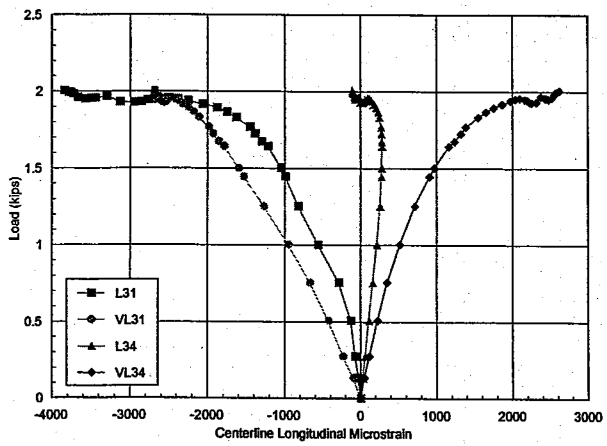

(a) Longitudinal

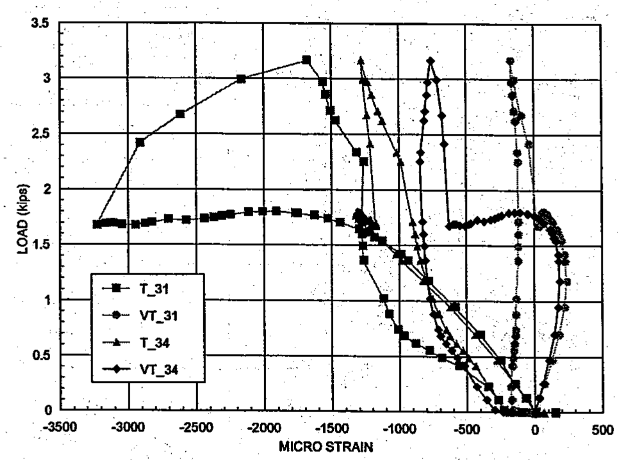

(b) Transverse

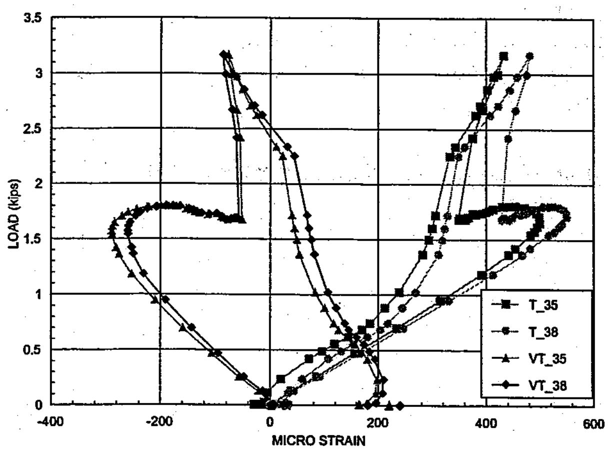

(c) Transverse

Fig. 3.18 - Load versus Valley Longitudinal and Transverse Strains for ADS 36

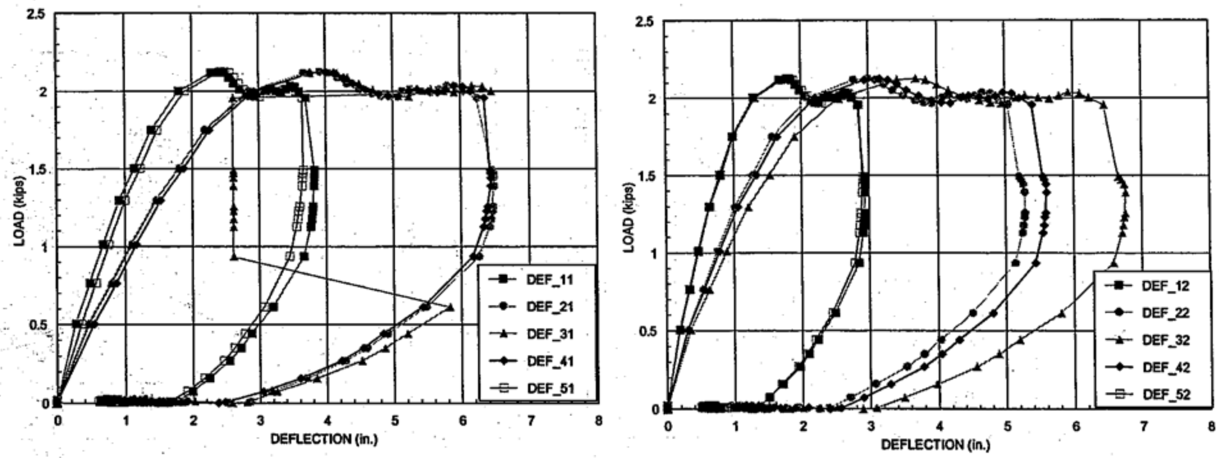

(a) Top (b) Bottom

Fig. 3.19 - Load vs Deflection Measured Along Top and Bottom of Hancor 36

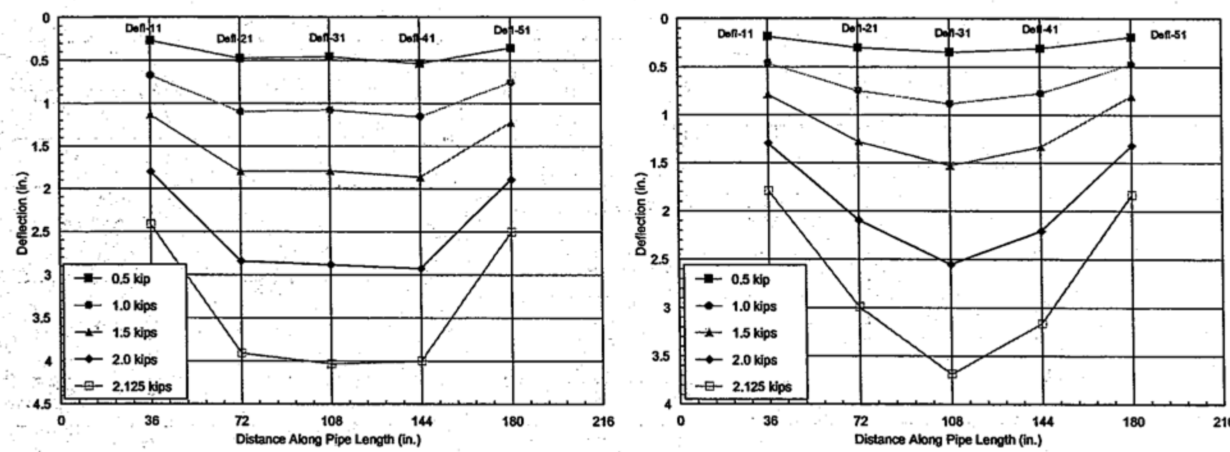

(a) Top (b) Bottom

Fig. 3.20 - Measured Top and Bottom Deflections at Sections Along Hancor 36

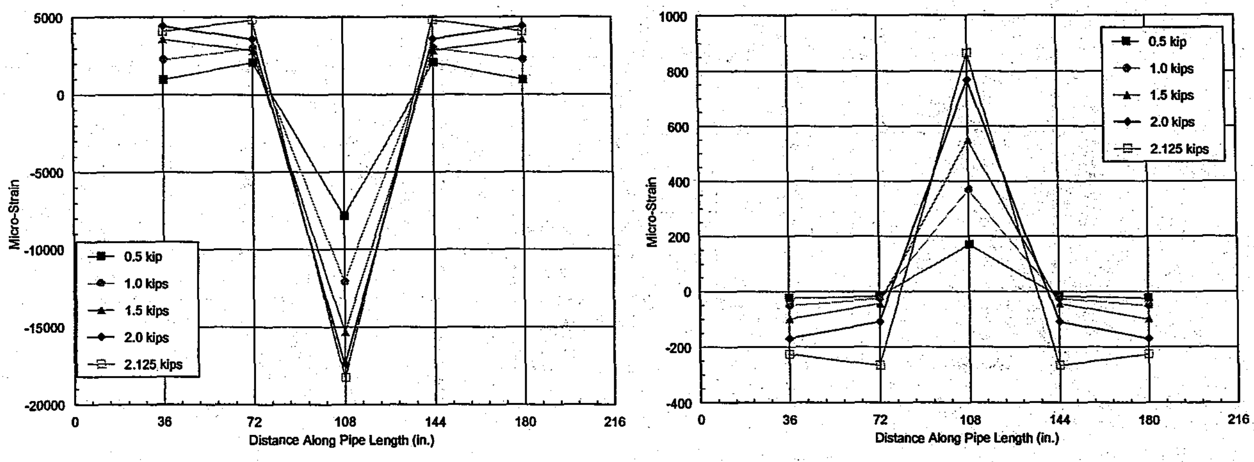

(a) Top Outer

(b) Bottom Outer

Fig. 3.21 - Measured Top and Bottom Outer Surface Strains at Sections Along Hancor 36

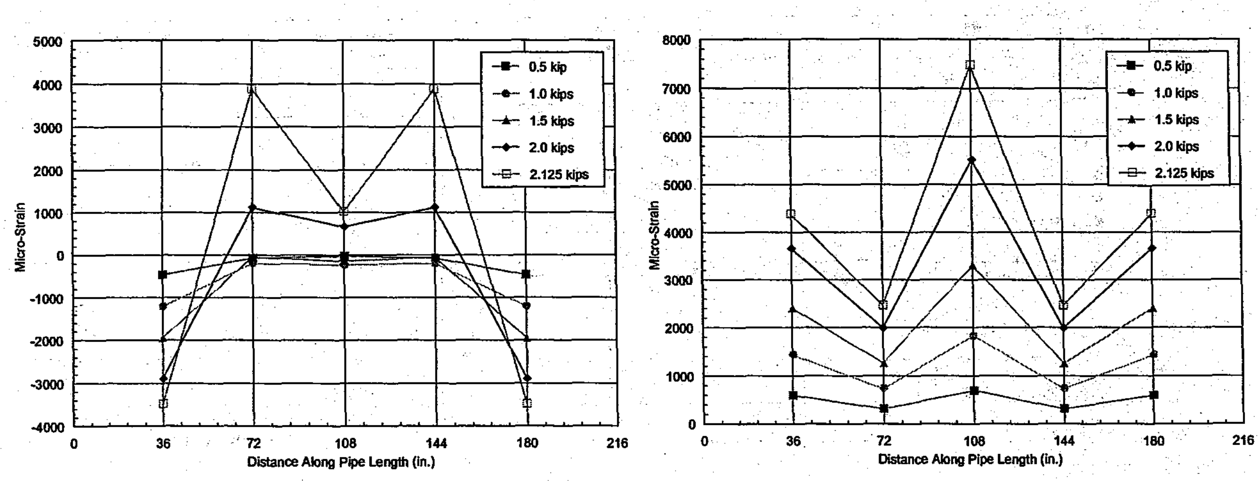

(a) Top Inner

(b) Bottom Inner

Fig. 3.22 - Measured Top and Bottom Inner Surface Strains at Sections Along Hancor 36 Specimen

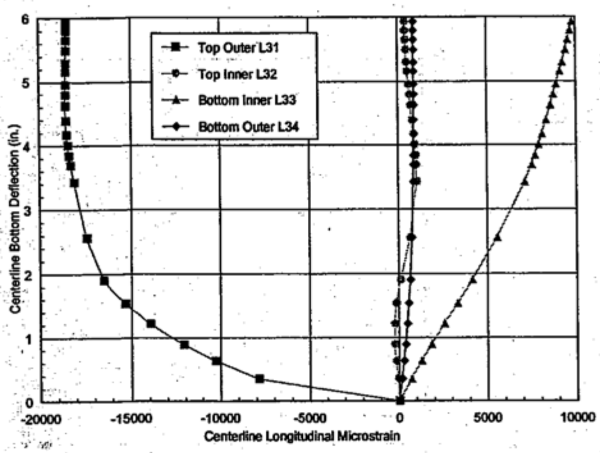

(a) Bottom Deflection

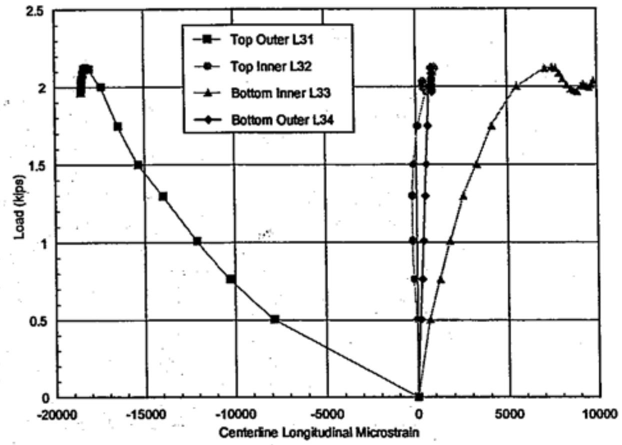

(b) Load

Fig. 3.23 Bottom Deflection and Load versus Longitudinal Strains at Centerline for Hancor 36 Specimen

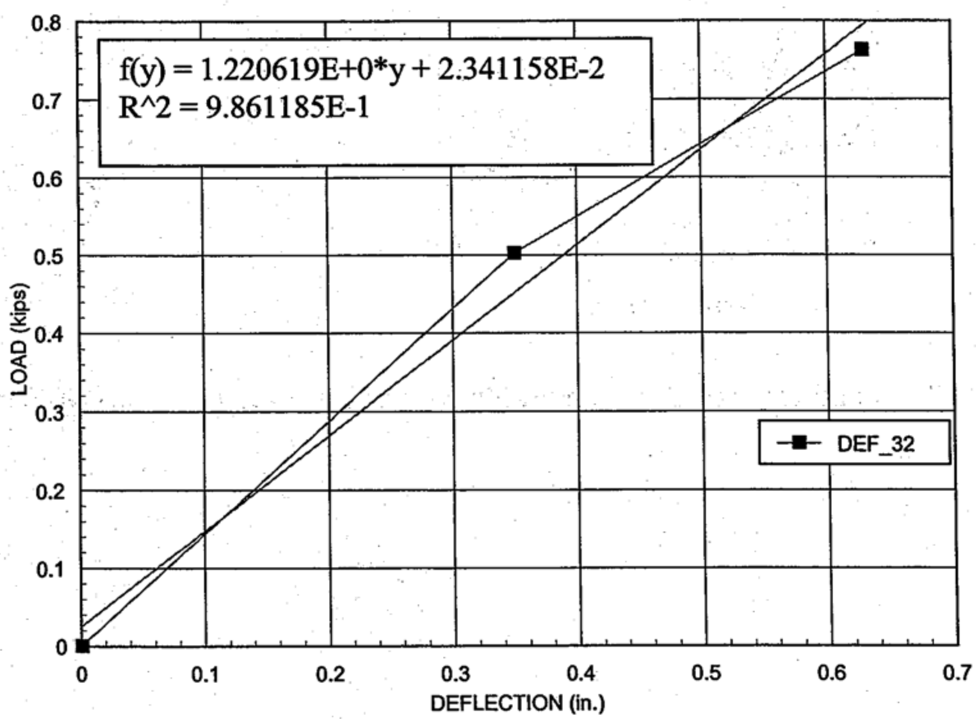

Fig. 3.24 - Slope of Load versus Bottom Deflection at Centerline for Hancor 36 Specimen

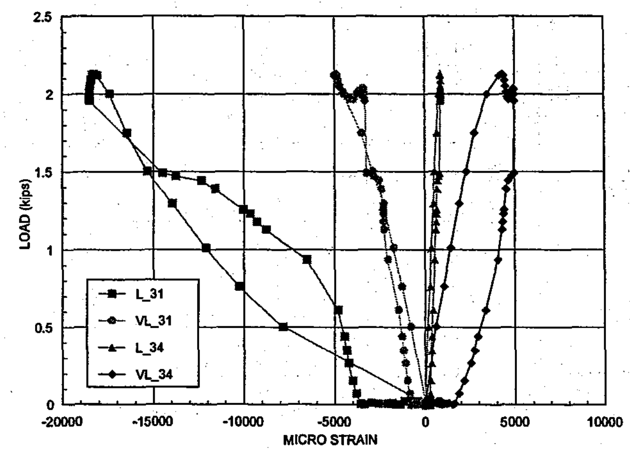

(a) Longitudinal

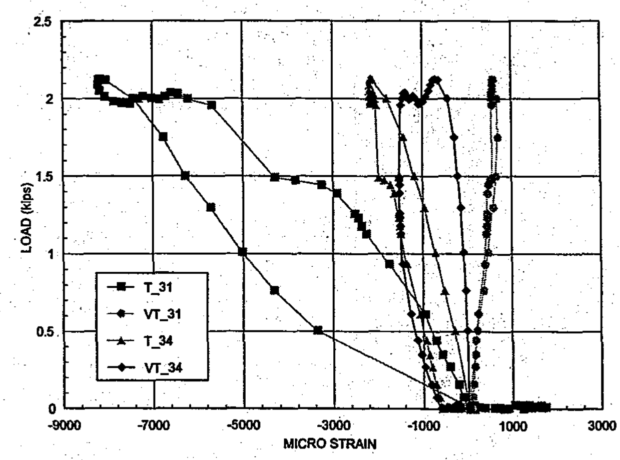

(b) Transverse

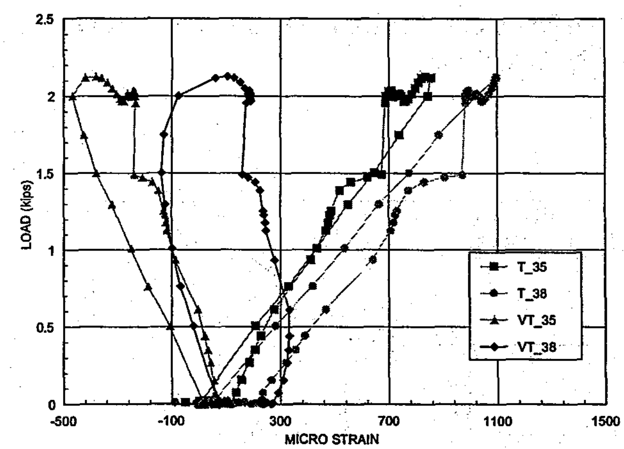

(c) Transverse

Fig. 3.25 - Load versus Valley Longitudinal and Transverse Strains for Hancor 36

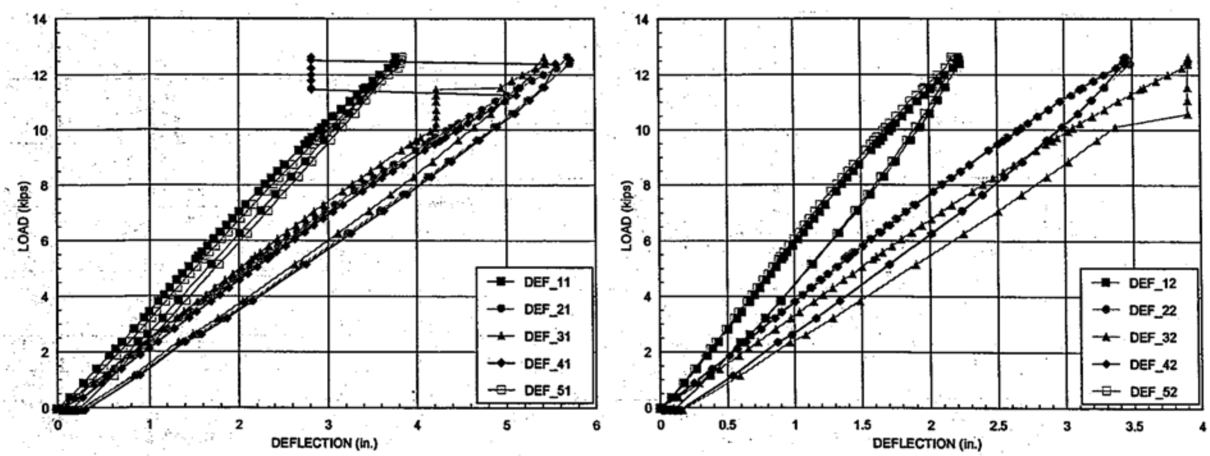

(a) Top (b) Bottom

Fig. 3.26 - Load vs Deflection Measured Along Top and Bottom of PVC 36

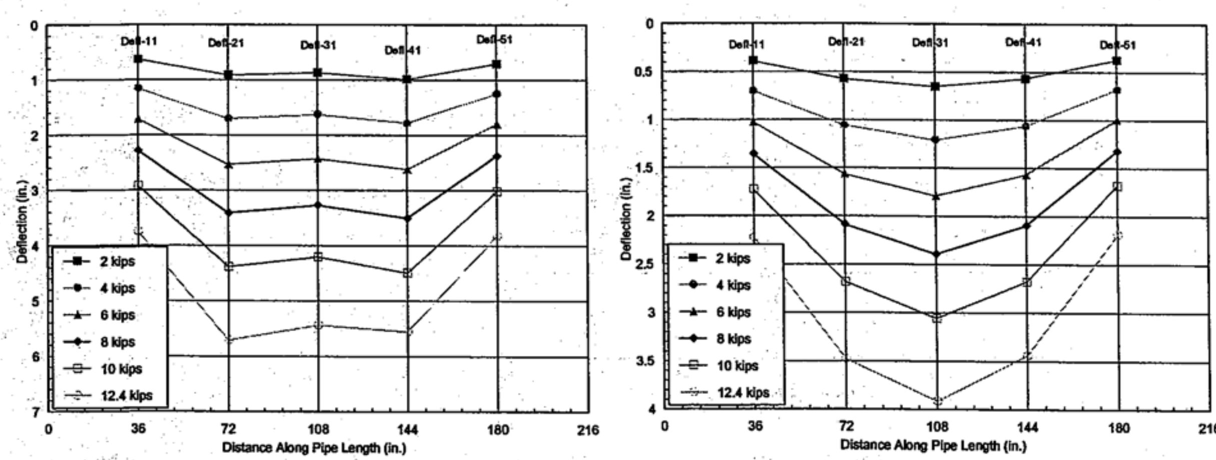

(a) Top (b) Bottom

Fig. 3.27 - Measured Top and Bottom Deflections at Sections Along PVC 36

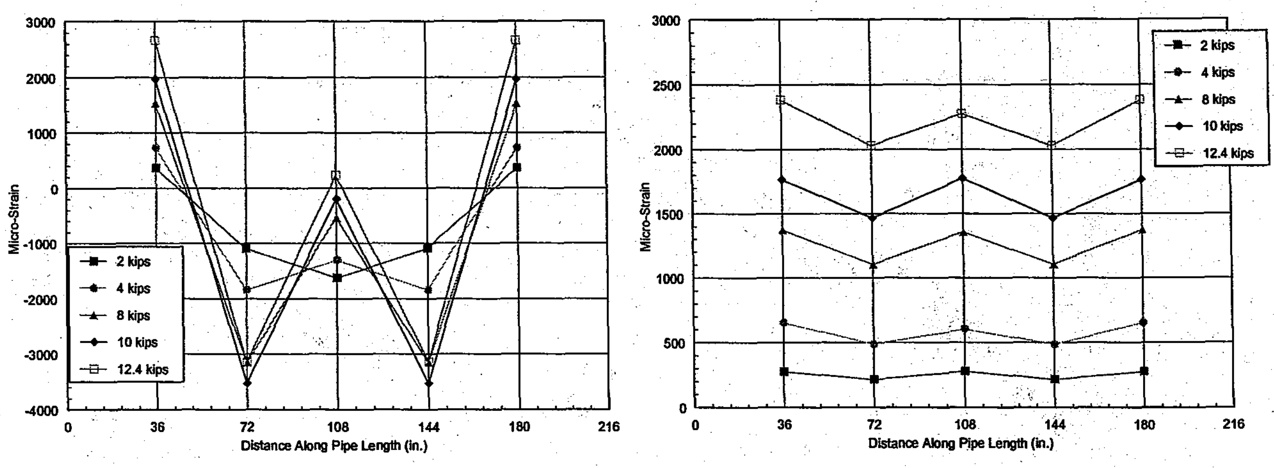

(a) Top Outer **(b) Bottom Outer**

Fig. 3.28 - Measured Top and Bottom Outer Surface Strains at Sections Along PVC 36 Specimen

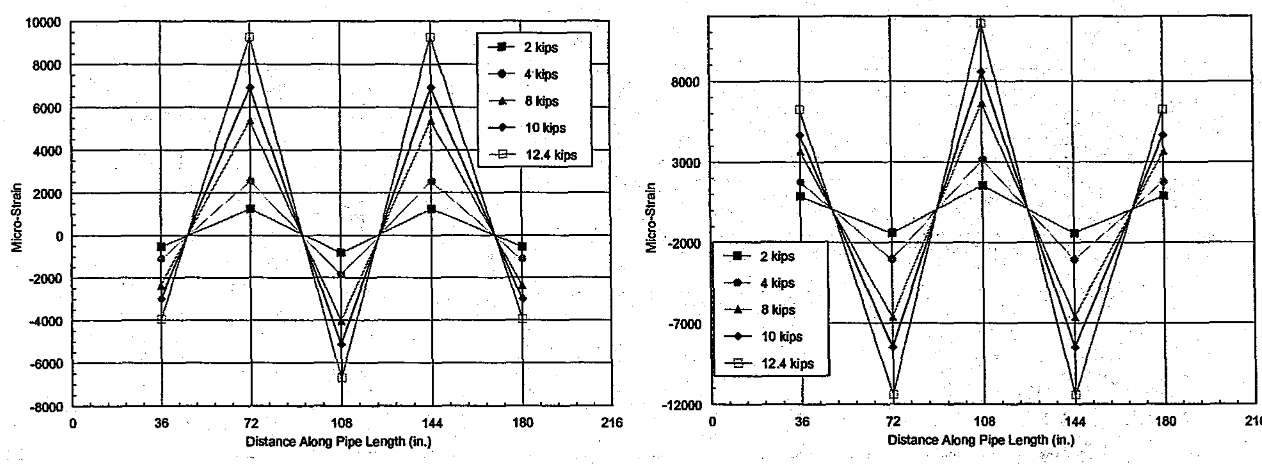

(a) Top Inner **(b) Bottom Inner**

Fig. 3.29 - Measured Top and Bottom Inner Surface Strains at Sections Along PVC 36 Specimen

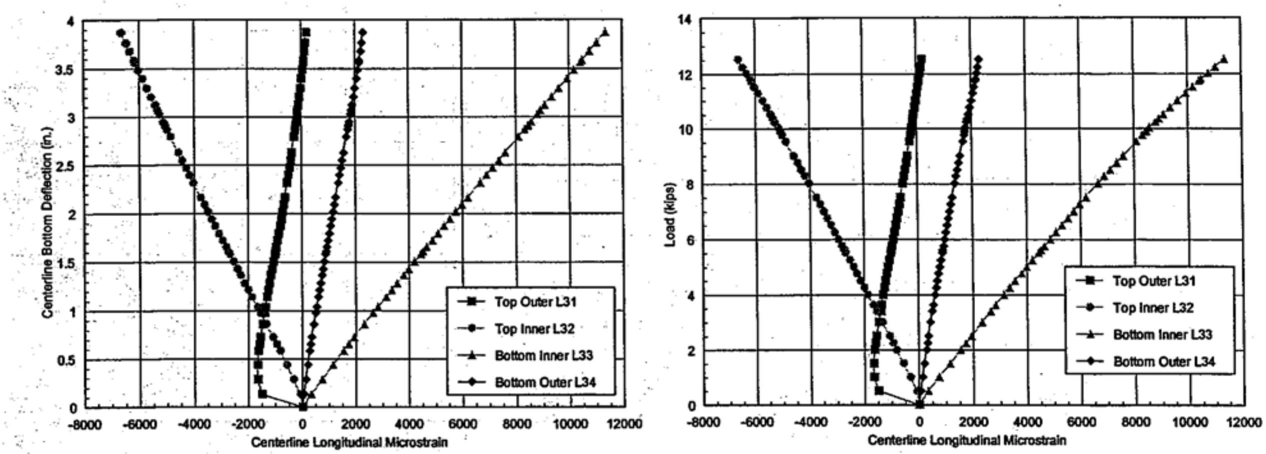

(a) Bottom Deflection

(b) Load

Fig. 3.30 Bottom Deflection and Load versus Longitudinal Strains at Centerline for PVC 36 Specimen

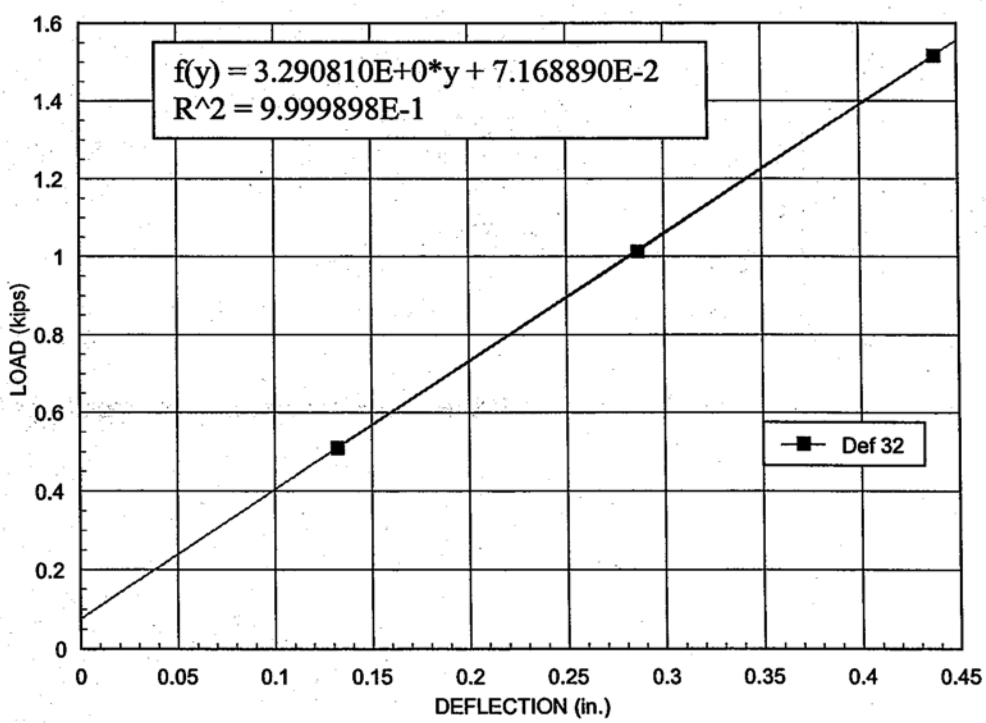

Fig. 3.31 - Slope of Load versus Bottom Deflection for PVC 36 Specimen at Centerline

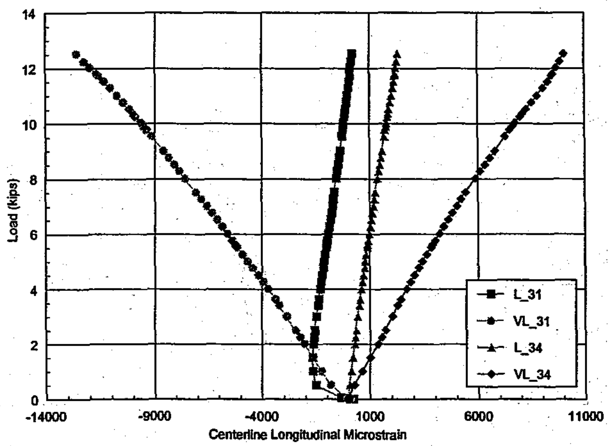

(a) Longitudinal

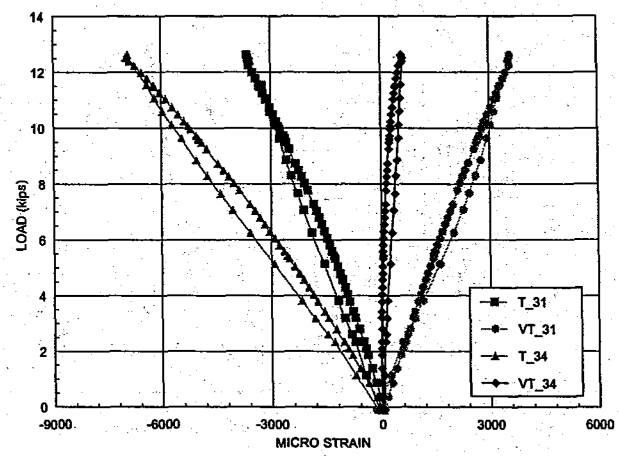

(b) Transverse

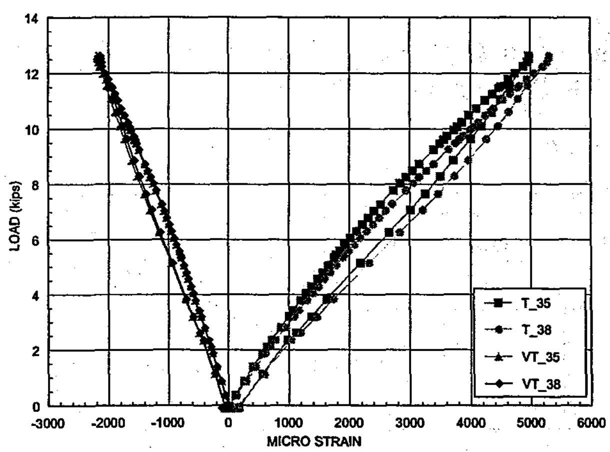

(c) Transverse

Fig. 3.32 - Load versus Valley Longitudinal and Transverse Strains for PVC 36

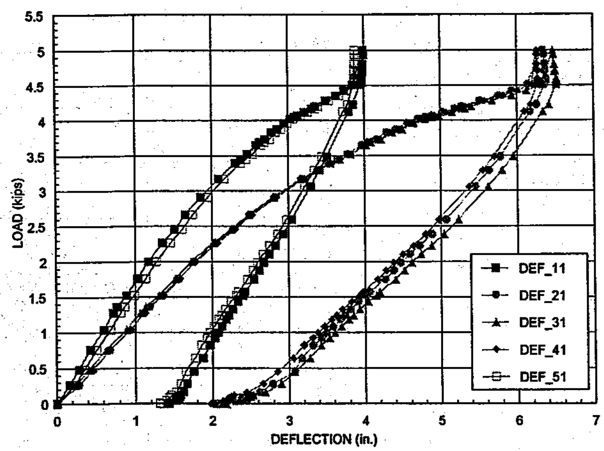

(a) Top

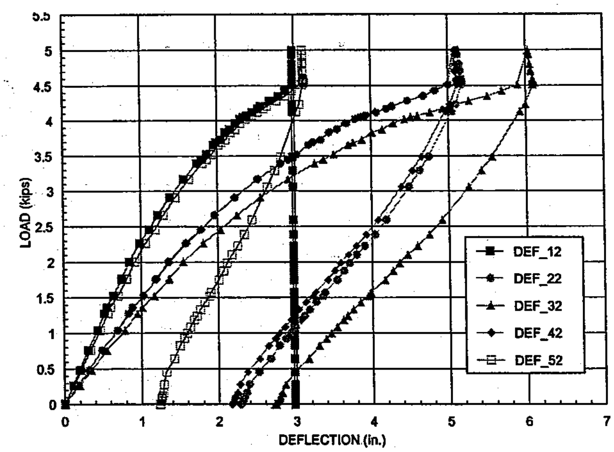

(b) Bottom

Fig. 3.33 - Load vs Deflection Measured Along Top and Bottom of Steel 36

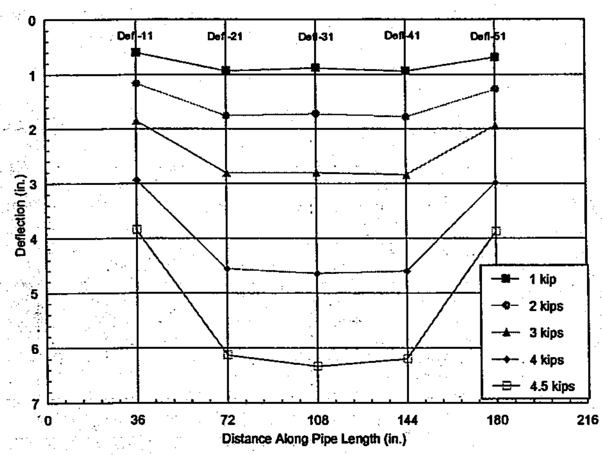

(a) Top

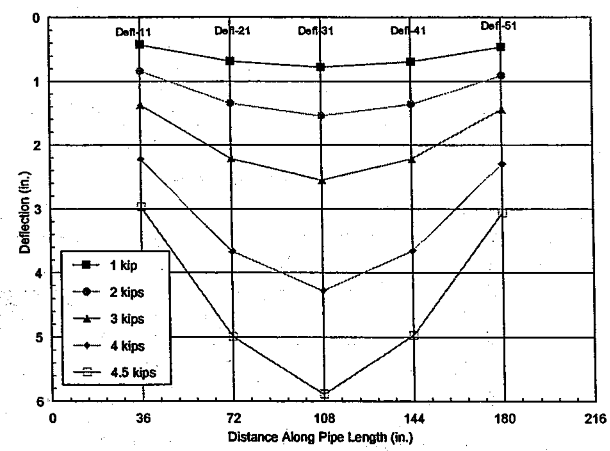

(b) Bottom

Fig. 3.34 - Measured Top and Bottom Deflections at Sections Along Steel 36

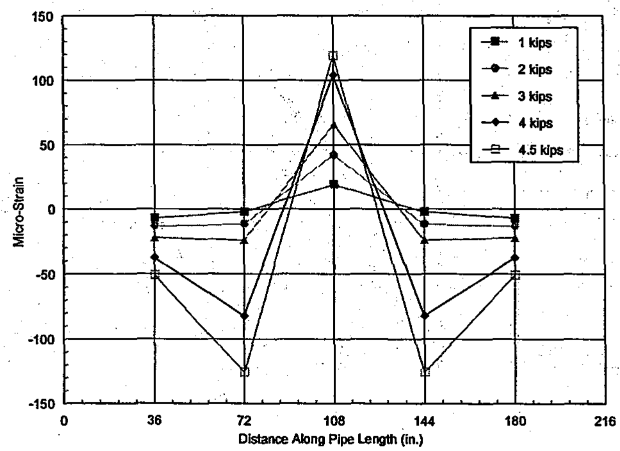

(a) Top Outer

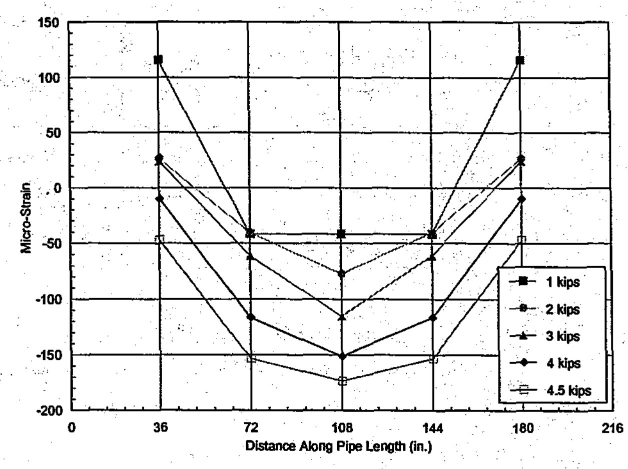

(b) Bottom Outer

Fig. 3.35 - Measured Top and Bottom Outer Surface Strains at Sections Along Steel 36 Specimen

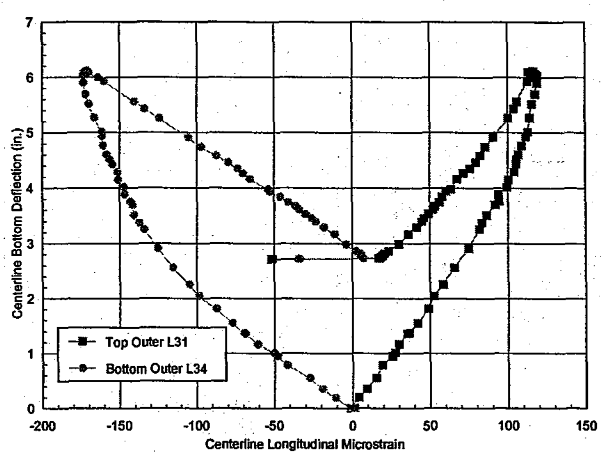

(a) Bottom Deflection

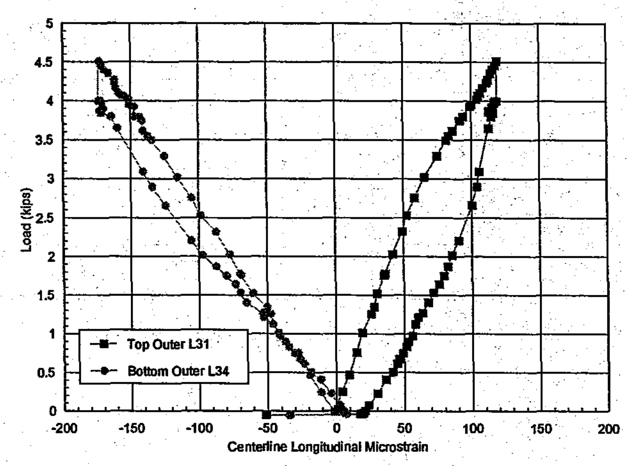

(b) Load

Fig. 3.36 - Bottom Deflection and Load versus Longitudinal Strains at Centerline for Steel 36 Specimen

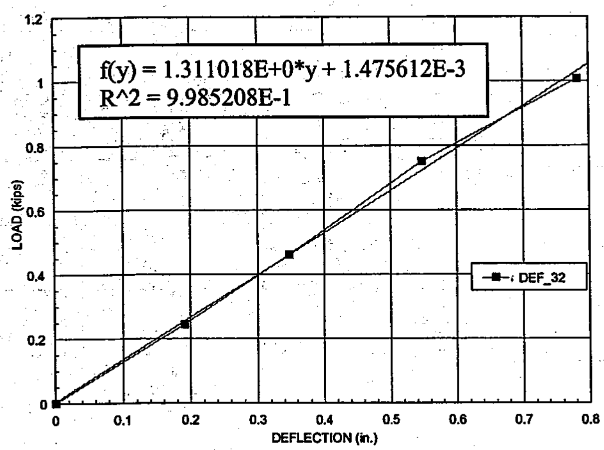

Fig. 3.37 - Slope of Load versus Bottom Deflection at Centerline for Steel 36

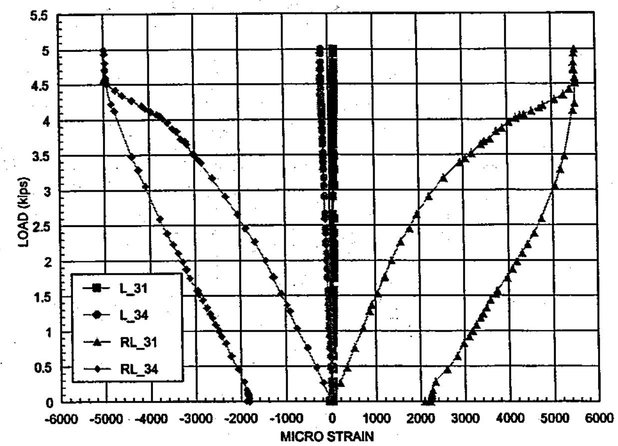

Fig. 3.38 - Load versus Valley Longitudinal Strains for Steel 36

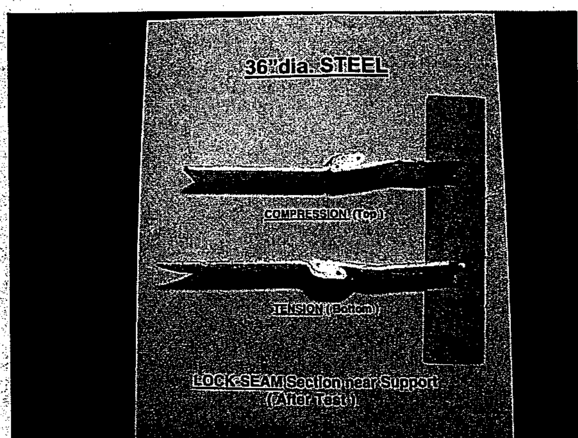

(a) Near Support

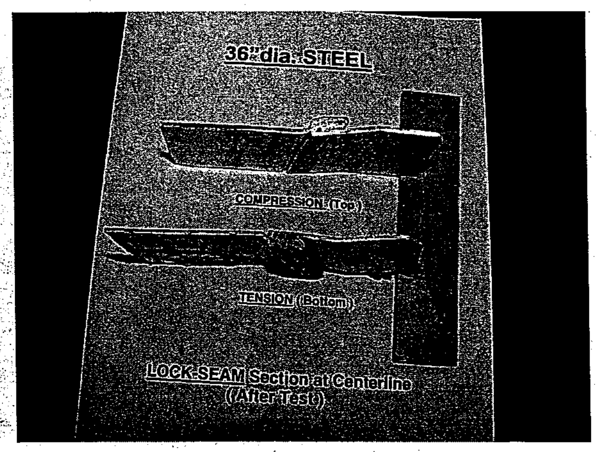

(b) At Centerline

Fig. 3.39 - Lock Seam Sections of Steel Specimen

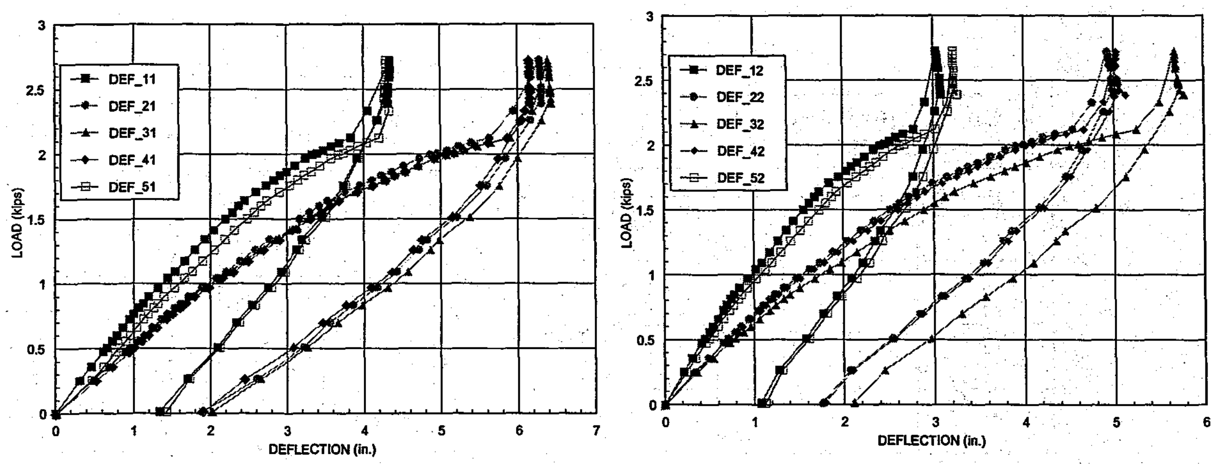

(a) Top **(b) Bottom**

Fig. 3.40 - Load vs Deflection Measured Along Top and Bottom of Aluminum 36

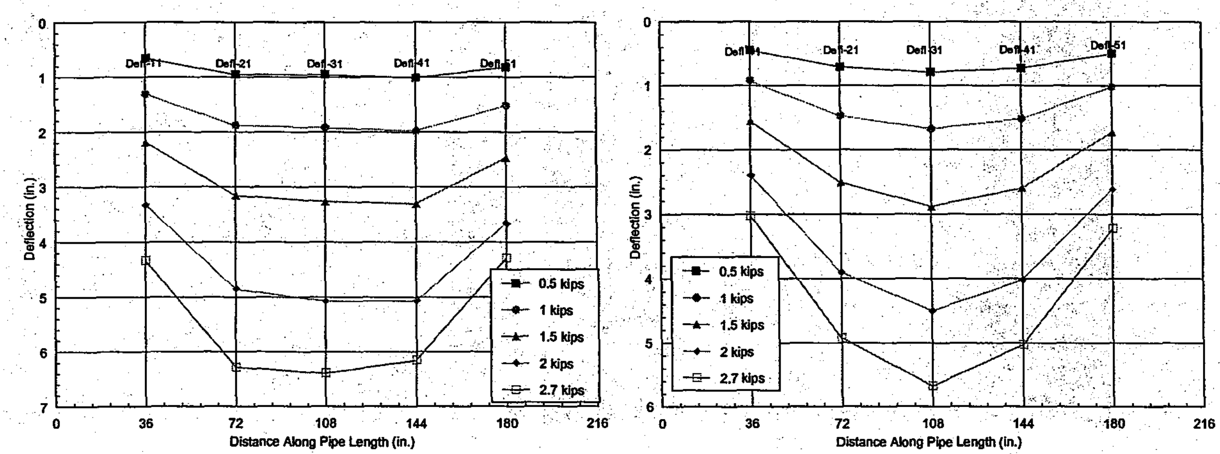

(a) Top **(b) Bottom**

Fig. 3.41 - Measured Top and Bottom Deflections at Sections Along Aluminum 36

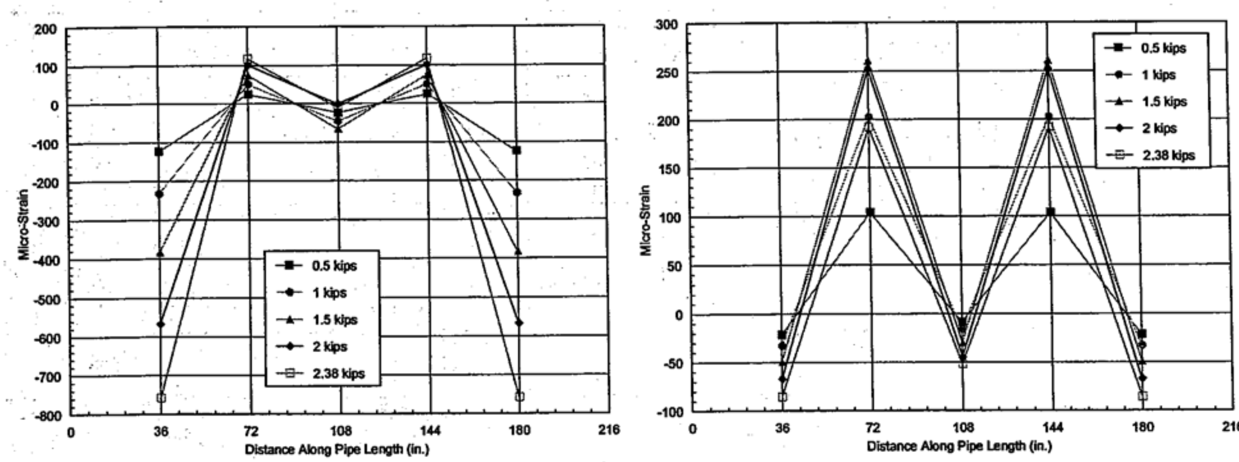

(a) Top Outer

(b) Bottom Outer

Fig. 3.42 - Measured Top and Bottom Outer Surface Strains at Sections Along Aluminum 36 Specimen

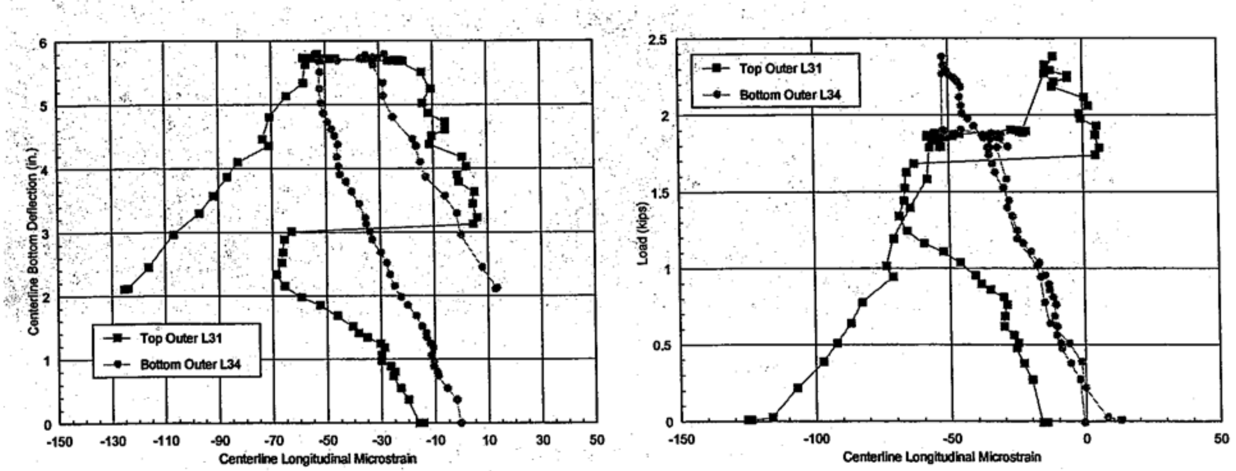

(a) Bottom Deflection

(b) Load

Fig. 3.43 Bottom Deflection and Load versus Longitudinal Strains at Centerline for Aluminum 36 Specimen

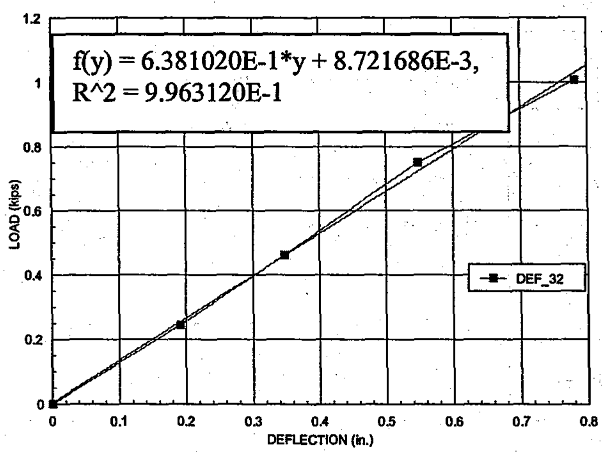

Fig. 3.44 - Slope of Load versus Bottom Deflection at Centerline for Aluminum 36

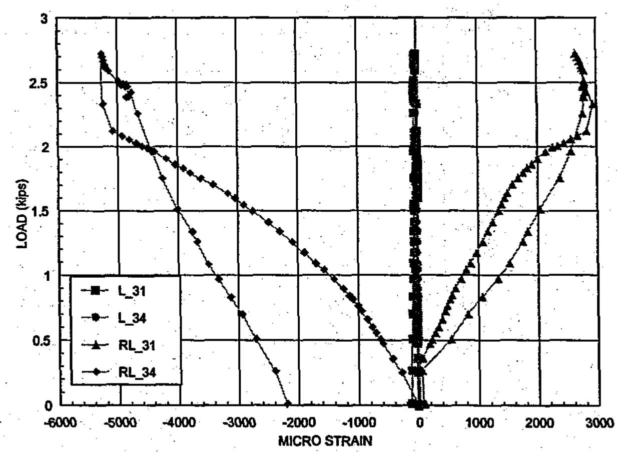

Fig. 3.45 - Load versus Valley Longitudinal Strains for Aluminum 36

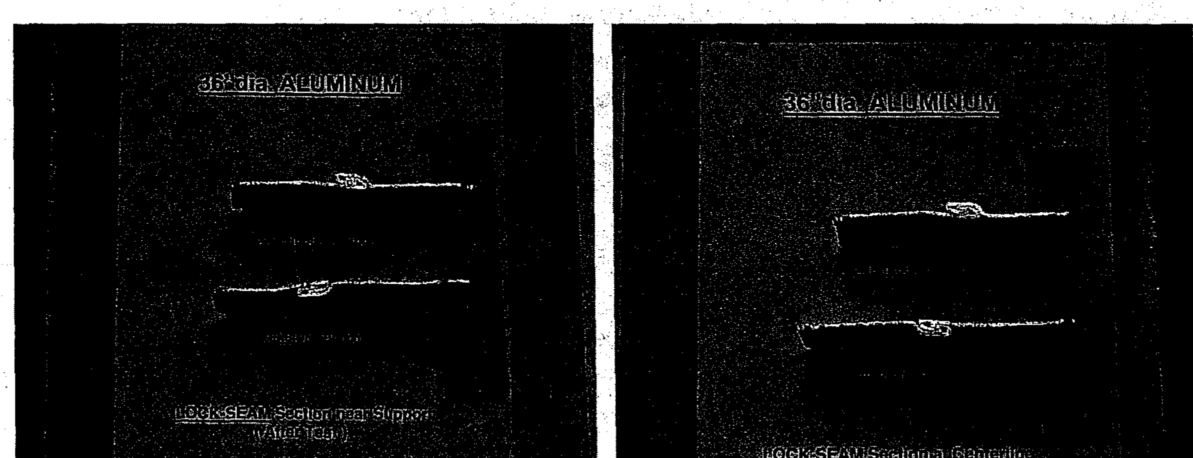

(a) Near Support **(b) At Centerline**

Fig. 3.46 - Lock Seam Sections of Aluminum Specimen

Chapter 4: Parallel Plate Loading Tests

4.1 Objectives

The objective of this test is to determine the load-deflection characteristics of flexible pipes under parallel-plate loading. The pipe stiffness (PS), the stiffness factor (SF), and the percentage pipe deflection (P) are determined from this test. The interrelations of dimensions and deflection properties for flexible pipes are: also evaluated in the study.

4.2 Experimental Program Apparatus

The hydraulic jack used in the testing has the capability of constant-rate-crosshead movement. The rate of head approach can be varied and was in the range of 0.05 to 150 in. per minute. The load could be applied to the flexible pipe through two parallel flat, smooth, and clean steel bearing plates. The steel plate at the top is welded to a NAT steel beam and the load applied to the center of the WF beam. The thickness of the plates is about 0.875 in, so as to minimize bending or deformation of the plate during testing. The plate length is slightly larger than the specimen length, and the plate width is approximately equal to the pipe contact width at maximum pipe deflection plus 6.0 in. The change in inside diameter was measured using LVDTs in three directions: parallel and perpendicular to the direction of loading, and 45° to the direction of loading. The LVDTs were used to measure to the nearest 0.01 in. Fig. 4.1 shows a typical experimental set-up for the test.

Test Specimens

The test specimens included two sizes: 36 in. and 48 in. diameter. The 36 in. diameter pipes were. of HDPE, PVC, aluminum and steel. One type of HDPE pipe had a 48-in. diameter. The 36-in. diameter pipe test specimens except PVC had a length equal to the pipe diameter, while the 48- in. diameter pipe specimen had a length of 40 inches. The PVC pipe specimens were of 13 inches length. The ends of the specimens were cut square and free of burrs and jagged edges. At least three specimens were tested for each pipe sample.

The average measured outside diameter (OD), inside diameter (ID) and lengths of the test specimens are presented in Table 4.1, along with the minimum pipe stiffness values specified by AASHTO M294 for HDPE and ASTM F679 for PVC pipes. Details of the, measured values of pipe diameters and geometries are given in Chapter 2.

Test Procedure

The pipe specimen is positioned with its longitudinal axis parallel to the: bearing plates; and: centered laterally in the test set-up. The LVDTs were installed in place (Fig. 4.1). The load was applied by means of a hydraulic jack on the center of a VVF beam.

The specimens were loaded at rates of 0.05 in. per minute, 0.5 in. per minute, 10 in. per minute and 150 in. per minute. The load-deflection measurements were recorded continuously and observations were made to identify liner cracking, crazing, wall cracking, wall delamination, rupture and wall buckling.

The test continued until the load on the specimen failed to increase with increasing deflection or the specimen exhibited a deformation of 30% of the average inside diameter. The tests were performed according to the ASTM D2412 Standard.

Test Program

Details of the parallel plate test program for pipe stiffness carried out in this study are presented in Table 4.2.

4.3 Description of Significant Pipe Events

Liner cracking or crazing --- the occurrence of a break or network of fine breaks in the liner visible to the unaided eye.

Wall cracking--- the occurrence of a break in the pipe wail visible to the unaided eye.

Wall delamination--- the occurrence of any separation in the components of the pipe wall visible to the unaided eye.

Rupture--- a crack or break extending entirely or partly though the pipe wall.

Wall buckling---any reverse curvature or deformation in the pipe wall that reduces the load carrying capability of the pipe.

4.4 Calculations

The pipe stiffness, PS, for any given deflection is given by:

$$\mathrm{PS} = \frac{F}{\Delta y} \tag{4.1}$$

The stiffness factor, SF, for any given deflection as follows:

$$\mathrm{SF} = 0.149r^3\,\mathrm{PS} \tag{4.2}$$

Where:

Δy = measured change in.the inside diameter in the direction of load application (in.),

F = the load applied to the pipe to produce a given percentage deflection, and

r = the mid-wall radius determined by subtracting the average wall thickness from the average outside diameter and dividing the difference by two (in.).

4.5 Results and Discussion

Overall Results

Table 4.3 summarizes the experimental results for a vertical deflection of 5% o and 10% of the diameter. Table 4.3a gives the vertical and horizontal deflections, whereas Table 4.3b provides the average PS values obtained from the tests. In the case of HDPE, PVC, and .metal flexible pipes, there was no evidence of wall buckling, rupture, cracking or delamination until the specimens exhibited a vertical deflection of 15% of the diameter.

Pipe-stiffness

The LVDTs recorded the change in the inside diameter of the test specimens, whereas the MTS measured the deformation of the pipe wall plus the change in the inside diameter. Only the PS values based on LVDT measurements are presented in the report. The PS values based on the MTS measurement are slightly smaller than those based on LVDT measured deformations. The PS values for all pipes are calculated for both 5% and 10% of the inside vertical diameter for different loading rates and are presented in Tables 4.4 to 4.9 for ADS 48, ADS 36, Hancor 36, PVC 36, Steel 36, and Aluminum 36, respectively. As expected, the higher the loading rate, the greater the PS value. It is observed that the PS values corresponding to 5% of the inside vertical diameter for the loading rate of 0.5 in. per minute are greater than the minimum value suggested by AASHTO and ASTM. Standards for both the HDPE and PVC pipes, see Table 4.1. The PS values for all the HDPE, PVC and metal pipes corresponding to the vertical deflection of 10% o of the inside diameter are smaller than those based on the vertical deformation of 5% of the inside diameter except one specimen for each PVC and aluminum pipe test series.

Load versus Deflections

The vertical deformation of the test specimens increased with increasing load. The HDPE and PVC pipes maintained a perfectly symmetric deformed shape, even at a relatively large vertical deformation of 20% of the inside diameter. However, the metal flexible pipes did not show any symmetry in the deformed shape, and thus, exhibited distinctly different behavior than that of HDPE and PVC pipes. The deformed shapes of the specimens for various levels of vertical deflections are presented in Figs. 4.3 to 4.8 for ADS 48, ADS 36, Hancor-36, PVC 36, Steel 36, and Aluminum 36, respectively. The curves representing the load versus the vertical and horizontal deflections are presented in Fig. 4.9 to 4.11 for ADS 4.8, APS 36, and Hancor 36, respectively, and in Fig. 4.12 for PVC 36, Steel 36, and Aluminum 36.

Vertical Deflection versus Horizontal Deflection Ratio

The vertical deflection-horizontal deflection ratios, Δ_v/Δ_x are summarized in Table 4.3a for 5% and 10% vertical deflections. As can be observed, the ratio Δ_v/Δ_x did not vary as the load rate increased. As the vertical deflection increased from 5% to 10%, the Δ_v/Δ_x ratio did not change for PVC pipes, it slightly increased for HDPE pipes, and it slightly decreased for metal pipes. For the load rate of 0.5in./min. and 5% deflection, the average Δ_v/Δ_x ranged from 1.25 to 1.46 for HDPE (highest average value achieved by Hancor 36), whereas it ranged from 1.49 to 1.64 for metal pipes and was equal to 1.49 for PVC.

4.6 Conclusions

The following conclusions are of interest:

(a) HDPE and PVC pipes tested according to ASTM and AASHTO Standards (vertical deflection (5%) and loading rate (0.5 in./min.) achieved a pipe stiffness, PS, higher than the minimum specified by the standards (Figs. 4.13 and 4.14). The PS values for all the HDPE, PVC and metal pipes corresponding to the vertical deflection of 10% inside diameter are smaller than those based on vertical deformation of 5% inside diameter (Figs. 4.15 and 4.16).

(b) Tests confirmed that for a given vertical deflection, the HDPE pipe stiffness (PS) substantially decreases with decrease in the loading rate and vice-versa.

(c) Up to a 15% vertical deflection, no sign of distress in the pipes was observed.

Table 4.1 - Geometry (Average values) and Minimum Specified PS of Specimens

Pipe Type	OD (in)	ID (in)	L (in.)	Minimum PS (psi)
ADS 48	52.320	47.016	40	18.14
ADS 36	36.00	41.5703	36	21.77
HANCOR 36	41.477	35.852	36	21.77
PVC 36	38.7734	35.5078	13	46.00
STEEL 36	36.313	35.836	36	--
ALUMINUM 36	37.28	35.852	36	--

Table 4.2 - Parallel Plate Test Program

Type of pipe	Load Rate (in/min.)	Number of Tests
ADS 48	0.05	1
	0.5	2
	10	1
	150	1
ADS 36	0.05	1
	0.5	2
	10	1
	150	1
Hancor 36	0.05	1
	0.5	2
	10	1
	150	1
PVC 36	0.05	1
	0.5	2
	10	1
	150	1
Steel 36	0.5	3
Alumimun 36	0.5	3

Table 4.3a - Summary of Experimental Results

Series	Load Rate/Specimen# (in./min.)	5% Vertical Deflection					10% Vertical Deflection				
		Load (Kips)	Load (Lbs/in.)	Δ_v (in.)	Δ_x (in.)	Δ_v/Δ_x	Load (Kips)	Load (Lbs/in.)	Δ_v (in.)	Δ_x (in.)	Δ_v/Δ_x
ADS 48	0.05	1.99	49.75	2.40	1.97	1.22	2.995	74.88	4.80	3.62	1.33
	0.5-1	2.65	66.25	2.40	1.91	1.26	4.03	100.75	4.80	3.61	1.33
	0.5-2	2,52	63.00	2.40	1.93	1.24	3.82	95.50	4.80	3.63	1.32
	0.5 Average	2.58	64.63	2.40	1.92	1.25	3.93	98.13	4.80	3.62	1.33
	10	3.46	86.50	2.445	2.22	1.10	5.24	131.00	4.81	3.83	1.26
	150	4.45	111.25	2.41	1.96	1.23	7.01	175.25	4.82	3.60	1.34
ADS 36	0.05	1.74	48.33	1.80	1.45	1.24	2.71	75.28	3.60	2.74	1.31
	0.5-1	2.35	65.28	1.80	1.45	1.24	3.68	102.22	3.60	2.69	1.34
	0.5-2	2.46	68.33	1.80	1.38	1.30	3.74	103.89	3.61	2.58	1.40
	0.5 Average	2.40	66.80	1.80	1.42	1.27	3.71	103.05	3.61	2.64	1.37
	10	3.17	88.06	1.83	1.48	1.24	4.86	135.00	3.60	2.62	1.37
	150	3.75	104.17	1.81	1.37	1.32	5.96	165.55	3.62	2.58	1.40
HANCOR 36	0.05	1.36	37.77	1.80	1.23	1.46	1.92	53.33	3.60	2.38	1.51
	0.5-1	1.58	43.89	1.81	1.19	1.52	2.49	69.17	3.60	2.39	1.51
	0.5-2	1.73	48.06	1.80	1.27	1.42	2.68	74.44	3.61	2.53	1.43
	0.5 Average	1.66	45.98	1.80	1.23	1.46	1.58	71.80	3.60	2.46	1.47
	10	2.37	65.83	1.81	1.17	1.55	3.62	100.56	3.60	2.41	1.49
PVC 36	0.5-1	1.28	90.46	1.81	1.27	1.43	2.34	180.00	3.60	2.51	1.43
	0.5-2	1.28	98.46	1.80	1.15	1.57	2.22	170.77	3.61	2.40	1.50
	0.5 Average	1.28	94.46	1.80	1.21	1.49	2.28	175.38	3.60	2.45	1.46
	10	1.32	101.54	1.82	1.22	1.50	2.22	170.77	3.60	2.37	1.52
Steel 36	0.5-1	2.19	60.83	1.80	1.42	1.27	2.75	76.39	3.60	2.70	1.33
	0.5-2	2.07	57.50	1.80	0.98	1.84	2.98	82.78	3.61	2.40	1.50
	0.5-3	2.19	60.83	1.80	1.00	1.80	3.05	84.72	3.60	2.38	1.51
	Average	2.15	59.72	1.80	1.13	1.64	2.93	81.30	3.60	2.49	1.45
Aluminium 36	0.5-1	0.94	26.11	1.80	1.40	1.29	1.43	39.72	3.60	2.82	1.28
	0.5-2	0.94	26.11	1.81	0.96	1.88	1.43	39.72	3.60	2.54	1.42
	0.5-3	0.94	26.11	1.80	1.38	1.30	1.39	38.61	3.60	2.74	1.31
	Average	0.94	26.11	1.80	1.25	1.49	1.42	39.35	3.60	2.70	1.34

Table 4.3b - Experimental Pipe Stiffness PS (Average Values)

Series	Load Rate (in./min)	PS for 5% Vert. Defl. (psi)	PS for 10% Vert. Defl. (psi)
(a) ADS 48	0.05	20.75	15.60
	0.5	26.91	20.44
	10	35.34	27.24
	150	46.10	36.39
(b) ADS 36	0.05	26.85	20.89
	0.5	37.09	28.62
	10	49.28	39.93
	150	57.51	45.72
(c) Hancor 36	0.05	20.93	14.82
	0.5	25.53	19.89
	10	36.47	27.89
	150	—	—
(d) PVC 36	0.5	54.62	48.64
(e) Steel 36	0.5	33.12	22.55
(f) Aluminium 36	0.5	13.03	12.01

Table 4.4 - Measured PS and SF of HDPE ADS 48" pipes

Pipe Stiffness (Parallel Plate Test)										
Pipe	**ADS 48**									
ASTM Formula		PS	=	F/ Δy						
Actual Formula		PS	=	(Load*1000)/(length*defl)						
		SF	=	0.149*r^3*PS			r = 24.832 in.			
vert defl (LVDT)										
Head Rate	Test #	**vert defl (inch)**		vert Load (Kips)		Length	PS (psi)		SF (lb-in^2)	
in. per minute		5%	10%	5%	10%	(inch)	5%	10%	5%	10%
0.05		-2.4001	-4.8006	-1.99219	-2.99531	40	20.75	15.60	47344.36	35588.11
0.5	1	-2.404	-4.8036	-2.65469	-4.02969	40	27.61	20.97	62985.26	47848.46
0.5	2	-2.403	-4.8026	-2.52031	-3.82344	40	26.22	19.90	59821.59	45408.72
10		-2.4449	-4.8129	-3.45625	-5.24375	40	35.34	27.24	80633.28	62143.23
150		-2.4134	-4.8174	-4.45	-7.0125	40	46.10	36.39	105171.79	83028.11

Table 4.5 - Measured PS and SF of HDPE ADS 36" pipes

Pipe Stiffness (Parallel Plate Test)										
Pipe	**ADS 36**									
ASTM Formula		PS	=	F/ Δy						
Actual Formula		PS	=	(Load*1000)/(length*defl)						
		SF	=	0.149*r^3*PS			r = 19.392 in.			
vert defl (LVDT)										
Head Rate	Test #	**vert defl (inch)**		vert Load (Kips)		Length	PS (psi)		SF (lb-in^2)	
in. per minute		5%	10%	5%	10%	(inch)	5%	10%	5%	10%
0.05		-1.8007	-3.6006	-1.74063	-2.70781	36	26.85	20.89	29178.58	22700.49
0.5	1	-1.8021	-3.6033	-2.35313	-3.68438	36	36.27	28.40	39413.89	30864.26
0.5	2	-1.8002	-3.605	-2.45625	-3.74219	36	37.90	28.83	41186.13	31333.49
10		-1.8998	-3.6112	-3.37031	-5.19063	36	49.28	39.93	53548.46	43387.32
150		-1.8113	-3.6218	-3.75	-5.96094	36	57.51	45.72	62494.93	49680.62

Table 4.6 - Measured PS and SF of HDPE HANCOR 36" pipes

Pipe Stiffness (Parallel Plate Test)										
Pipe	**HAN 36**									
ASTM Formula		PS	=	F/ Δy			r = 19.332 in.			
Actual Formula		PS	=	(Load*1000)/(length*defl)						
		SF	=	0.149*r^3*PS						
vert defl1 (LVDT)										
Head Rate	Test #	**vert defl1 (inch)**		vert Load (Kips)		Length	PS (psi)		SF (lb-in^2)	
in. per minute		5%	10%	5%	10%	(inch)	5%	10%	5%	10%
0.05		-1.8012	-3.6024	1.13086	1.92246	36	-20.93	-14.82	-22529.36	-15958.26
0.5	1	-1.8086	-3.6024	1.5832	2.48788	36	-24.32	-19.18	-26176.83	-20651.79
0.5	2	-1.8012	-3.6097	1.73398	2.67636	36	-26.74	-20.60	-28787.47	-22170.93
10		-1.8086	-3.6048	2.3748	3.61874	36	-36.47	-27.89	-39265.24	-30018.51

Table 4.7 - Measured PS and SF of PVC 36" pipes

Pipe Stiffness (Parallel Plate Test)										
Pipe	PVC 36									
ASTM Formula		PS	=	F/ Δy						
Actual Formula		PS	=	(Load*1000)/(length*defl)						
		SF	=	0.149*r^3*PS			r = 18.570 in.			
vert defl1 (LVDT)										
Head Rate	Test #	vert defl1 (inch)		vert Load (kips)		Length	PS (psi)		SF (lb-in^2)	
in. per minute		5%	10%	5%	10%	(inch)	5%	10%	5%	10%
0.5	1	-1.8061	-3.60481	1.28164	2.3371	13	54.58	49.87	52.080	47.586
0.5	2	-1.80363	-3.60727	1.28164	2.22402	13	54.66	47.42	52.157	45.285
10	1	-1.81594	-3.6000	1.31933	2.2240	13	56.02	47.52	53.455	45.345

Table 4.8 - Measured PS and SF of Steel 36" pipes

Pipe Stiffness (Parallel Plate Test)										
Pipe	STEEL 36									
ASTM Formular		PS	=	F/ Δy			r = 18.037 in.			
Actual Formular		PS	=	(Load*1000)/(length*defl)						
		SF	=	0.149*r^3*PS						
vert defl1										
Head Rate	Test #	vert defl1 (inch)		vert Load (Kips)		Length	PS (psi)		SF (lb-in^2)	
in. per minute		5%	10%	5%	10%	(inch)	5%	10%	5%	10%
0.5	1	-1.8036	-3.6048	2.18632	2.75175	36	-33.67	-21.20	-29441.82	-18540.65
0.5	2	-1.8012	-3.6073	2.07324	2.97792	36	-31.97	-22.93	-27957.17	-20050.85
0.5	3	-1.8012	-3.6048	2.18632	3.05331	36	-33.72	-23.53	-29482.03	-20572.49

Table 4.9 - Measured PS and SF of Aluminum 36" pipes

Pipe Stiffness (Parallel Plate Test)										
Pipe	ALUM 36									
ASTM Formula		PS	=	F/ Δy			r = 18.248			
Actual Formula		PS	=	(Load*1000)/(length*defl)						
		SF	=	0.149*r^3*PS						
vert defl1 (LVDT)										
Head Rate	Test #	**vert defl1 (inch)**		vert Load (Kips)		Length	PS (psi)		SF ($lb\text{-}in^2$)	
in. per minute		5%	10%	5%	10%	(inch)	5%	10%	5%	10%
0.5	1	-1.8036	-3.6048	0.94238	1.43242	36	-14.51	-14.22	-13140.39	-12877.55
0.5	2	-1.8086	-3.6024	0.94238	1.43242	36	-14.47	-11.05	-13104.57	-10000.32
0.5	3	-1.8676	-3.6024	0.94238	1.39472	36	-14.51	-10.75	-13173.10	-9737.12

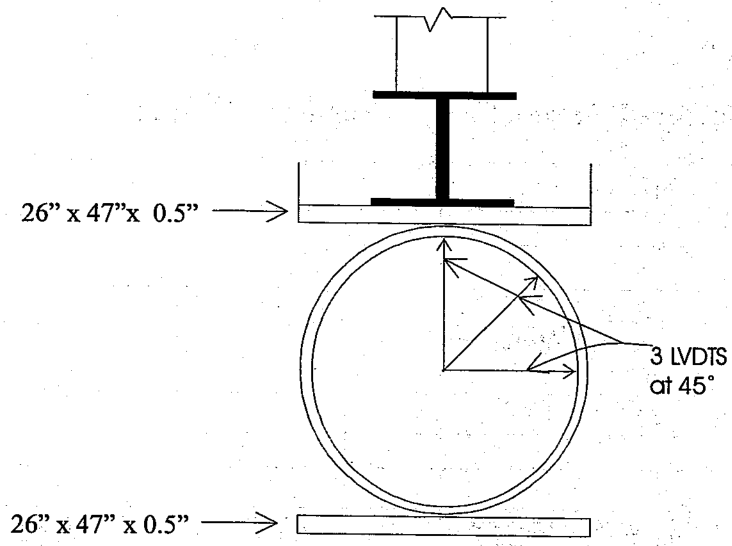

Fig. 4.1 - LVDT Experimental Set-up

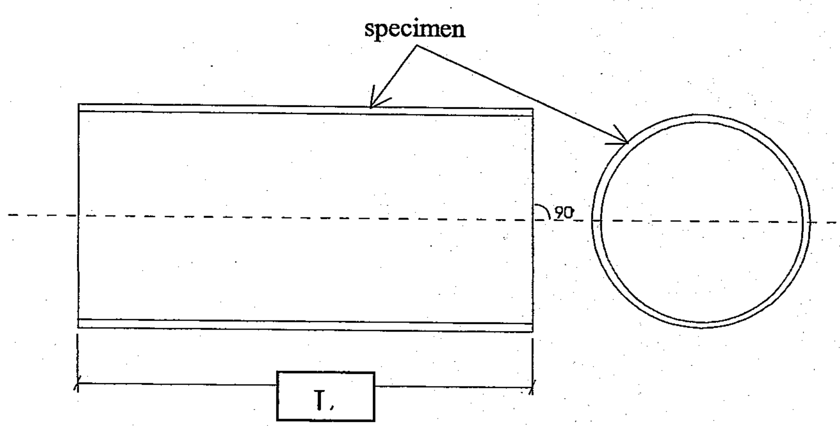

Fig. 4.2 - Test Specimen

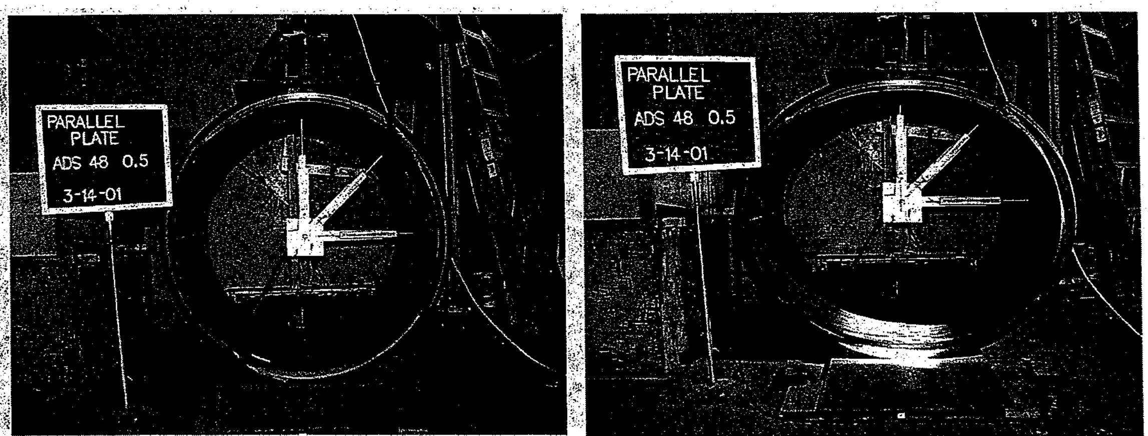

(a) ADS48 under Parallel Plate Test (b) Deformed Shape of ADS 48"

Fig. 4.3 - Views of ADS 48 Pipe Specimen During Parallel Plate Test

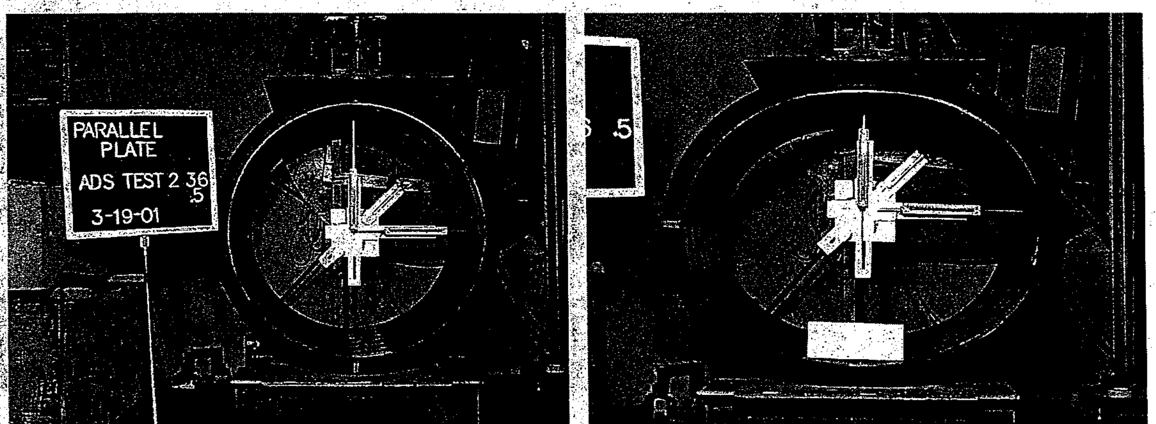

(a) ADS 36 under Parallel Plate Test (b) Deformed Shape of ADS 36"

Fig. 4.4 - Views of ADS 36 Pipe Specimen During Parallel Plate Test

(a) Hancor 36 under Parallel Plate Test (b) Deformed Shape of Hancor 36"

Fig. 4.5 - Views of Hancor 36 Pipe Specimen During Parallel Plate Test

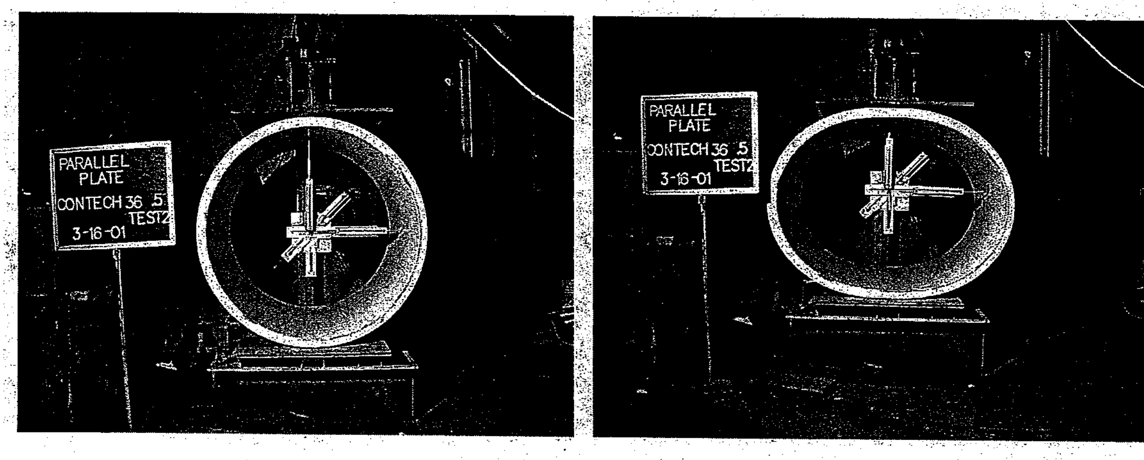

(a) PVC 36 under Parallel Plate Test (b) Deformed Shape of PVC 36"

Fig. 4.6 - Views of PVC Pipe Specimen During Parallel Plate Test

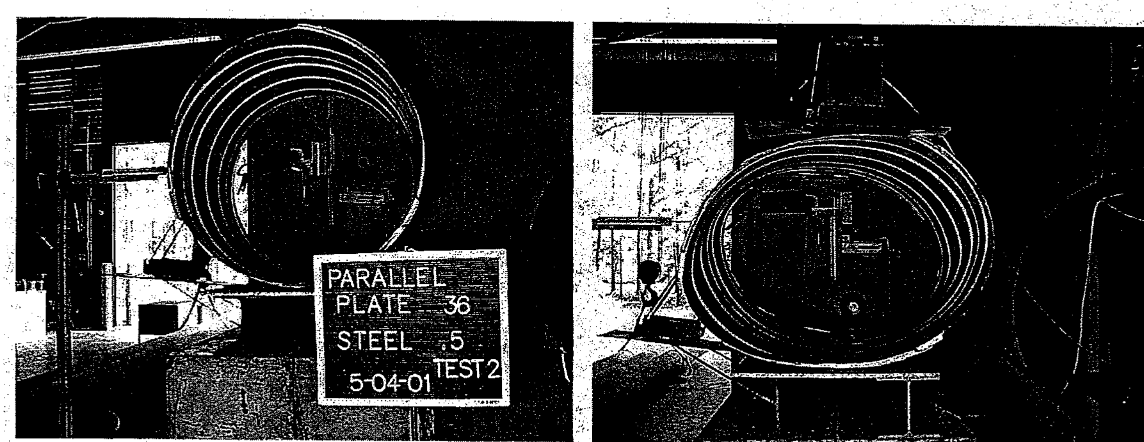

(a) Steel 36 under Parallel Plate Test (b) Deformed Shape of Steel 36"

Fig. 4.7 - Views of Steel Pipe Specimen During Parallel Plate Test

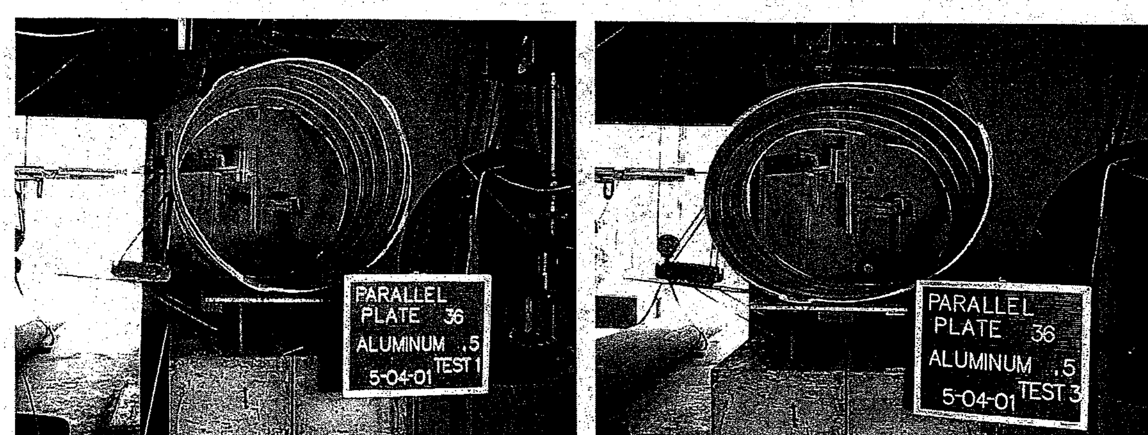

(a) Aluminum 36 under Parallel Plate Test (b) Deformed Shape of Aluminum 36"

Fig. 4.8 - Views of Aluminum Pipe Specimen During Parallel Plate Test

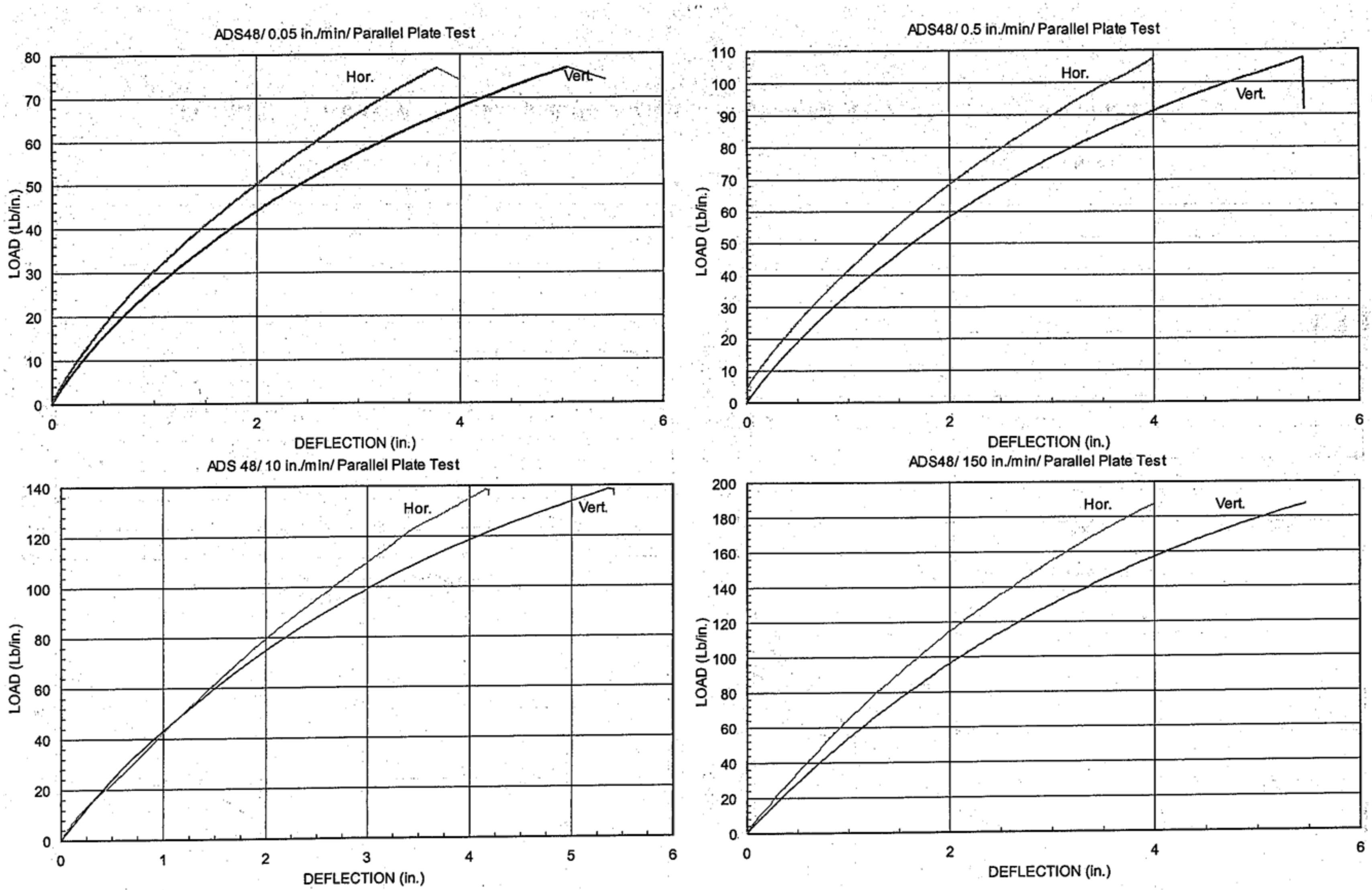

Fig. 4.9 - Load versus Vertical and Horizontal Deflections for ADS 48 Under Parallel Plate Test

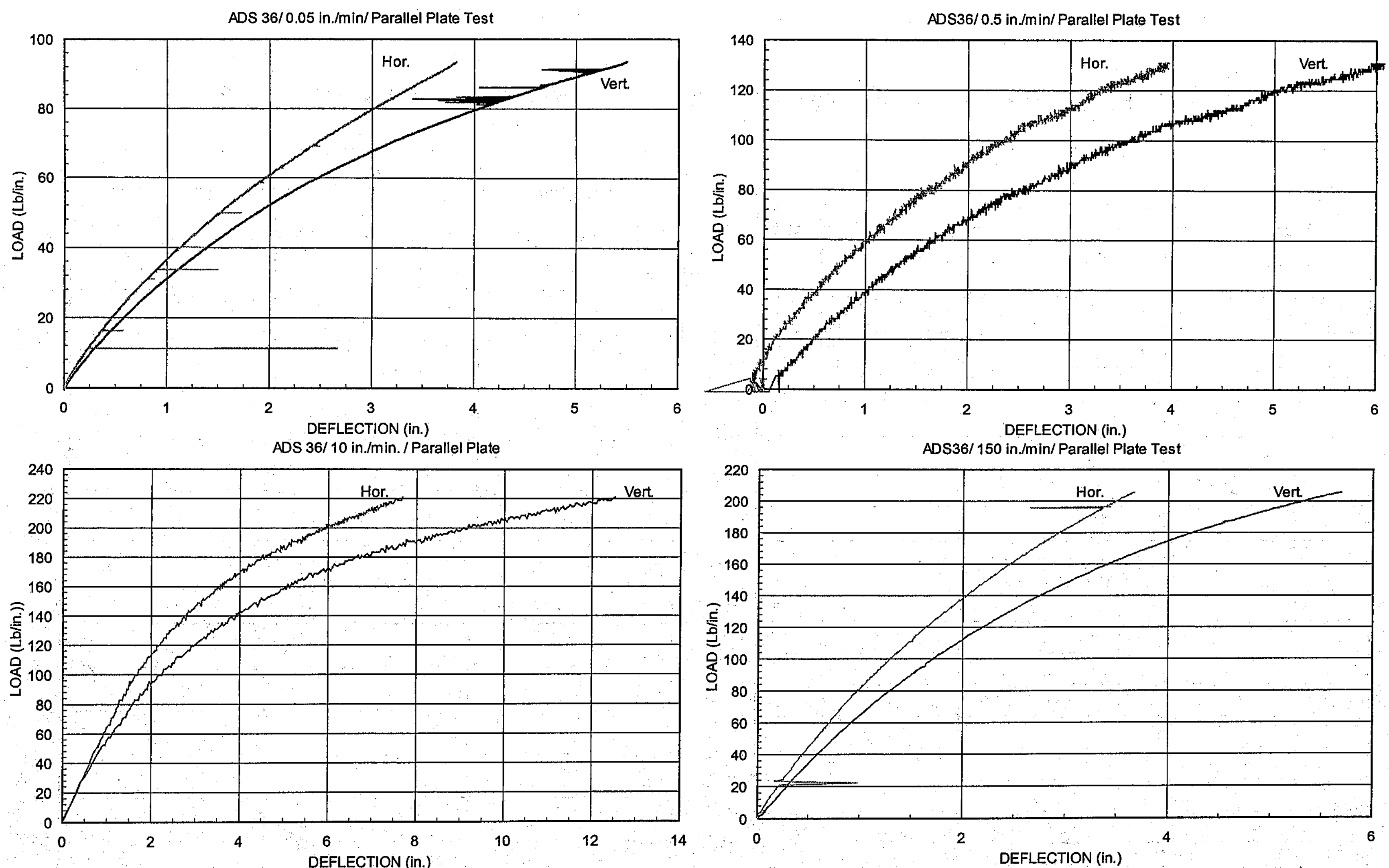

Fig. 4.10 - Load versus Vertical and Horizontal Deflections for ADS 36 Under Parallel Plate Test

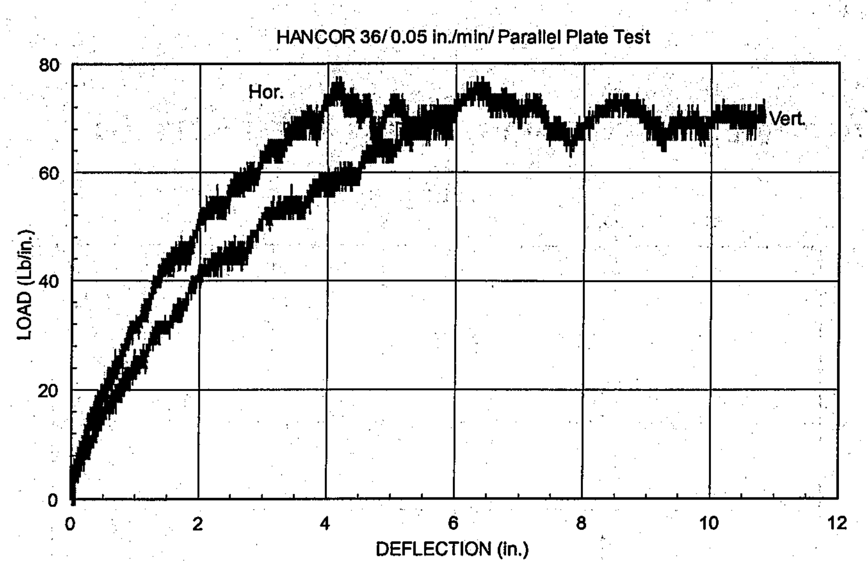

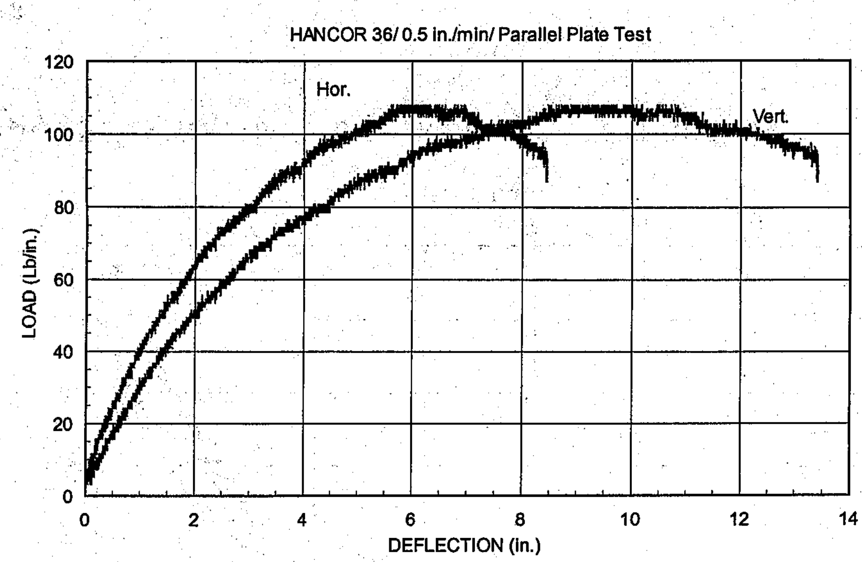

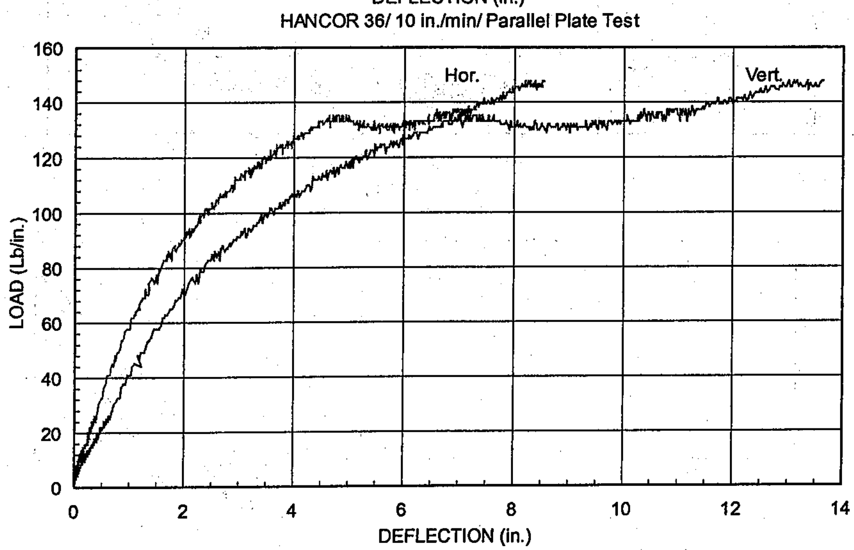

Curves for 150 in./min. loading rate not available

Fig. 4.11 - Load versus Vertical and Horizontal Deflections for HANCOR 36 Under Parallel Plate Test

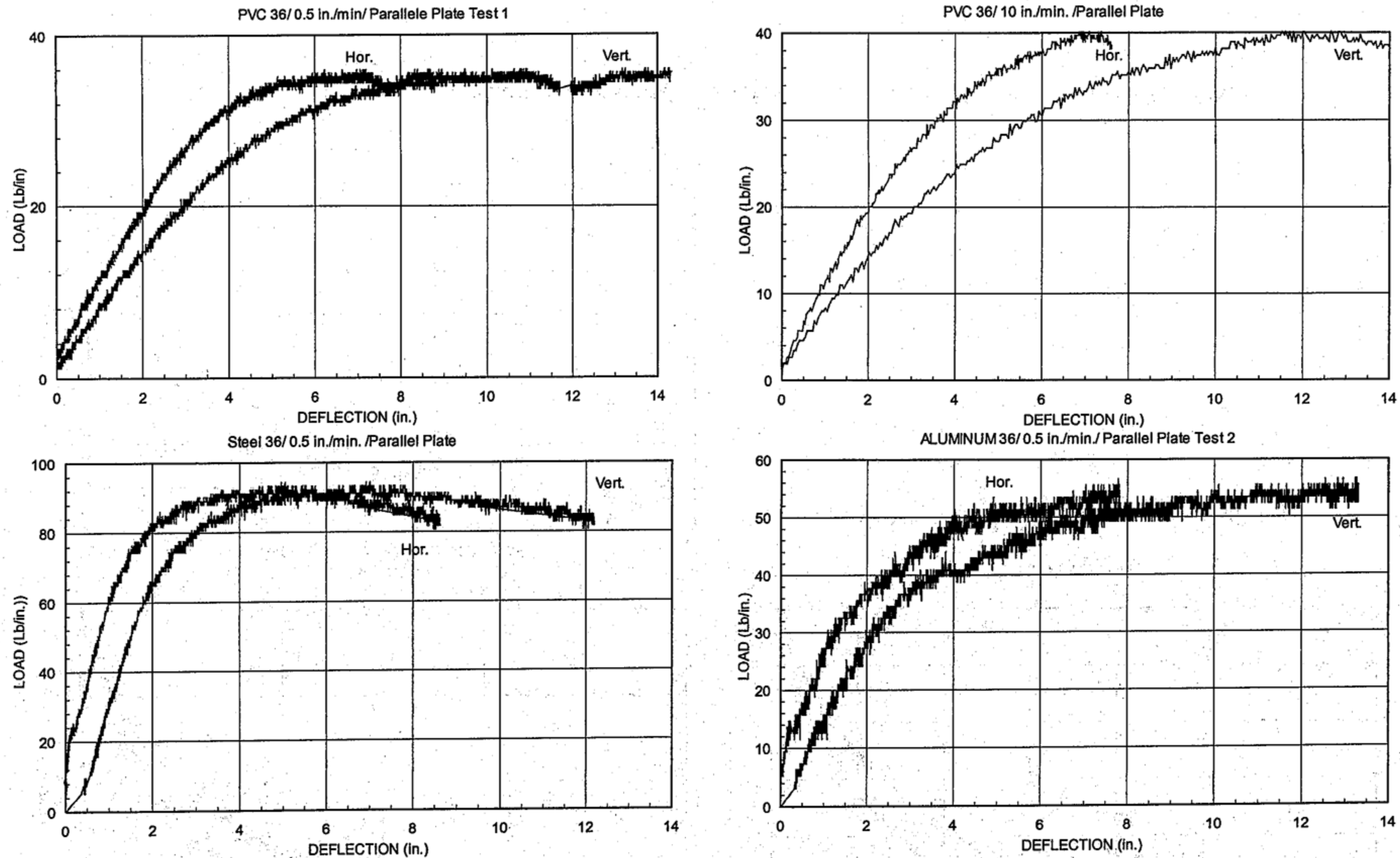

Fig. 4.12 - Load versus Vertical and Horizontal Deflections for PVC 36, Steel and Aluminum Under Parallel Plate Test

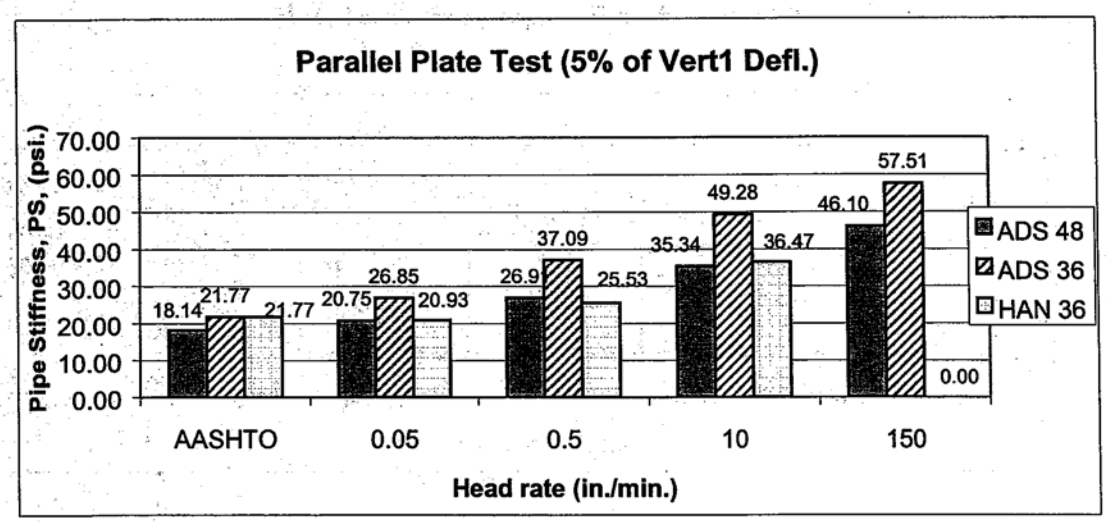

Fig. 4.13 - Comparison of Measured PS Values at 5% Vertical Deflection for HDPE Pipes at Different Loading Rates

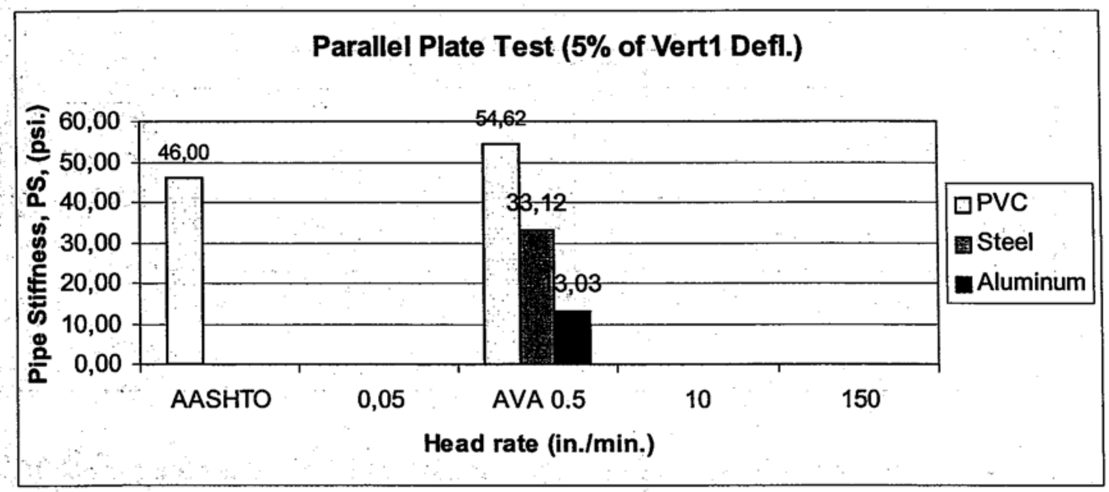

Fig. 4.14 - Comparison of Measured PS Values at 5% Vertical Deflection for 36" PVC and Metal Pipes at a Loading Rate of 0.5 in./min.

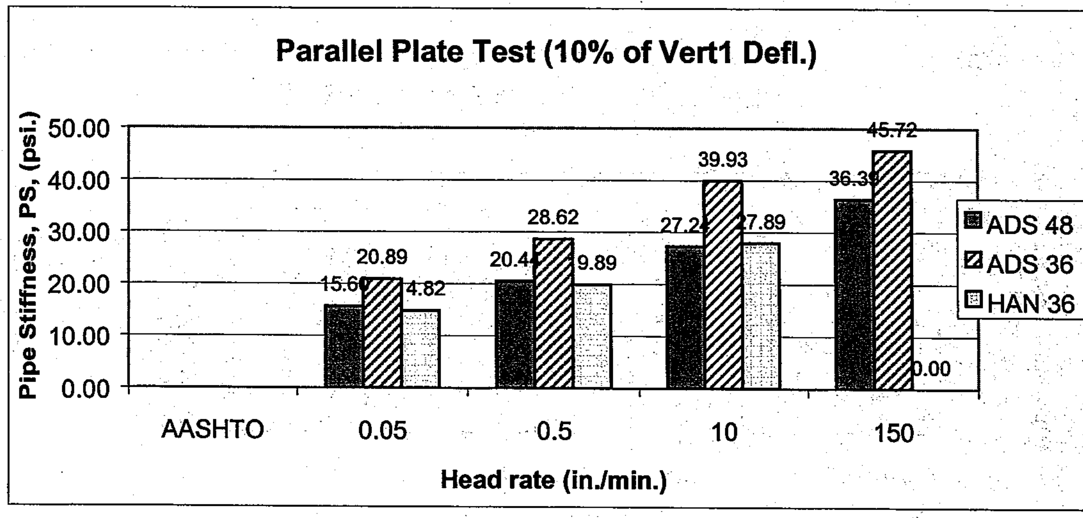

Fig. 4.15 - Comparison of Measured PS Values at 10% Vertical Deflection for HDPE Pipes at Different Loading Rates

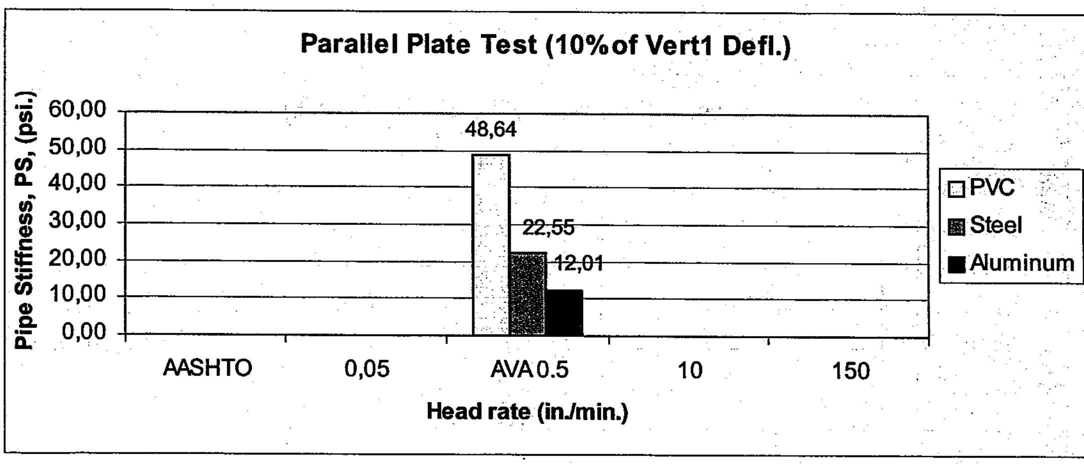

Fig. 4.16 - Comparison of Measured PS Values at 10% Vertical Deflection for 36" PVC and Metal Pipes at a Loading Rate of 0.5 in./min.

Chapter 5: Flattening Test

5.1 Objectives

The objective of this test is to evaluate pipe performance when subjected to flattening between parallel plates until the pipe's inside diameter is reduced by a certain predetermined percent of its original diameter. The specimen is considered to have, passed the test, if no splitting, cracking, breaking, or separation of ribs or seams, or both has occurred. These phenomena should be observed under normal light with unaided eyes.

5.2 Apparatus, Test Specimens and Procedure

The hydraulic jack used in the testing has the capability of constant-rate-crosshead movement. The rate of the head approach can be varied and was in the range of 0.05 to 150 in. per minute. The flattening tests were performed in conjunction with the parallel plate tests. Therefore, the apparatus, test specimens and procedure are identical to those pertaining to the parallel plate tests (see chapter 4 for details). For the flattening tests, no continuous load-deflection readings were recorded. However, for each of the flattened position considered, observations were made to identify splitting, cracking, breaking, or separation of ribs or seams, or both.

5.3 Observations on Behavior of Pipes Flattened According to Standards

AASHTO M294 (for HDPE) and ASTM F949-00 (for PVC) require that HDPE and PVC pipes be flattened between parallel plates until the inside diameter is reduced by:

- HDPE: 20%
- PVC: [100 - 3.43 ID/(OD - ID)], that is approximately 62% ° for the PVC pipe under investigation.
- Note that no flattening test is required for metal pipes.

The following observations were made within the vertical deflection ranges outlined above:

(a) <u>HDPE Pipes (AASHTO M294)</u>

- Less *than 15% vertical deflection*

No wall buckling and other unsymmetrical deformations were observed for all the HDPE pipes tested. All the pipes deformed in an elliptical shape.

- At 15% vertical deflection

At a vertical deflection of 15% o of the diameter, wall buckling was observed around the springline in the outside wall in the case of HDPE Hancor pipe (Fig. 5.1).

- At 20% vertical deflection
  - ADS 48: Scattered local wall buckling was observed around the pipe's springline (Fig. 5.2).
  - ADS 36: Scattered local wall buckling was observed in only certain areas of pipe's springline.
  - Hancor 36: Wall buckling, which was observed at a vertical deflection of 15% diameter on the exterior surface, became more noticeable.

(b) PVC Pipe (ASTM F949-00)

- Up to 20% vertical deflection
  - No wall buckling and other unsymmetrical deformations were observed for all
  - PVC pipes. All the pipes deformed in an elliptical shape (Fig. 5.3).

- At 30% vertical deflection
  - Most PVC specimens tested at loading rates of 0.05, 0.5 and 150 in./min exhibited wall rupture either at the invert or at the crown at vertical deflections ranging from 30 to 36%. The pipe failed suddenly with a loud noise as a result of the wall rupture (see Figs. 5.4a and b).

- At 36% vertical deflection
  - Fig. 5.5a to c present some of the views of the pipe at a vertical deflection of 36% of the diameter. From these figures, reverse curvature at the crown and at the invert, as well as inside wall buckling were clearly observed.

- At 60% vertical deflection
    - All PVC specimens tested at a load rate of 10 in./min. could be flattened up to 60% deflection without rupture (see Fig. 5.22d).

5.4 Observations on Behavior of Pipes Flattened Up to 60%

5.4.1 HDPE ADS 48" Pipe

Flat invert/crown was attained at a deflection of approximately 30% (Fig. 5.6b). No reverse curvature was observed until 42% deflection (Fig. 5.6c and d).

With increasing vertical deflection to 30% of the pipe's diameter, the extent of wall buckling gradually increased and developed along the specimen length (Figs. 5.2b and 5.7). A crack was observed on the inside wall as seen in Fig. 5.7. Fig. 5.8 shows a bulge in a portion of the wall. Wall buckling occurred primarily in the region of the pipe's springline and at a vertical deflection of 42% of the diameter (Fig. 5.9). No buckling was observed on the outside of the pipe wall.

5.4.2 HDPE ADS 36" Pipe

Flat invert/crown prior to reverse curvature was attained at a deflection of approximately 30% (Fig. 5.10b). Reverse curvature initiated at 36% deflection (Fig. 5.l0c). As the vertical deflection increased to 30% of the diameter, the area of wall buckling gradually increased. Excessive wall buckling was observed mainly on the springline of the left and right inside surfaces (Figs. 5.11 to 5.14). The test pipe specimen was then compressed to a vertical deflection of 59% of the diameter. The distance between some corrugations became longer, while the others shortened (Fig. 5.15). The crown region of the test pipe went into reverse curvature prior to reaching the vertical deflection of 59% of the diameter (Fig. 5.10d). However, the invert region of the specimen maintained almost a flat surface except at the center portion of the supporting steel plate (Fig. 5.16).

5.4.3 HDPE HANCOR 36" Pipe

Flat invert/crown prior to reverse curvature was attained at a deflection of approximately 45% (Fig. 5.17a). Reverse curvature initiated at 20% deflection (Fig. 5.17b) and was clearly apparent as the. deflection attained 30% (Figs. 5.17c). When the vertical deflection value increased to 59% of the diameter, both the pipe region in the invert as well as at the crown exhibited almost identical reverse curvature shapes (Fig. 5.17d). In general, pipe properties of HDPE RANCOR 36" pipe are similar to HDPE ADS 36" pipe. The deformation behavior of HDPE RANCOR 36" pipes are displayed in Figs. 5.17 to 5.21.

In the case of HDPE RANCOR 36" pipes, wall buckling on the exterior surface became noticeable even at a vertical deflection of 15% o of the diameter. Moreover, a break in the rib was evident on the exterior surface of the pipe wall (Fig. 5.21).

5.4.4 PVC 36" Pipe

Flat invert/crown prior to reverse curve was attained at a deflection of approximately 30% (Fig. 5.22b). All PVC specimens tested at a load rate of 10 in./min. could be flattened up to 60% deflection without rupture (Fig. 5.22d). However, as outlined earlier, most PVC specimens tested at loading rates of 0.05, 0.5 and 150 in./min. exhibited wall, rupture either at the invert or at the crown at a vertical deflection ranging from 30 to 36%.

5.4.5 Steel and Aluminum 36" Pipes

Both the aluminum and steel pipes did not exhibit reverse curvature as clearly as the HDPE pipes. Fig. 5.23a) to d) shows views of the behavior of the aluminum, pipe under parallel plates for different deflection levels. Note the highly unsymmetrical deflected shapes of the aluminum pipe specimen. Similarly, Fig 5.24a) to d) shows that the behavior of the steel 36" pipe is similar to that of the aluminum 36" pipe.

5.5 Conclusions

The following conclusions are of interest with regard to the flattening tests:

(a) All the HDPE pipes passed the flattening test since no splitting, cracking, breaking, or separation of ribs or seams, or both, were observed under normal light with unaided eyes.

(b) The PVC pipes tested at 0.05, 0.5 and 1.50 in./min. ruptured either at the crown or at the invert after the occurrence of reverse curvature, at a vertical deflection ranging from 30% to 36%. However, only the PVC pipe specimens tested at 10 in./min. could be flattened up to 60% vertical deflection without failure. These pipe specimens did not experience any splitting, cracking, breaking, or separation of ribs or seams, or both, and therefore passed the flattening test.

Also, results indicated the following:

(c) For HDPE pipes, up to 15% vertical deflection, no wall buckling or unsymmetrical deformed shapes were observed.

(d) At 15% vertical deflection, wall buckling initiated at the area of the springline in the outside wall of Hancor 36.

(e) At 20% vertical deflection, scattered local wall buckling initiated in the area of the springline in the inside wall for all HDPE pipes.

(f) PVC pipe performed well up to 20% vertical deflection. No wall buckling or unsymmetrical deformed shapes were observed. Between 20 to 30% vertical deflection, inside wall buckling was noticeable.

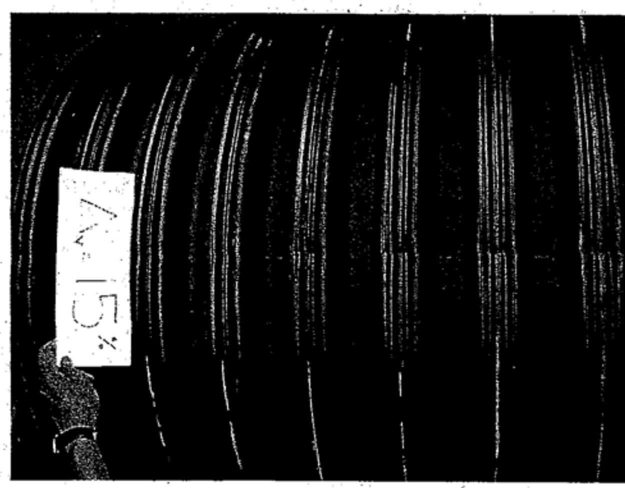

Fig. 5.1 - Wall Buckling on the Outside of Hancor 36 Pipe at Vertical Deflection of 15%

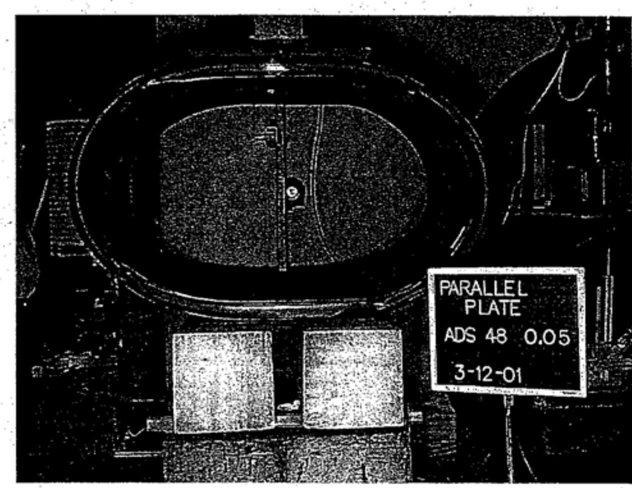

Fig. 5.2a - Deformed Shape of HDPE ADS 48" Pipe at Vertical Deflection of 20% Diameter

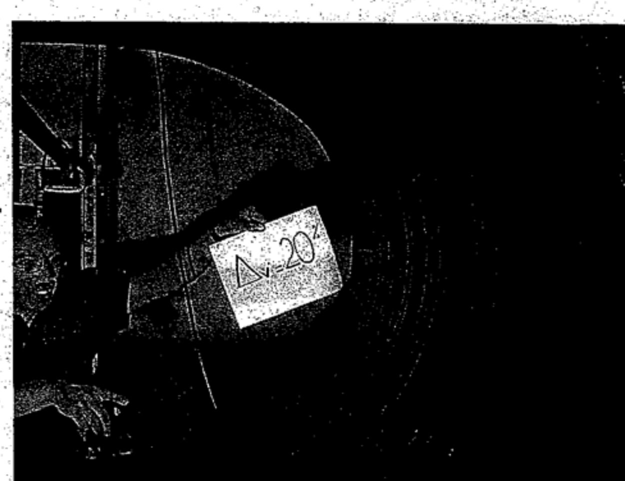

Fig. 5.2b - Scattered Wall local Buckling at Vertical Deflection of 20% Diameter

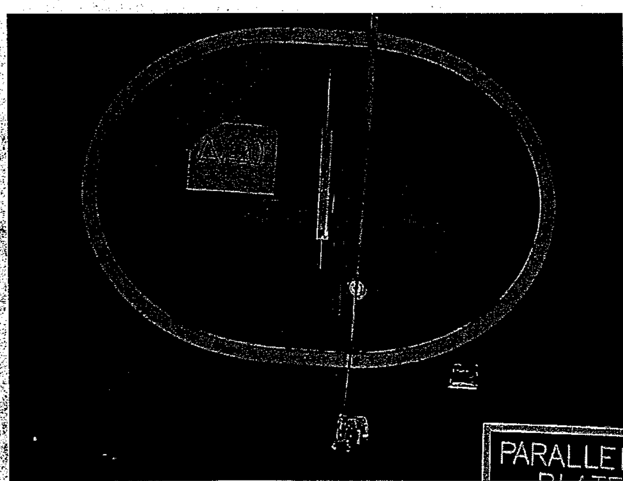

Fig. 5.3 - Deformed Elliptical Shape of PVC 36" Pipe at the Vertical Deflection of 20%

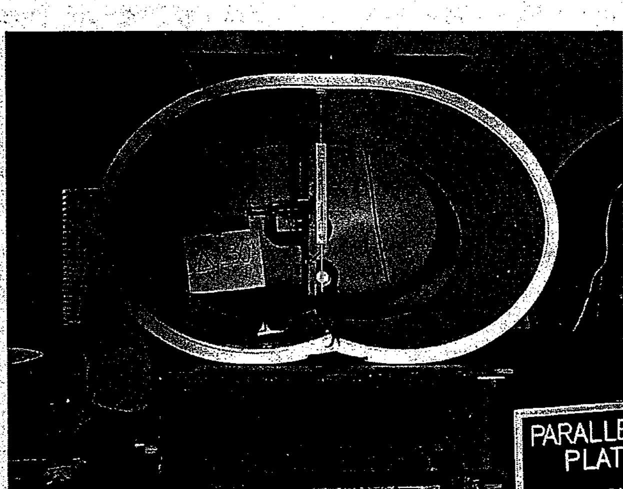

Fig. 5.4a - Failure of PVC Due to Wall Rupture in the Invert Region with Reverse Curvature at the Vertical Deflection of 30% Diameter

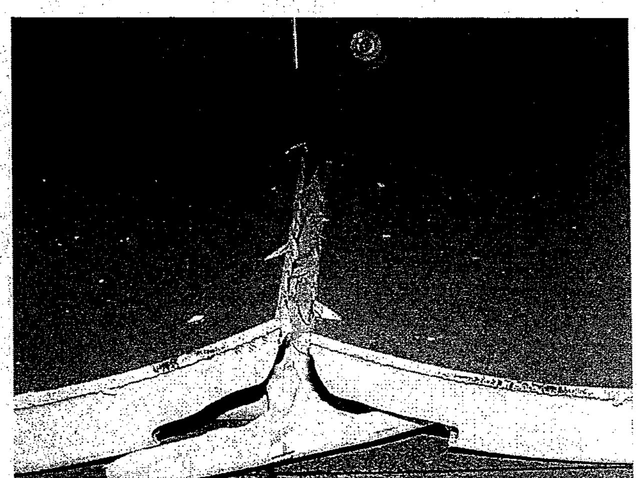

Fig. 5.4b - Close up View of invert Rupture of PVC 36" Pipe at the Vertical Deflection of 30% Diameter

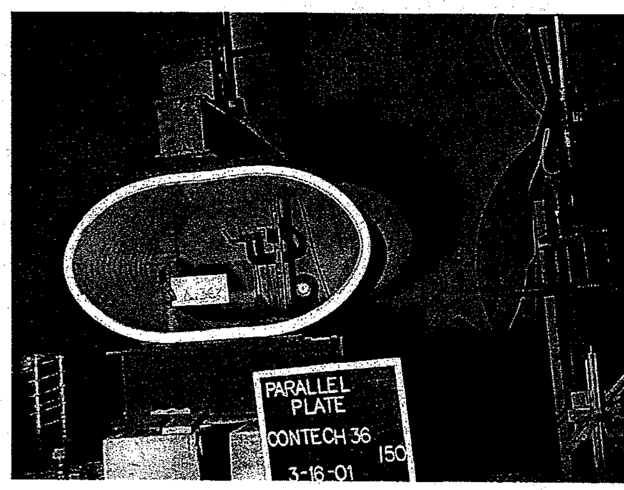

Fig. 5.5a - Deformed Elliptical Shape of PVC 36" Pipe at the Vertical Deflection of 36%

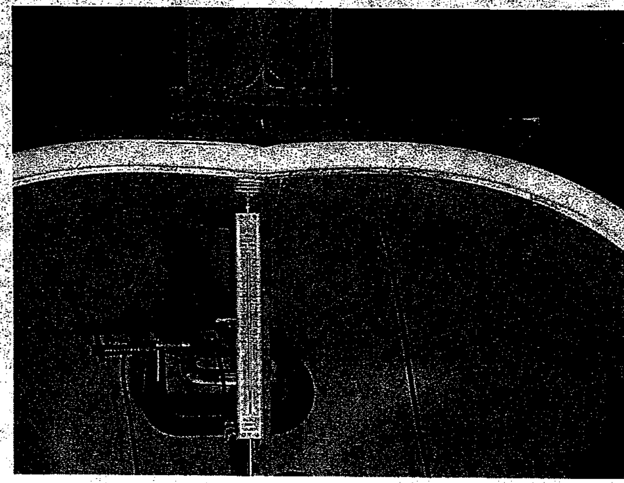

Fig. 5.5b - Close up View of Crown of PVC 36" Pipe at the Vertical Deflection of 36%

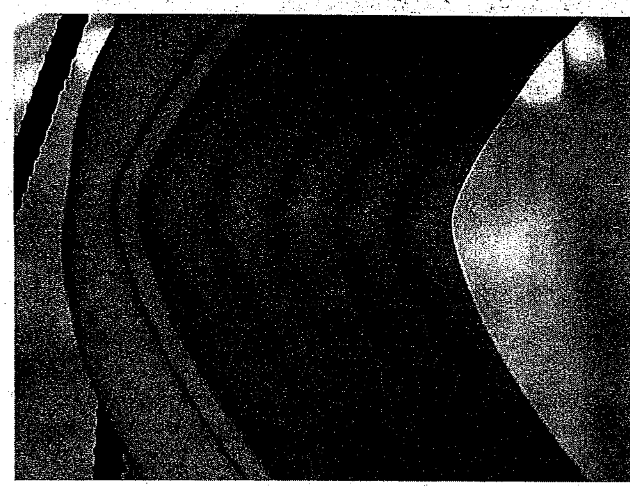

Fig. 5.5c - Wall Buckling at Springline of PVC 36" Pipe at the Vertical Deflection of 36%

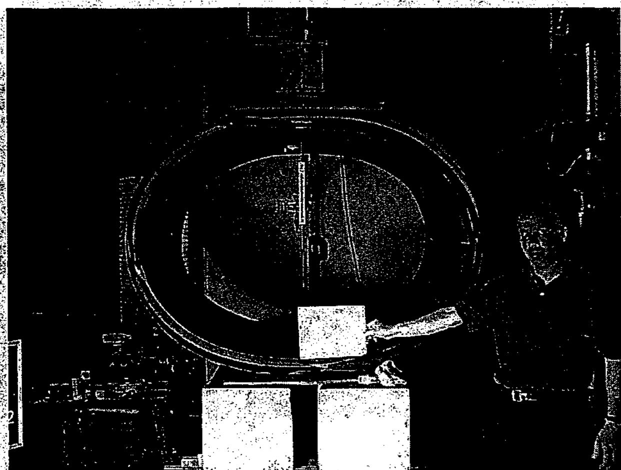

a) At approximately 20% deflection

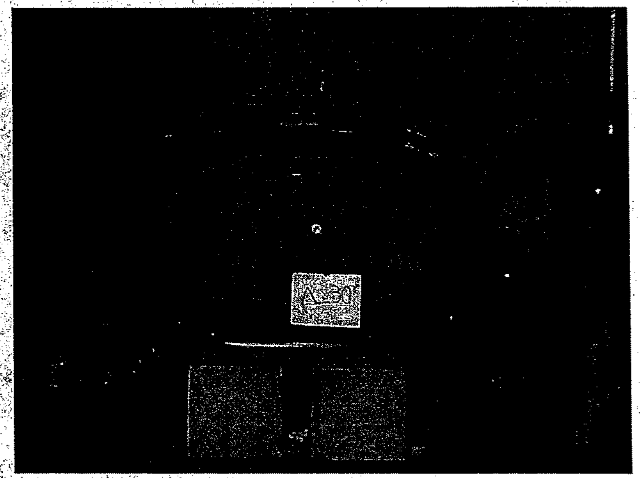

b) At approximately 30% deflection

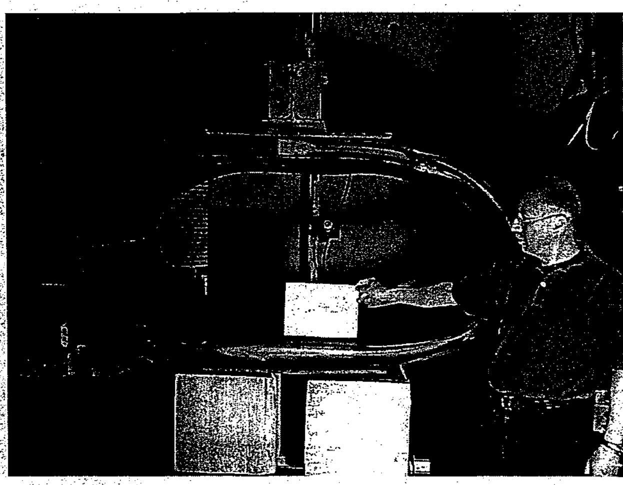

c) At approximately 42% deflection

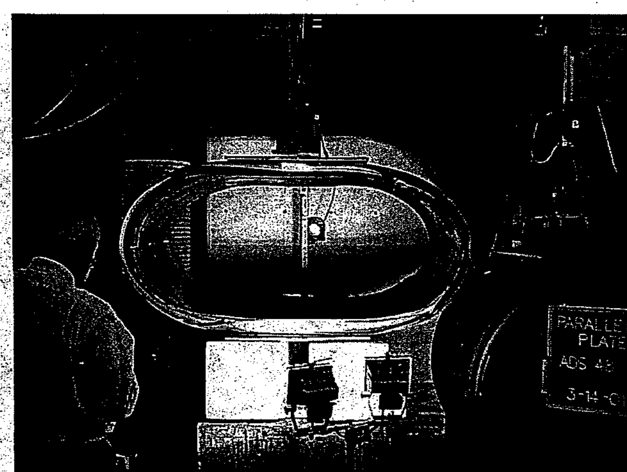

d) At approximately 42% deflection

Fig. 5.6 - Deformed Shapes of HDPE ADS 48" Pipe Under Parallel Plates at Different Vertical Deflections

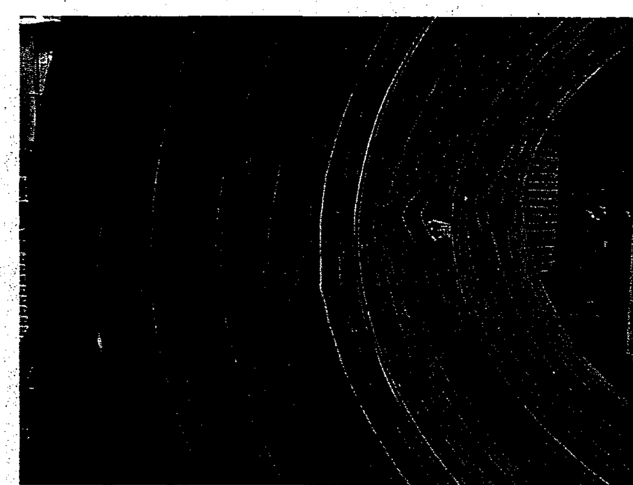

Fig. 5.7 - Extensive Inside Wall Local Buckling and One Wall Cracking at Vertical Deflection of 30% Diameter – ADS48

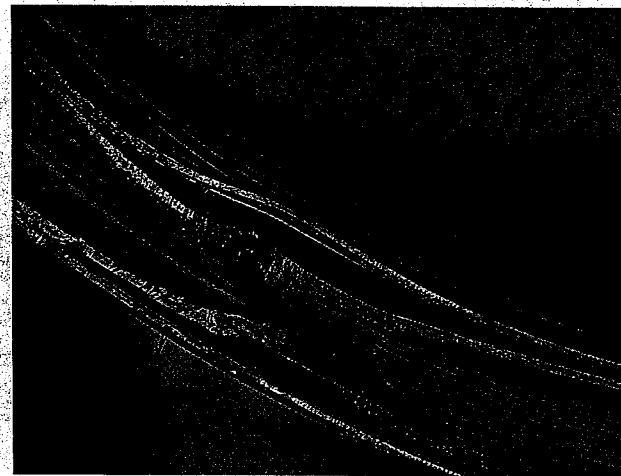

Fig. 5.8 - Part Edge Area Bulging at Vertical Deflection of 30% Diameter –ADS48

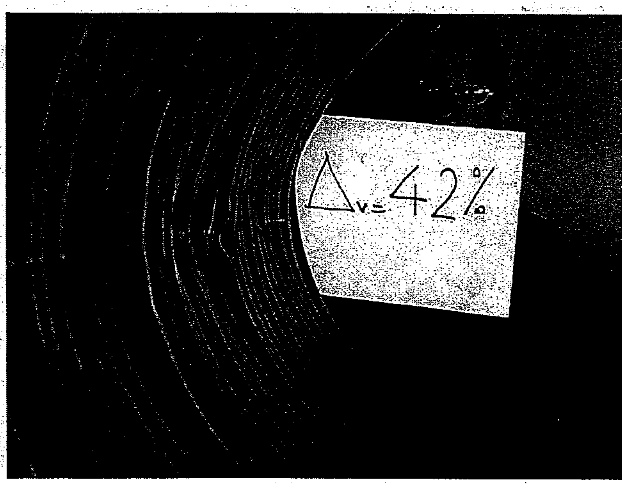

Fig. 5.9 - Wide-Spread Wall Buckling at Vertical Deflection of 42% Diameter-ADS48

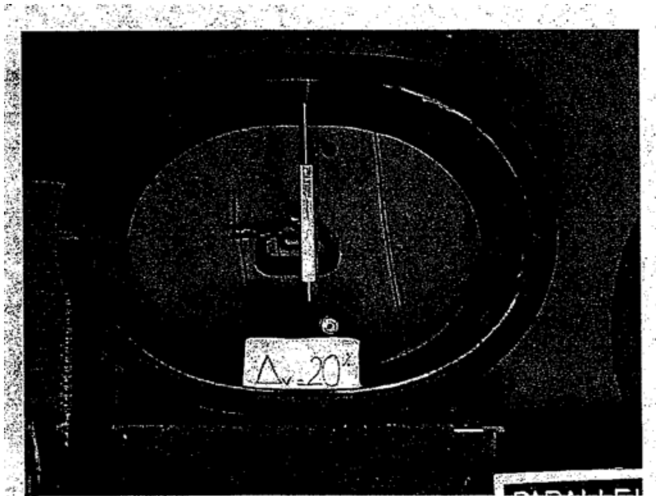

a) At approximately 20% deflection

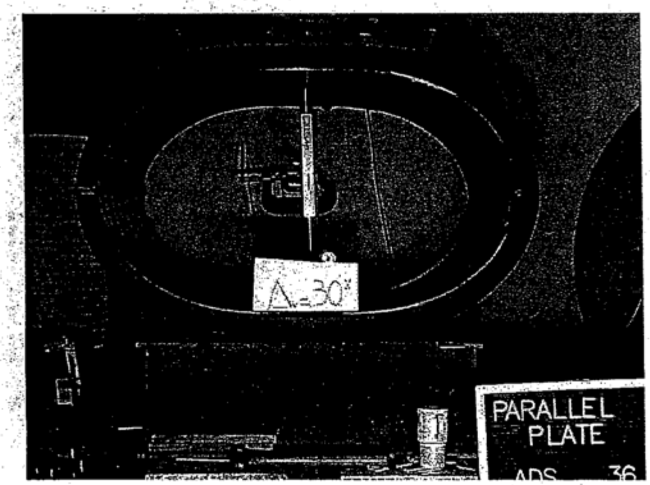

b) At approximately at 30% deflection

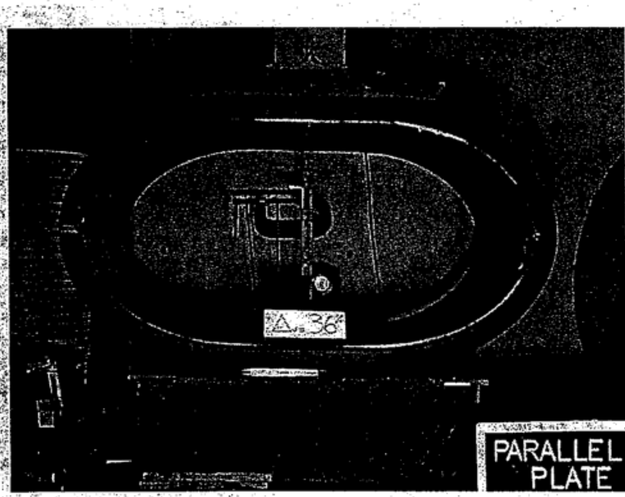

c) Initiation of reverse curve at crown and invert at 36%

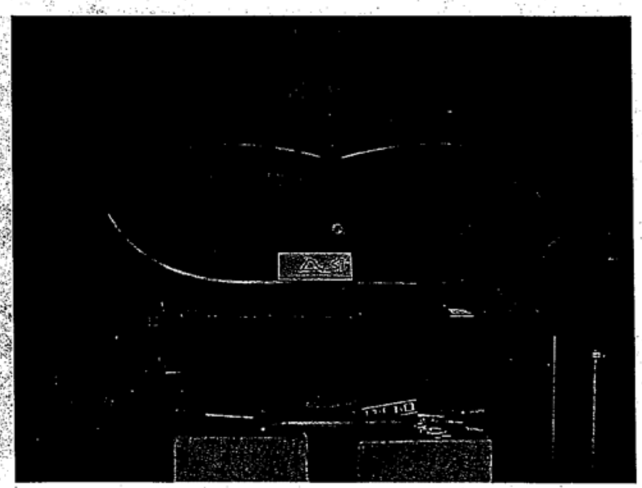

d) Reverse curve at crown and invert at 59%

Fig. 5.10 - Deformed Shapes of HDPE ADS 36" Pipe Under Parallel Plates at Different Vertical Deflections

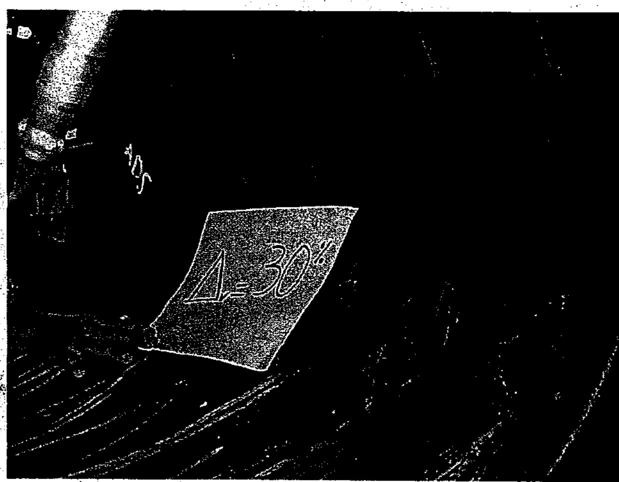

Fig. 5.11 - Inside Wall Deformation at the Vertical Deflection of 20% Diameter - ADS36

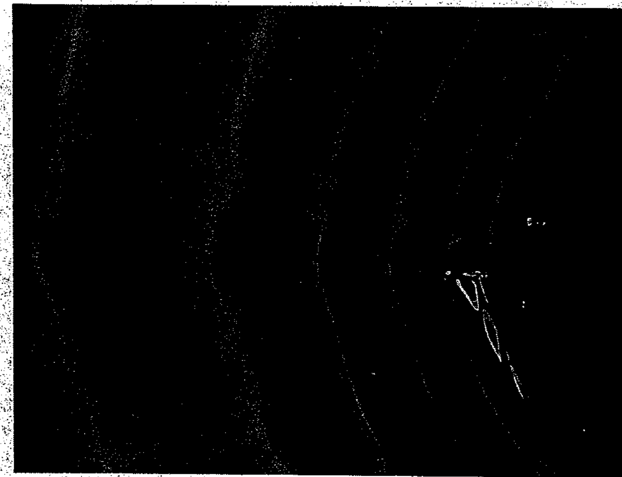

Fig. 5.12 - Wide Spread Wall Buckling Forming a Line in the Area of Springline at the Vertical Deflection of 30% Diameter – ADS36

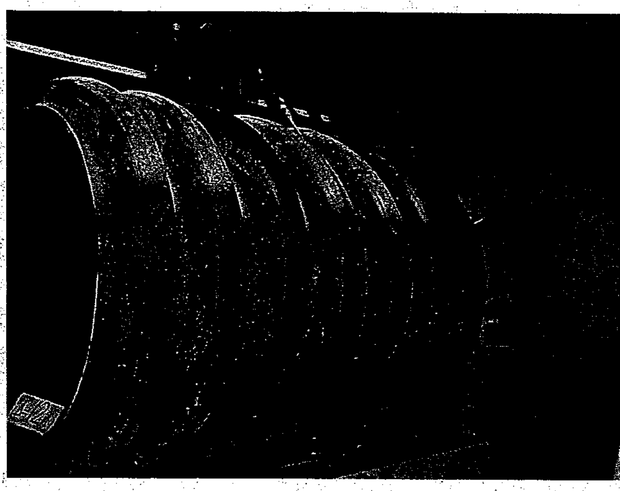

Fig. 5.13 - Outside Wall Buckling at the Vertical Deflection of 30% Diameter – ADS36

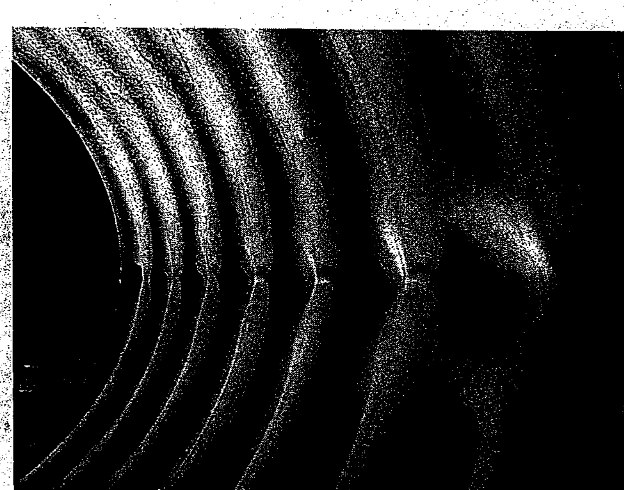

Fig. 5.14 - Wide Spread Inside Wall Buckling at the Vertical Deflection of 36% Diameter – ADS36

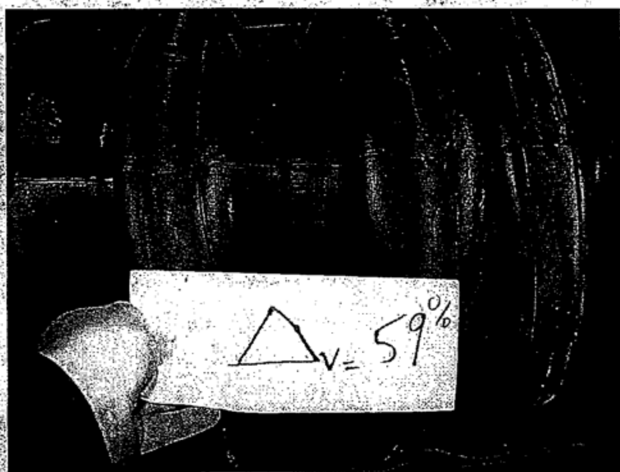

Fig. 5.15 - Deformation of the Outside Surface at Pipe Springline at the Vertical Deflection of 59% Diameter – ADS36

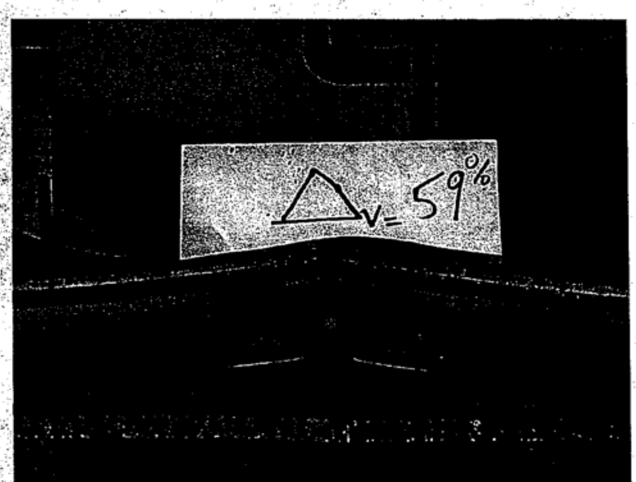

Fig. 5.16 - Lightly Reversed Curvature of Invert Region at the Vertical Deflection of 59% Diameter – ADS36

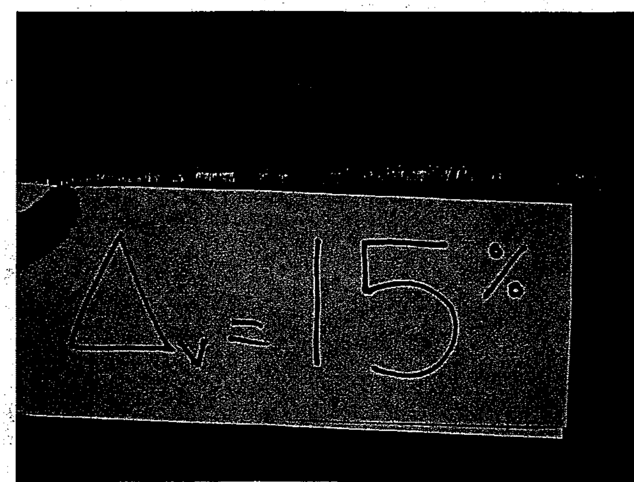

a) Flat invert/crown at approximately 15% deflection

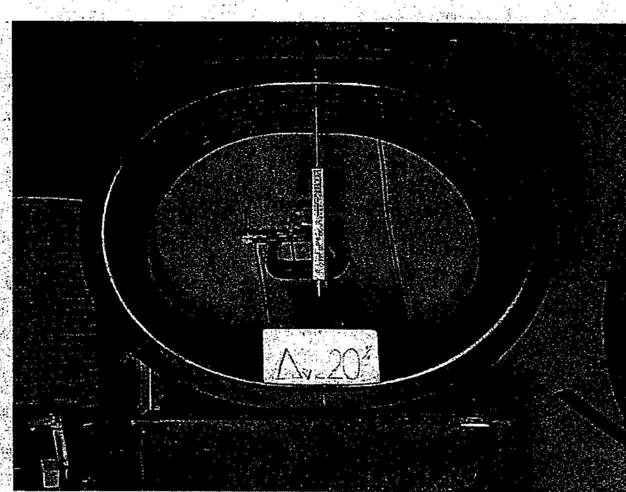

b) Initiation of reverse curve at crown and invert at 20%

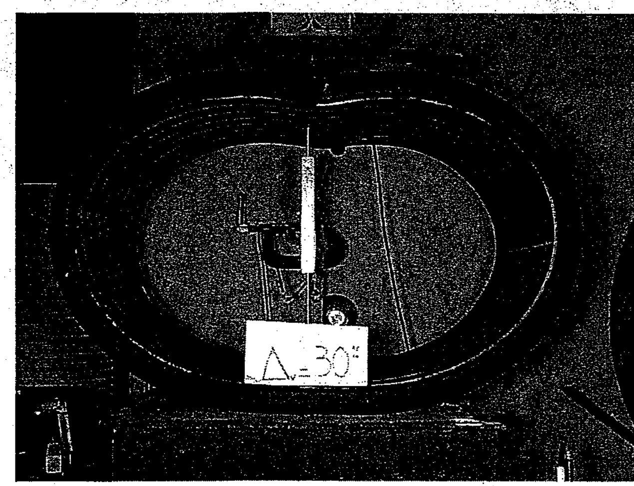

c) Reverse curve at crown and invert at 30%

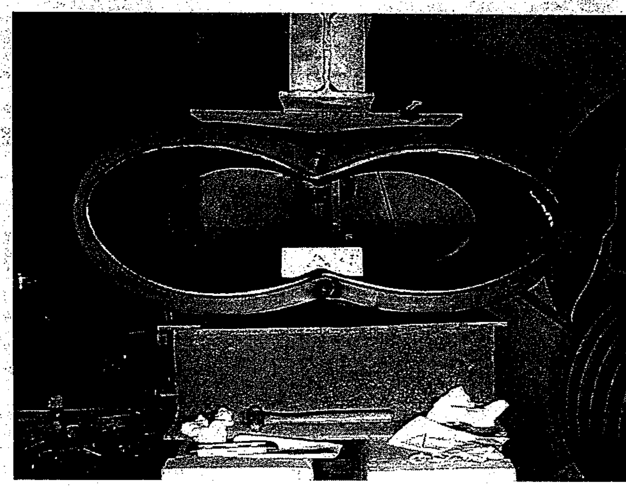

d) Reverse curve at crown and invert at 59%

Fig. 5.17 - Deformed Shapes of HDPE Hancor 36" Pipe Under Parallel Plates at Different Deflections

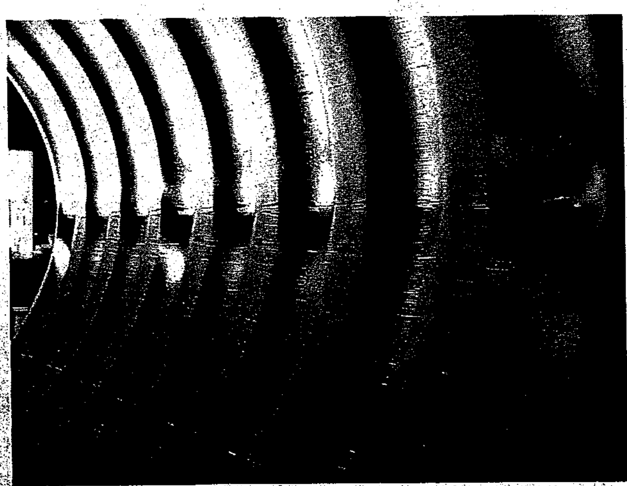

Fig. 5.18 - Inside Wall Buckling at the Springline of HDPE Hancor 36" Pipe at the Vertical Deflection of 30% Diameter

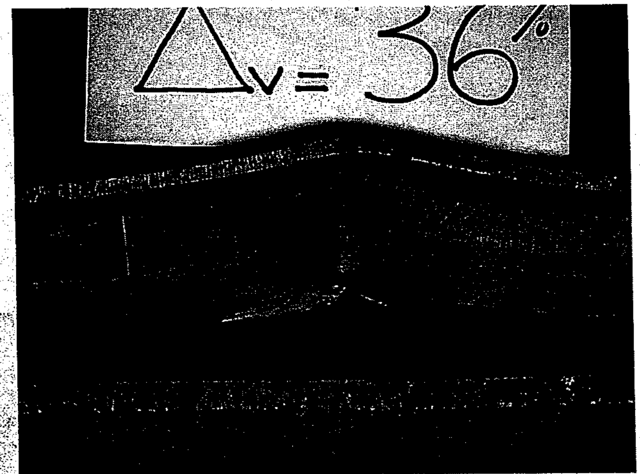

Fig. 5.19 - Deformation of the Invert Region of HDPE Hancor 36" Pipe at the Vertical Deflection of 36% Diameter

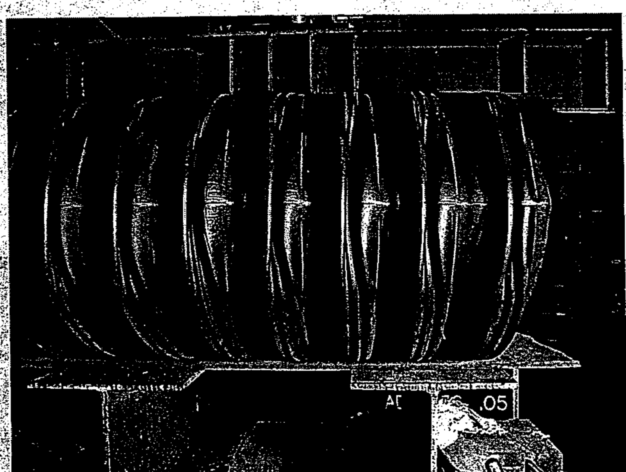

Fig. 5.20 - Extensive Wall Buckling on the Exterior Surface of HDPE Hancor 36" Pipe at the Vertical Deflection of 59% Diameter

Fig. 5.21 - Breaking of Rib of HDPE Hancor 36" Pipe at the Vertical Deflection of 59% Diameter

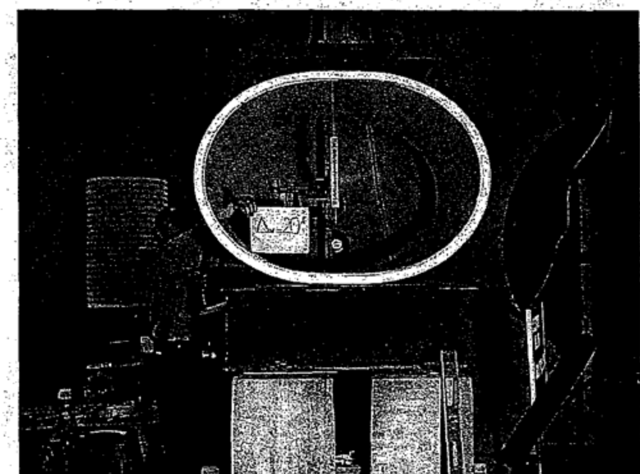

a) At approximately 20% deflection

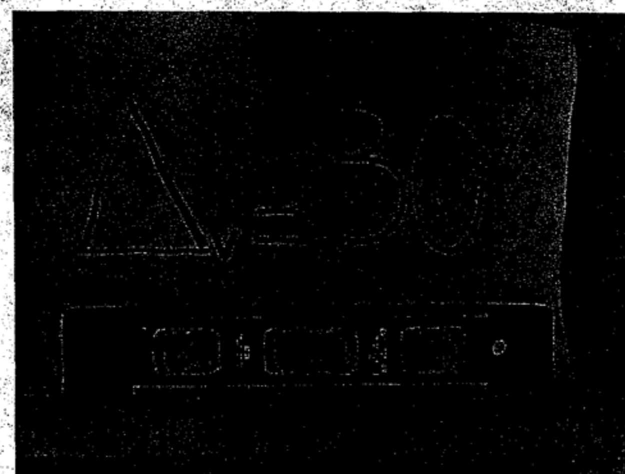

b) Flat crown and invert prior to reverse curve at 30%

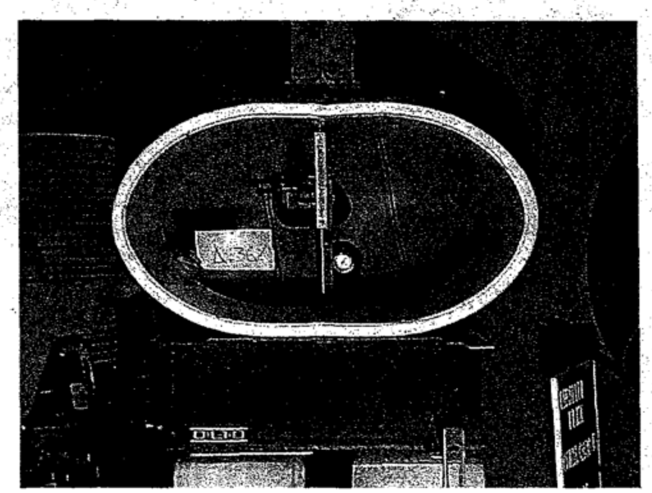

c) Initiation of reverse curve at crown and invert at 36%

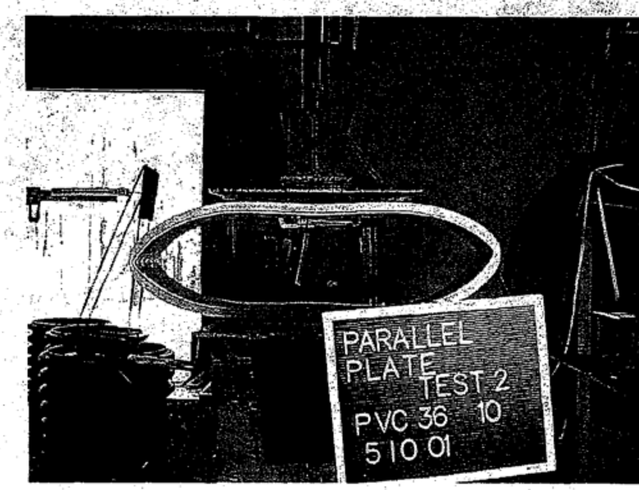

d) Deformed shape at 60% (for 10 in./min only)

Fig. 5.22 - Deformed Shapes of PVC 36" Pipe Under Parallel Plates at Different Vertical Deflections

a) At 0% deflection

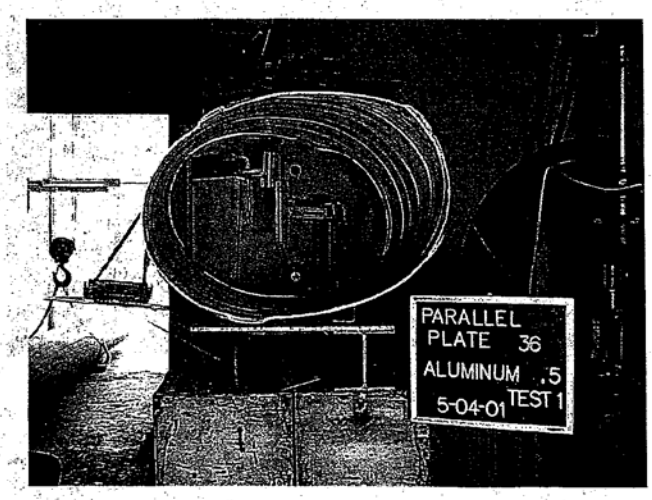

b) Overall elliptical deformed shape at approximately 15%

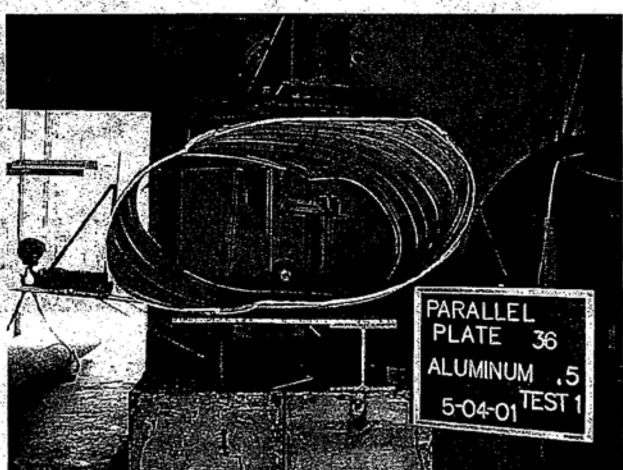

c) Overall unsymmetrical deformed shape at 36%

d) Material yielding at approximately 36%

Fig. 5.23 - Deformed Shapes of Aluminum 36" Pipe Under Parallel Plates at Different Vertical Deflections

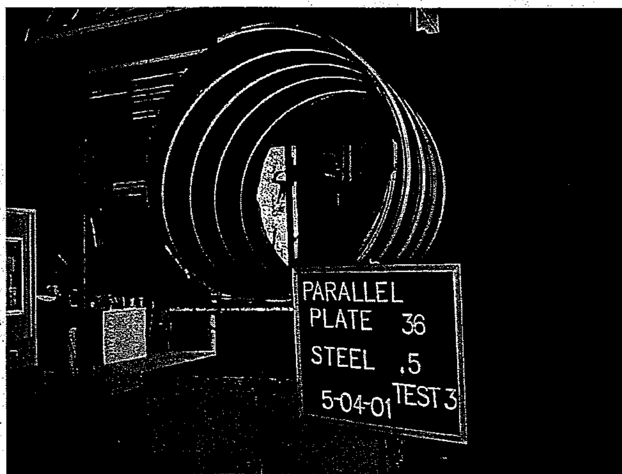

a) At 0% deflection

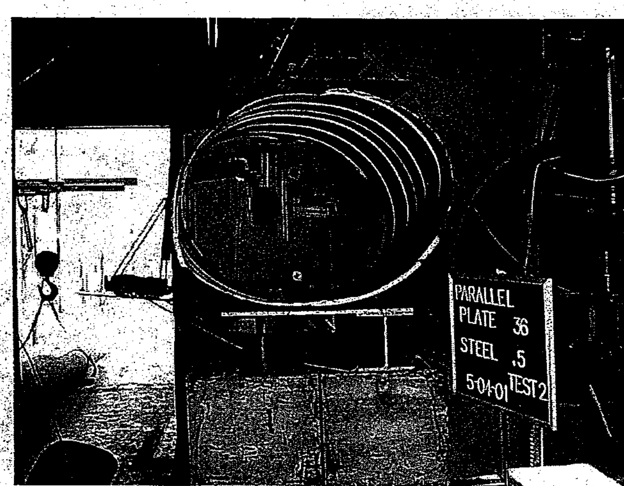

b) Overall elliptical deformed shape at approximately 15%

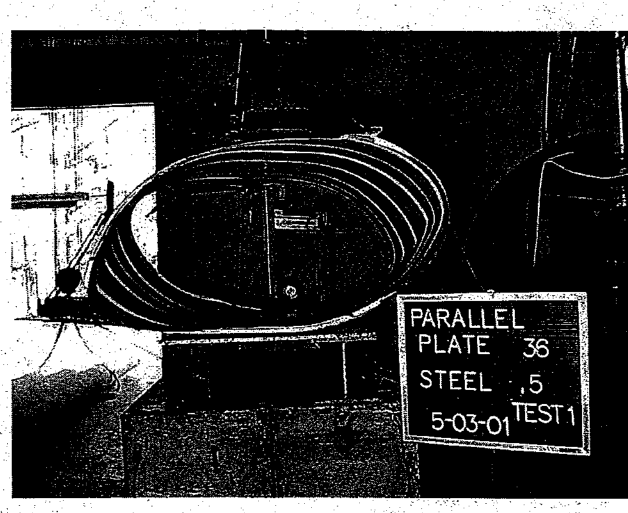

c) Overall unsymmetrical deformed shape at 36%

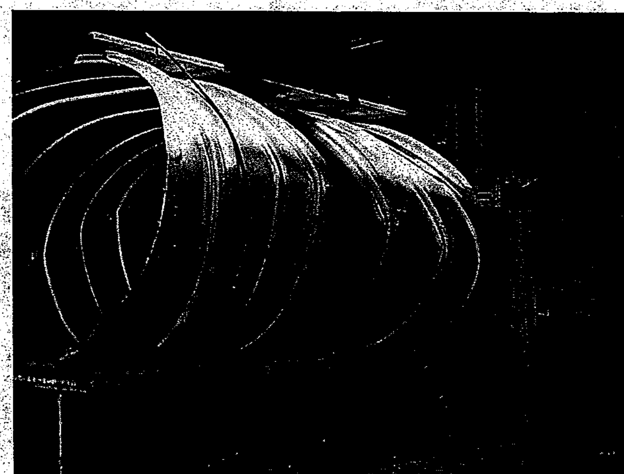

d) Material yielding at approximately 36%

Fig. 5.24 - Deformed Shapes of Steel 36" Pipe Under Parallel Plates at Different Vertical Deflections

Chapter 6: Curved Beam Stiffness Test

6.1 Scope and Objectives

Pipe stiffness (PS) obtained from the parallel-plate loading test (ASTM D2412), is widely used in the modified Spangler equation to obtain an approximate pipe deformation. In the field, reacting forces in response to all external forces are shared by the pipe and the soil element of the pipe-soil composite structure, but in the ASTM D2412 test, the only restraint is in the vertical direction (Gabriel & Goddard, 1999). In the parallel-plate loading test, wall bending is considered as the most dominant effect while ring compression is the least. An alternative measure of pipe stiffness has been proposed by Gabriel & Goddard (1999). In their method, a curved specimen, subtending an arc of 90°, cut from a production run pipe, is loaded at both end (pined-pined constraints) with external compressive forces. At the same magnitude of loading, the curved beam is believed to have less bending moment in the walls at the springline than the parallel plate test. Thus, a greater proportion of the wall's compression and a lesser proportion of the wall's bending moment makes up the response of the curved beam than that of the parallel plate test. Hence, it is claimed that the curved beam stiffness test approximates more closely the field condition of the buried pipe.

The objective of this section is to find the pipe stiffness by using the above curved beam approach. Investigating the pipe behavior (Load vs. deflection, Deflection vs. strains, etc.) under the curved beam conditions for different loading rates is another objective pursued in this part of the study.

6.2 Experimental Program Apparatus

A hydraulic jack with a varying rate of crosshead movement is used to apply external forces for the tests. A load cell is used to continuously record, this external compressive force with time before and during the periods of loading. The reaction frames were made from 3/8 I-beam steel structure and 3/8 steel plates. A special device is fabricated and welded to the testing frame to hold the thermoplastic specimen. Typical setups for thermoplastic and metal specimens, can be seen in Figs. 6.4 to 6.9. Two deflectometers (LVDT) are used to continuously measure both vertical and horizontal displacements of the test specimens, Fig.

6.1. Strain gages were also installed on one specimen (load rate of 0.5 in./min.) of each series to monitor the strains on the concave wall (inner wall) and the convex wall (outer wall) of the pipe, as shown in Fig. 6.2.

Test specimen

The test specimens are cut from randomly selected sections. The longitudinal length of the test specimens cut from ADS 48" pipes is 40 inches. The length of 36 inches was chosen for the test specimens cut from 36-in. diameter HDPE, PVC, aluminum and steel pipes. The longitudinal edges of the test specimen were made to have a smooth plane, free of jagged edges and burrs. Fig. 6.3 illustrates the test specimens cut from a 40-in. (48-in. diameter pipe) and 36-in. (36-in. diameter pipe) width ring. Table 6.1 presents the geometric properties of the specimens.

Test Procedure

The average of three measurements of the longitudinal length at mid- and quarter-points of the arc of the curved specimen is first determined. The test is conducted by applying a nearly instantaneous load to the longitudinally cut edges of the 90° section of the specimen until 10% shortening of the chord connecting the longitudinal edges is attained. Four different rates of the crosshead 0.05, 0.5, 10, and 150 in./min. were used during the loading of each pipe. Load and displacement readings were continuously recorded. The load versus displacement for various rates of the cross-head movement was plotted for different types of specimens.

Test Program

Details of the curved-beam test program carried out in this study are presented in Table 6.2.

6.3 Time-Independent Pipe Stiffness, K(0)

The time-independent pipe stiffness, K(0) in pounds per square inch is calculated using the following procedure:

i) Percent displacement (% displacement) is calculated by dividing the change in vertical displacement of the chord length of the specimen, by its original chord length, and then multiplying by 100.

ii) "The time-dependent pipe stiffness, K(t) is calculated from the load-vertical displacement data at five points from 2% to 4% displacements as given by the equation below:

$$K(t) = F /(L.\Delta y) \tag{6.1}$$

Where, F = measured load at the specified deflection on the full length of the curved beam specimen in pounds (lbs.), Δy = the specified displacement for each percent deflection in inches (in),. L = the length of test curved beam test specimen in inches (in.).

iii) The time-dependent stiffness values, K(t) versus the % displacements are plotted.

iv) A linear least squares curve is fitted through the points between 2% and 4% displacements.

v) The straight line is extrapolated linearly to the y-axis intercept giving the time-dependent K(0).

6.4 Presentation and Discussions of Results

Overall Behavior

Views of specimens ready for testing (i.e., initial state of deformation), during testing (i.e., deformed state), and at failure, are respectively presented in Figs. 6.4 to 6.9. for ADS 48", ADS 36", Hancor 36", PVC 36", Steel 36" and Aluminum 36". Table 6.3 summarizes the characteristic values corresponding to 5% and 10% vertical ring deflection. It is observed that the vertical/horizontal deflection ratio (Δ_v/Δ_x) is higher for 5% vertical deflection than for 10% vertical deflection. Also, the ratio (Δ_v/Δ_x) did not vary as the loading rate was varied. For 5% vertical deflection, the average value of (Δ_v/Δ_x) was 1.09 for ADS 48", 1.08 for ADS 36", 1.20 for Hancor 36, 1.14 for PVC 36", 1.04 for Steel 36", and 1.11 for Aluminum 36".

Load versus Deflections

The curves representing the applied load versus the vertical and horizontal deflections are shown in Figs. 6.10 to 6.15 for ADS 48", ADS 36", Hancor 36", PVC 36", Steel 36" and Aluminum 36", respectively.

Load versus Strains and Vertical Deflection versus Strains

The curves representing the applied load versus strain readings on the one hand and the vertical deflection versus the strain readings on the other, are shown in Figs. 6.16 to 6.21 for respectively ADS 48", ADS 36", Hancor 36", PVC 36", Steel 36" and Aluminum 36". Table 6.4 summarizes the values of the strains recorded in the different pipes for 5% and 10% vertical deflections and the corresponding applied loads. From this table, the following observations can be formulated: (a) At a vertical deflection of 5% of the diameter, the tensile strains at the outer surface were similar for all the pipes and varied between 15,292με and 18,026με; (b) The compressive strains varied considerably from one type of pipe to another. At the vertical deflection of 5% of the diameter, it was equal to 17με for ADS 48", 6,627με for ADS 36", 14,078με for Hancor 36", 12,169με for PVC 36", 3,710με for Steel 36" and 1,395με for Aluminum 36".

Time-Independent Pipe Stiffness

A linear least square fit of time dependent stiffness, K(t), versus the vertical displacement in percentage of the original chord length, is presented in Figs. 6.22a to 6.22f for ADS 48", ADS 36", Hancor 36", PVC 36", Steel 36" and Aluminum 36", respectively.

The time-independent pipe stiffness, K(0) corresponding to the y-axis intercepts of the curves was determined for each of the twelve tests of the program, and the results are summarized in Table 6.5. The average pipe stiffness (PS) values obtained from the parallel plate tests (see chapter 4) are also given between parentheses for comparison purposes. From this table, the following observations can be made: (a) for HDPE pipes, the time-independent pip e stiffness, K(0) increased as the loading rate increased; (b) for PVC, no noticeable variation of K(0) with the loading rate was observed; (c) the K(0) values are 2 to 3 times greater than the PS values obtained from the parallel plate tests.

6.5 Conclusions

The following conclusions can be drawn:

(a) The K(0) values increase with the loading rate. They are 2 to 3 times greater than the PS values determined by the parallel plate test.

(b) For a vertical deflection of 5% of the diameter, the tensile strain in the outer wall was approximately equal to 18,000με (i.e., 1,980 psi) for all HDPE, 17,000gs (i.e., 6,800 psi) for PVC and 16,000με (i.e., 60 ksi for steel and 21 ksi for aluminum) for metal pipes. The compressive strain in the inner wall ranged from 0 to 14,000gs for plastic pipes and from 1,400με to 3,700με for metal pipes.

Table 6.1 - Geometric Properties of Arch Specimens

Pipe Type	ID (in.)	OD (in.)	Chord Length $(OD/\sqrt{2})$ (in.)
ADS 48	47.02	52.32	40.00
ADS 36	36.00	41.57	29.39
HANCOR 36	35.71	41.48	29.33
PVC 36	35.51	38.77	27.41
STEEL 36	35.84	36.31	25.68
ALUMINUM 36	35.85	37.28	26.36

Table 6.2 - Curved-Beam Test Program

Type of Pipe	Load Rate (in/min.)	Number of Tests
ADS 48	0.05	2
	0.5	2
	10	2
	150	2
ADS 36	0.05	2
	0.5	2
	10	2
	150	2
Hancor 36	0.05	2
	0.5	2
	10	2
	150	2
PVC 36	0.5	2
Steel 36	0.5	2
Aluminum 36	0.5	2

Table 6.3 - Summary of Experimental Results

Series	Load Rate/Specimen #	5% Vertical Deflection				10% Vertical Deflection			
	(in./min.)	Load (Lbs/in.)	Δ_v (in.)	Δ_x (in.)	Δ_v/Δ_x	Load (Lbs/in.)	Δ_v (in.)	Δ_x (in.)	Δ_v/Δ_x
ADS 48	0.05-1	84.26	2.402	2.24	1.07	88.39	4.800	4.05	1.19
	0.05-2	70.00	2.401	2.34	1.03 (1.05)[a]	73.32	4.800	4.06	1.18 (1.18)
	0.5-1	104.34	2.408	2.15	1.12	110.31	4.365	3.75	1.16
	0.5-2	94.26	2.406	2.28	1.06 (1.09)	97.77	3.258	2.95	1.10 (1.13)
	10-1	144.80	2.399	2.02	1.19	151.37	4.761	3.88	1.23
	10-2	140.08	2.390	2.14	1.12 (1.15)	142.15	4.776	3.91	1.22 (1.22)
	150-1	189.65	2.343	2.185	1.07	197.38	4.791	4.07	1.18
	150-2	180.20	2.355	2.228	1.06 (1.06)	178.48	4.825	4.20	1.15 (1.16)
ADS 36	0.05-1	82.03	1.804	1.77	1.02	82.25	3.605	3.20	1.13
	0.05-2	77.04	1.801	1.70	1.06 (1.04)	77.17	3.602	3.01	1.20 (1.16)
	0.5-1	107.60	1.806	1.59	1.14	110.33	3.607	3.04	1.19
	0.5-2	112.63	1.801	1.76	1.02 (1.08)	109.45	3.60	3.19	1.13 (1.16)
	10-1	142.80	1.804	1.58	1.14	139.45	3.66	3.00	1.22
	10-2	148.48	1.779	1.38	1.29 (1.22)	145.44	3.64	2.91	1.25 (1.24)
	150-1	148.48	1.779	1.383	1.29	146.31	4.791	4.07	1.17
	150-2	146.66	1.897	1.708	1.11 (1.20)	138.54	4.825	4.20	1.15 (1.16)
HANCOR 36	0.05-1	59.94	1.803	1.66	1.09	57.42	3.605	2.98	1.21
	0.05-2	61.50	1.801	1.58	1.14 (1.11)	62.19	3.602	2.90	1.24 (1.2)
	0.5-1	73.35	1.801	1.51	1.20	72.66	3.605	2.84	1.27
	0.5-2	76.47	1.801	1.52	1.20 (1.20)	80.16	3.602	2.82	1.28 (1.27)
	10-1	81.11	1.784	1.37	1.30	77.34	3.629	2.71	1.34
	10-2	84.76	1.767	1.51	1.17 (1.24)	76.30	3.585	2.85	1.26 (1.30)
	150-1	111.24	1.695	1.54	1.10	87.85	3.15	2.67	1.18
	150-2	114.11	1.730	1.45	1.19 (1.15)	107.20	3.69	2.95	1.25 (1.22)
PVC 36	0.05-1	85.11	1.801	1.74	1.04	99.57	3.602	3.22	1.12
	0.05-2	126.43	1.801	1.64	1.10 (1.07)	119.14	2.53	2.23	1.13 (1.13)
	0.5-1	132.07	1.801	1.58	1.14	129.77	3.607	2.93	1.23
	0.5-2	151.00	1.804	1.58	1.14 (1.14)	152.17	3.604	2.92	1.23 (1.23)
	10-1	164.97	1.813	1.62	1.12	188.15	3.597	2.93	1.23
	10-2	158.12	1.828	1.58	1.16 (1.14)	175.22	3.620	2.89	1.25 (1.24)
	150-1	162.54	1.767	1.52	1.16	205.77	3.718	2.92	1.27
	150-2	162.85	1.887	1.62	1.16 (1.16)	191.54	3.607	2.84	1.27 (1.27)
Steel 36	0.5-1	60.50	1.801	1.77	1.02	42.32	3.602	3.18	1.13
	0.5-2	49.31	1.806	1.71	1.06 (1.04)	32.68	3.605	3.05	1.18 (1.16)
Aluminum 36	0.5-1	25.56	1.806	1.64	1.10	20.40	3.605	3.02	1.19
	0.5-2	21.57	1.804	1.62	1.11 (1.11)	15.45	3.602	2.95	1.22 (1.21)

Note: [a] values between parentheses are average values for the load rate considered.

Table 6.4 - Strain Readings for 5% and 10% Vertical Deflection (Loading Rate = 0.5 in./min)

Pipe Type	Vertical Deflection (%)	Vertical Deflection (in.)	Inner SG ($\mu\varepsilon$)	Outer SG ($\mu\varepsilon$)
ADS 48	5	2.406	-17	18 026
	10	3.258[a]	-17	24 402
ADS 36	5	1.395[a]	-6 627	18 726[a]
	10	3.53	-8 390	
HANCOR 36	5	1.801	-14 078	17 932
	10	3.604	-20 361[a]	28 121[a]
			(Δ_v = 3.03 in.)	(Δ_v = 2.78 in.)
PVC 36	5	1.804	-12 169	17 091
	10	---	-19 777[a]	23 765[a]
			(Δ_v = 3.31 in.)	(Δ_v = 2.27 in.)
Steel 36	5	1.806	-3 710	15 854
	10	3.605	-11 119	25 398[a]
				(Δ_v = 2.57 in.)
Aluminum 36	5	1.804	-1 395	15 292
	10	3.602	-2 819	20 357

Note: [a] Maximum/minimum recorded values

Table 6.5 - Time-Independent Pipe Stiffness K (0)

	Load Rate	Test No.	K(0)*	R^{2**}
(a) ADS 48	0.05	1	62.74	0.99
		2	53.04	0.99
		Mean	57.89 (20.75)	
	0.5	2	74.14	0.99
		1	76.31	0.99
		Mean	75.22 (26.91)	
	10	1	113.26	0.997
		2	109.60	0.99
		Mean	111.43 (35.34)	
	150	1	140.8	0.99
		2	144.7	0.99
		Mean	142.8 (46.10)	
(b) ADS 36	0.05	1	93.08	0.99
		2	87.46	0.99
		Mean	90.27 (26.85)	
	0.5	1	113.66	0.99
		2	132.5	0.99
		Mean	123.08 (37.09)	
	10	1	158.27	0.99
		2	153.08	1.00
		Mean	155.68 (49.28)	
	150	1	153.23	1.00
		2	163.12	0.99
		Mean	158.18 (57.51)	
(c) Hancor 36	0.05	1	70.80	0.99
		2	65.62	0.99
		Mean	68.21 (20.93)	
	0.5	1	79.72	1.00
		2	69.00	1.00
		Mean	74.36 (25.53)	
	10	1	82.95	1.00
		2	93.2	1.00
		Mean	88.08 (36.47)	
	150	1	136.70	0.99
		2	121.26	1.00
		Mean	128.98 (-)	
(d) PVC 36	0.05	1	83.77	0.99
		2	141.36	1.00
		Mean	112.56 (-)	
	0.5	1	117.98	1.00
		2	133.94	1.00
		Mean	125.96 (54.62)	
	10	1	137.12	1.00
		2	130.70	1.00
		Mean	133.91 (-)	
	150	1	124.35	0.99
		2	130.78	1.00
		Mean	127.56 (-)	
(e) Steel 36	0.5	1	110.0	0.98
		2	90.8	0.92
		Mean	100.2 (33.12)	
(f) Aluminum 36	0.5	1	34.65	1.00
		2	34.78	0.97
		Mean	34.71 (13.03)	

* The average pipe stiffness (PS) values obtained from the parallel plate tests are given between parentheses.
** Coefficient of Determination

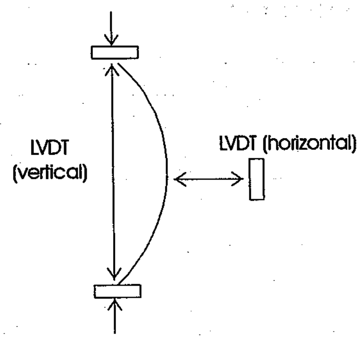

Figure 6.1 - Schematic of Locations of Vertical and Horizontal Deflectometers

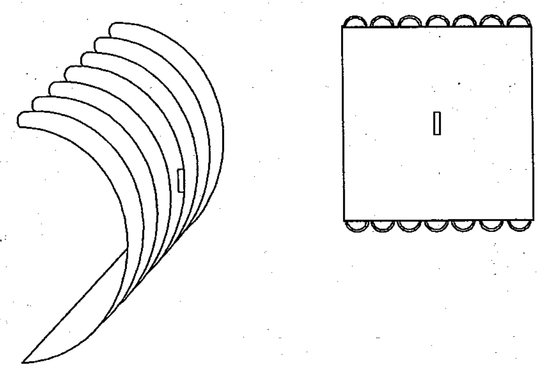

Figure 6.2 - Schematic of Locations of Strain Gages on the Inner and Outer Pipe Walls

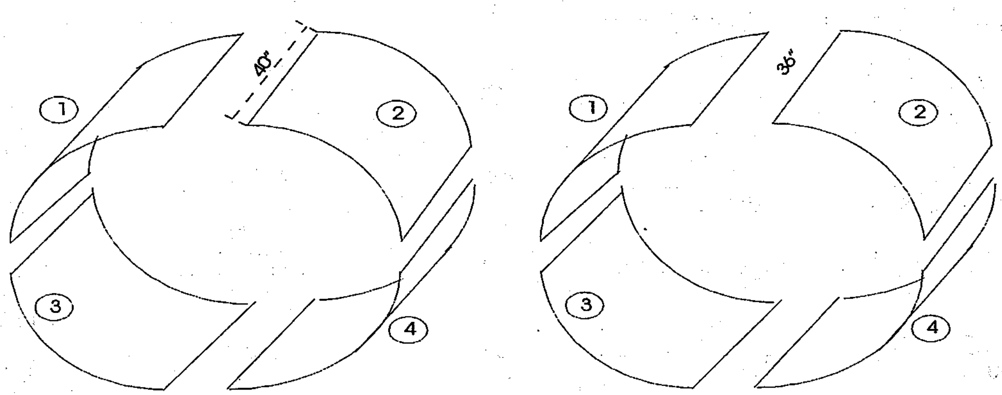

a) 48 in. Diameter Pipe **b) 36 in. Diameter Pipe**

Figure 6.3 - Pipe Ring Cut Into 4 Test Specimens

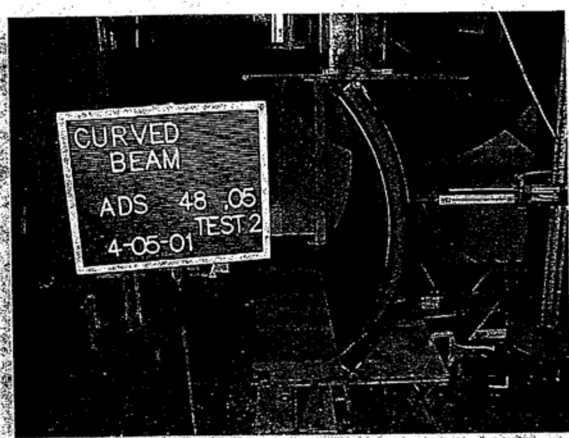

a) Initial shape prior to testing

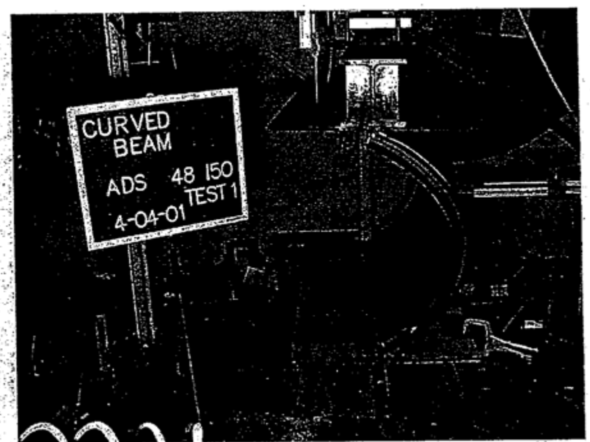

b) Deformed shape during testing

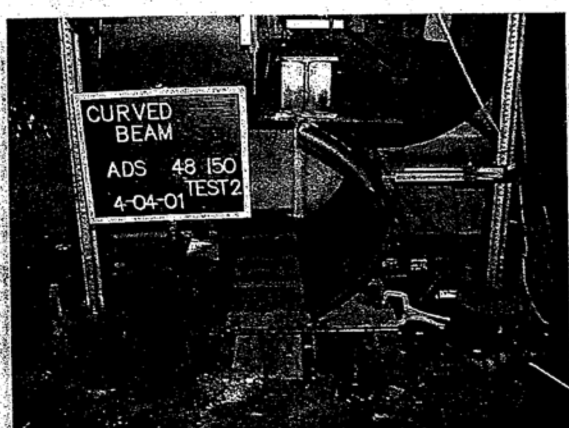

c) Deformed shape at failure

d) Local buckling at failure

Fig. 6.4 - Views of ADS 48 Specimen at Different Deformed Shapes During Curved-Beam Tests

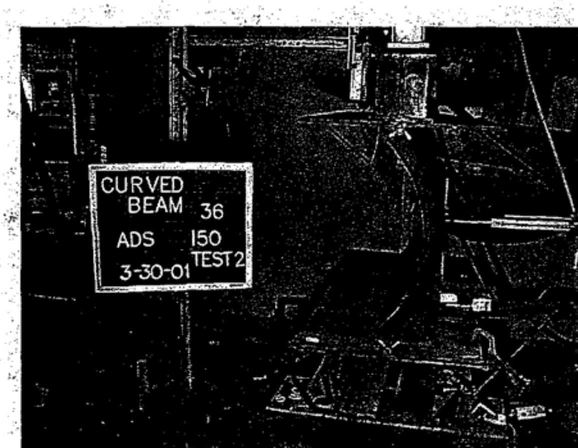

a) Initial shape prior to testing

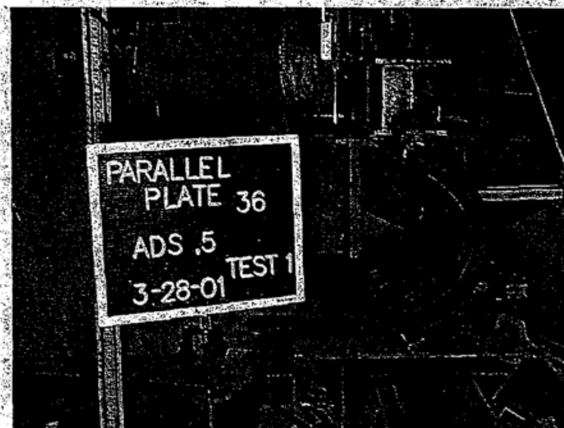

b) Deformed shape during testing

c) Deformed shape at failure

d) Rupture at failure

Fig. 6.5 - Views of ADS 36 Specimen at Different Deformed Shapes During Curved-Beam Tests

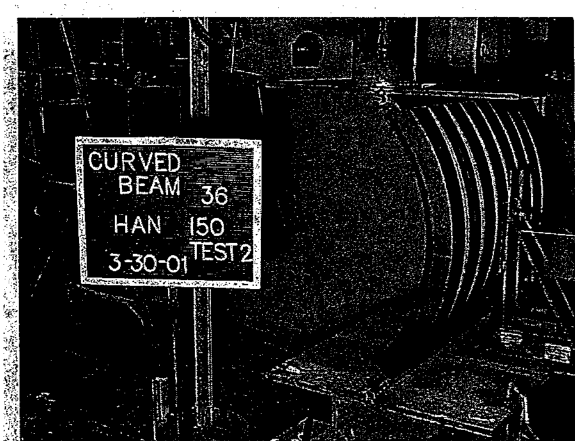

a) Initial shape prior to testing

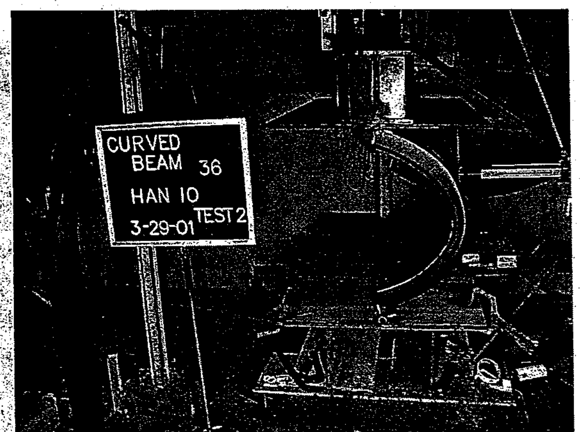

b) Deformed shape during testing

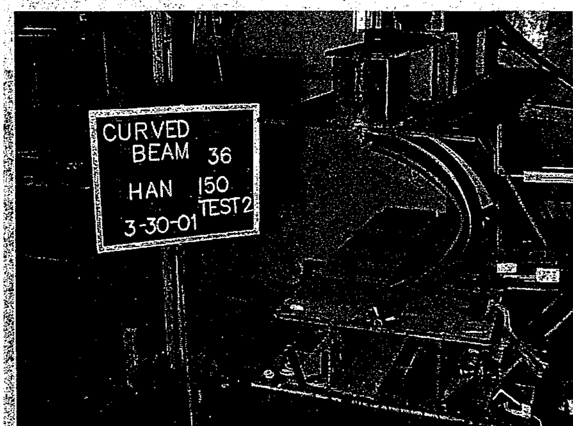

c) Deformed shape at failure

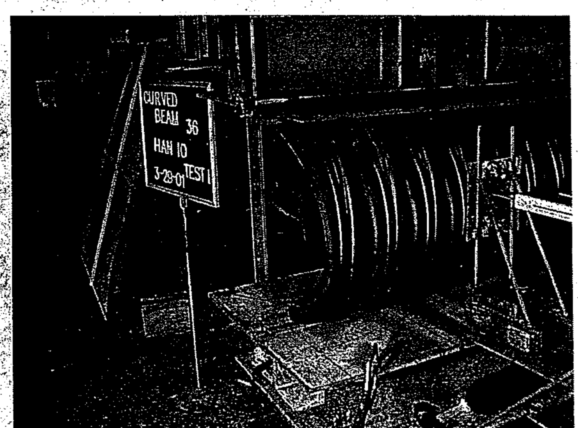

d) Corrugation buckling at failure

Fig. 6.6 - Views of HANCOR 36 Specimen at Different Deformed Shapes During Curved-Beam Tests

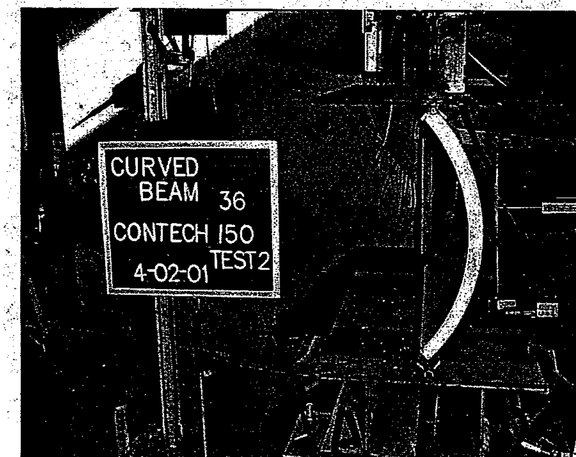

a) Initial shape prior to testing

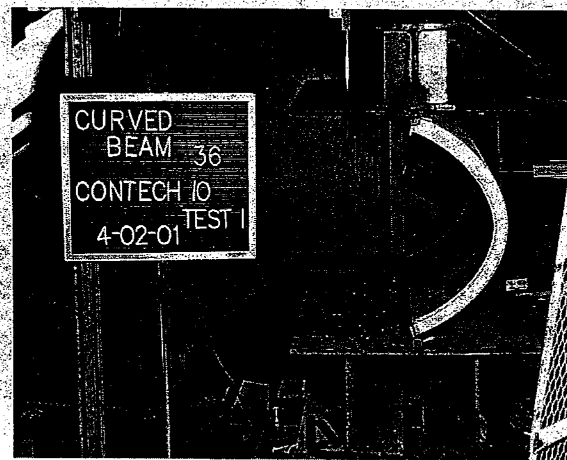

b) Deformed shape during testing

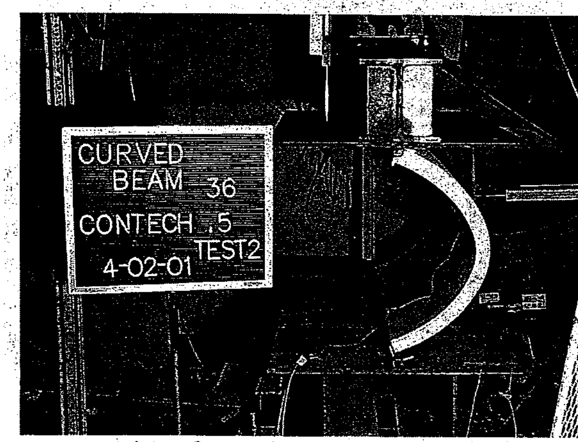

c) Deformed shape at failure

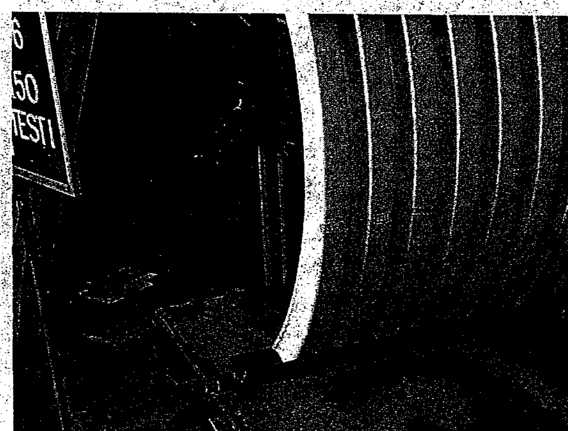
d) Line of buckling at failure

Fig. 6.7 - Views of PVC 36 Specimen at Different Deformed Shapes During Curved-Beam Tests

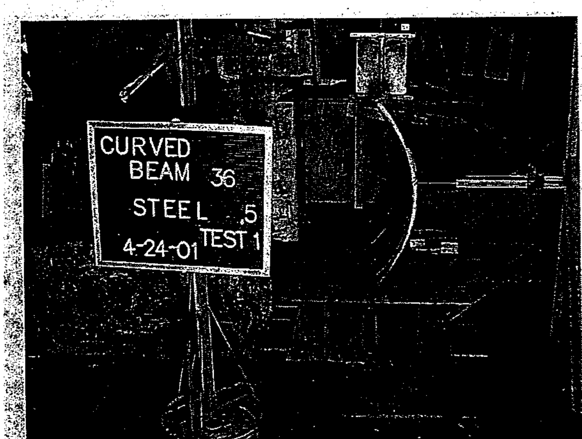

a) Initial shape prior to testing

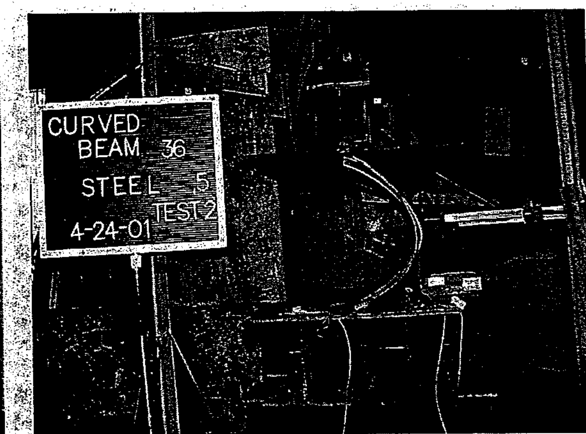

b) Deformed shape during testing

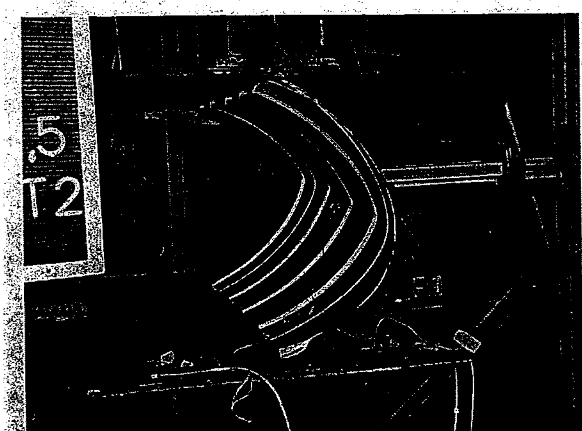

c) Deformed shape at failure

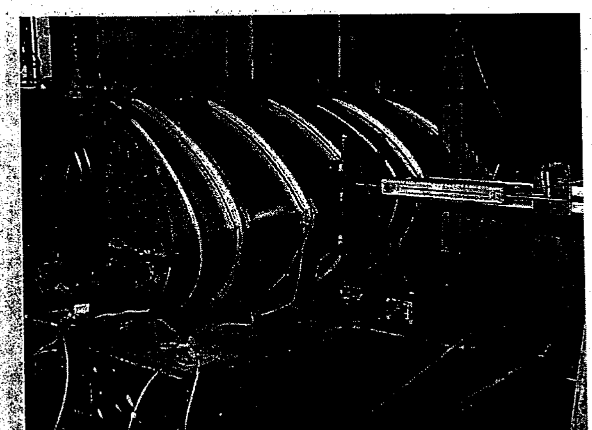
d) Yielding of steel at failure

Fig. 6.8 - Views of STEEL 36 Specimen at Different Deformed Shapes During Curved-Beam Tests

a) Initial shape prior to testing

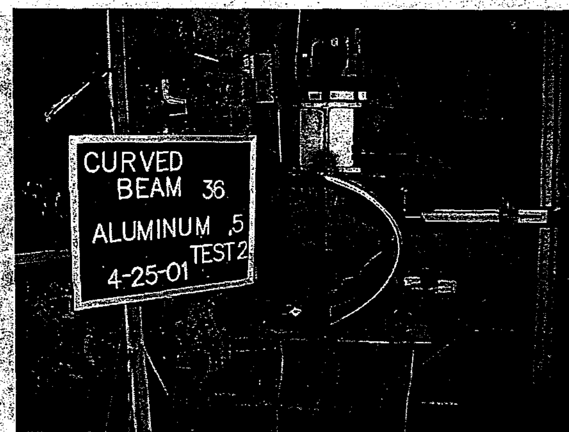

b) Deformed shape during testing

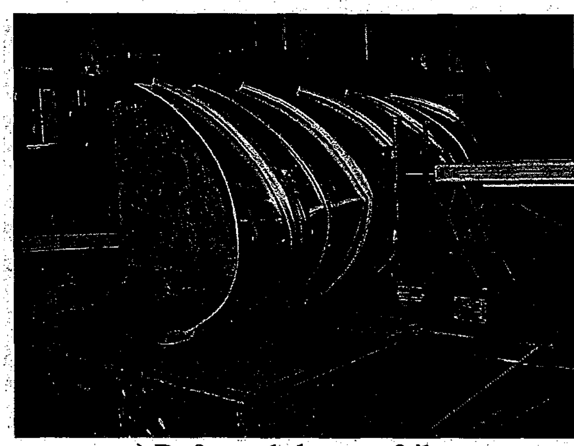

c) Deformed shape at failure

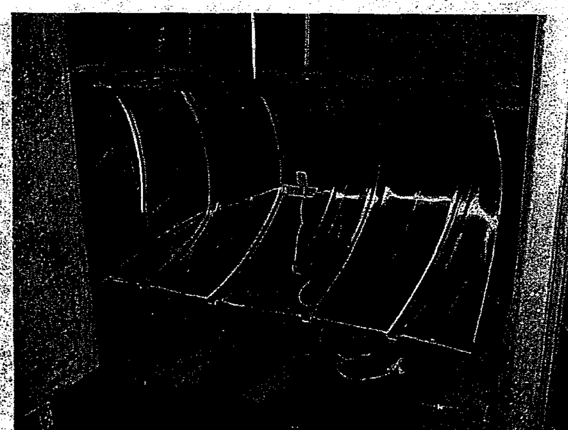

d) Yielding of aluminum at failure

Fig. 6.9 - Views of ALUMINUM 36 Specimen at Different Deformed Shapes During Curved-Beam Tests

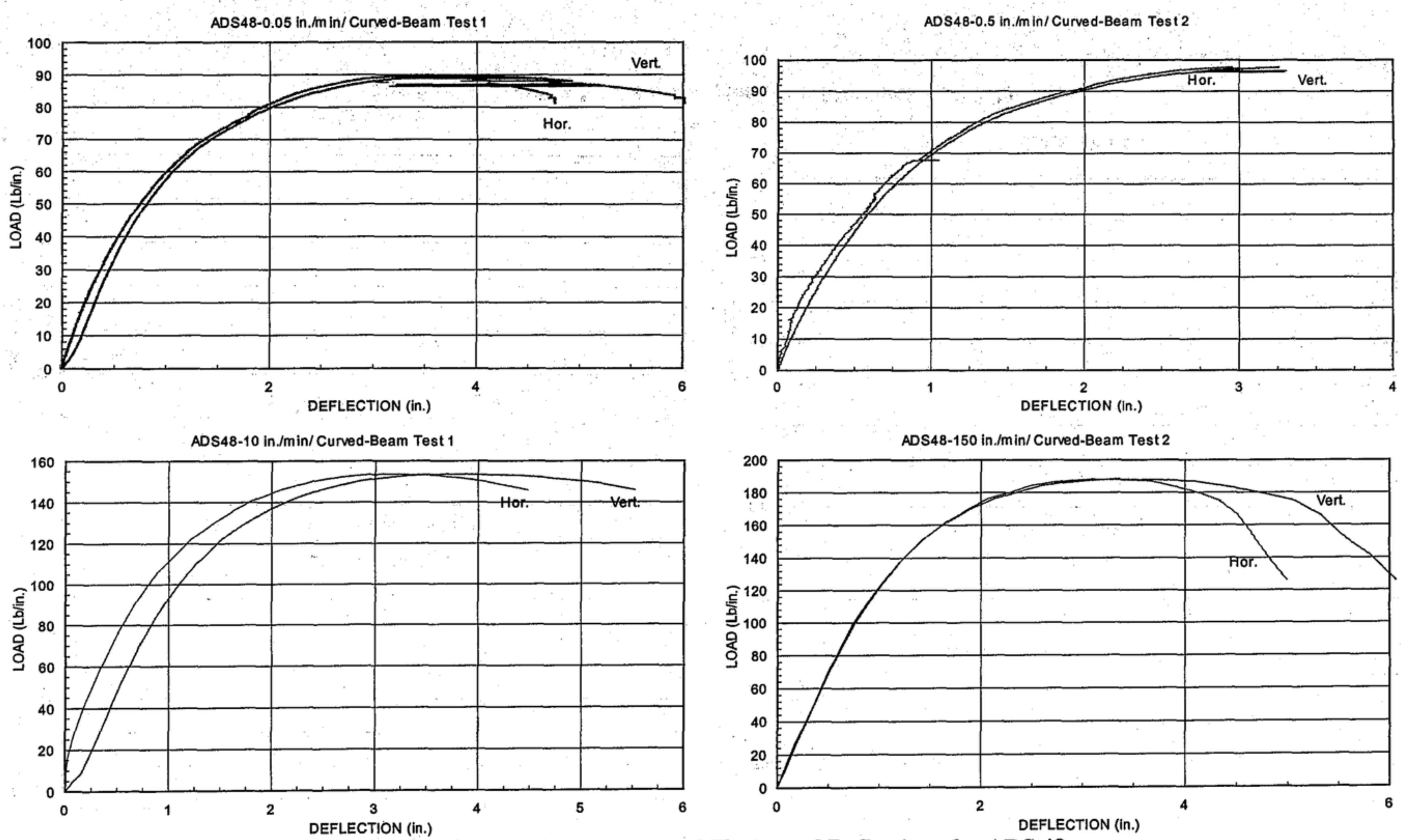

Fig. 6.10 - Load vs Vertical and Horizontal Deflections for ADS 48

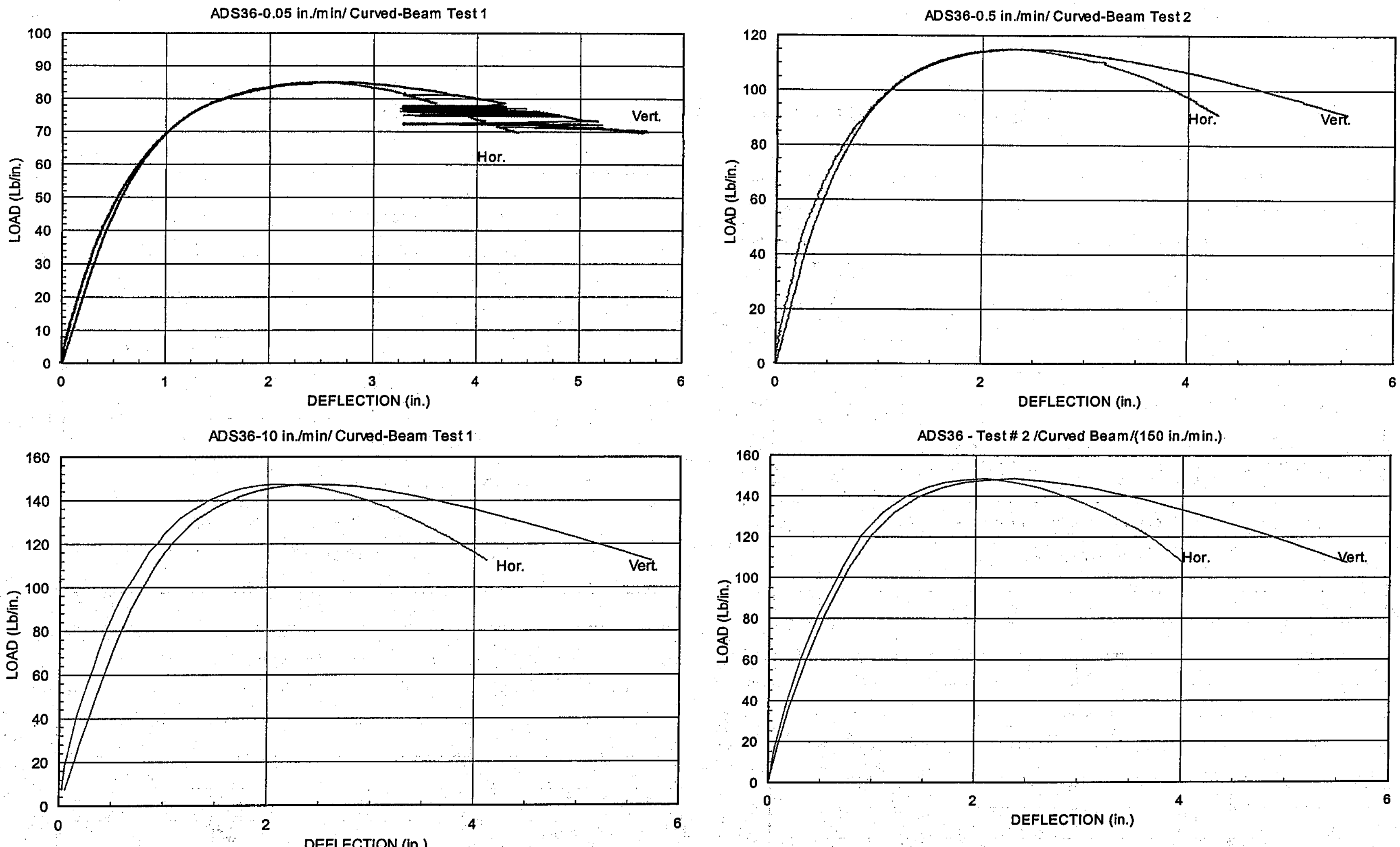

Fig. 6.11 - Load vs Vertical and Horizontal Deflections for ADS 36

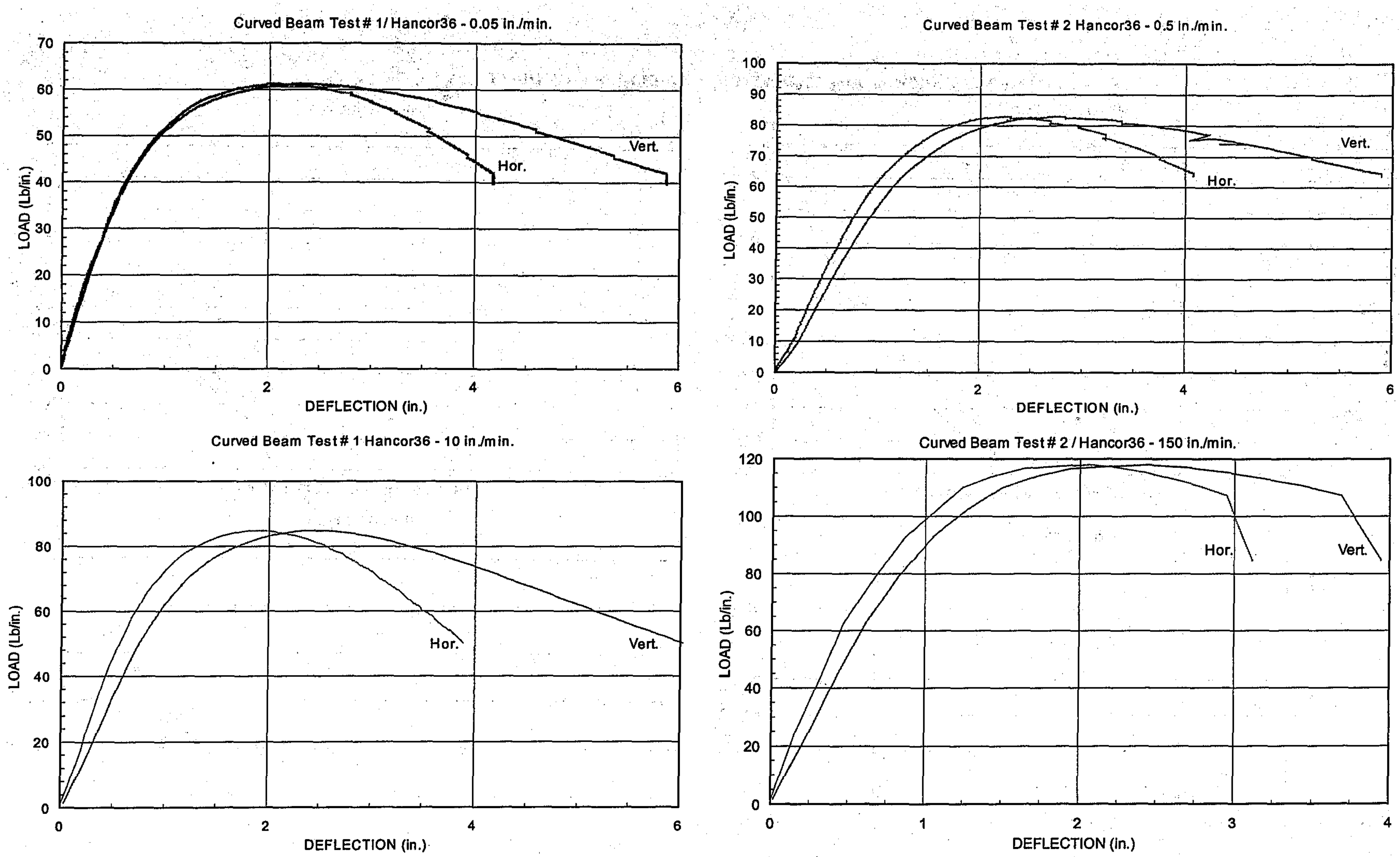

Fig. 6.12 - Load vs Vertical and Horizontal Deflections for Hancor 36

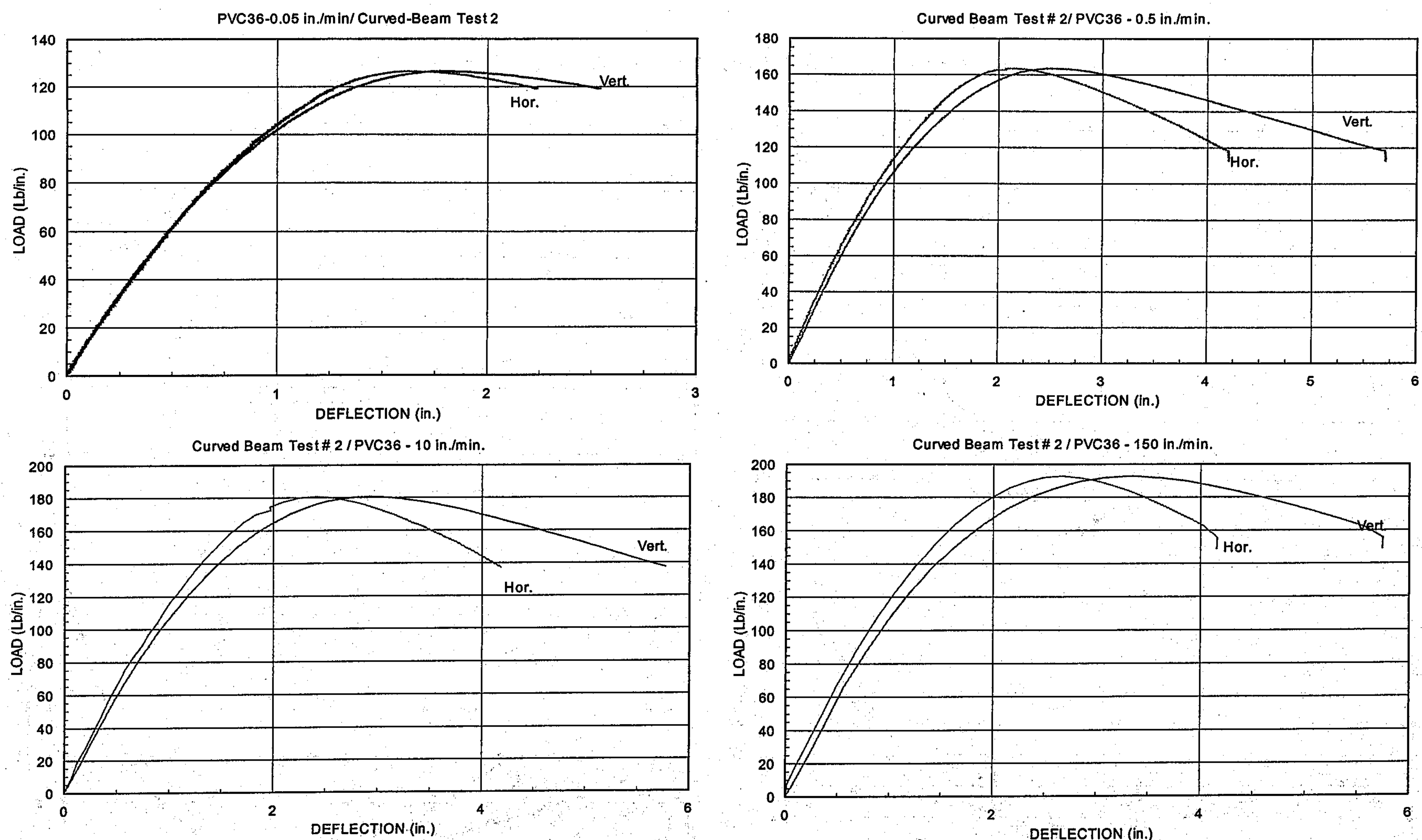

Fig. 6.13 - Load vs Vertical and Horizontal Deflections for PVC 36

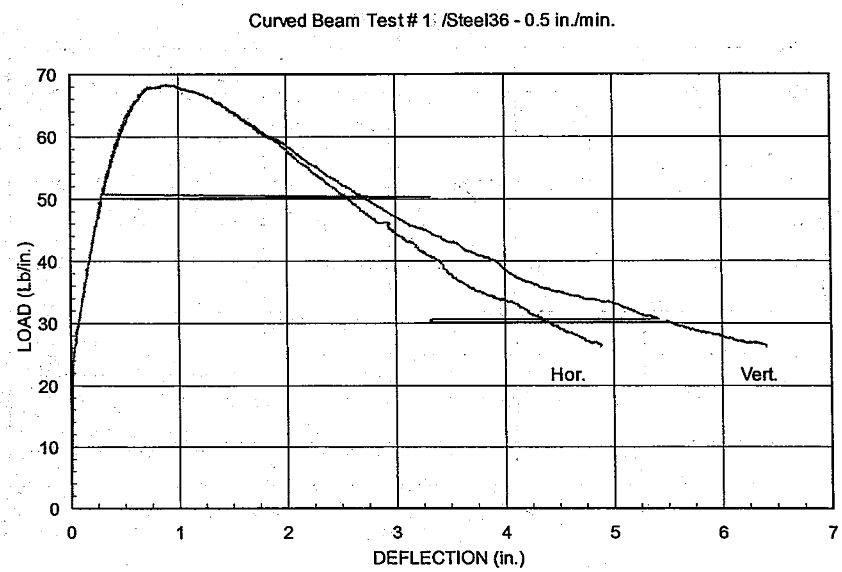

Fig. 6.14 - Load vs Vertical and Horizontal Deflections for Steel 36

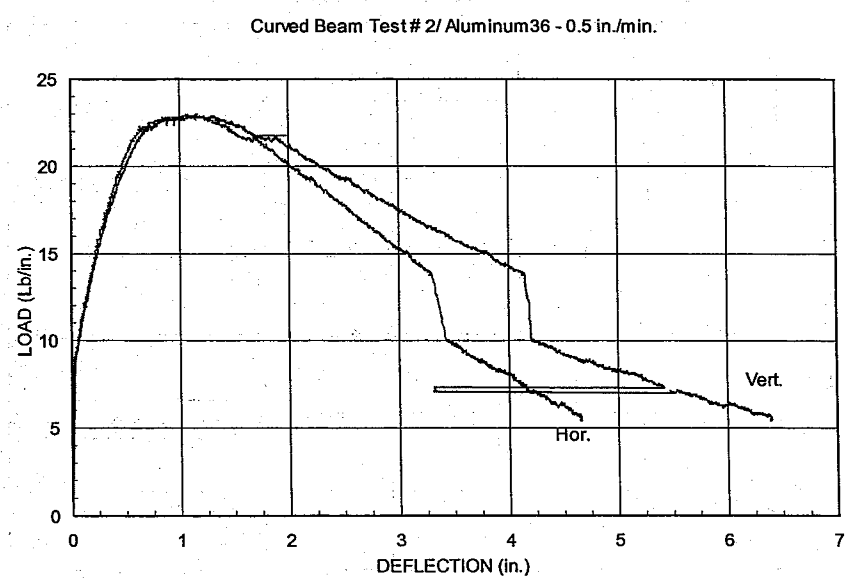

Fig. 6.15 - Load vs Vertical and Horizontal Deflections for Aluminum 36

(a) Load vs Strains

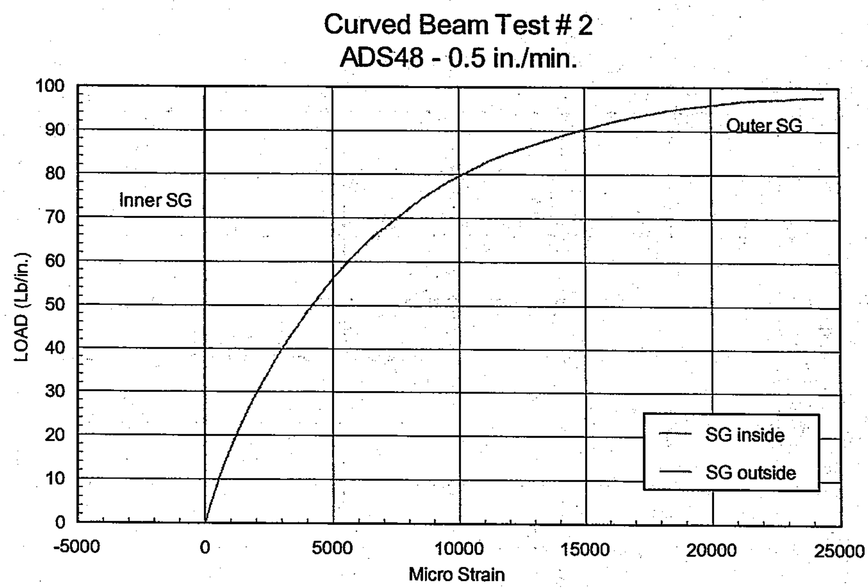

(b) Vertical Deflection vs Strains

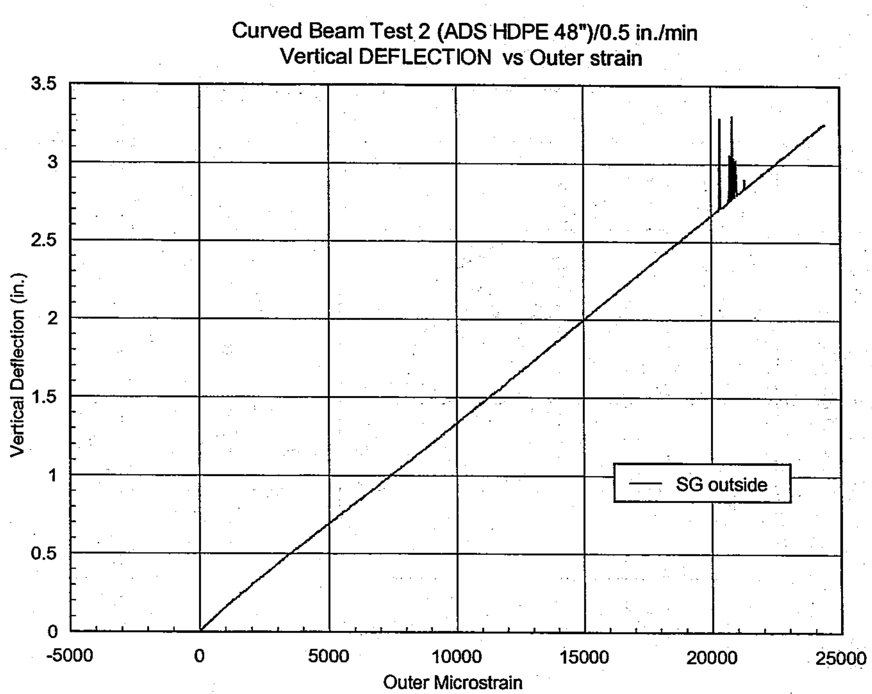

Fig. 6.16 - Load and Vertical Deflection vs Strains for ADS 48

(a) Load vs Strains

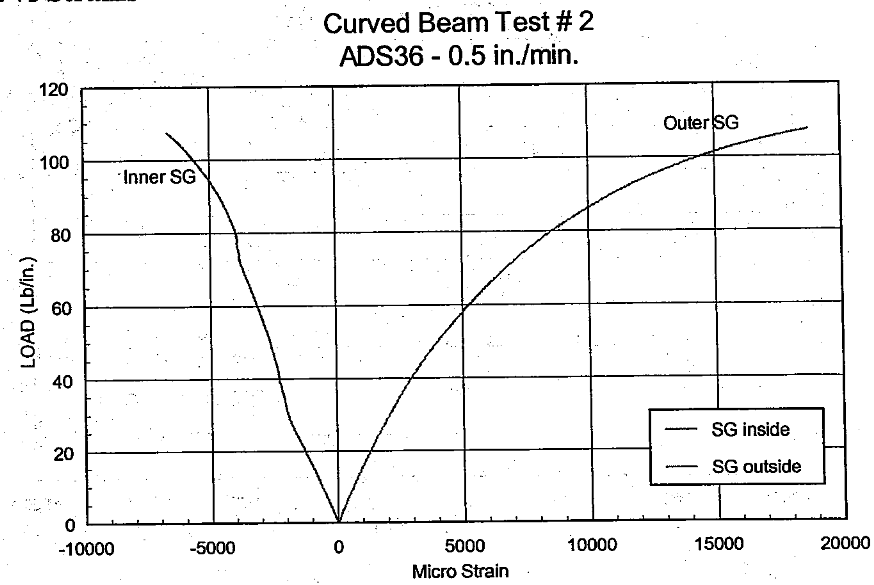

(b) Vertical Deflection vs Strains

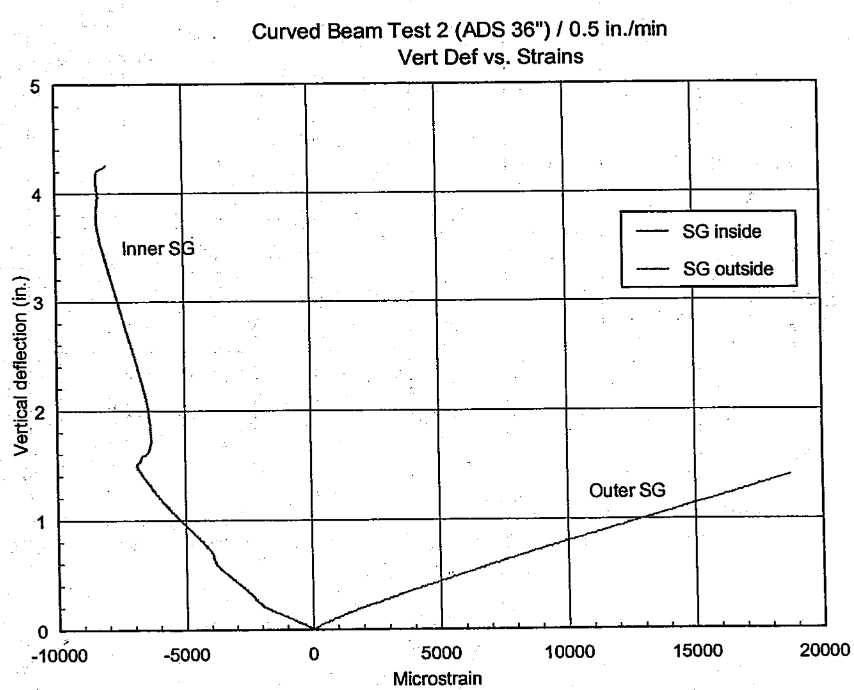

Fig. 6.17 - Load and Vertical Deflection vs Strains for ADS 36

(a) Load vs Strains

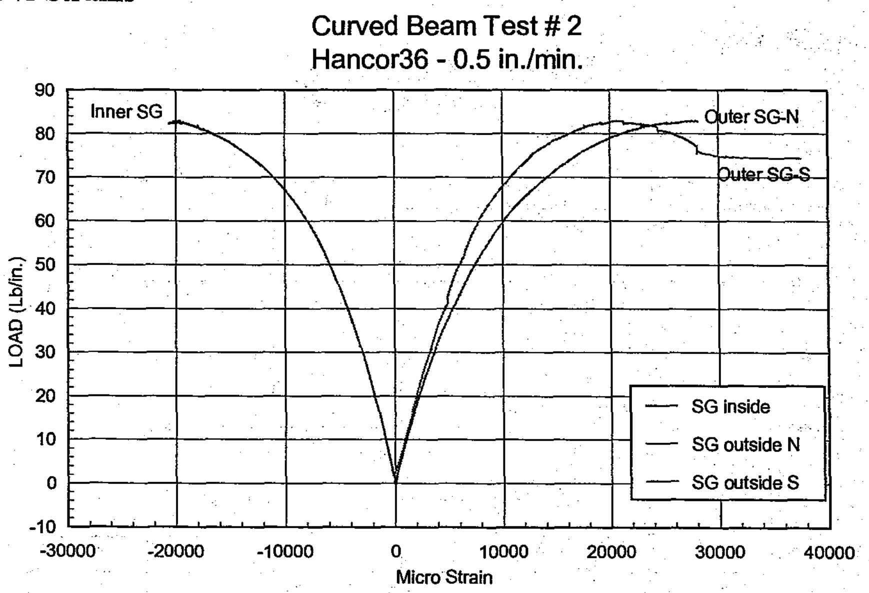

(b) Vertical Deflection vs Strains

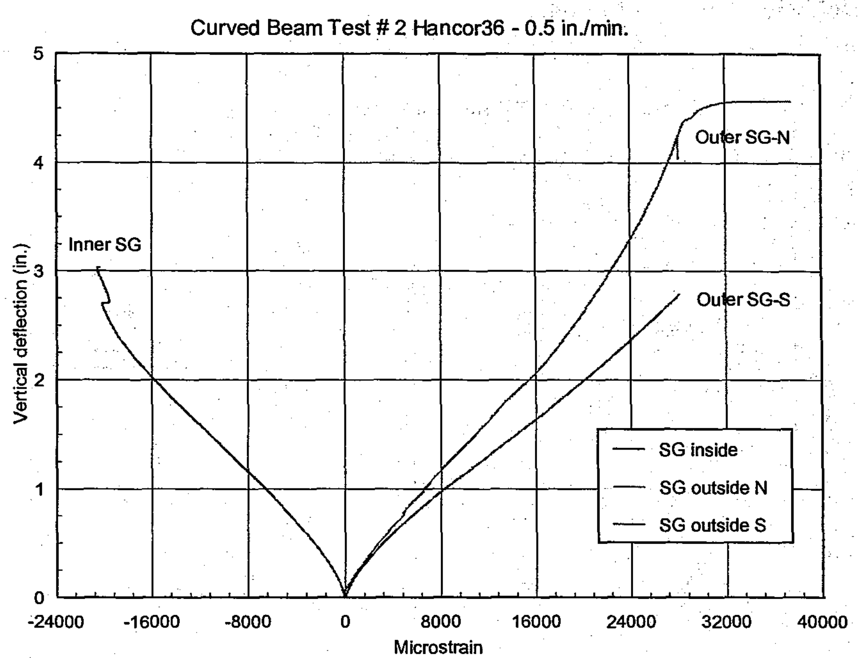

Fig. 6.18 - Load and Vertical Deflection vs Strains for Hancor 36

(a) Load vs Strains

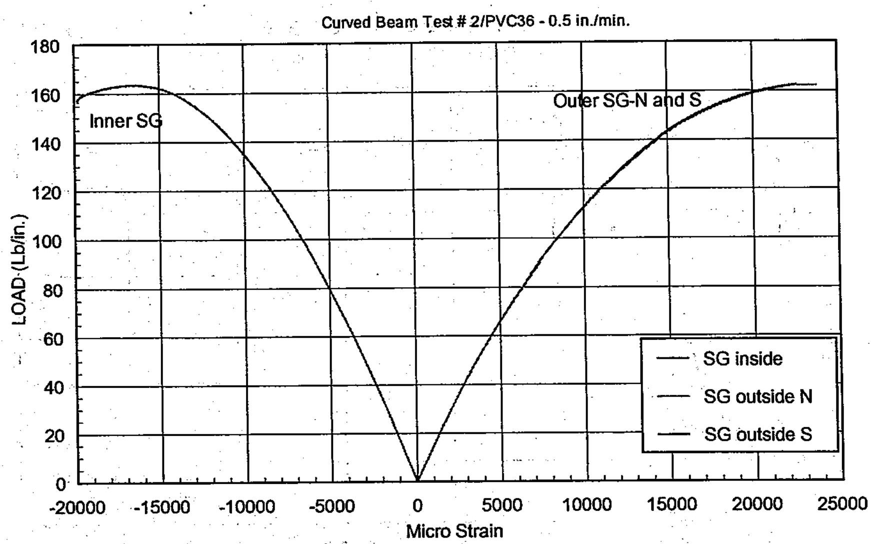

(b) Vertical Deflection vs Strains

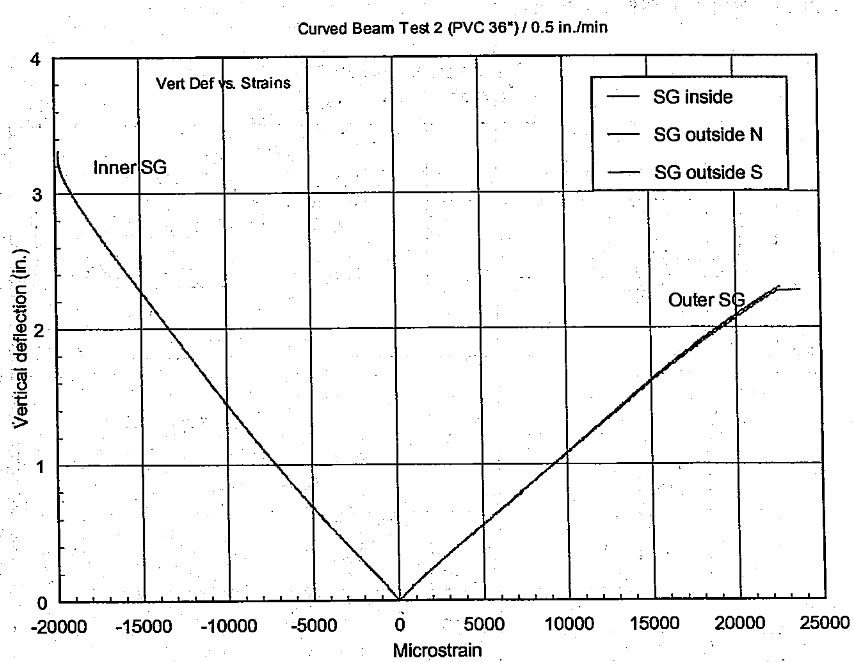

Fig. 6.19 - Load and Vertical Deflection vs Strains for PVC 36

(a) Load vs Strains

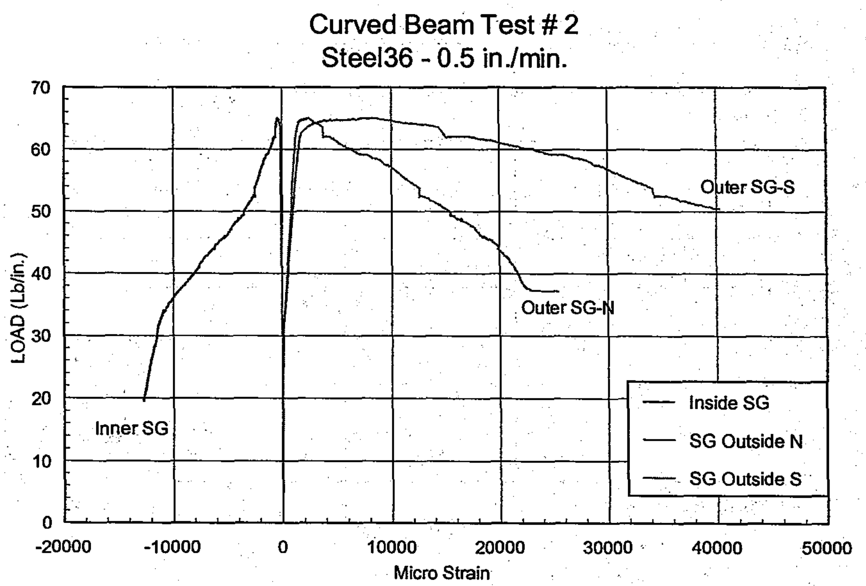

(b) Vertical Deflection vs Strains

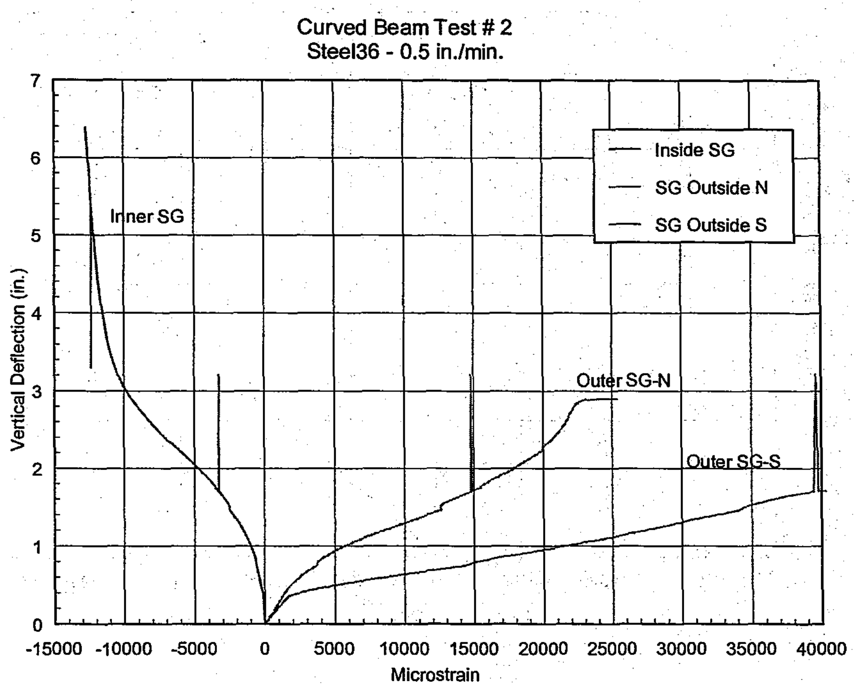

Fig. 6.20 - Load and Vertical Deflection vs Strains for Steel 36

(a) Load vs Strains

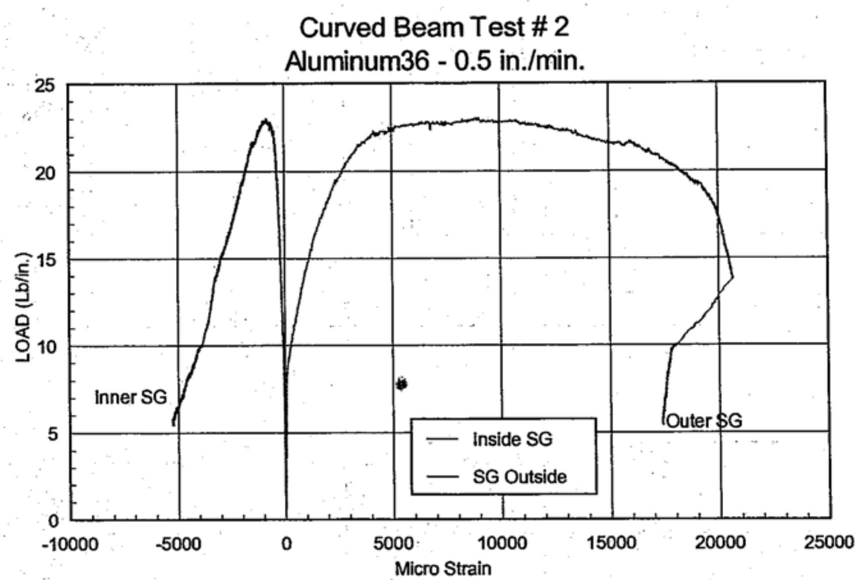

(b) Vertical Deflection vs Strains

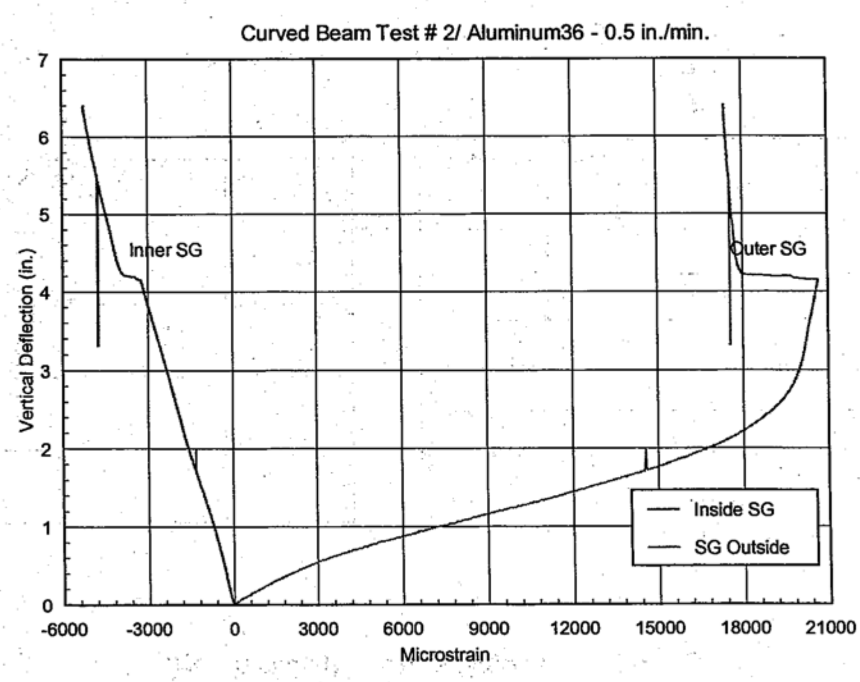

Fig. 6.21 - Load and Vertical Deflection vs Strains for Aluminum 36

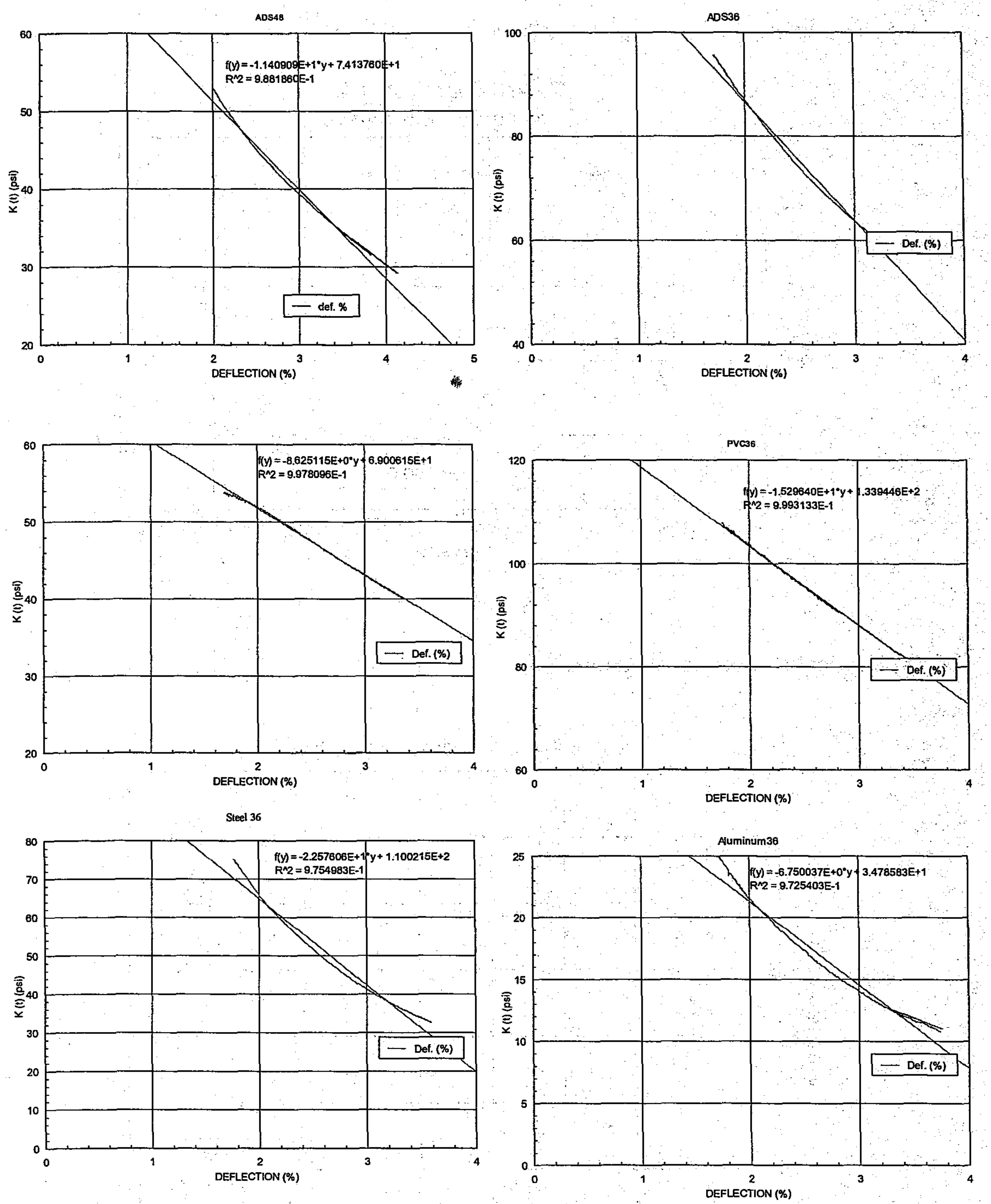

Fig. 6.22 - Typical Curve Fittings for K(0)

Chapter 7: Joint Integrity Test

7.1 Objectives

The objective of this test is to identify any damage of the joints of the HDPE and PVC pipes at the minimum specified deflection of 20% of the nominal pipe diameter. The evaluation of PS of jointed specimens under parallel plate is another objective pursued in this part of the study. The maximum radial distances between pipe and fittings, or between bell and spigot are also recorded during the test and after load removal.

7.2 Experimental Program Apparatus

The hydraulic jack used in the testing has the capability of constant-rate-crosshead movement. The rate of head approach was 0.5 in. per minute. The load could be applied to the flexible pipe through two parallel flat, smooth, and clean steel bearing plates resting over wooden planks. These wooden planks were positioned between the pipe crown and the steel plate on either side of the joint to enable uniform load application similar to the parallel plate testing. The steel plate at the top is welded to a WF steel beam and the load is applied to the center of the WF beam. The thickness of the plates was about 0.875 in., so as to minimize bending or deformation of the plate during testing. The plate length was slightly larger than he specimen length, and the plate width was approximately equal to the pipe contact width at maximum pipe deflection plus 6.0 in. The change in inside diameter was measured using LVDTs in three directions: parallel and perpendicular to the direction of loading, and 45° to the direction of loading. The LVDTs were used to measure to the nearest 0.01in. Fig. 7.1 shows atypical experimental set-up for the test.

Test Specimens

The test specimens (Fig. 7.2) included two sizes: 36-in. and 48-in. diameters. The 36-in. diameter pipes consisted of HDPE and PVC pipes. One type of HDPE pipe was of 48 in. diameter. The test specimens had a total length of 36 inches for the 36-in. diameter pipes and 48 inches for the 48-in. diameter pipe. The ends of specimens were. cut square and free of burrs and jagged edges.

The outside diameter (OD) and the inside diameter (ID) of the test specimens as well as the details of the bell and spigot at the joint for all the pipe types were documented in Chapter 2

Test Procedure

The pipe sections were positioned with its longitudinal axis parallel to the bearing plates and centered laterally in the test set-up. The LVDTs were installed in place (Fig. 7.1). The load was applied through a hydraulic jack on the center of a WF beam.

The connected pipe and fitting were loaded at rates of 0.5 in. per minute. The load-deflection measurements were recorded continuously and observations were made of the pipe connections.

Test Program

Table 7.1 presents details of the test program carried out in this study on joint integrity."

7.3 Observations and Discussion

Pipe *Stiffness*

The pipe stiffness values for jointed specimens under parallel plate were calculated using the same procedure as that outlined in chapter 4, and are presented in Table 7.2 for 5% and 10% vertical deflections. The average values for specimens with no joints are also provided between parentheses for comparison and discussion.

Results show that for HDPE pipes the PS values of specimens with joints, although slightly smaller than, are very similar to corresponding specimens with no joints. For PVC pipes, however, the PS of specimens with joints is substantially greater than that of corresponding specimens with no joints, that is, the increase of the PS average value due to the presence of the joint is 37% and 46% for 5% and 10% vertical deflections, respectively.

Gaps and Openings

Generally, all the specimens with joints behaved satisfactorily for deflections below 10%, where no significant deformations were observed. The maximum openings in this range of deflection was 0.25 inch. As the vertical deflection increased, so did the joint openings and the radial gaps between the two walls. However, the maximum openings and radial gaps observed were relatively small with a maximum opening of 0.75 in. and a maximum radial gap of 1.5 in. for 30 % vertical deflection.

HDPE ADS 48 pipes

Before the joint integrity test, the inside wall surface at the joint of the HDPE ADS 48" pipe presented some irregularities in the radial gap. The initial radial gap at the joint ranged from 0.22 in. to 0.68 in., as presented in Table 7.3. During the test and as the vertical load increased, the radial gap at the joint increased as presented in Table 7.3 for 15% and 30 % vertical deflection. Vertically the maximum radial gap corresponding to 30% vertical deflection was 0.42 in. (crown/invert), whereas it was 1.25 in. in the horizontal direction (springline). Small gaps were also observed at the haunch and shoulder area. Initial joint openings in the longitudinal direction were also observed (approximately 0.2 in. max.), but did not open significantly wider as the load increased. Wall buckling was observed at approximately 30% vertical ring deflection (see Fig. 7.10b). No cracks were observed during the test.

Figs 7.7 to 7.10 show views of the behavior of the ADS 48" pipe joint during the course of the joint integrity test. The diameter recovery was almost complete 24 hours after the end of the test (ID after 24 hour recovery = 45.8 in., compared to original ID = 47.0 in.).

HDPE ADS 36" pipes

Before joint integrity test, the inside wall surface at the joint of the HDPE ADS 36" pipe was smooth. During the test, radial gaps first appeared at the springline area of the specimen joint. With increasing vertical deflection, radial gaps widened and spread to the haunch and shoulder area. Table 7.4a presents the radial gaps recorded for 15% and 30% vertical deflection. The maximum radial gap observed was approximately 0.6 in. at the springline, for 30% vertical deflection.

In addition, openings in the longitudinal direction were also observed, as presented in Table 7.4b for 15% and 30 % vertical deflection. For 30% vertical deflection, the maximum opening in the longitudinal direction was 0.4 in. at the crown/invert, whereas it was 0.75 in. at the springline. No wall buckling and cracks were observed during the test.

Figs 7.11 to 7.15 show views of the behavior of the ADS 36" pipe joint during the course of the joint integrity test. The diameter recovery, was almost complete 24 hours after the end of the test (ID after 24 hour recovery = 35 in., compared to original ID,= 36.0 in.).

HDPE HANCOR 36" pipes

Before the joint integrity test, the inside wall surface at the joint of the HDPE HANCOR pipe was smooth. During the load application, the two parts of the specimen did not deform to the same extent, thereby, creating radial gaps.

The recorded radial gaps at the joint are presented in Table 7.5a for 15% and 30 % vertical deflection. The maximum gap at 30% vertical deflection was 0.63 in. at the crown/invert, whereas it was 1.0 in. at the springline. Openings in the longitudinal direction were also observed. The maximum longitudinal opening observed at 30% vertical deflection was approximately 0.75 in. at the crown/invert. No longitudinal opening was observed at springlines.

At 30% vertical deflection, wall buckling was observed at both the crown and invert.

Figs 7.15 to 7.18 show views of the behavior of the Hancor 36" pipe joint during the course of the joint integrity test. The diameter recovery was almost complete 24 hours after the end of the test (ID after 24 hour recovery = 35.0 in., compared to original ID = 35.85 in.).

PVC 36" pipes

Before the joint integrity test, the inside wall surface at the joint of the PVC 36" pipe was smooth. Under the load application, the two specimens did not deform to the same extent. However, the radial gap between the pipes at the springline was larger than at other areas. The recorded radial gaps are presented in Table 7.6 for 15% and 30 % vertical deflection.

The maximum gap for 30% vertical deflection was 1.5 in. at the springlines. No gap was observed at the crown/invert. No significant joint openings in the longitudinal direction were observed. Prior to the failure, reverse curvature was observed at both the invert and the crown of the pipe.

Figs 7.19 to 7.21 show views of the behavior of the PVC 36" pipe joint during the course of the joint integrity test. The diameter recovery was almost complete 24 hours after the end of the test (ID after 24 hour recovery = 34.25 in., compared to original ID = 35.5 in.).

7.4 Conclusions

The following conclusions can be drawn from the joint integrity results:

(a) Up to 10% vertical deflection, all the pipes behaved satisfactorily with no signs of cracks or excessive gaps.

(b) The radial gaps and longitudinal openings were small and reached 1.5 in. and 0.75 in., respectively, for 30% vertical deflection.

(c) For HDPE ADS 48" and 36" diameter pipes, the presence of joints results in a slight reduction (10% maximum for 5% vertical deflection) of the PS values.

(d) For HDPE Hancor 36", the presence of joints resulted in an increase (23% for 5% vertical deflection) of the PS value.

(e) For PVC pipes, the presence of joints resulted in a significant increase (37% for 5% vertical deflection) of the PS value.

Table 7.1 - Joint Integrity Test Program

Series	Load Rate (in/min.)	Number of Tests
ADS 48	0.5	2
ADS 36	0.5	2
Hancor 36	0.5	2
PVC 36	0.5	2
Steel 36	0.5	2
Aluminum 36	0.5	2

Table 7.2 - Experimental Pipe Stiffness (Load Rate = 0.5 in./min.)

Series	Specimen	5% Vertical Deflection			10% Vertical Deflection		
		Load (Lbs/in.)	Defl. (in.)	PS (psi)	Load (Lbs/in.)	Defl. (in.)	PS (psi)
(a) ADS 48	0.5-1	60.47	2.406	25.13	96.59	4.806	20.10
	0.5-2	57.32	2.404	23.84	89.52	4.800	18.65
	0.5-mean			**24.49**			**19.37**
				(26.91)			(20.44)
(b) ADS 36	0.5-1	54.45	1.806	30.15	90.05	3.600	25.01
	0.5-2	68.05	1.813	37.54	98.42	3.602	27.33
	0.5-mean			33.85			26.17
				(37.09)			(28.62)
(c) HANCOR 36	0.5-1	59.68	1.801	33.14	86.90	3.600	24.14
	0.5-2	53.40	1.801	29.65	86.90	3.605	24.11
	0.5-mean			**31.40**			**24.12**
				(25.43)			(19.89)
(d) PVC 36	0.5-1	139.26	1.806	77.11	258.63	3.600	71.84
	0.5-2	129.84	1.804	72.09	254.44	3.605	70.58
	0.5-mean			**74.60**			**71.20**
				(54.62)			(48.64)

Note: [a] Values between parentheses are average PS values of pipes with no join,t from Table 4.3b

Table 7.3 - Radial Gap at Joint versus Vertical Deflection for ADS 48

Location	Initial Gap (in.)	Gap at 15% Vertical Deflection (in.)	Gap at 30% Vertical Deflection (in.)
Crown	0.4225	0.5470 (0.1245)*	0.84 (0.4175)
Invert	0.6810	0.8740 (0.1930)	1.10 (0.4190)
Springline West	0.2190	0.6400 (0.4210)	1.33 (1.1110)
Springline East	0.3475	1.0325 (0.6850)	1.60 (1.2525)

Note: * Values between parentheses are net values due to ring deflection.

Table 7.4a - Radial Gap at Joint versus Vertical Deflection for ADS 36

Location	Initial Gap (in.)	Gap at 15% Vertical Deflection (in.)	Gap at 30% Vertical Deflection (in.)
Crown	0.0	0.0	0.0
Invert	0.0	0.0	0.0
Springline West	0.0	0.25	0.60
Springline East	0.0	0.25	0.60

Table 7.4b - Joint Opening versus Vertical Deflection for ADS 36

Location	Initial Opening (in.)	Opening at 15% Vertical Deflection (in.)	Opening at 30% Vertical Deflection (in.)
Crown	0.0	0.40	0.40
Invert	0.0	0.40	0.40
Springline West	0.0	0.25	0.75
Springline East	0.0	0.50	0.75

Table 7.5a - Radial Gaps at Joint versus Vertical Deflection for Hancor 36

Location	Initial Gap (in.)	Gap at 15% Vertical Deflection (in.)	Gap at 30% Vertical Deflection (in.)
Crown	0.0	0.0	0.63
Invert	0.0	0.0	0.63
Springline West	0.0	0.50	1.00
Springline East	0.0	0.50	0.875

Table 7.5b - Joint Opening versus Vertical Deflection for Hancor 36

Location	Initial Opening (in.)	Opening at 15% Vertical Deflection (in.)	Opening at 30% Vertical Deflection (in.)
Crown	0.0	0.50	0.75
Invert	0.0	0.50	0.75
Springline West	0.0	0.00	0.0
Springline East	0.0	0.00	0.0

Table 7.6 - Radial Gap at Joint versus Vertical Deflection for PVC 36

Location	Initial Gap (in.)	Gap at 15% Vertical Deflection (in.)	Gap at 30% Vertical Deflection (in.)
Crown	0.0	0.00	0.0
Invert	0.0	0.00	0.0
Springline West	0.0	0.60	1.50
Springline East	0.0	0.60	1.50

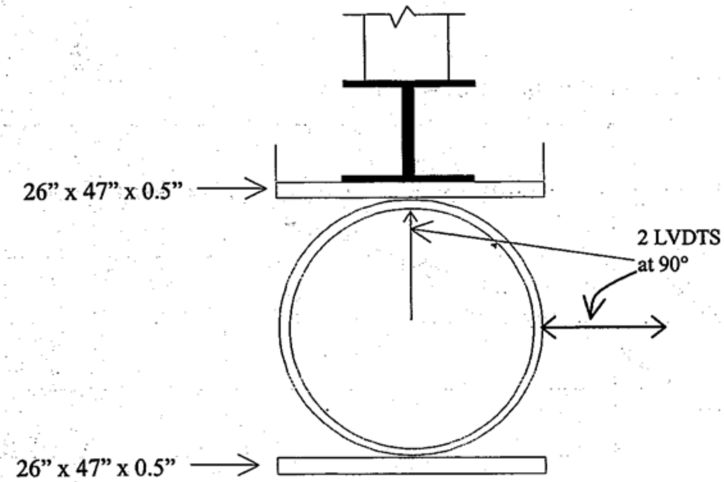

Fig. 7.1 - LVDT Experimental Set-up

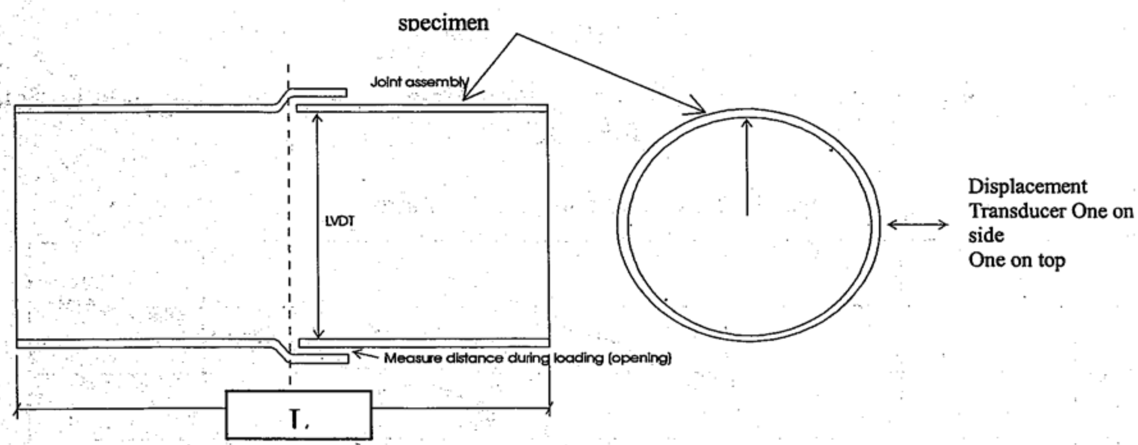

Fig. 7.2 - Test Specimen

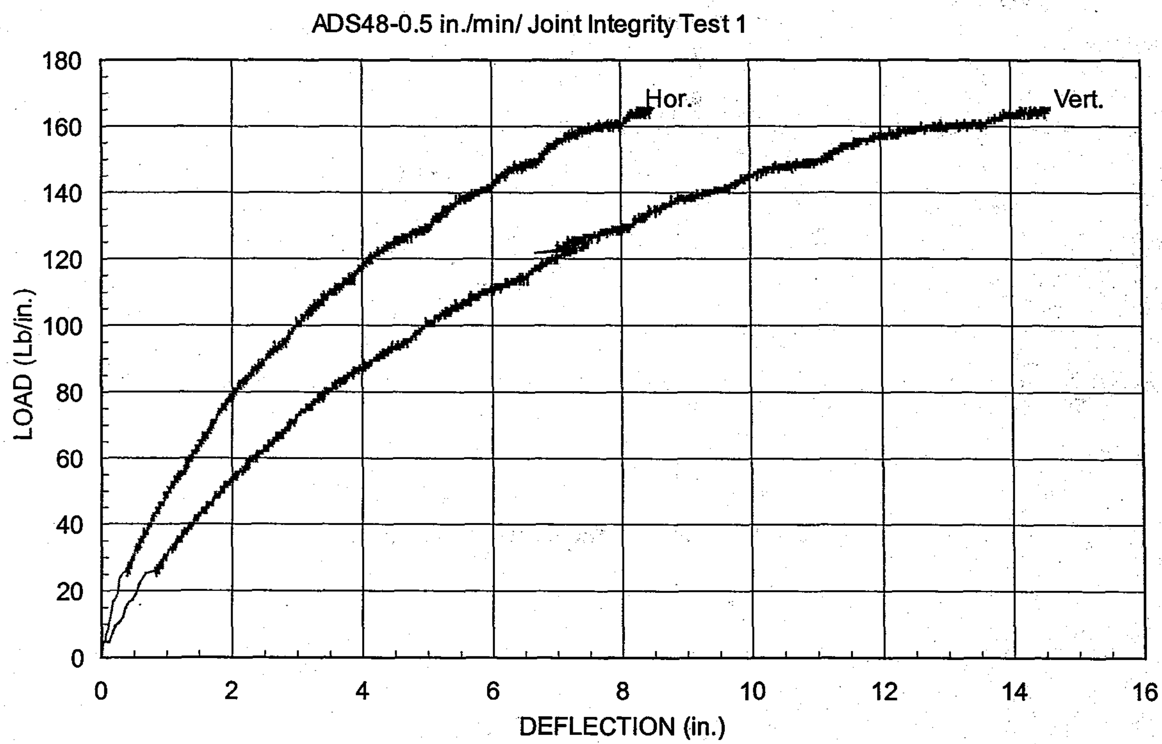

Fig. 7.3 - Load versus Vertical (Shortening) and Horizontal (Elongation) Deflections for ADS 48

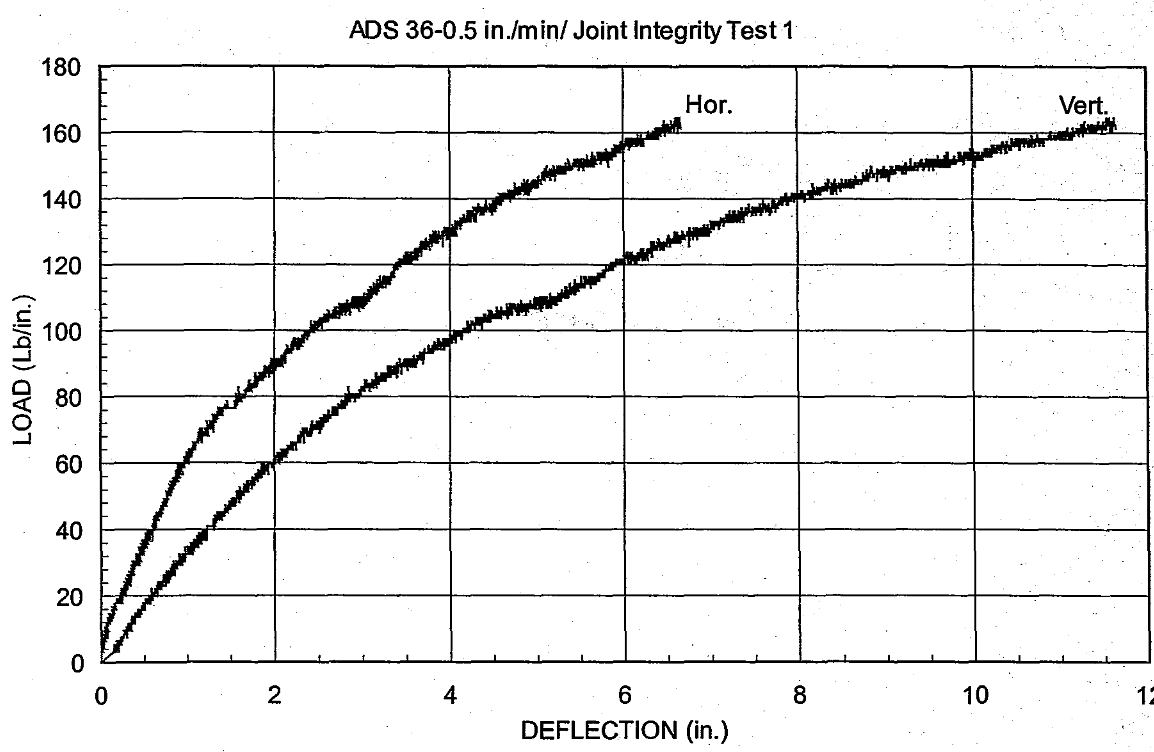

Fig. 7.4 - Load versus Vertical (Shortening) and Horizontal (Elongation) Deflections for ADS 36

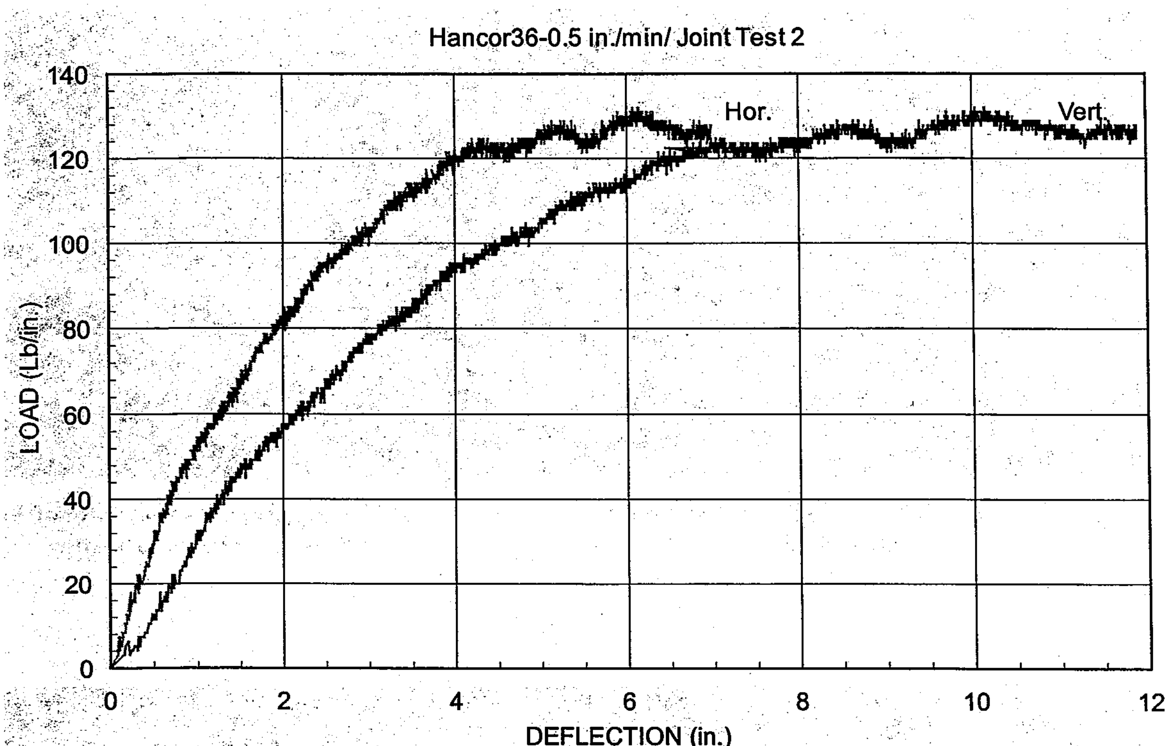

Fig. 7.5 - Load versus Vertical (Shortening) and Horizontal (Elongation) Deflections for Hancor 36

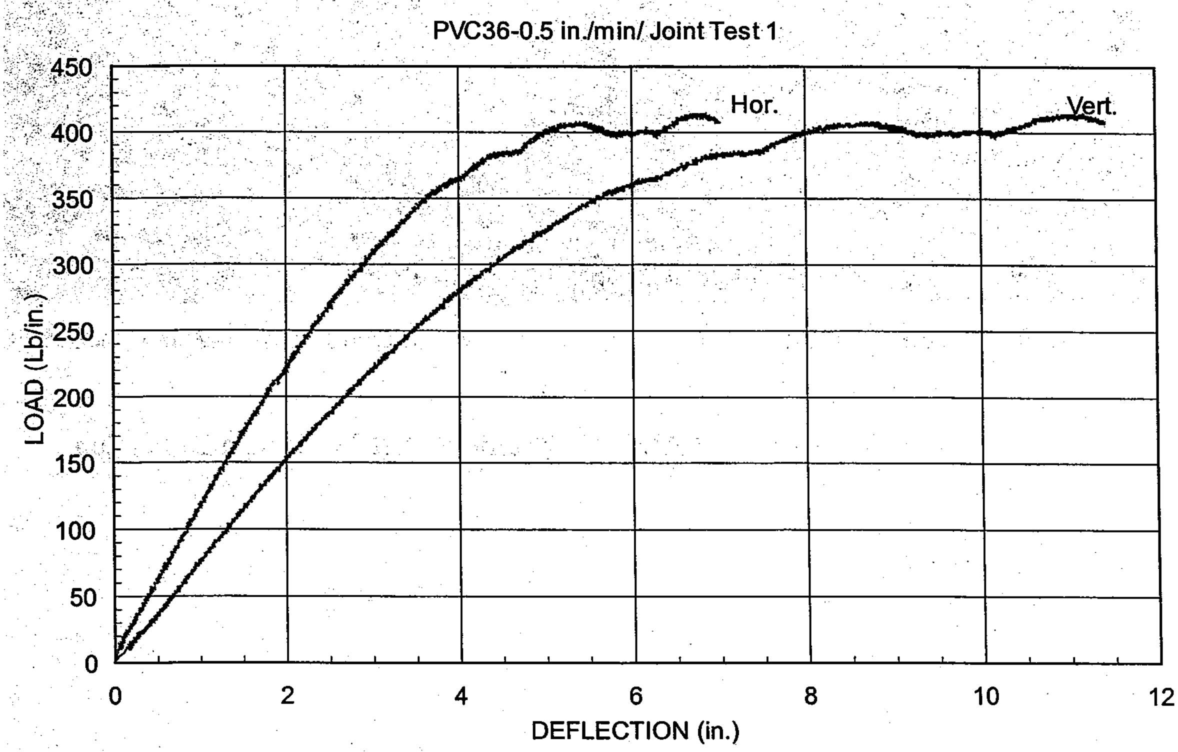

Fig. 7.6 - Load versus Vertical (Shortening) and Horizontal (Elongation) Deflections for PVC 36

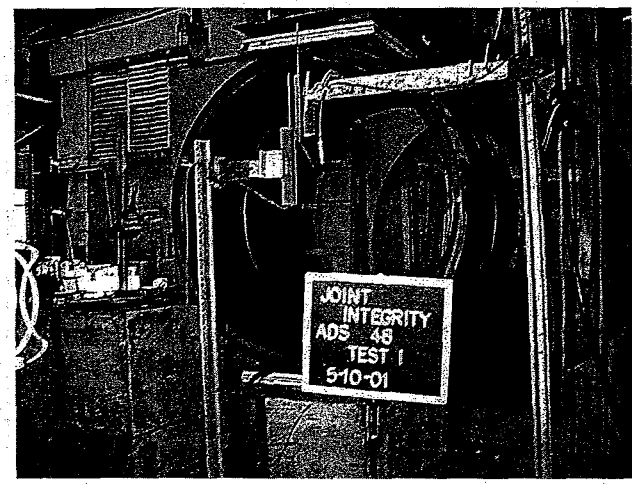

Fig. 7.7 - Joint Integrity Test Setup for ADS 48" Pipe

Fig. 7.8 - Exterior View of Joint of ADS 48 Specimen Prior to Testing

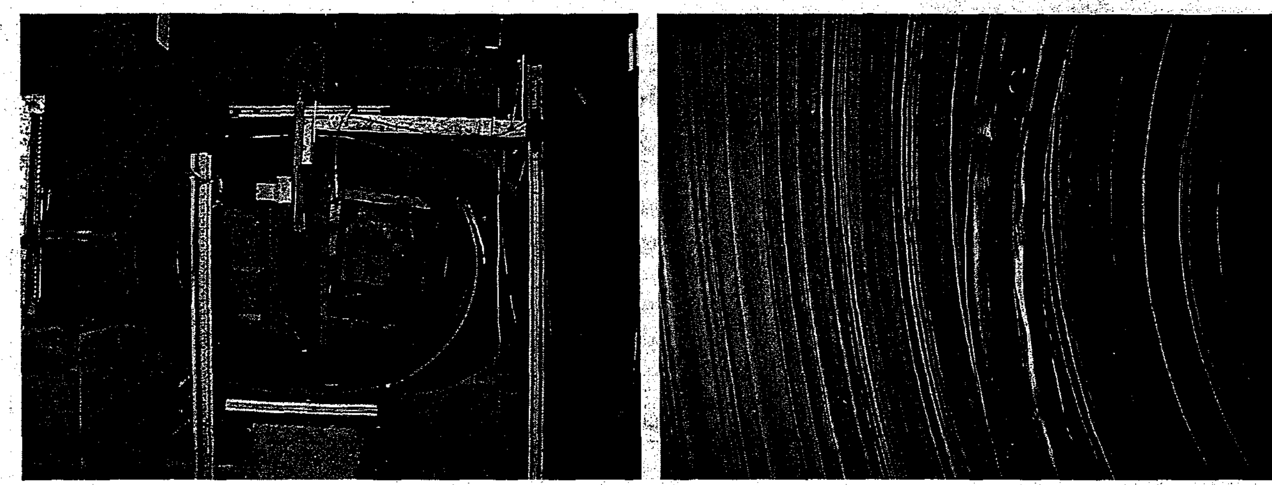

(a) Deformed Shape of ADS48 at 20% Defl.

(b) Interior of ADS48 at 15% to 20% Defl.

Fig. 7.9 - Behavior of Joint of ADS 48 Specimen at 20% vertical Deflection

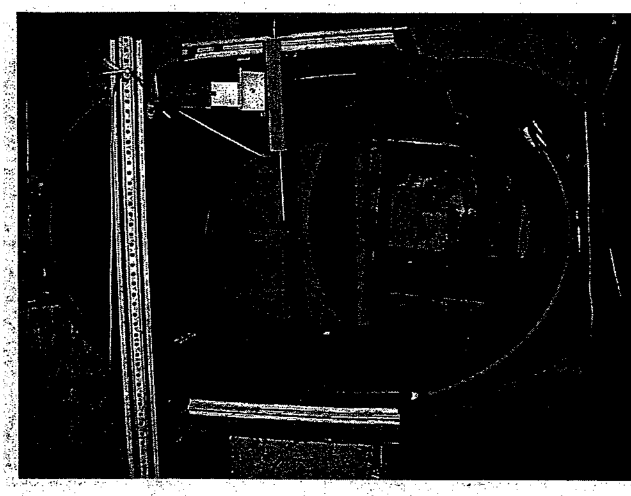

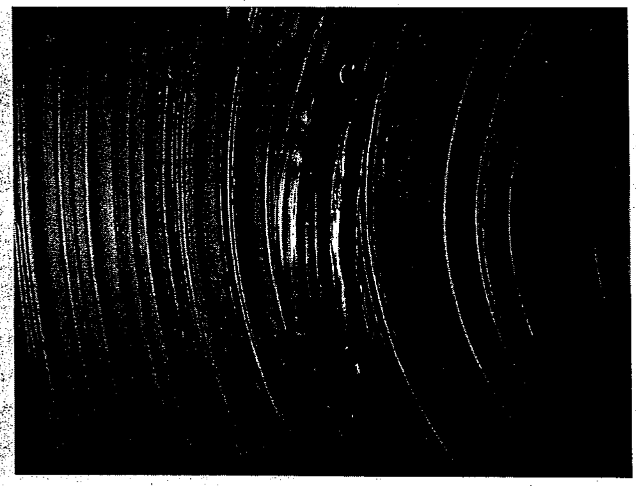

(a) Deformed Shape of ADS48 at 30% Defl. **(b) Interior of ADS48 at 30% Defl.**

Fig. 7.10 - Behavior of Joint of ADS 48 Specimen at 30% vertical Deflection

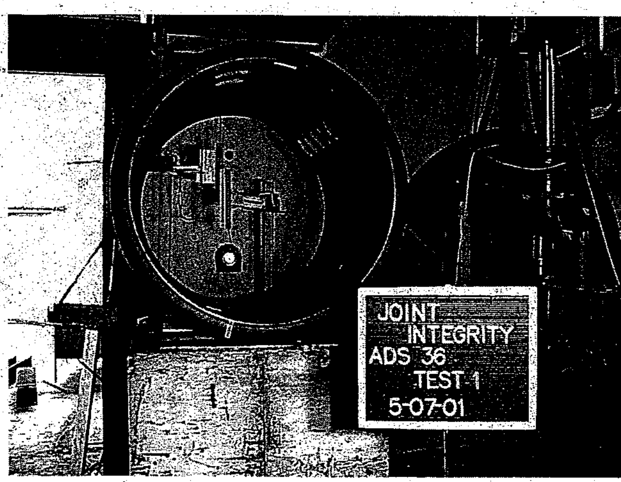

Fig. 7.11 - Joint Integrity Test Setup for HDPE ADS 36" Pipe

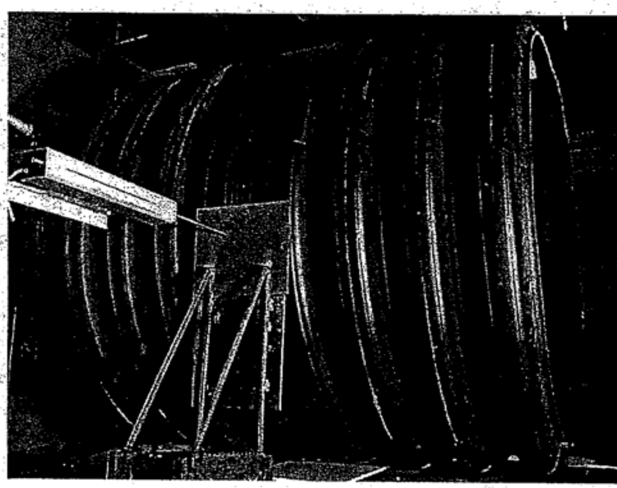

Fig. 7.12a -Exterior View of ADS36 Prior to Test

Fig. 7.12b -Interior View of ADS36 Prior t
Test

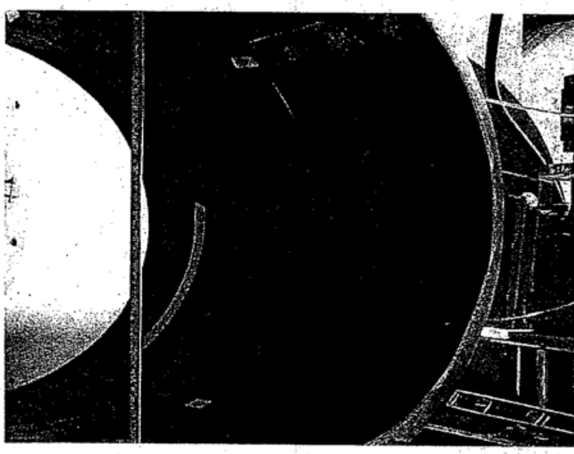

(a) Gap at Spingline for ADS36 at 10% Defl.

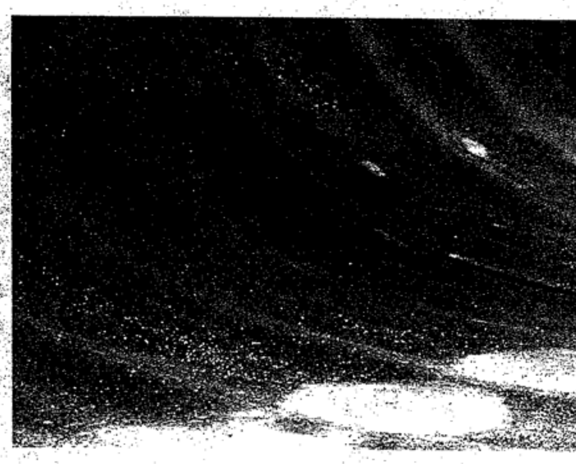

(b) Gap at Invert for ADS36 at 20% Defl.

Fig. 7.13 - Behavior of Joint of ADS 36 Specimen at 10% and 20% Vertical Deflection

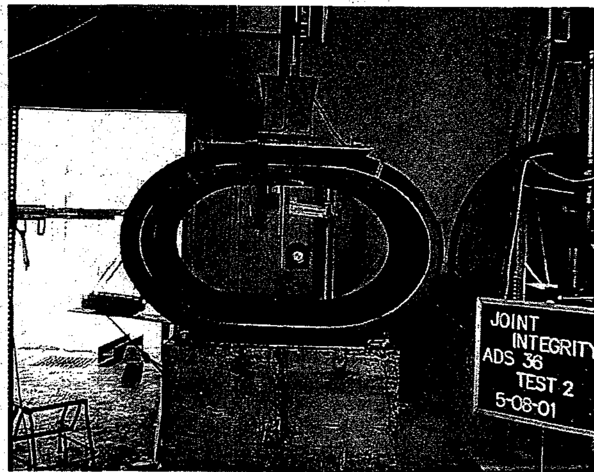

(a) Deformed Shape of ADS36 at 33% Defl.

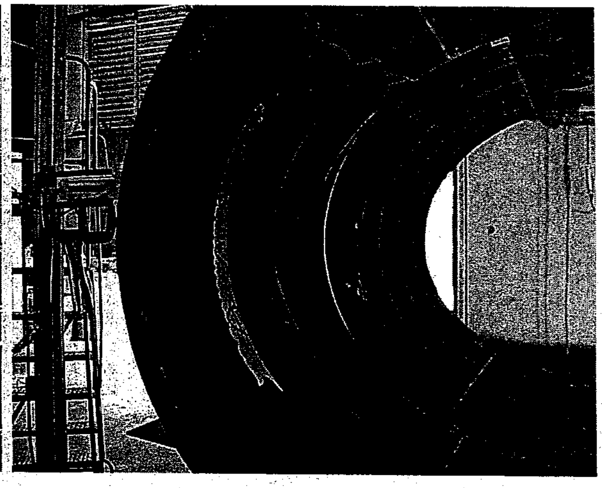

(b) Interior of ADS36 Joint at Springline/ 33%Defl.

(c) Interior of ADS36 Joint at Haunch at 33% Defl.

(d) Shoulder of ADS36 Joint at 33% Defl.

Fig. 7.14 - Behavior of Joint of ADS 48 Specimen at 30% Vertical Deflection

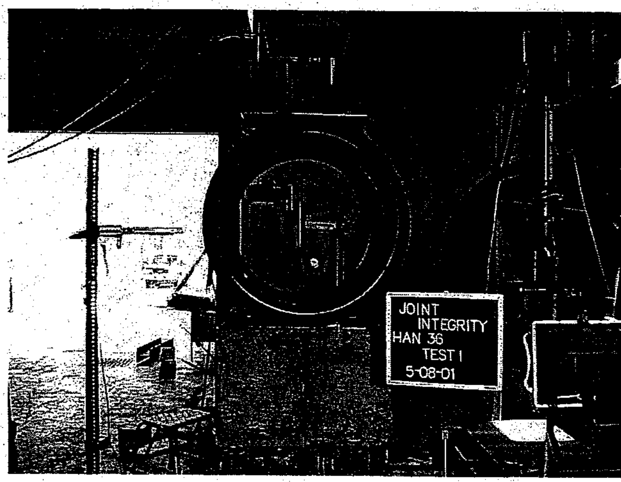

Fig. 7.15 - Joint Integrity Test Setup for HDPE Hancor 36" Pipe

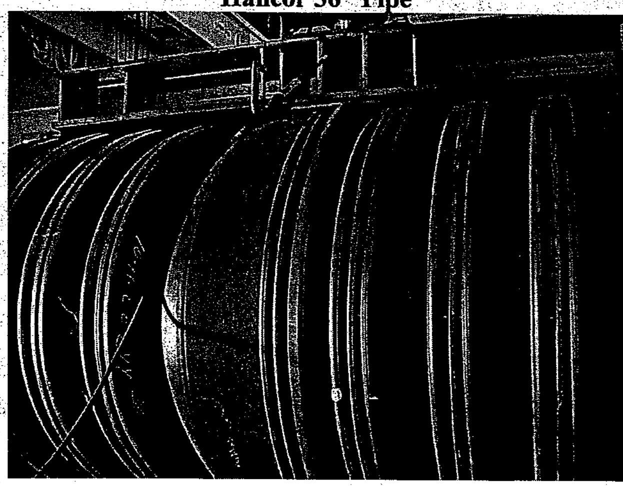

Fig. 7.16a -Exterior View of Hancor36 Prior to Test

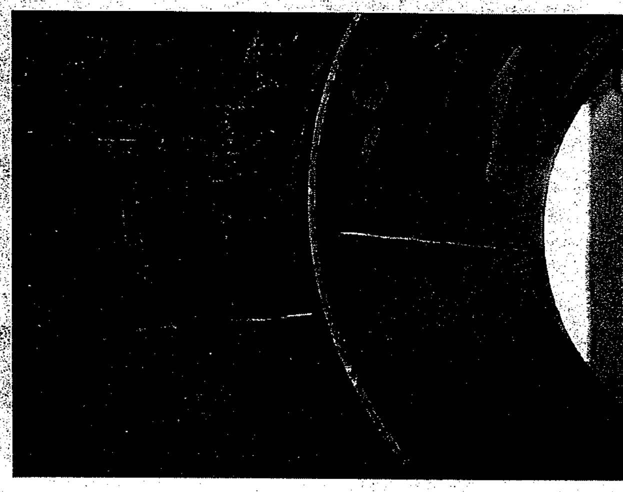

Fig. 7.16b -Interior View of Hancor36 Prior to Test

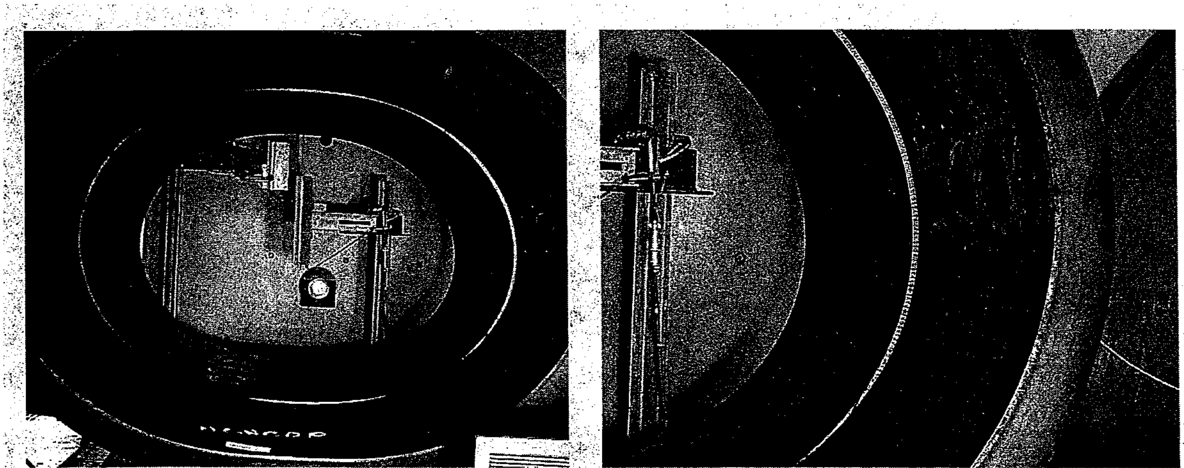

(a) Deformed Shape for Hancor36 at 15% to 20% Defl.

(b) Gap at Invert for hancor36 at 15% Defl.

Fig. 7.17 - Behavior of Joint of Hancor 36 Specimen at 15% and 20% Vertical Deflection

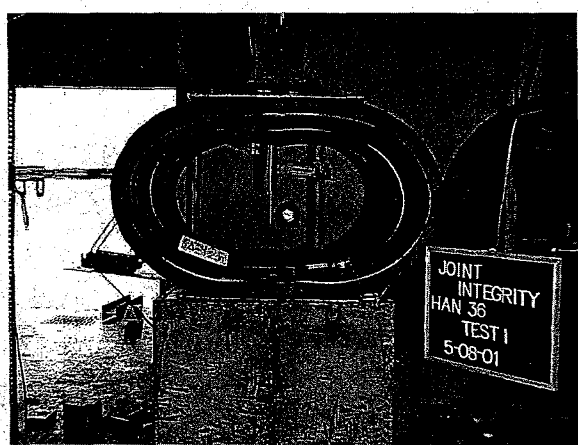

(a) Deformed Shape of Hancor36 at 33% Defl.

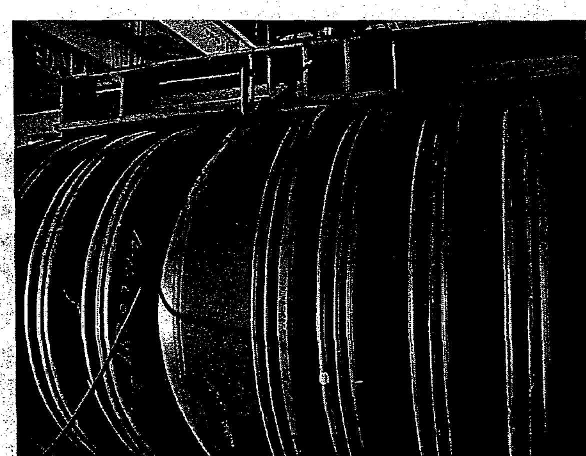

(b) Exterior View of Hancor 36 at 30% Defl.

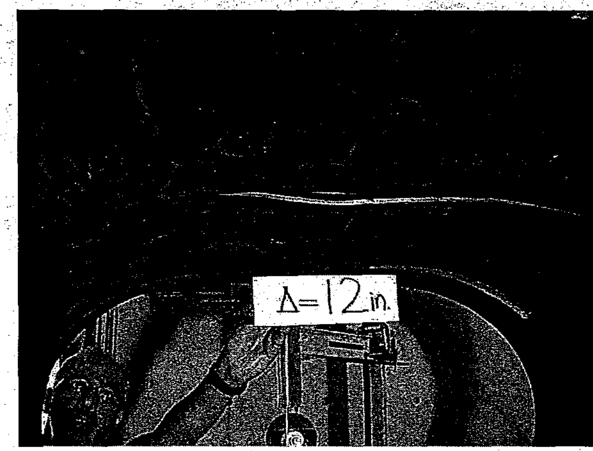

(c) View of Crown of Hancor 36 at 30% Defl.

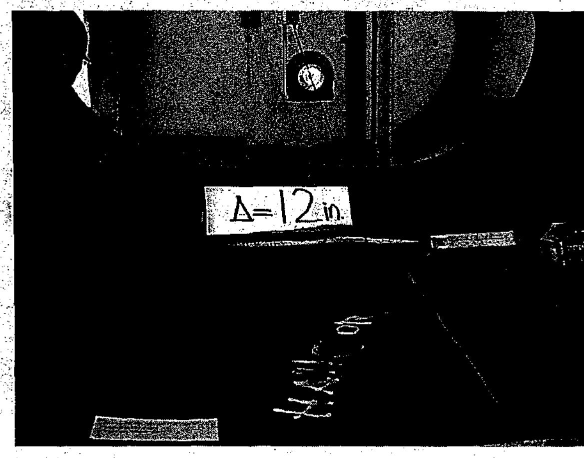

(d) View of Invert of Hancor 36 at 30% Defl.

Fig. 7.18 - Behavior of Joint of Hancor 36 Specimen at 30% and 33% vertical Deflection

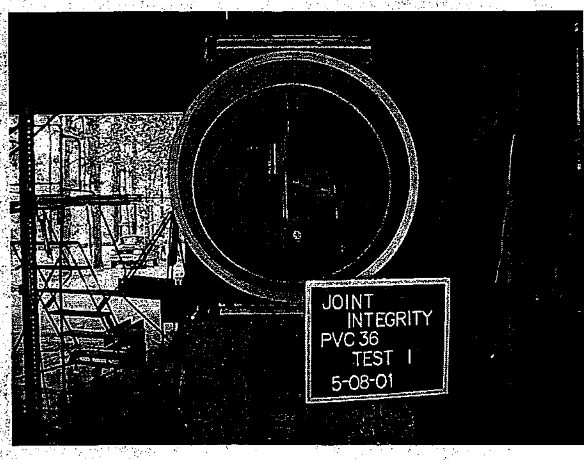

(a) Joint Integrity Test Setup for PVC 36" Pipe

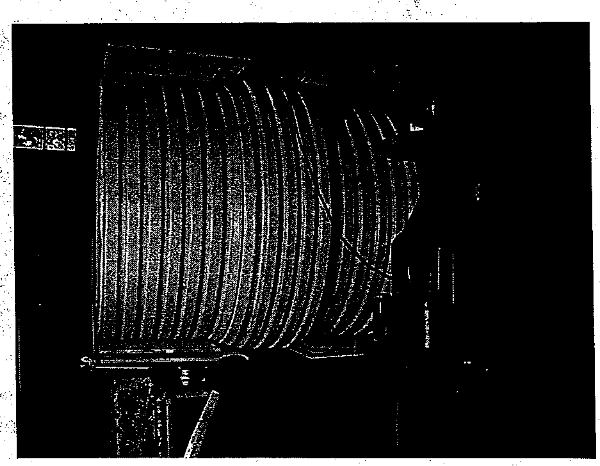

(b) Exterior View of PVC36 Prior to Test

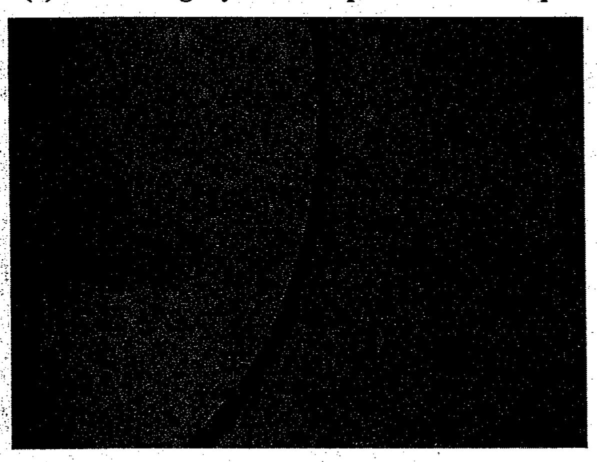

(c) Interior View of PVC36 Prior to Test

Fig. 7.19 - Joint Integrity Test Setup for PVC 36" pipe

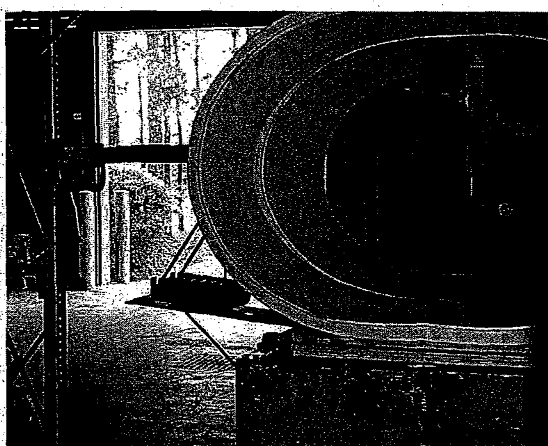

Fig. 7.20 - Behavior of Joint of PVC 36 Specimen at 30% vertical Deflection

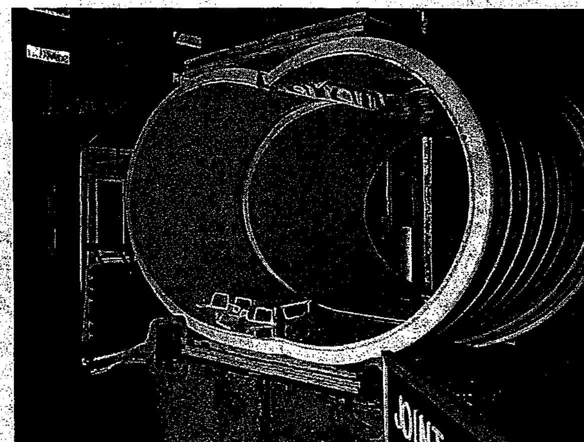

Fig. 7.21 - Failure of PVC 36" Pipe at 33% Vertical Deflection

Chapter 8: Tensile Tests on Dumbbell-Shaped Speciens

8.1 Scope and Objectives

The objective of this test was to determine the tensile properties of an HDPE coupon cut from the ADS D-wall-type pipe in the form of a dumbbell-shaped (dog bone shaped) specimen. The specimens were tested under predetermined cross-head speed and ambient conditions. The tensile properties include the tensile strength, percent elongation, the modulus of elasticity and Poisson's ratio. Most of the test procedure and method of calculating tensile properties follow closely the approach described in ASTM D-638, Standard Test Method for Tensile Properties of Plastics.

8.2 Experimental Program

Two types of specimens were used in the test The first type (Type A) is of double wall type since the pipe configuration is of a D-type pipe as described in section 4.1.3 of AASTHO M 294-98, "Standard Specification for Corrugated Polyethylene Pipe 300- to 1200-mm Diameter", and the second type (Type B) has only one wall thickness, cut into half from the first type. Figs. 8.1 and 8.2 show the configurations of the test specimens Type A and Type B, respectively.

Apparatus

The testing device shown in Figure 8.3 was specially fabricated. The specimen was held in place by connecting steel rods at both ends. The rods pass through the infill mortar between the inner and outer walls. A hydraulic jack having a constant rate-of-head movement was used to apply the tensile force. The two ends of the specimen were free to move into alignment upon load application so that the longitudinal axis of the specimen would coincide with the direction of the applied load. The applied load was measured using the load cell/ gage pressure. The change in length of the specimen, and the axial,. and transverse strains were recorded using LVDTs and strain gages, respectively.

Test Specimens

The test specimen was first cut from the flexible pipe in the form of longitudinal strips 11.2in. x 28 in. The coupon was then machined to obtain the shape shown in Fig. 8.4, ensuring one weld at the center of the specimen. The coupon was than machined to obtain the dumbbell-shaped specimen (Dog bone shape), and then instrumented as shown in Fig. 8.5.

Test Procedure

All strain gages were installed on the specimen and the specimen aligned so as to ensure the longitudinal axis of the specimen to be coincident with the direction of the applied load. The tensile force was applied at a constant rate-of-head speed of 0.5 in. per minute until the specimen failed. The data acquisition system was used to continuously record both transverse strain and axial strain simultaneously. The applied tensile load and the corresponding elongation of the specimen were also continuously recorded.

Test Program

Table 8.1 presents the details of the testing program.

8.3 Calculations

i) Ultimate tensile strength

Ultimate tensile strength, σ_u, is calculated by dividing the maximum load at rupture, F_b, in newtons (or pounds-force) by the original cross-sectional area, A, of the specimen m square metres (or square inches).

ii) Modulus of elasticity

First, a graph of stress versus strain of the specimen is plotted. The initial linear portion of the stress-strain curve is extended, and the modulus of elasticity, E, is given by the slope of this straight line, which is calculated by dividing the difference in stress corresponding to any segment on the straight line by the corresponding difference in strain.

iii) Poisson's ratio

The axial and transverse strains obtained from the test are plotted against the applied load. Straight lines are drawn through each set of points for both the axial, ε_a, and the transverse, ε_t, strains. One of any section in the linear portion of the graph is selected and the change in strain is determined. Then, Poisson's ratio, μ, is calculated using Eq. (8.1) shown below:

$$\mu = -\text{(change in transverse strain)} / -\text{(change in axial strain)} \qquad (8.1)$$

8.4 Results and Observations

i) Type A specimen

Table 8.2 summarizes the experimental results for tension test Type A for the ADS 48" pipe. It presents the maximum forces and corresponding stresses, and the recorded strains in the longitudinal and transverse directions. The table also provides the apparent modulus of elasticity and Poisson's ratio for each test which are determined by using the example curve fittings shown in Fig. 8.7. Fig. 8.6 shows the load versus the longitudinal and transverse strains curves for the four Type A tests. Typical views of the specimens at failure are presented in Fig. 8.8.

ii) Type B specimen

Table 8.3 summarizes the experimental results for tension test Type B for the ADS 48" pipe. It presents the maximum forces and corresponding stresses, and the recorded strains in the longitudinal and transverse directions. The table also provides the apparent modulus of elasticity and Poisson's ratio for each test, which are determined by using the example fittings shown in Fig. 8.10. Fig. 8.9 shows the load versus the longitudinal and transverse strains curves for the four Type B tests. Typical views of the specimens at failure are presented in Fig. 8.11.

iii) Observations

- The single wall specimen (Type B) exhibited apparent tensile properties superior to those of the double wall specimen (Type A).
- The average maximum tensile strength achieved by Type B was 2935 psi compared to 2049 psi for Type A specimen. The average apparent modulus of elasticity was 413 ksi for Type B versus 282.5 ksi for Type A. The average maximum longitudinal strain was similar for both types and attained approximately 1.1%. The maximum transverse strain was substantially lower for Type A (double wall: 1,248με) than for Type B (single wall: 5,596με).

8.5 Conclusions

Results indicate that Type A test (Double wall dumbbell shape) underestimates the tensile strength of the D-wall-type pipes such as the ADS 48". Results also indicate that the seam behavior under tensile stresses is satisfactory in view of the maximum strength achieved.

Table 8.1 - Type A and B Test Program

Test Type	Description	Number of Tests
Type A	Double Wall	4
Type B	Single Wall	4

Table 8.2 - Summary of Results for Tests Type A

Test#	Maximum Load (Lbs)	Maximum Stress, σ_u[(a)] (psi)	Modulus of Elasticity[(a)] (psi)	Max. Long. Strain ($\mu\varepsilon$)	Max. Transv. Strain ($\mu\varepsilon$)	Poisson's Ratio, μ	Rupture Mode
1	1132	2258	301860	9591[(B)]	1528	0.146	Inside wall
2	1138	2270	235503	13247[(T)]	1234	0.093	Inside wall
3	1028	2051	231958	16004[(L1)]	1413	0.109	Inside wall
4	810	1616	360622	6840[(L1)]	816	0.143	Inside at weld
Average	1027	2049	282486	11420	1248	0.123	--

Notes: [(a)] Based on a thickness of (0.071 in. × 2 walls) and an average measured width of 3.53 inches, that is $A = 0.5013\ in^2$

[(b)] B, T, L1 = Bottom, Top, and L1 strain gages

Table 8.3 - Summary of Results for Tests Type B

Test#	Maximum Load (Lbs)	Measured Thickness (in.) (area(-in^2))	Maximum Stress, σ_u[(a)] (psi)	Modulus of Elasticity[(a)] (psi)	Max. Long. Strain ($\mu\varepsilon$)	Max. Transv. Strain ($\mu\varepsilon$)	Poisson's Ratio, μ	Rupture Mode
1	611	3.54 (0.2513)	2431	745386	3670	4286	0.101	Seam
2	492	3.58 (0.2542)	1935	238090	11337	3256	0.325	Wall
3	904	3.48 (0.2471)	3658	313980	14636	7565	0.357	Wall
4	929	3.52 (0.2499)	3717	353062	14293	7276	0.378	Wall
Average	734	3.53 (0.2506)	2935	412629	10984	5596	0.290	---

Note: [(a)] Based on a thickness of 0.071 inches and measured widths as indicated.

(a) Front View

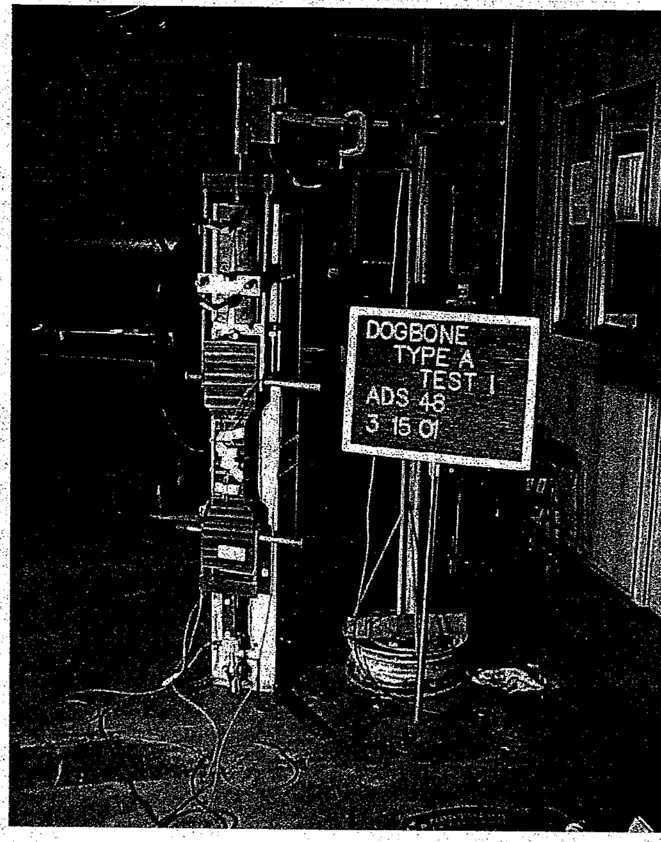

(b) Side View

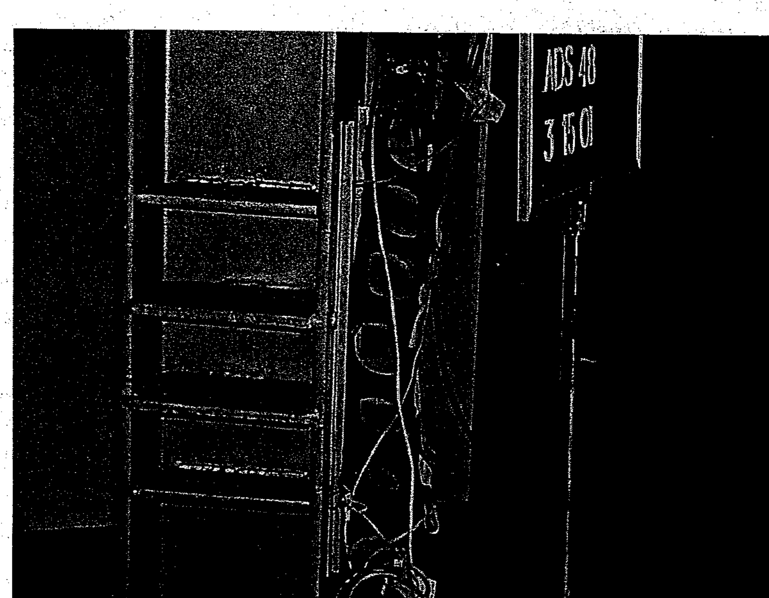

Fig, 8.1 - Double wall type specimen (Type A)

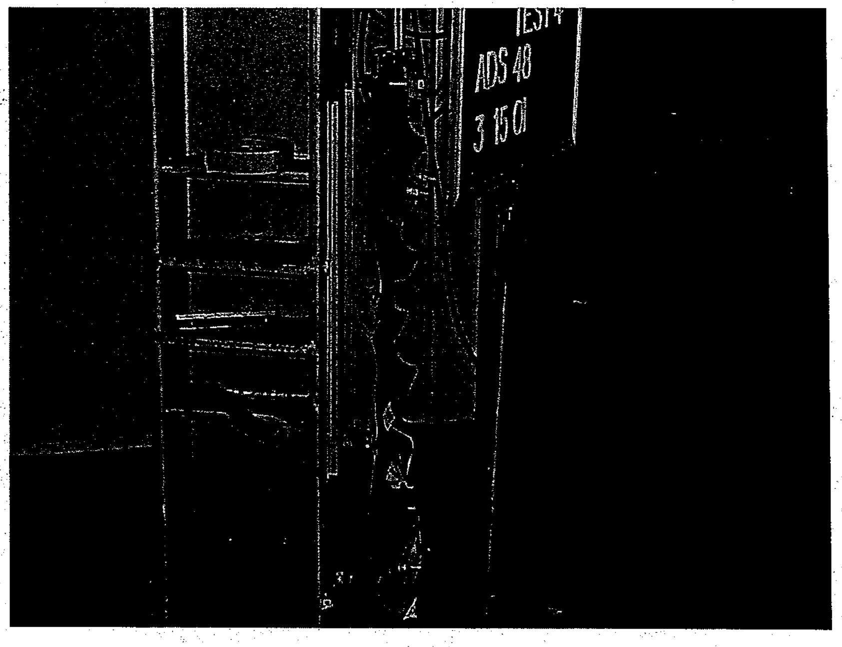

Fig. 8.2 - Single Wall Type Specimen (Type B)

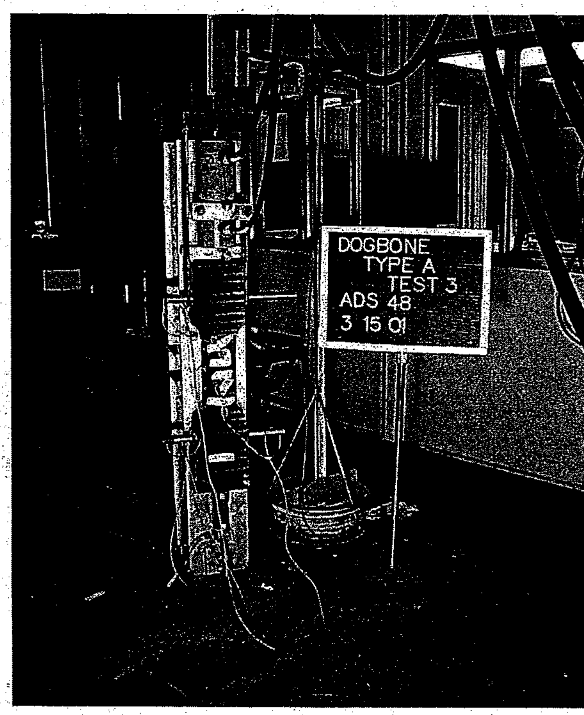

Fig. 8.3 - Typical Test Setup

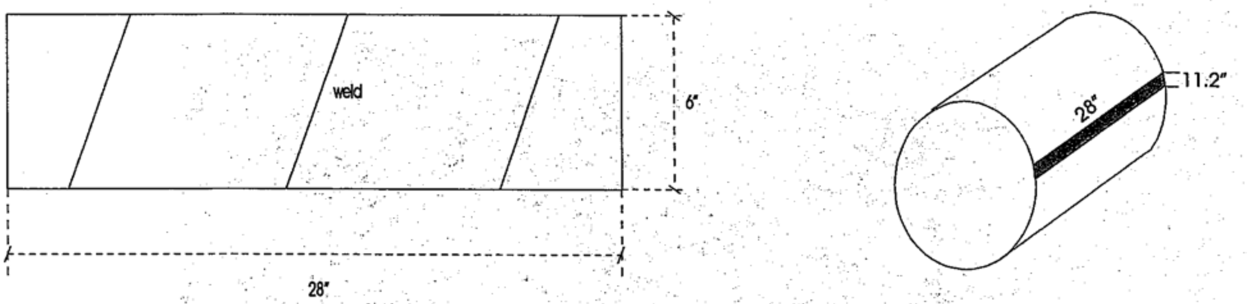

Fig. 8.4 - Specimen Cut in the Form of Longitudinal Strip from the Pipe

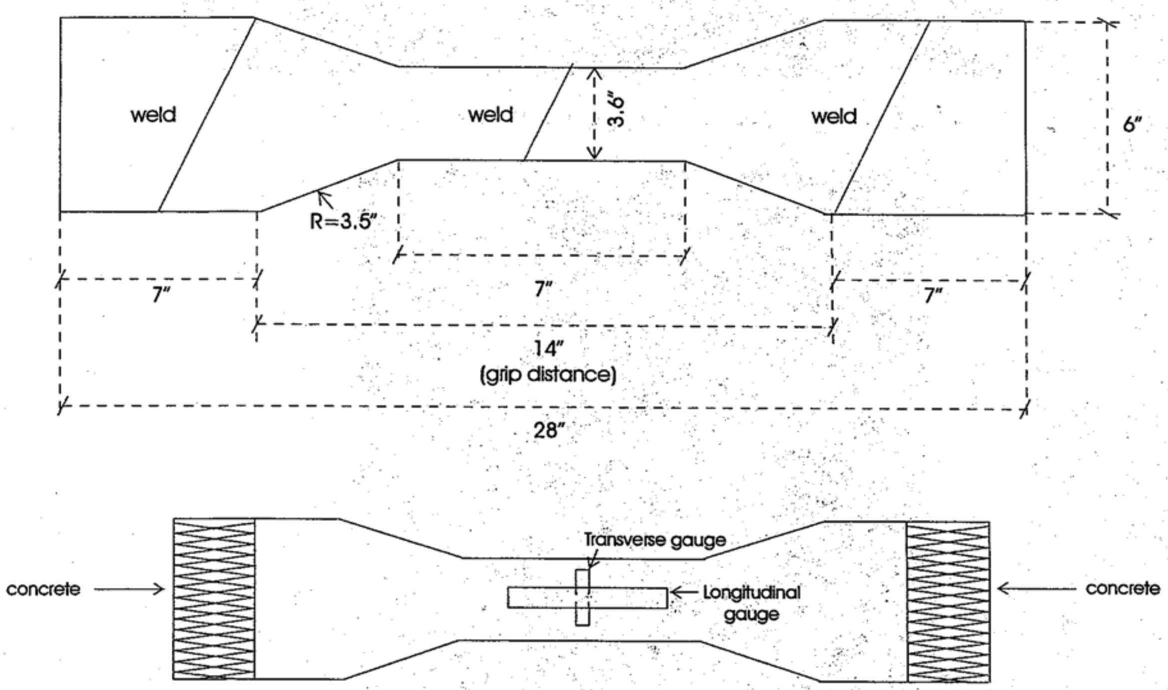

Fig. 8.5 - Specimen Cut Into Dumbbell-Shape (Dogbone Shape)

(a) Test # 1

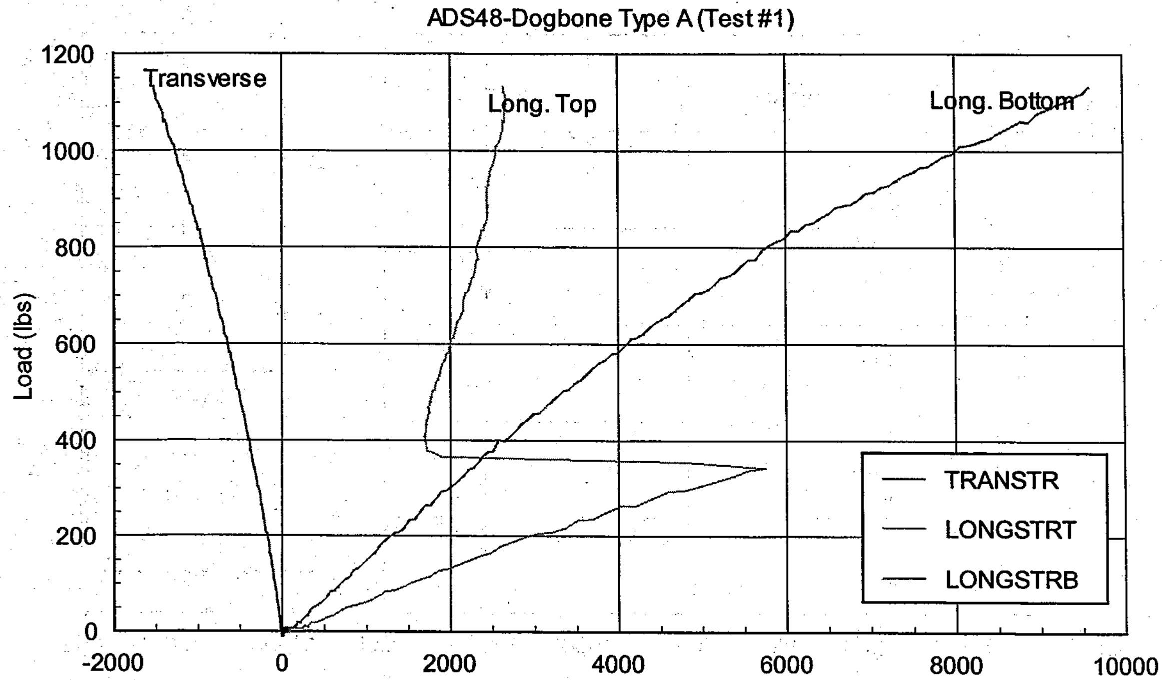

(b) Test # 2

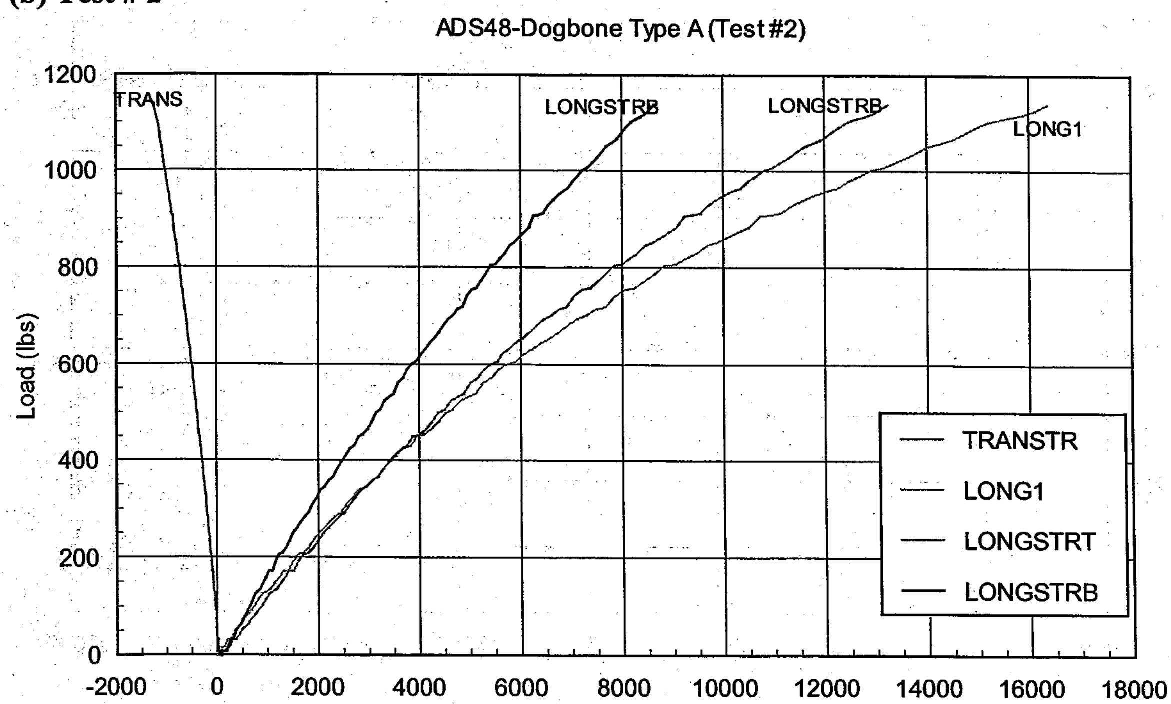

(c) Test # 3

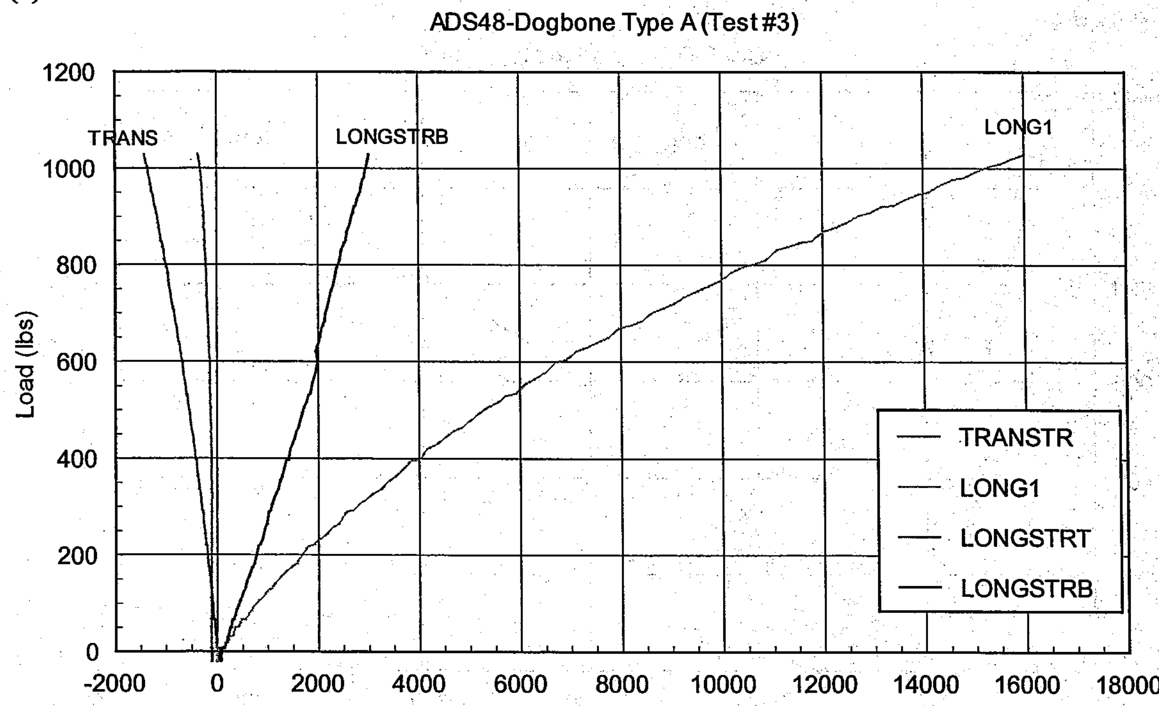

(d) Test # 4

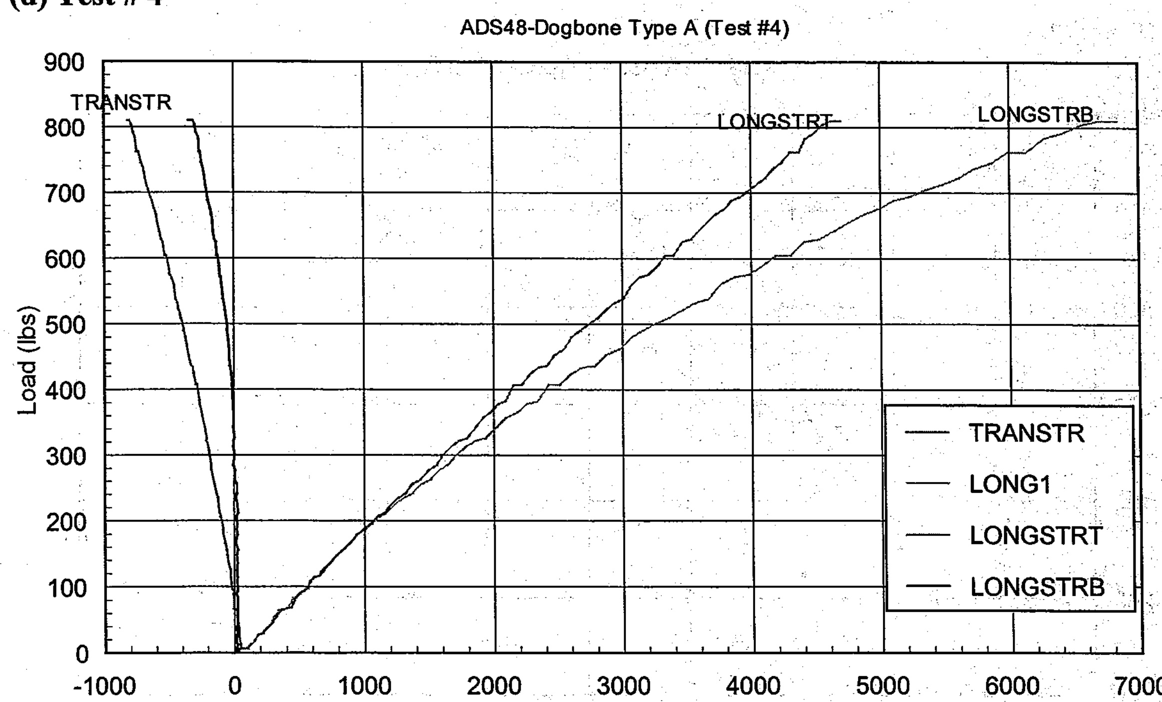

Figure 8.6 - Load vs. Axial and Transverse Strain for Type A Specimen

(a) Modulus of elasticity

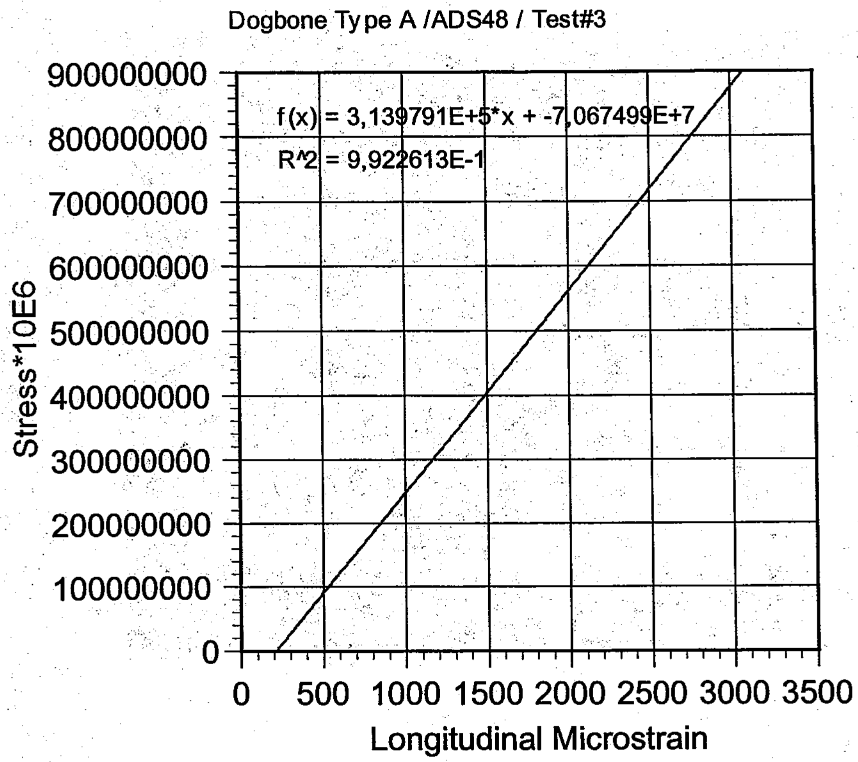

(b) Poisson's ratio

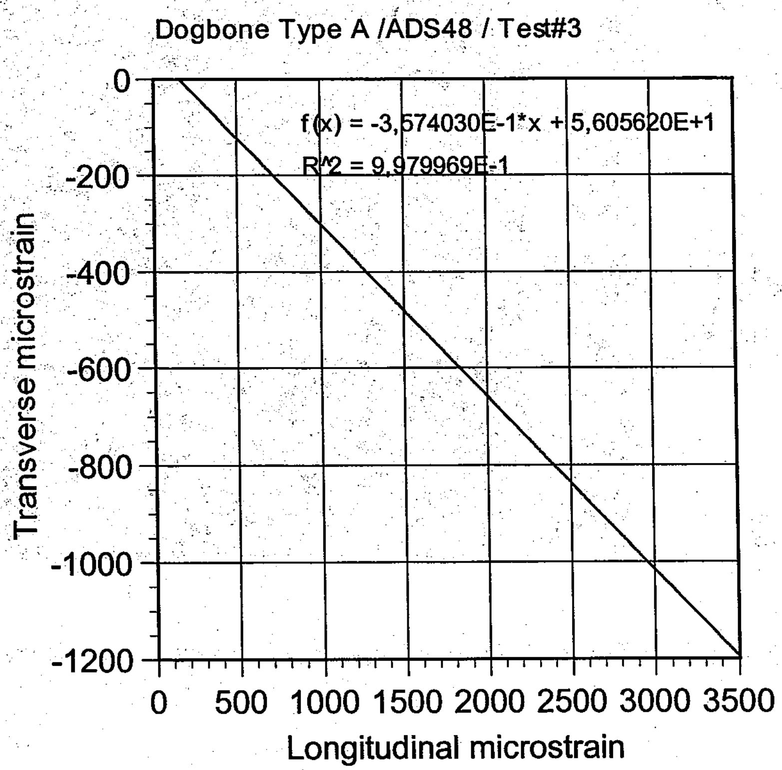

Fig. 8.7 - Typical Curve Fittings for Modulus and Poisson's Ratio for Type A

(a) General View

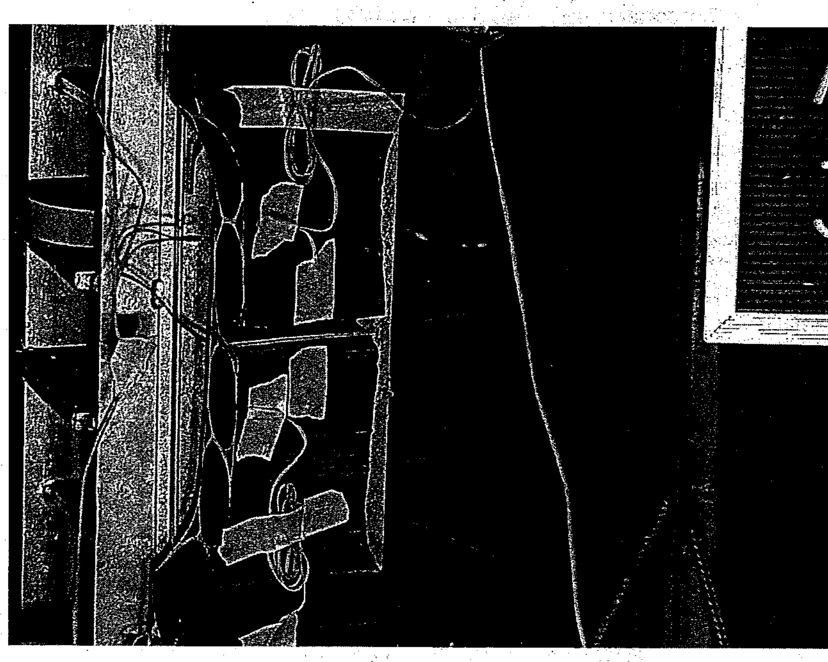

(b) Close-up View

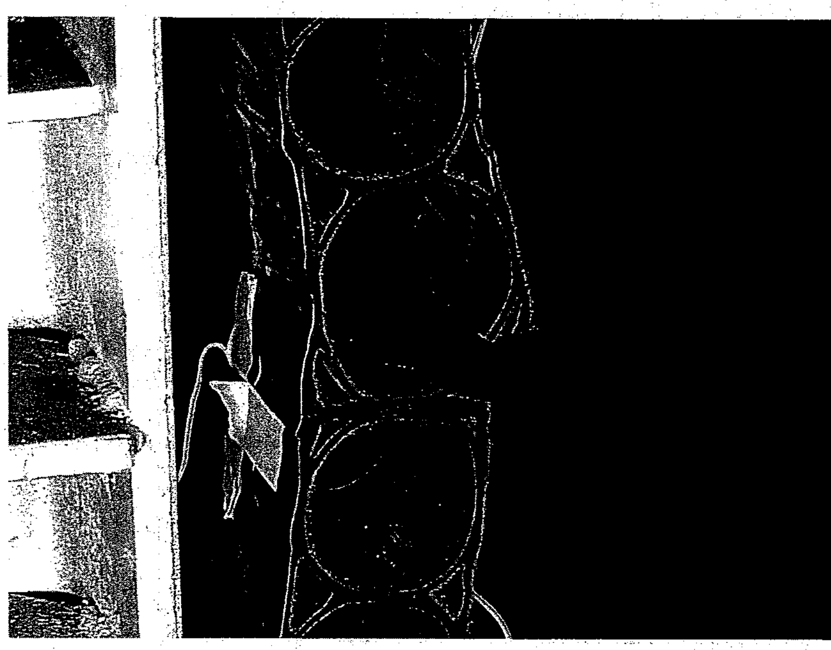

Fig. 8.8 - Typical Views of Specimens Type A at Failure

(a) Test # 1

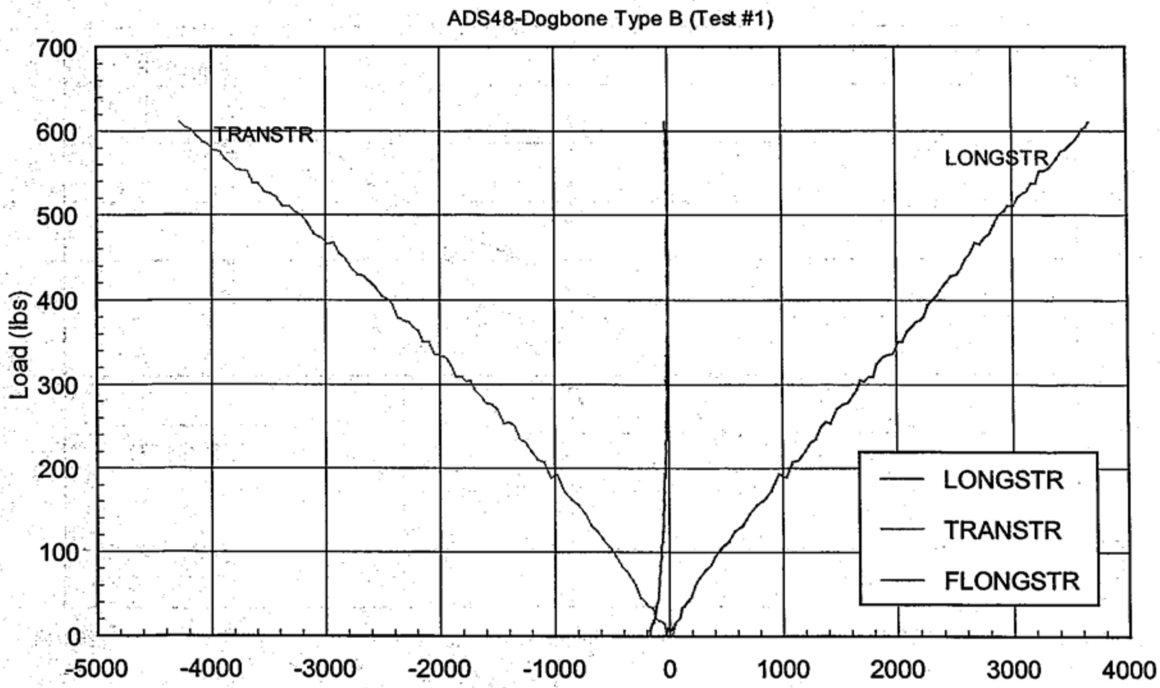

(b) Test # 2

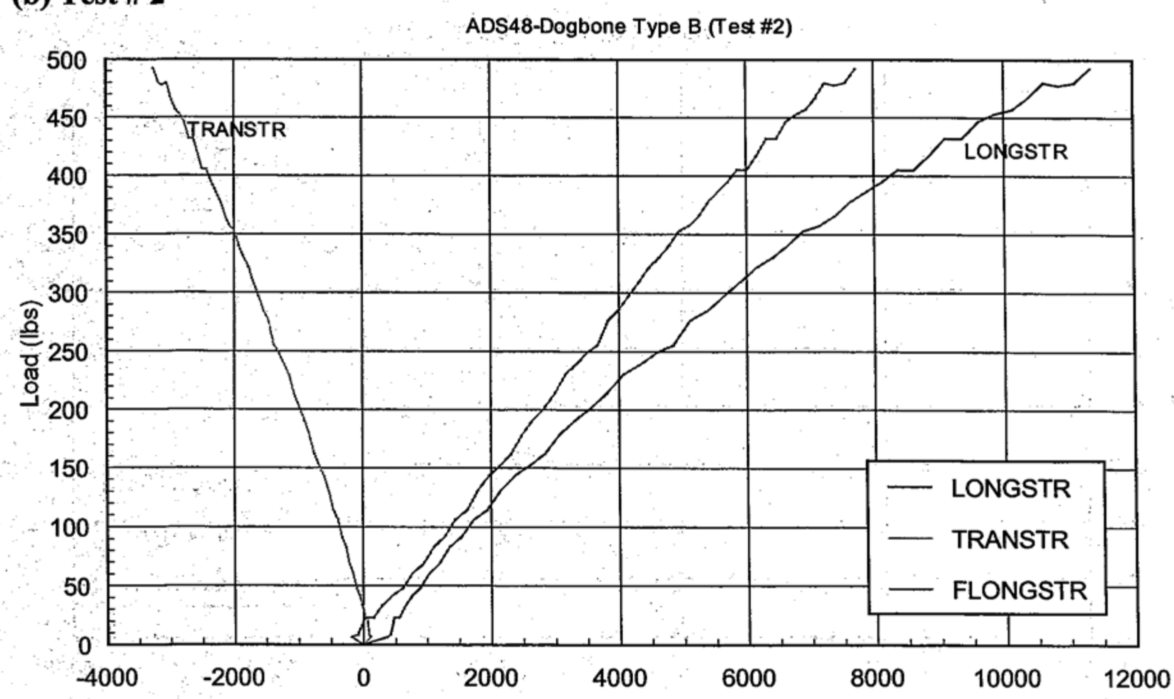

(c) Test # 3

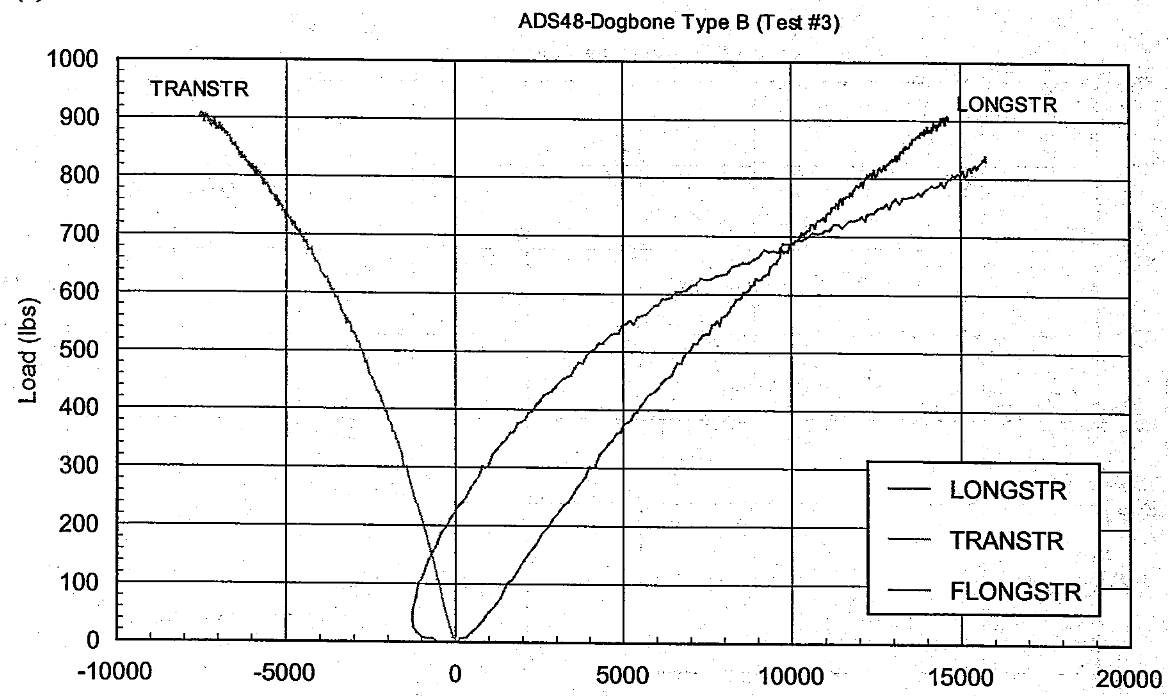

(d) Test # 4

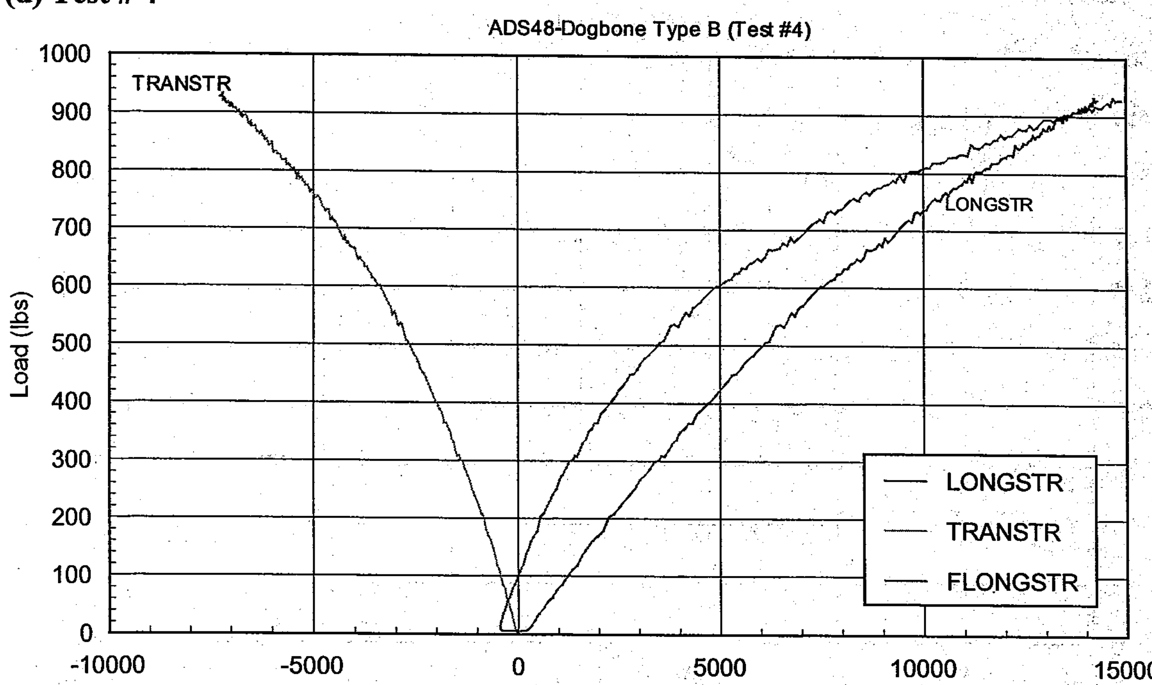

Fig. 8.9 - Load vs. Axial and Transverse Strain for Type B Specimen

(a) Modulus of elasticity

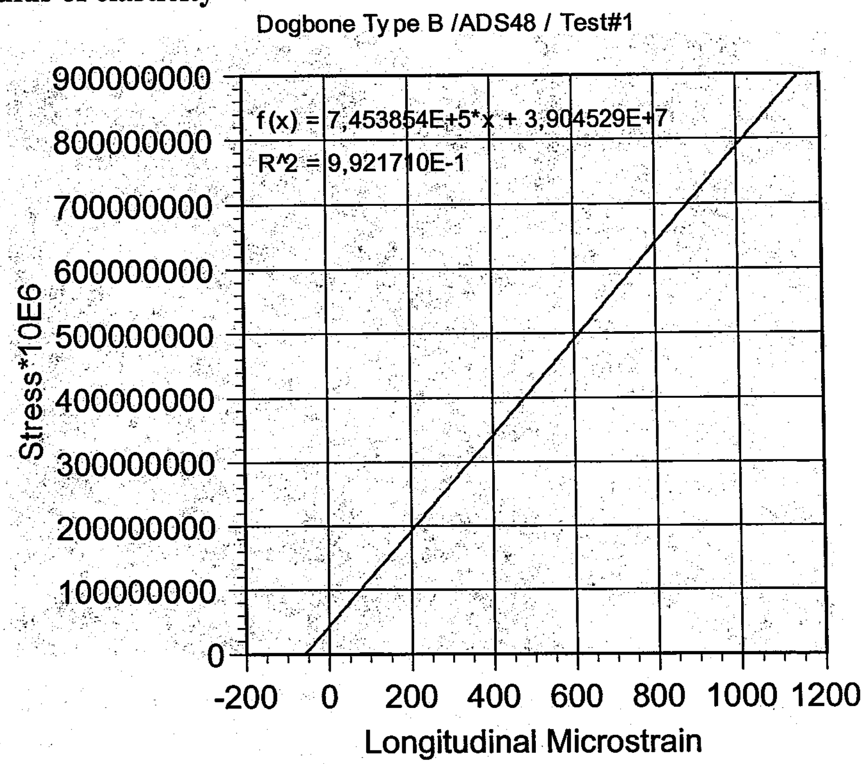

(b) Poisson's ratio

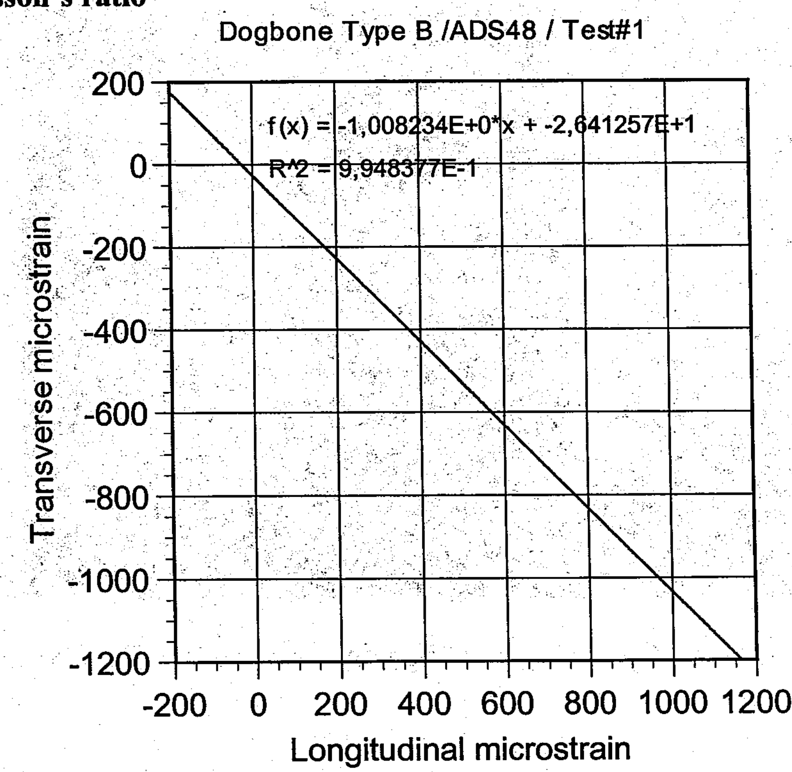

Fig. 8.10 - Typical Curve Fittings for Modulus and Poisson's Ratio for Type B

(a) General View

(b) Lose-up View

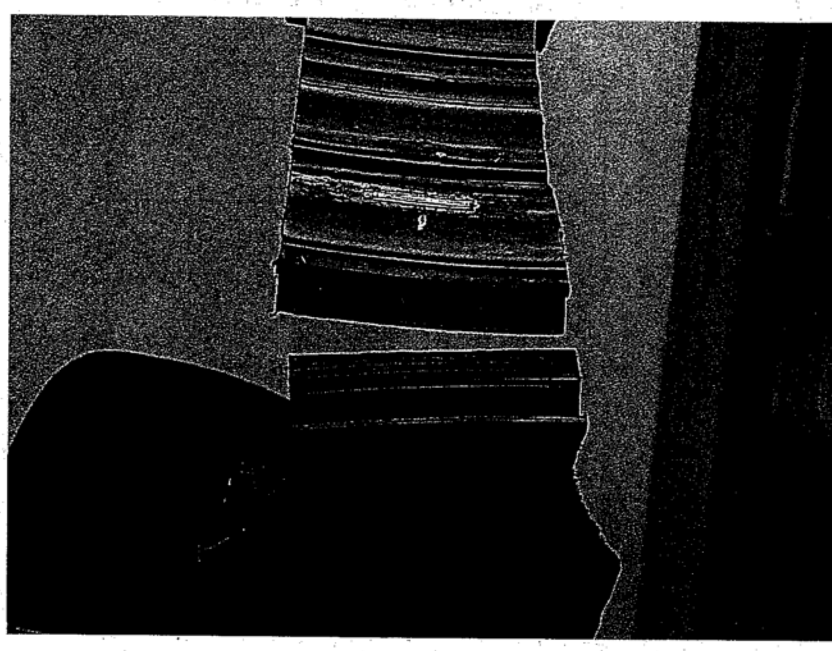

Fig. 8.11 - Typical Views of Specimens Type B at Failure

Chapter 9: Tensile Tests on Full-Ring Specimens

9.1 Scope and Objectives

In this test, an apparent hoop tensile strength is determined by utilizing a split disk test fixture. The test specimen, a full-diameter, full-thickness ring cut from the pipe, is tested under a predetermined cross-head speed and ambient conditions. The test procedure and method of calculation follow closely the ASTM D2290, Standard Test Method for Apparent Hoop Tensile Strength of Plastic or Reinforced Plastic Pipe by Split Disk Method.

The apparent tensile strength rather than a true tensile strength is obtained due to the bending moment induced by the change in contour of the ring between the two disk sections as they separate. The tensile strength obtained will provide reasonably accurate information for plastic pipe when employed under conditions approximating those under which the tests are performed. The vertical diametric strain and the modulus of elasticity will also be computed from the results of this test.

9.2 Experimental Program

Apparatus

Two different configurations of the split disk test fixtures, based on two pipe-diameter sizes (48" and 36" pipe diameters), were specially fabricated. The test fixtures were both made by using 3/8"smooth rigid steel semi-circular pipes. Steel plates of 3/8" thickness cut in a segmental shape were welded to the-machined steel' pipes to reinforce the fixtures. Figs. 9.1 and 9.2 show the test fixtures for the 36" and 48" diameter pipes respectively. These fixtures were then attached to the lifting arms of forklift using steel rods welded to the steel plates. Fig. 9.3 illustrates an overall setup for the 36" diameter pipe tests. The major difference between the two fixtures is that the test fixture for the 48-in. diameter pipe had two hydraulic jacks in order to have a uniform load application on the test specimens. On the other hand, the test fixture for the 36-in diameter pipes required only one jack, but with a larger piston diameter for the load application.

Test Specimen

The length of the HDPE 36" diameter specimens was chosen as 15.5 in., whereas the length of the PVC 36" pipes was 8.75 in. to ensure that at least two or three corrugations or spiral ribs were included on the specimens. Figure 9.4 shows the length of the specimen as well as dimensions of the reduced section for the HDPE 36", diameter pipe. The length of the 48" diameter specimen was chosen as 40 inches. Fig. 9.5 shows both the length and the dimension of the reduced section for the HDPE 48" diameter specimens. The reduced cross sections were located at 180° from each other and machined such that the specimens were free of sharp corners to avoid stress concentrations.

Test Procedure

Once the test fixture, either for the 36" or 48"diameter pipes, was secured to the forklift, the inside surface of the test specimen was lubricated and then mounted on the test fixture. The test specimen was aligned to the center of the split disk specimen holder. The testing was performed at a speed of 0.5 inch per minute. The tensile load was continuously recorded by using the data acquisition system until the specimens completely ruptured. A deflectometer was also used to record the elongation along the direction of the load application (see Fig. 9.3).

Test Program

Details of the split disk test program are presented in Table 9.1. The reduced lengths as well as the area of the reduced sections for the two walls are also provided in the table.

9.3 Calculations

i) Apparent tensile strength

The apparent tensile strength, σ_a(psi), of the specimen is calculated by dividing the maximum tensile load, F_u(lbs) by the cross-sectional areas of the reduced sections A_m (in.^{2}), as shown below:

$$\sigma_a = F_u / 2A_m \qquad (9.1)$$

Where,

A_m	=	minimum cross-sectional area,
	=	d x b, in.^{2}
d	=	thickness at minimum area; in. (= wall area in.^{2} /in.), and
b	=	width at minimum area, in.

ii) Vertical diametric strain

The vertical diametric strain is calculated by dividing the elongation in the direction of the load application by the original nominal pipe diameter.

9.4 Test Results and Observations

Figs 9.6, 9.7, and 9.8 illustrate the test setup and the deformations of the HDPE specimens ADS 48", ADS 36", and Hancor 36", respectively. Figs 9.9, 9.10, and 9.11 show the deformations of the PVC specimens and the cracking of the steel and aluminum specimens, respectively. Typical load versus vertical diametric strain for ADS 48", ADS 36", Hancor 36", PVC, steel, and aluminum specimens are presented respectively in Figs. 9.12, 9.13, 9.14, 9.15, 9.16, and 9.17.

The following observations can be made:

(a) All the HDPE pipes achieved a similar maximum apparent tensile strength of approximately 2700 psi (see Table 9.2). However, the maximum radial strain was higher for ADS 48" (19.08%), compared to ADS 36" (10.45%) and to Hancor 36" (11.11%).

(b) All the HDPE pipes also achieved a similar apparent modulus of elasticity (see Table 9.3a) of approximately 70 ksi.

(c) The PVC pipe achieved a maximum apparent tensile stress of 5,258 psi, a maximum tensile radial strain of 2.92%, and an average apparent modulus of elasticity of 271 ksi.

(d) The steel and aluminum pipes achieved respectively a maximum apparent tensile stress of 46,249 psi and 32,063 psi, a maximum tensile radial strain of 1.96% and 1.59%, and an average apparent modulus of elasticity of 4,886 ksi and 2,977 ksi.

9.5 Conclusions

Results show that apparent tensile strength under split disk tests are lower than those under tensile tests on small dog bone specimens with no welds (see chapter 10). However, they are higher than those achieved on dumbbell shape specimens with welds for ADS 48 (see chapter 8).

Table 9.1 - Experimental Program for Split Disk Tests

Series	Load Rate (in./min.)	Number of Tests	Reduced Length of Specimen (one wall) (in.)	Unit Area of Specimen (in^2/in.)	Total Area of Reduced Section (in^2)
ADS 48	0.5	3	34.00	0.581[b]	39.508
ADS 36	0.5	3	14.25	0.401[b]	11.429
HANCOR 36	0.5	3	13.38	0.375[c]	10.035
PVC 36	0.5	3	7.75[a]	0.411[d]	6.371
Steel 36	0.5	3	23.00	0.0593[d]	2.730
Aluminiun 36	0.5	3	23.00	0.0474[d]	2.181

Notes: [a] Measured ($\neq$from written procedure where it was 7.25 in.)
[b] From Manufacturer Product Information Sheet
[c] From Hancor, inc., Drainage Hand book
[d] From Contech (Fax of June 28, 2001). Original values given in in^2/ft.
[e] Two wall section

Table 9.2 - Summary of Results for Split Disk Tests

Series	Test #	Maximum Load (kips)	Total area of Reduced Section ($in.^2$)	Maximum Apparent Stress (psi)	Maximum Radial Strain [a] (%)	Maximum Elongation (in.)
ADS 48	1	102.62	39.508		16.23	7.79
	2	98.79	39.508		21.52	10.33
	3	106.47	39.508		19.50	9.36
	Average	102.63	39.508	2598	19.08	9.16
ADS 36	1	32.34	11.429		8.86	3.19
	2	32.57	11.429		12.17	4.38
	3	30.78	11.429		10.33	3.72
	Average	31.90	11.429	2791	10.45	3.76
HANCOR 36	1	27.22	10.035		10.11	3.64
	2	28.30	10.035		14.31	5.15
	3	26.44	10.035		8.92	3.21
	Average	27.32	10.035	2722	11.11	4.00
PVC 36	1	32.49	6.371		2.59	0.933
	2	33.96	6.371		3.53	1.270
	3	34.04	6.371		2.64	0.950
	Average	33.50	6.371	5258	2.92	1.051
Steel 36	1	127.62	2.730		1.88	0.677
	2	121.67	2.730		1.83	0.657
	3	129.50	2.730		2.17	0.780
	Average	126.26	2.730	46249	1.96	0.705
Aluminum 36	1	66.79	2.181		1.60	0.576
	2	64.28	2.181		1.55	0.559
	3	78.71	2.181		1.62	0.583
	Average	69.93	2.181	32063	1.59	0.573

Note: [a] Maximum elongation divided by nominal pipe diameter multiplied by 10^6.

Table 9.3a - Calculations for Apparent Modulus of Elasticity for HDPE Pipes

Test#		Loads (kips)	Total Area (in^2)	Stress (psi)	Elongation (in.)	Diameter (in.)	Strain	Apparent Modulus of Elasticity (psi)
a) ADS 48								
#1	R1	10.2246			0.598			
	R2	25.5408			0.849			
	ΔR	15.3162	39.508	387.67	0.251	48	0.0052	74 137
#2	R1	10.7173			0.317			
	R2	26.2390			0.578			
	ΔR	15.5217	39.508	392.87	0.210	48	0.0054	72 755
#3	R1	10.3067			0.512			
	R2	25.0071			0.733			
	ΔR	14.7004	39.508	372.10	0.221	48	0.0046	80 817
							Average	**75 903**
b) ADS 36								
#1	R1	5.1954			0.522			
	R2	15.1209			0.957			
	ΔR	9.9255	11.429	868.45	0.435	36	0.0121	71 872
#2	R1	5.1178			0.677			
	R2	15.6637			1.144			
	ΔR	10.5459	11.429	922.73	0.467	36	0.0130	71 131
#3	R1	5.4280			0.743			
	R2	15.1209			1.159			
	ΔR	9.6929	11.429	848.10	0.416	36	0.0116	73 393
							Average	**72 132**
c) HANCOR								
#1	R1	5.1178			0.760			
	R2	15.2760			1.280			
	ΔR	10.1582	10.035	1012.28	0.52	36	0.0144	70 081
#2	R1	5.5055			0.561			
	R2	15.276			1.068			
	ΔR	9.7705	10.035	973.64	0.507	36	0.0141	69 134
#3	R1	5.5055			0.554			
	R2	15.1209			1.093			
	ΔR	9.6154	10.035	958.19	0.539	36	0.015	63 998
							Average	**67 738**

Table 9.3b - Calculations for PVC and Metal Pipes

Test#		Loads (kips)	Total Area (in^2)	Stress (psi)	Elongation (in.)	Diameter (in.)	Strain	Apparent Modulus of Elasticity (psi)
d) PVC 36								
#1	R1	5.3505			0.2977			
	R2	15.2760			0.5044			
	ΔR	9.9255	6.371	1557.92	0.2067	36	0.0057	271 335
#2	R1	5.5055			0.3469			
	R2	15.4310			0.5610			
	ΔR	9.9255	6.371	1557.92	0.2141	36	0.0059	261 958
#3	R1	5.5055			0.2190			
	R2	15.1209			0.4134			
	ΔR	9.6154	6.371	1509.25	0.1944	36	0.0054	279 491
							Average	**270 928**
e) Steel 36								
#1	R1	20.6955			0.06890			
	R2	52.366			0.15994			
	ΔR	31.6705	2.730	11601	0.0904	36	0.0025	4 640 366
#2	R1	20.0684			0.09596			
	R2	50.4846			0.16486			
	ΔR	30.4162	2.730	11141	0.0689	36	0.0019	5 863 929
#3	R1	21.0091			0.30266			
	R2	50.4846			0.39616			
	ΔR	29.4755	2.730	10797	0.0935	36	0.0026	4 152 649
							Average	**4 885 648**
f) Aluminum 36								
#1	R1	15.3649			0.27805			
	R2	29.1619			0.34203			
	ΔR	13.80	2.181	6326	0.0640	36	0.0018	3 514 443
#2	R1	15.3649			0.24114			
	R2	30.1026			0.32480			
	ΔR	14.74	2.181	6757	0.0837	36	0.0023	2 937 962
#3	R1	15.0513			0.1698			
	R2	30.7297			0.2756			
	ΔR	15.6784	2.181	7189	0.1058	36	0.0029	2 478 838
							Average	**2 977 081**

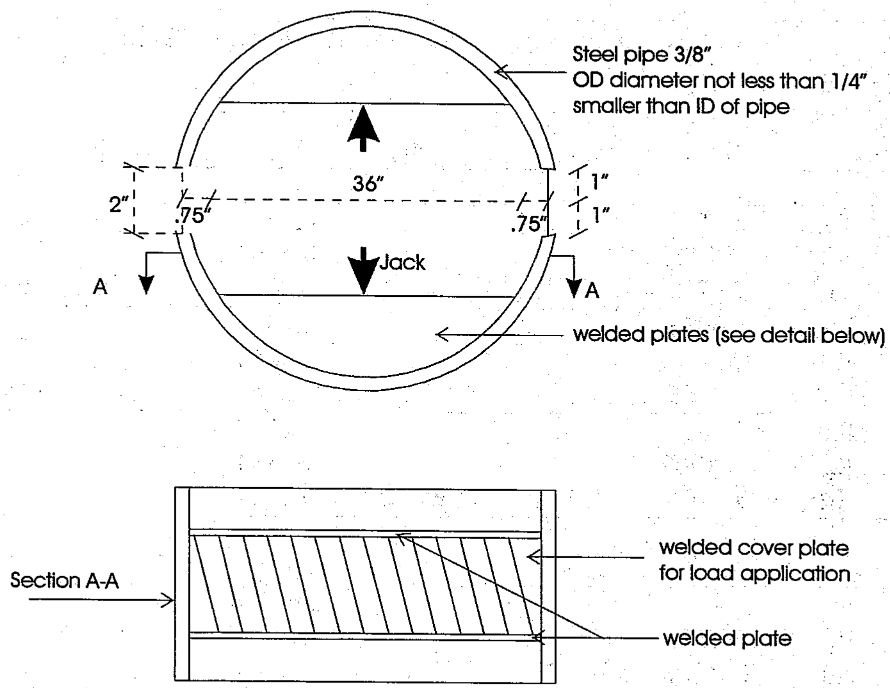

Fig. 9.1 - Test fixture for the 36" diameter pipe

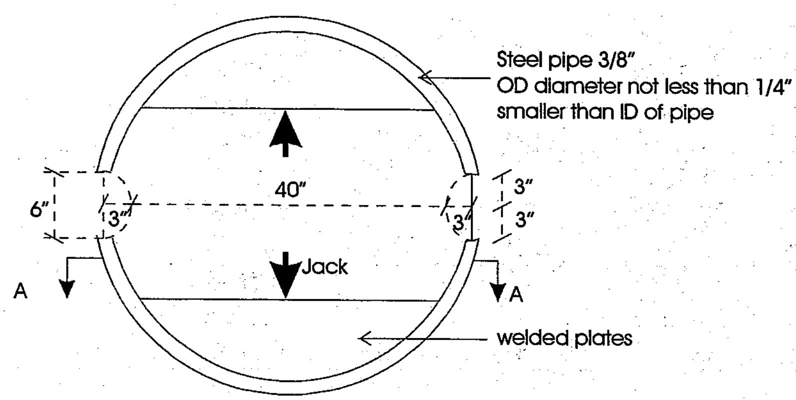

Fig. 9.2 - Test fixture for the 48" diameter pipe

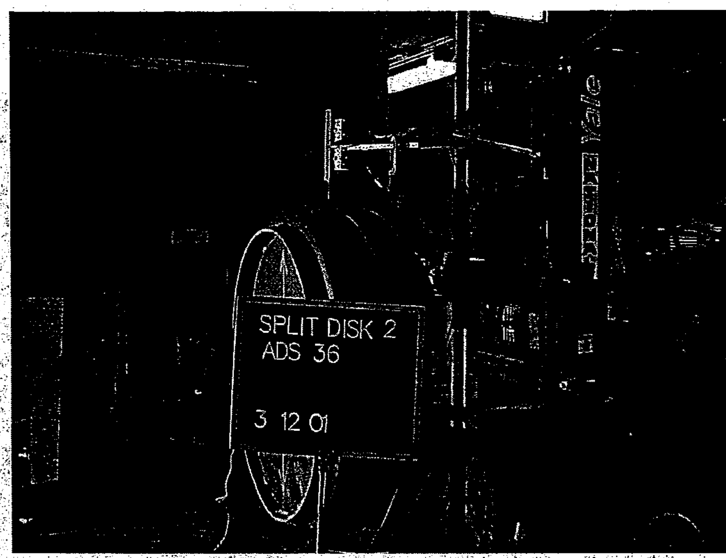

Fig. 9.3 - Overall Configuration of the Test Fixture for Testing the 36" Diameter Pipe

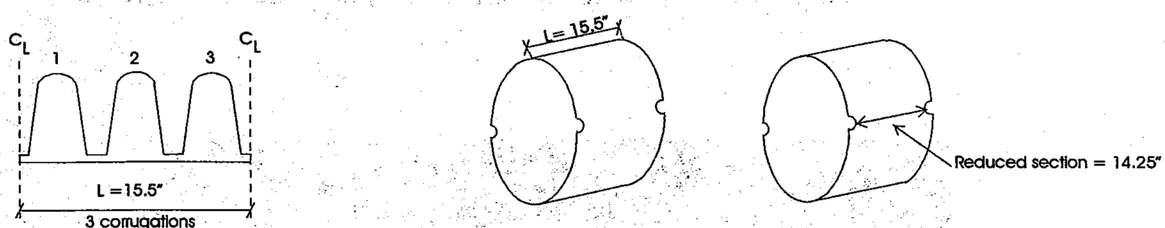

Figure 9.4 - HDPE 36" diameter specimen configurations

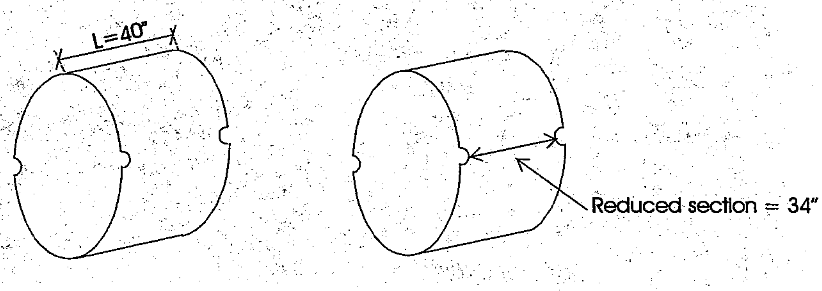

Figure 9.5 - HDPE 48" diameter specimen configurations

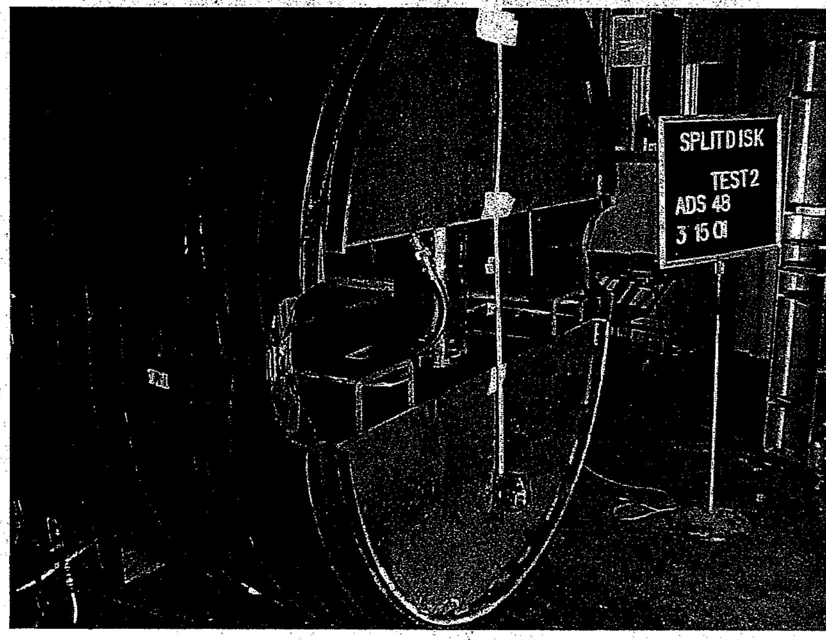

Fig. 9.6 - Deformation of ADS 48 specimen specimen under tensile load

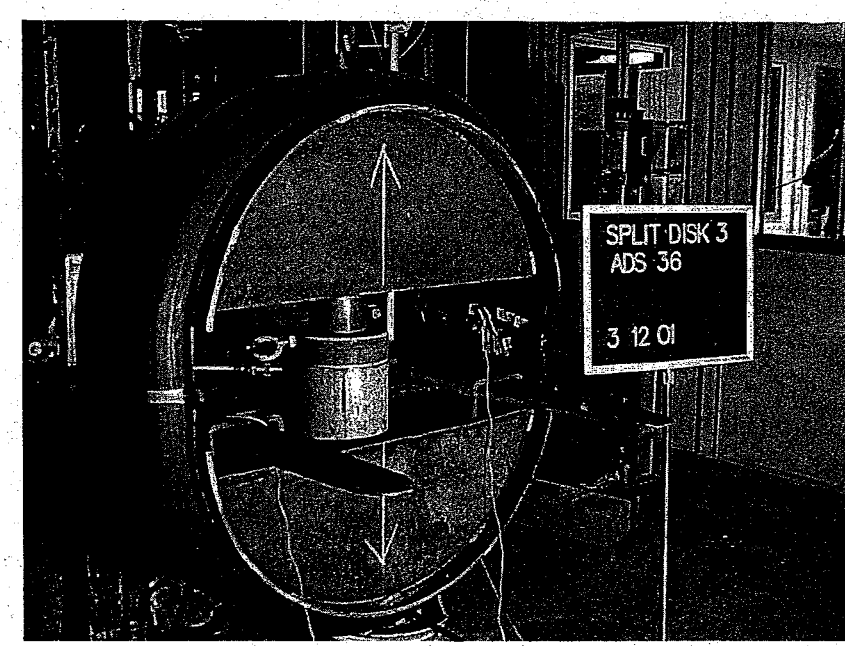

Fig. 9.7 - Deformation of ADS 36 specimen under tensile load

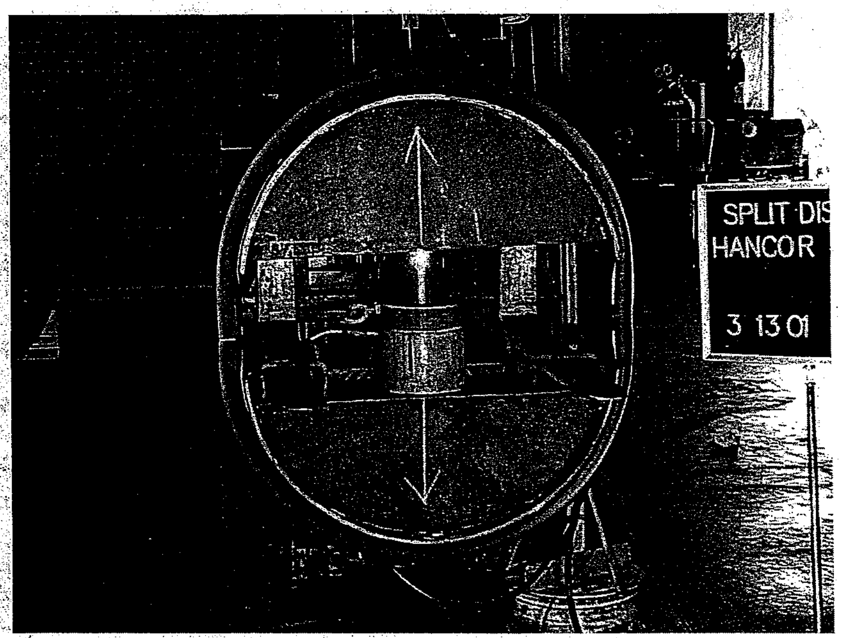

Fig. 9.8 - Deformation of HANCOR 36 specimen under tensile load

Fig. 9.9 - Deformation of PVC specimen under tensile load

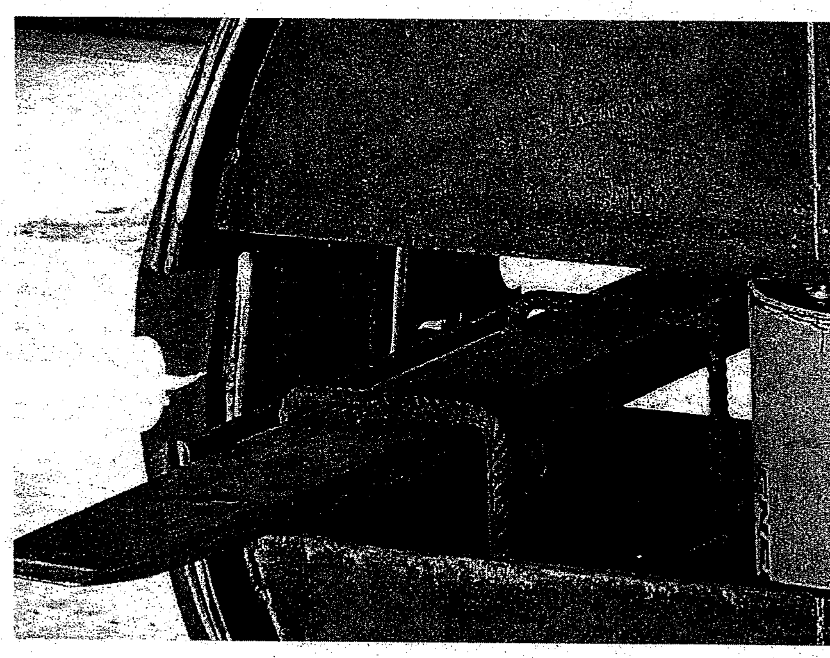

Fig. 9.10 - External cracking of steel specimen

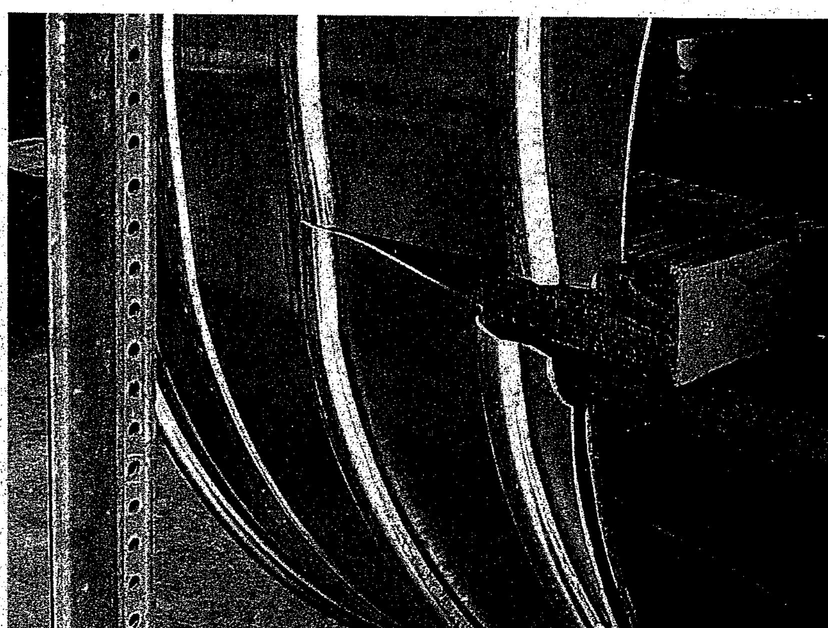

Fig. 9.11 - External cracking of aluminum specimen

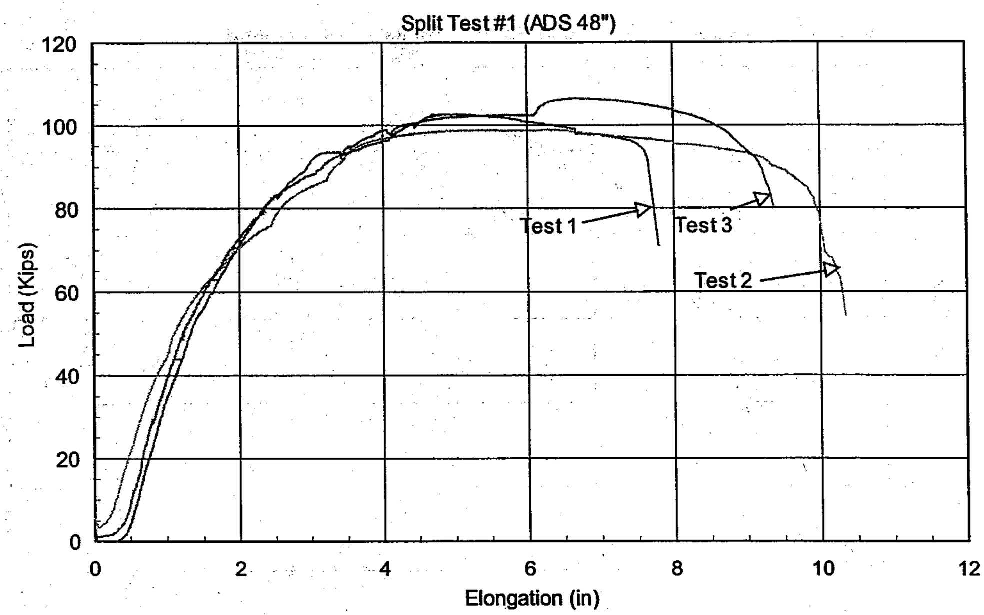

Fig. 9.12 - Load vs. Vertical Diametral Change for ADS 48 specimen

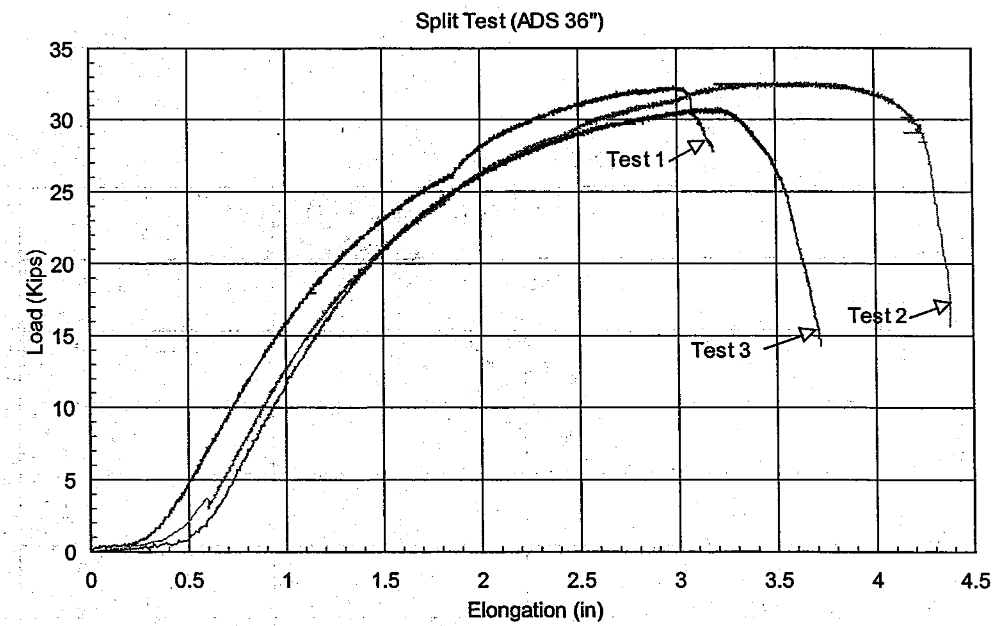

Fig. 9.13 - Load vs. Vertical Diametral Change for ADS 36 Specimen

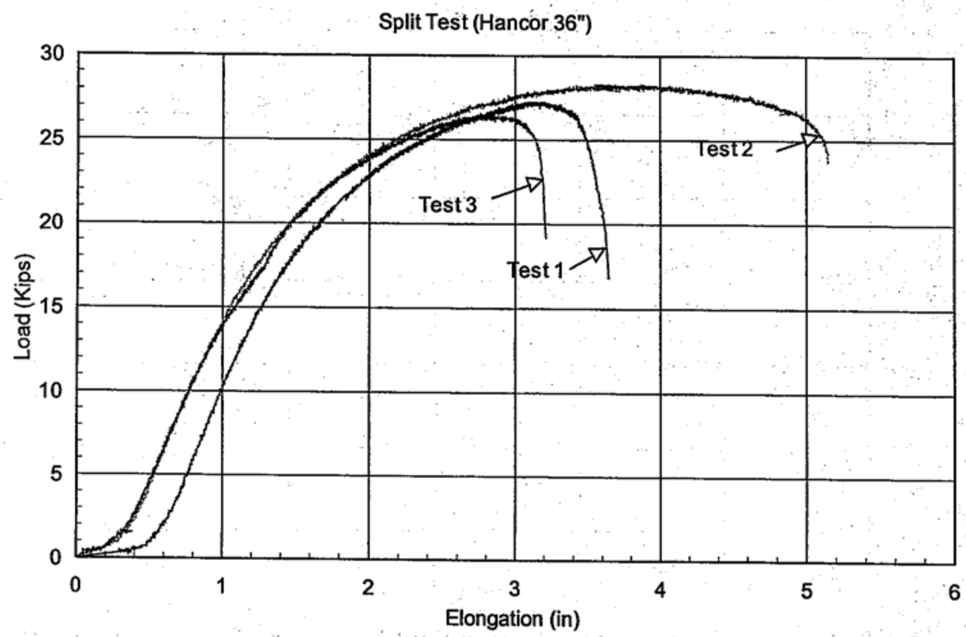

Fig. 9.14 - Load vs. Vertical Diametral Change for HANCOR 36 Specimen

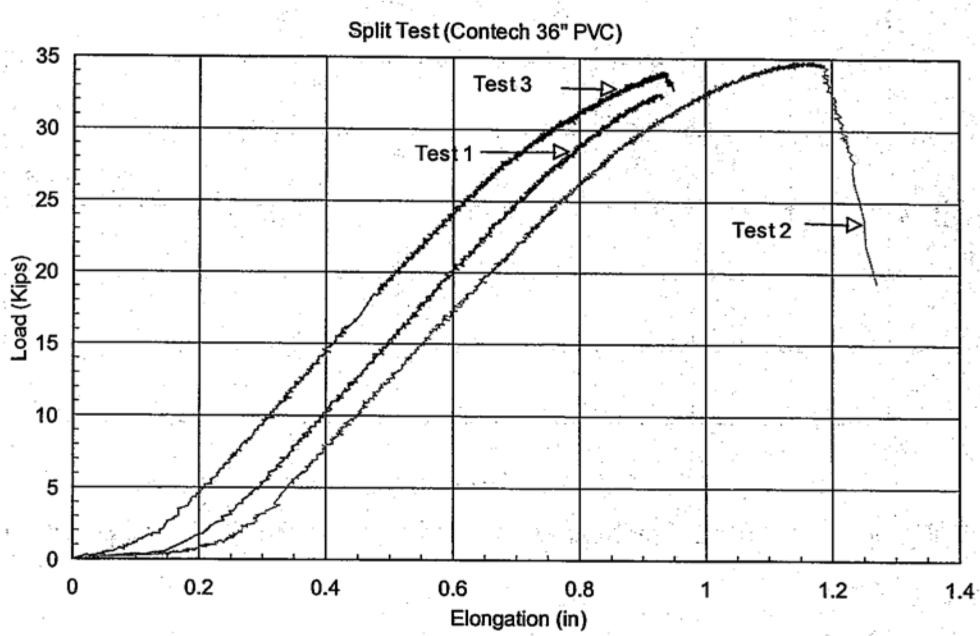

Fig. 9.15 - Load vs. Vertical Diametral Change for PVC 36 Specimen

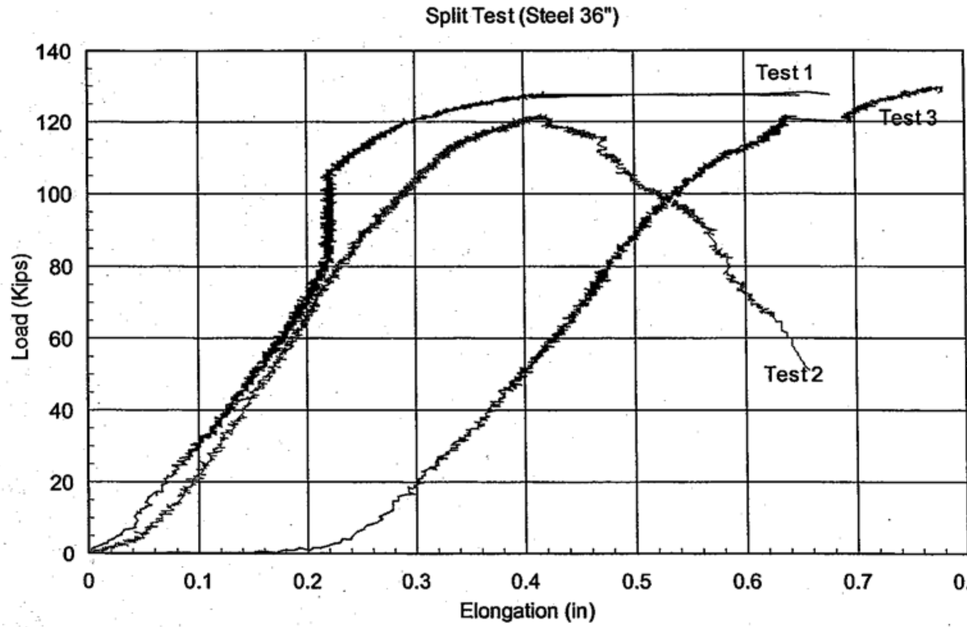

Fig. 9.16 - Load vs. Vertical Diametral Change for Steel 36 Specimen

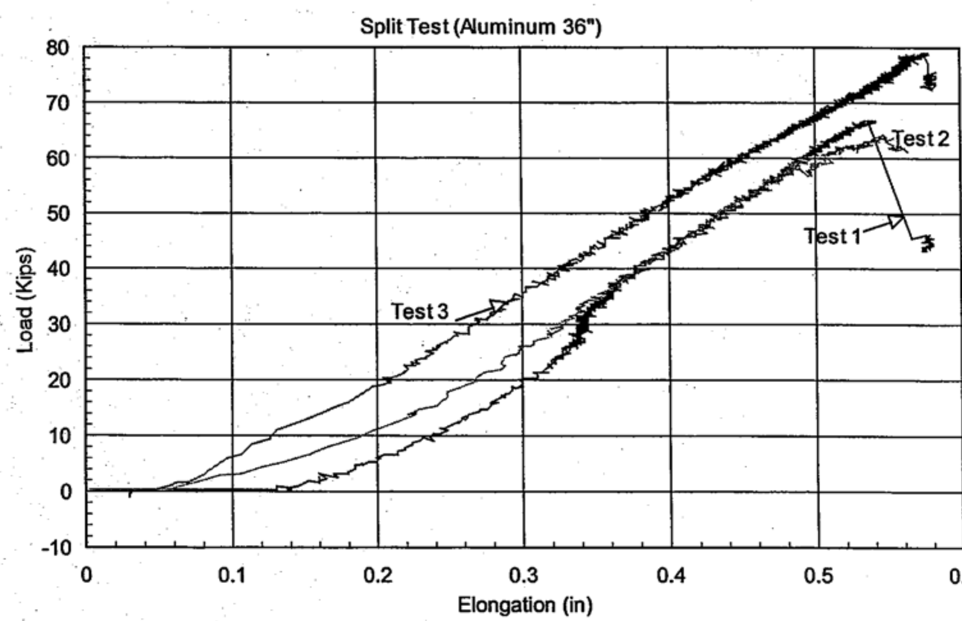

Fig. 9.17 - Load vs. Vertical Diametral Change for Aluminum 36 Specimen

Chapter 10: Tensile Tests on 10 Inch - Dog Bone Specimens

10.1 Objectives

The objective of this test was to determine he tensile properties of an HDPE coupon cut from the pipe specimen in the form of a dog bone shaped specimen. The specimens were tested under predetermined cross-head speed and ambient conditions. The tensile properties include the tensile strength, the percent elongation, the modulus of elasticity and Poisson's ratio. Most of the test procedure and method of calculating tensile properties closely follow the approach described in ASTM D-638, Standard Test Method for Tensile Properties of plastics.

10.2 Experimental program Apparatus

A 110-kip (500 kN), servo-hydraulic, tensile testing machine (Type MTS 810, for example see Fig. 10.2) was used for the dog bone tension tests. The machine is equipped with a Testar digital interface and is controlled by a computer program. In addition, the MTS machine was equipped with special grips to hydraulically control the pressure. The tests were performed at a displacement rate ranging from 0.05 in./min. to 150 in./min.(see Program, :Table 10.1). The applied load was measured using a load cell. The change in length of the specimen and the axial and transverse strains were recorded using LVDTs and strain gages, respectively.

Test Specimens

The test specimen was first cut from the flexible pipe in the form of longitudinal strips 1.13 in. x 9.7 in. The coupon was then machined to obtain the dog bone shape shown in Fig. 10.1. No welds or seams were allowed in the specimens, except those specimens designated by Steel 36 - seam and Aluminum 36 - seam, in which a seam lock was introduced at the middle of the specimens (see Figs. 10.12 and 10.13).

Test Procedure

Longitudinal and transverse strain gages were installed on the specimen and the specimen was aligned so as to ensure its longitudinal axis to be coincident with the direction of the applied load. For plastic pipe specimens, the tensile force was applied at a constant rate-of-head speed of 0.05, 0.5 10 and 150 in. per minute until the specimen failed. For metal pipes, the tensile force was applied at a constant rate-of-head speed of 0.5 in. per minute until the specimen failed. The data acquisition system was used to continuously record both transverse strain and axial strain simultaneously. The applied tensile load, as well as the corresponding elongation of the specimen was also continuously recorded.

Test Program

Table 10.1 presents the details of the testing program including the number of tests and the load rates.

10.3 Calculations

i) Ultimate tensile strength

The ultimate tensile strength, σ_u, is calculated by dividing the maximum load at failure, F_b in newtons (or pounds-force) by the original cross-sectional area, A of the specimen in square metres (or square inches).

ii) Modulus of elasticity

First, a graph of stress versus strain of the specimen is plotted. The initial linear portion of the stress-strain curve is extended, and the modulus of elasticity, E is given by the slope of this straight line, which is calculated by dividing the difference in stress corresponding to any segment on the straight line by the corresponding difference in strain.

iii) Poisson's ratio

The axial and transverse, strains obtained from the test are plotted against the applied load. Straight lines are drawn through each set of points for both the axial, ε_a, and the transverse, ε_t, strains. One of any section in the linear portion of the graph is selected and the change in strain is determined. Then, Poisson's ratio, μ, was calculated using Eq. (10.1) shown below:

$$\mu = -(\text{change in transverse strain}) / (\text{change in axial strain}) \quad (10.1)$$

10.4 Results and Observations

Experimental results are provided in Tables 10.2a and 10.2b for plastic and metal pipes, respectively, while, average values are summarized in Tables 10.3a and 10.3b. Photographs of the specimens during testing are presented in Figs. 10.2 to 10.13.

The curves of the stress versus longitudinal and transverse strains for the various loading rates considered are presented in Fig. 10.14 for ADS 48", Fig. 10.15 for ADS 36", 10.16 for Hancor 36" Fig. 10.17 for PVC 36", Fig. 10.18 for Steel 36"and Aluminum 36"and Fig. 10.19 for the seam locks of steel and aluminum pipes.

From these results, the following observations are made:

(a) Results for ADS 48 show scatter and seem inconsistent (see Table 10.3a). This is due to the difficulty of measuring the thickness of the specimen due to the surface irregularities of the pipe wall from which the specimens were cut.

(b) For HDPE pipes, the modulus of elasticity generally increased as the loading rate increased.

(c) The maximum average value of the modulus of elasticity (E) achieved by ADS 48" was 100 ksi, whereas it attained 154 ksi and 147 ksi for ADS 36" and Hancor 36", respectively. For PVC 36", the maximum average modulus of elasticity was 451 ksi. For 0.5 in./min. the average values of E were 69 ksi, 96 ksi, 117 ksi and 381 ksi for ADS 48", ADS 36", Hancor 36" and PVC 36", respectively.

(d) For HDPE pipes, the maximum stress increased as the loading rate increased. It varied between 3.11 ksi and 4.63 ksi for ADS 48", 2.80 ksi and 4.78 ksi for ADS 36", and 2.97 ksi and 4.79 ksi for Hancor 36. For PVC 36" pipe, the average maximum stress did not vary noticeably with the loading rate (between 5.18 and 6.64 ksi). For a loading rate of 0.5 in./min, the values of the maximum stress achieved by ADS 48", ADS 36" Hancor 36" and PVC 36" are, respectively, 3.47 ksi, 3.48 ksi, 3.59 ksi and 6.02 ksi.

(e) Steel and Aluminum achieved an average maximum tensile stress of 55.8 ksi and 33.1 ksi, respectively, and an average modulus of elasticity of 25,028 ksi and 9,272 ksi, respectively.

(f) The apparent maximum stresses achieved by the Steel and Aluminum seam lock specimens are 8.40 ksi and 4.00 ksi, respectively. The apparent modulus of elasticity is 1,150 ksi for Steel seam lock and 687 ksi for Aluminum seam lock.

10.5 Conclusions

The following conclusions can be formulated:

(a) The moduli of elasticity of the different pipes are within the range of values specified by the AASHTO code.

(b) The tensile strengths of the different pipes are in conformity with the AASHTO code.

Table 10.1 - Dog Bone Tension Test Type C Program

Type of Pipe	Load Rate (in/min.)	Number of Tests
ADS 48	0.05	2
	0.5	2
	10	2
	150	2
ADS 36	0.05	2
	0.5	2
	10	2
	150	3
Hancor 36	0.05	2
	0.5	2
	10	2
	150	2
PVC 36	0.05	2
	0.5	2
	10	2
	150	2
Steel 36	0.5	3
Aluminium 36	0.5	3
Steel 36 - Seam	0.5	2
Aluminium 36 - Seam	0.5	3

Table 10.2a – Experimental Results for Plastic Pipes

Type	Specimen	Width in	Thickness in	Cross section in²	Maximum force kips	Maximum stress ksi	Strain at max stress -	Modulus of elasticity ksi
ADS 48	0.05 - 1	0.735	0.339	0.2495	0.752	3.01	0.121	96
	0.05 - 2	0.740	0.339	0.2509	0.804	3.20	0.142	69
	0.5 - 1	0.742	0.328	0.2437	0.837	3.43	0.129	71
	0.5 - 2	0.732	0.339	0.2484	0.870	3.50	0.119	66
	10 - 1	0.737	0.336	0.2475	1.056	4.27	0.113	97
	10 - 2	0.737	0.337	0.2480	1.103	4.45	0.105	103
	150 - 1	0.733	0.328	0.2403	1.063	4.42	0.100	91
	150 - 2	0.733	0.335	0.2457	1.189	4.84	0.090	66.00
ADS 36	0.05 - 1	0.742	0.115	0.0850	0.250	2.94	0.073	77
	0.05 - 2	0.747	0.125	0.0933	0.248	2.66	0.091	52
	0.5 - 1	0.751	0.117	0.0875	0.312	3.56	0.086	101
	0.5 - 2	0.750	0.116	0.0871	0.296	3.40	0.084	90
	10 - 1	0.753	0.125	0.0939	0.353	3.76	0.072	153
	10 - 2	0.752	0.119	0.0891	0.354	3.97	0.076	154
	150 - 1	0.759	0.111	0.0840	0.400	4.76	0.046	141
	150 - 2	0.746	0.117	0.0876	0.423	4.83	0.055	110
	150 - 3	0.747	0.110	0.0823	0.390	4.74	0.046	126
Hancor 36	0.05 - 1	0.767	0.093	0.0710	0.212	2.99	0.080	102
	0.05 - 2	0.757	0.095	0.0719	0.213	2.96	0.080	107
	0.5 - 1	0.753	0.111	0.0836	0.292	3.49	0.089	109
	0.5 - 2	0.750	0.111	0.0836	0.308	3.69	0.102	125
	10 - 1	0.753	0.108	0.0812	0.365	4.49	0.060	136
	10 - 2	0.759	0.126	0.0953	0.400	4.20	0.073	147
	150 - 1	0.749	0.117	0.0879	0.411	4.68	0.050	154
	150 - 2	0.753	0.111	0.0836	0.410	4.90	0.049	141
PVC 36	0.05 - 1	0.740	0.157	0.1160	0.760	6.55	0.025	398
	0.05 - 2	0.750	0.181	0.1358	0.844	6.21	0.029	379
	0.5 - 1	0.745	0.184	0.1370	0.768	5.61	0.017	402
	0.5 - 2	0.750	0.179	0.1343	0.739	5.50	0.026	343
	0.5 - 3	0.747	0.187	0.1400	0.974	6.96	0.027	397
	10 - 1	0.758	0.189	0.1429	1.111	7.77	0.029	497
	10 - 2	0.752	0.191	0.1438	0.792	5.51	0.017	406
	150 - 1	0.748	0.186	0.1391	0.638	4.59	0.013	367
	150 - 2	0.752	0.181	0.1365	0.789	5.78	0.015	378

Table 10.2b – Experimental Results for Metal Pipes

Type	Specimen	Width in	Thickness in	Cross section in^2	Maximum force kips	Maximum stress ksi	Strain at max stress -	Modulus of elasticity ksi
STEEL 36	0.5 - 1	0.756	0.070	0.0532	2.941	55.24	0.037	23,354
	0.5 - 2	0.753	0.072	0.0540	3.001	55.62	0.074	25,408
	0.5 - 3	0.763	0.076	0.0577	3.259	56.51	0.064	26,322
ALU 36	0.5 - 1	0.747	0.076	0.0570	1.778	31.18	0.033	8,641
	0.5 - 2	0.753	0.070	0.0530	1.819	34.28	0.032	9,913
	0.5 - 3	0.753	0.072	0.0546	1.841	33.74	0.029	9,262
SEAM STEEL 36	0.5 - 1	1.025	0.071	0.0731	0.619	8.48	0.013	954
	0.5 - 2	1.019	0.072	0.0730	0.608	8.32	0.011	1,255
SEAM ALU 36	0.5 - 1	1.041	0.073	0.0763	0.312	4.09	0.024	791
	0.5 - 2	1.040	0.072	0.0753	0.297	3.95	0.013	562
	0.5 - 3	1.024	0.074	0.0754	0.299 (b)	3.97 (b)	0.010	709

Note : (b) Correponding to first yield

Table 10.3a – Experimental Average Results for Plastic Pipes

Make	Specimen	Maximum stress ksi	Strain at max stress -	Modulus of elasticity ksi
ADS 48	0.05	3.11	0.132	82
	0.5	3.47	0.124	69
	10	4.36	0.109	100
	150	4.63	0.095	78
ADS 36	0.05	2.80	0.082	65
	0.5	3.48	0.085	96
	10	3.87	0.074	154
	150	4.78	0.049	126
Hancor 36	0.05	2.97	0.080	104
	0.5	3.59	0.096	117
	10	4.35	0.067	141
	150	4.79	0.050	147
PVC 36	0.05	6.38	0.027	389
	0.5	6.02	0.023	381
	10	6.64	0.023	451
	150	5.18	0.014	372

Table 10.3b – Experimental Average Results for Metal Pipes

Type	Specimen	Maximum stress ksi	Strain at max stress -	Modulus of elasticity ksi
STEEL 36	0.5	55.79	0.058	25,028
ALU 36	0.5	33.07	0.031	9,272
SEAM STEEL 36	0.5	8.40	0.012	1,105
SEAM ALU 36	0.5	4.00	0.016	687

(a) Specimen cut in the form of longitudinal strip from the pipe

(b) Specimen cut into dogbone shape

(c) Instrumentation with strain gages

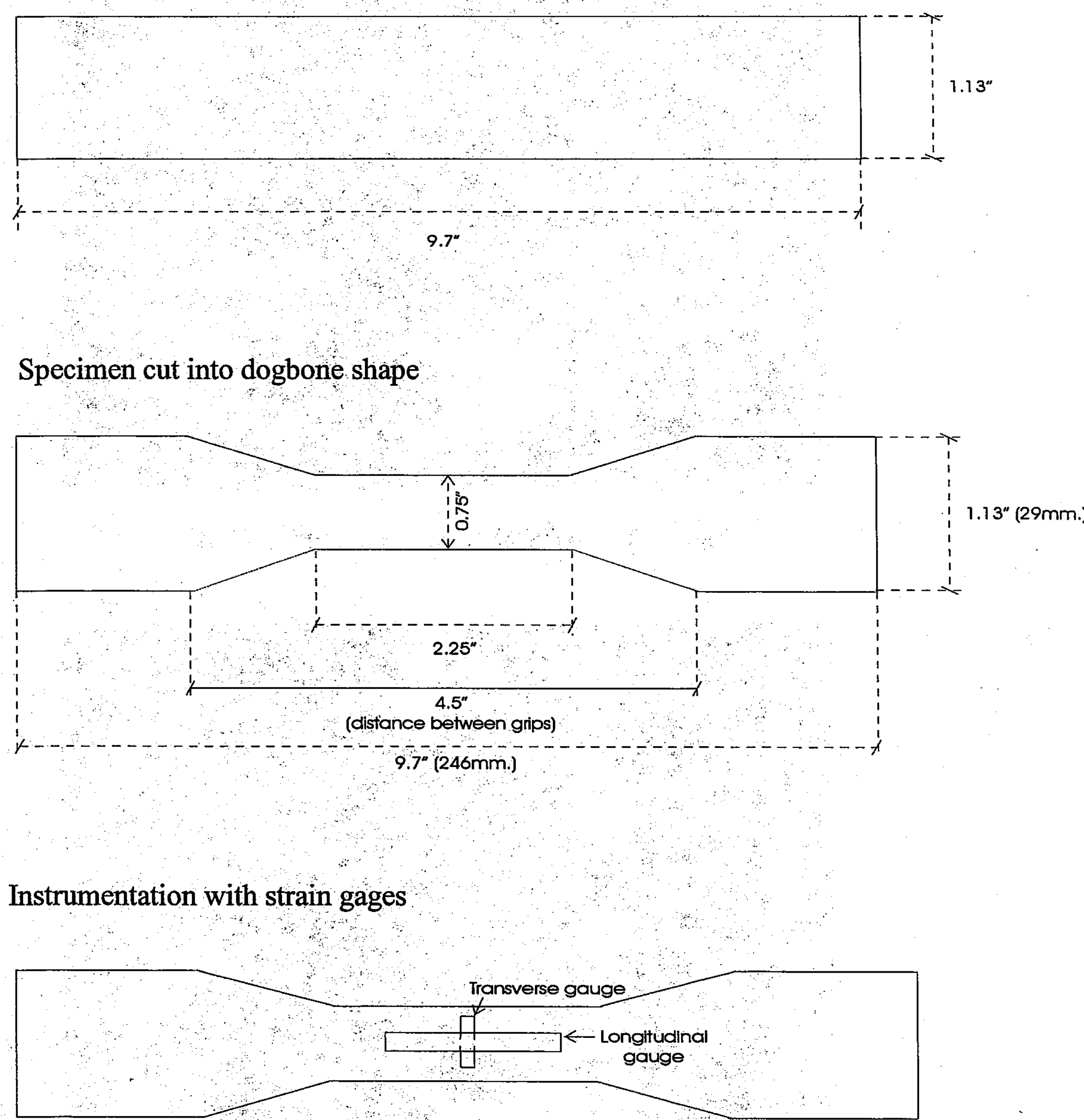

Fig. 10.1 - Details of Specimens

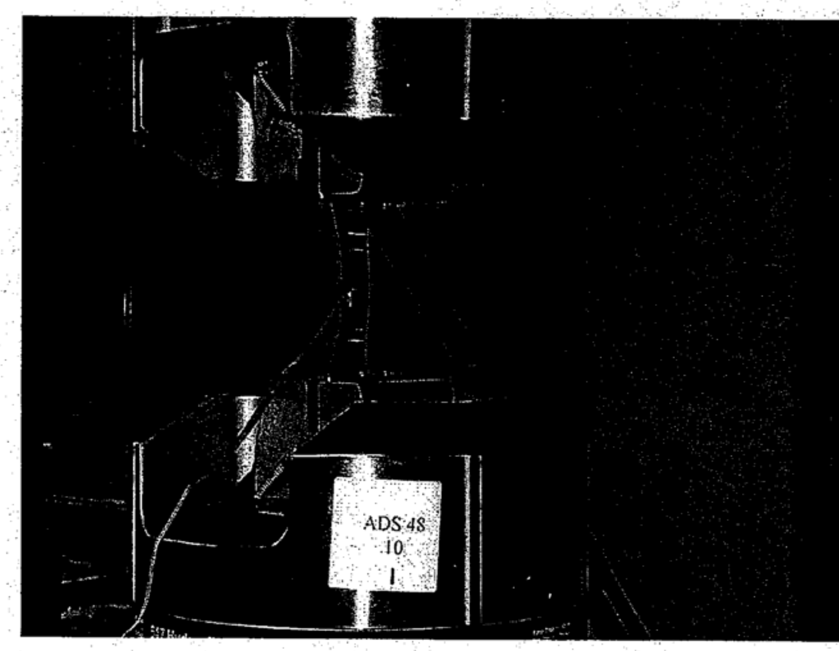

Fig. 10.2 - ADS 48 Specimen During Testing

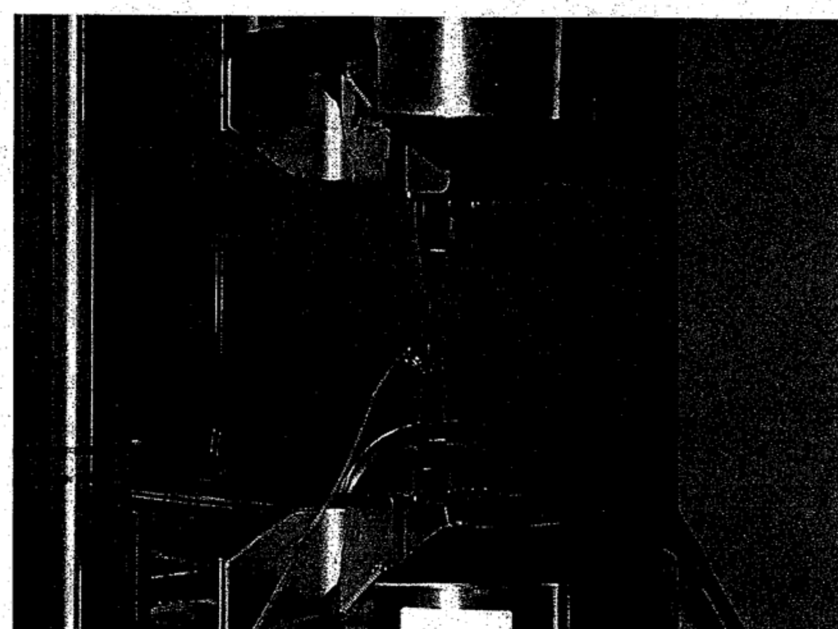

Fig. 10.3 - ADS 48 Specimen Prior to Failure

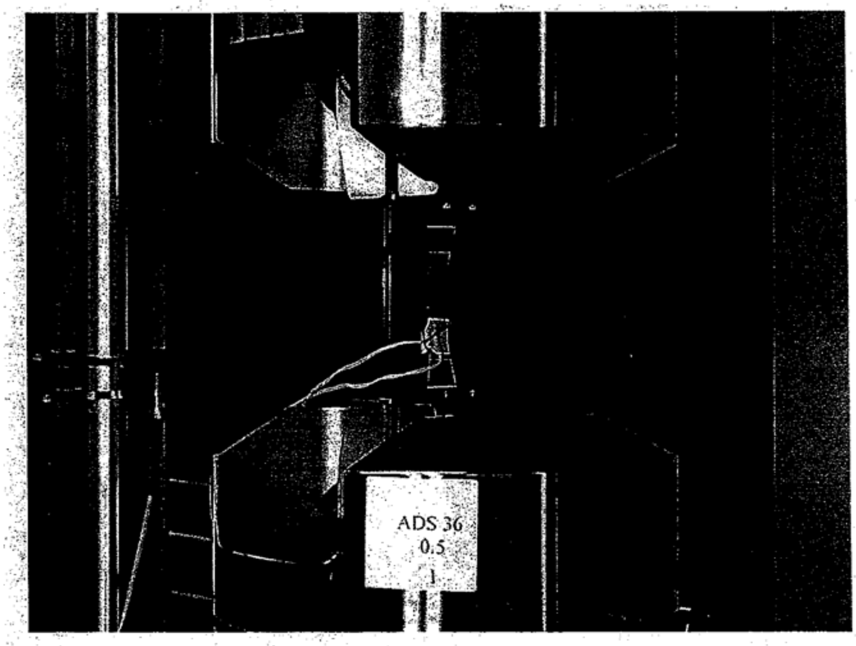

Fig. 10.4 - ADS 36 Specimen During Testing

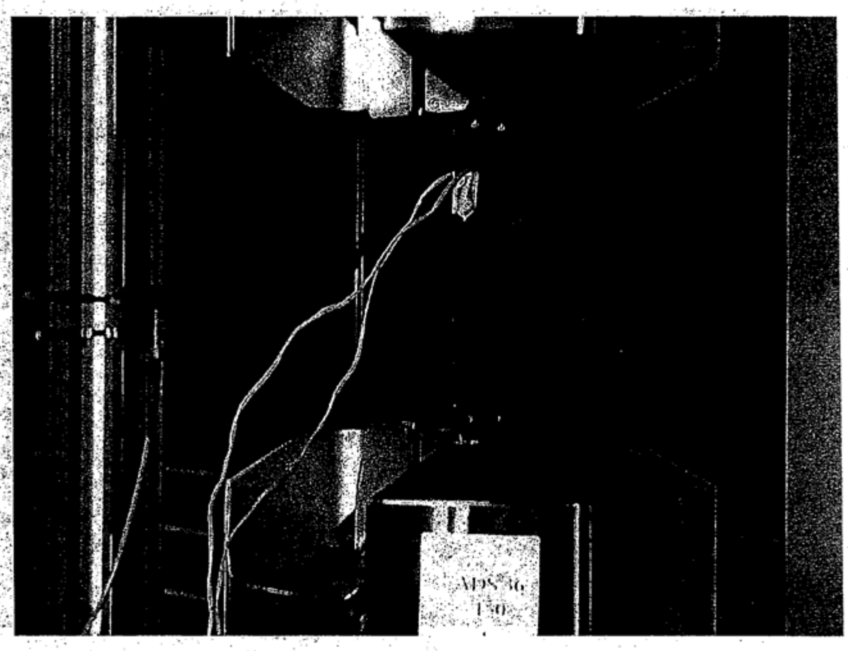

Fig. 10.5 - ADS 36 Specimen at Failure

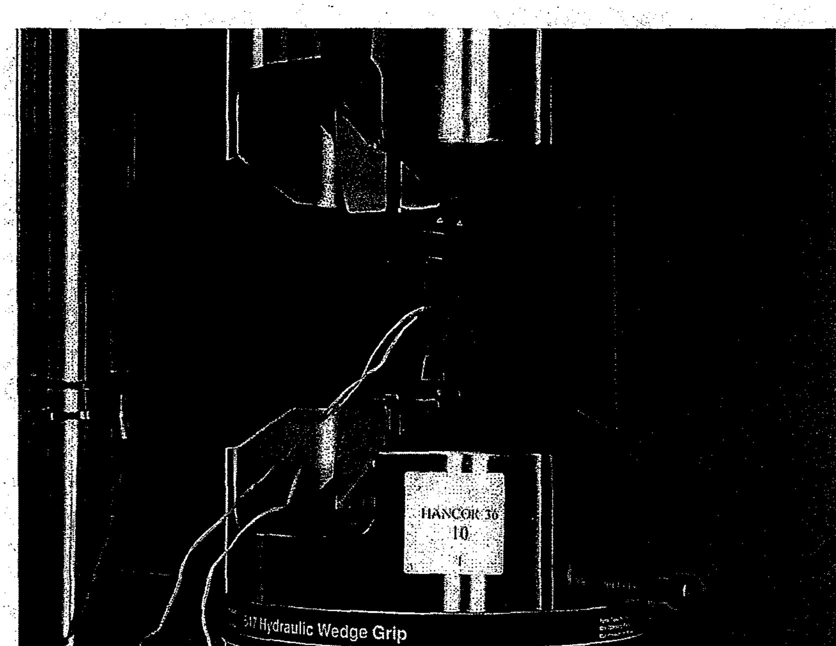

Fig. 10.6 - Hancor 36 Specimen During Testing

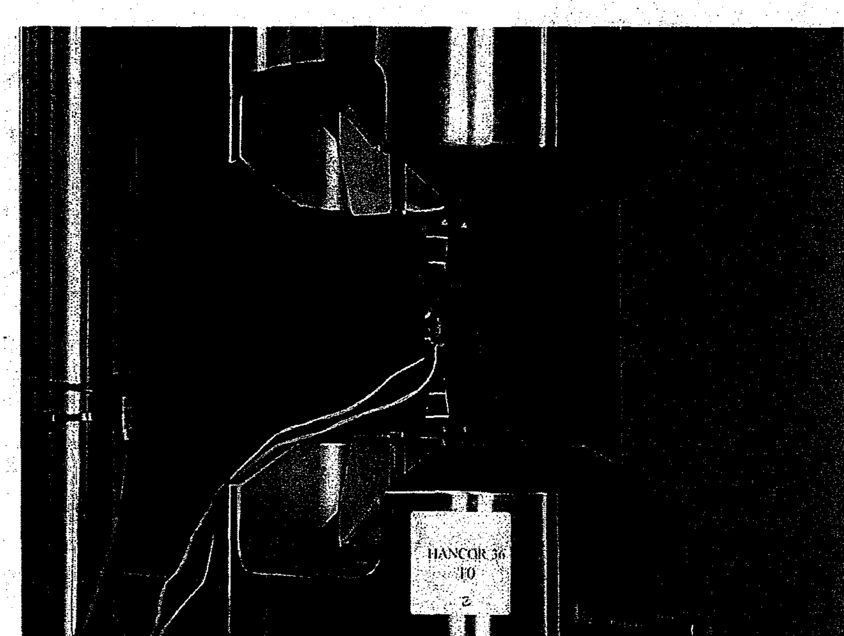

Fig. 10.7 - Hancor 36 Specimen at Failure

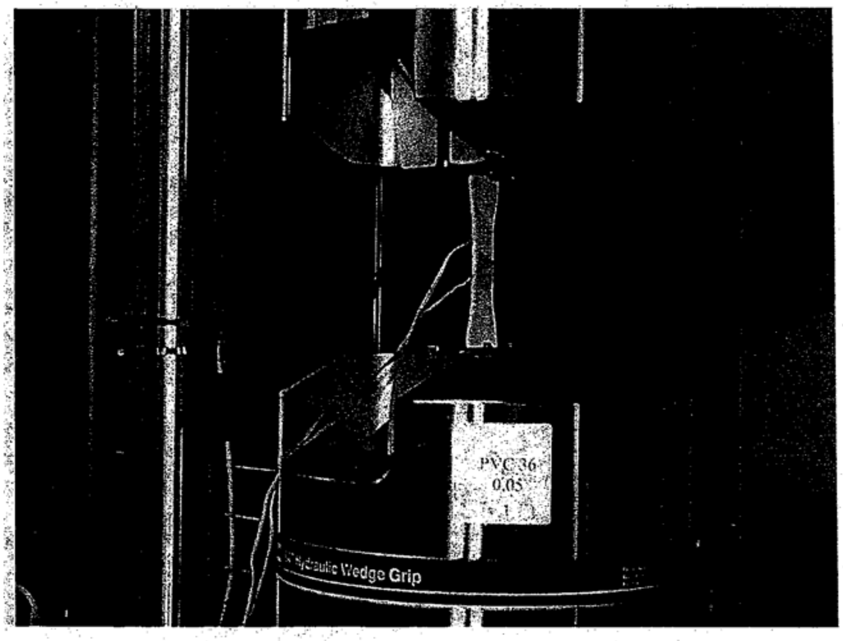

Fig. 10.8 - PVC 36 Specimen During Testing

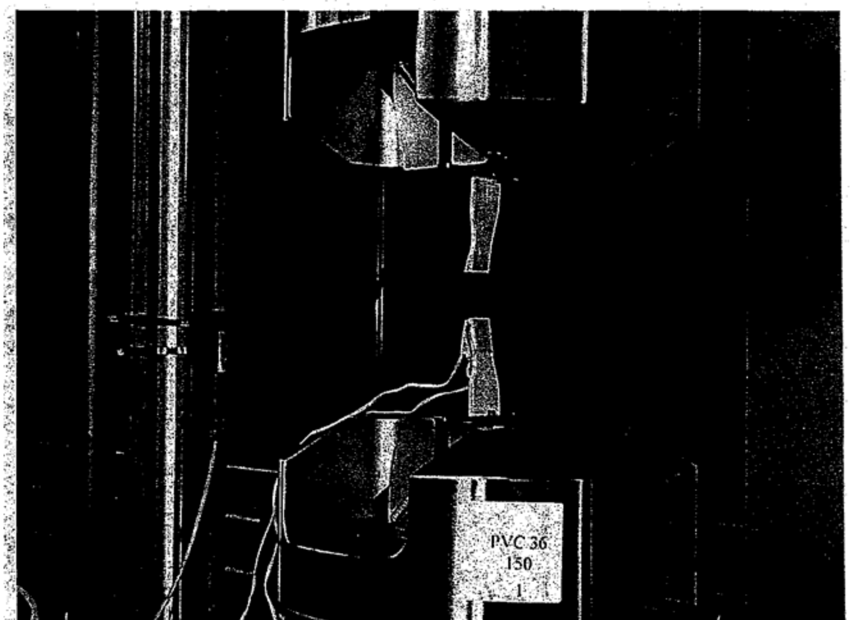

Fig. 10.9 - PVC 36 Specimen at Failure

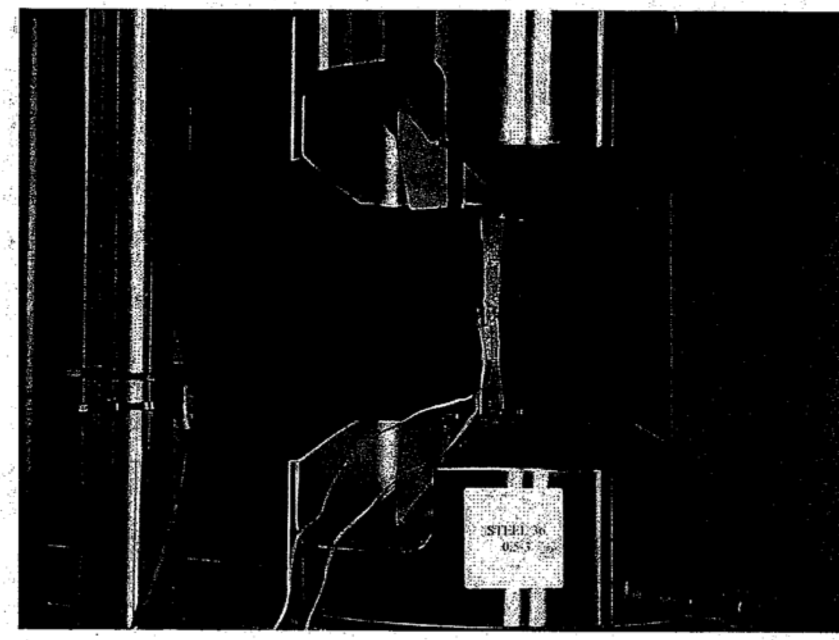

Fig. 10.10 - Steel 30 Specimen at Failure

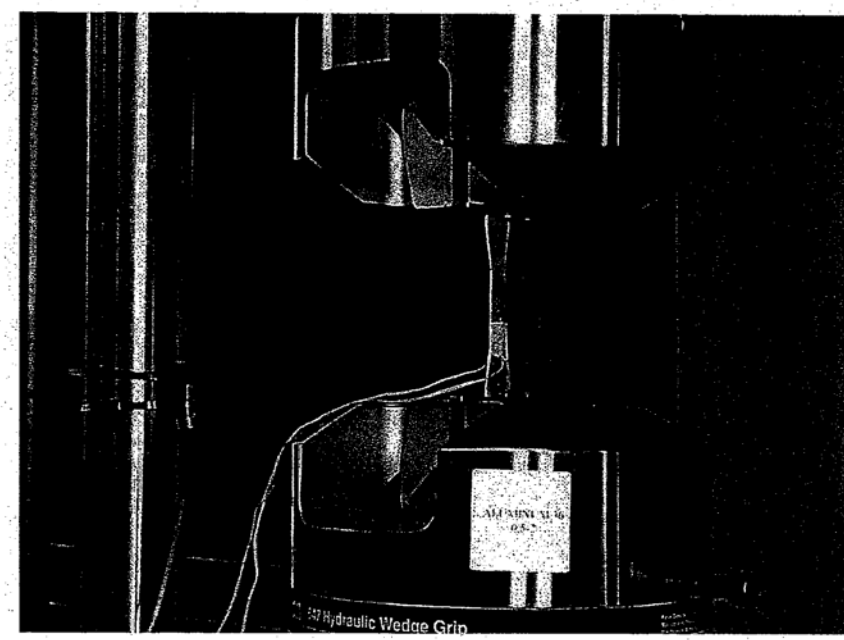

Fig. 10.11 - Aluminum Specimen During Testing

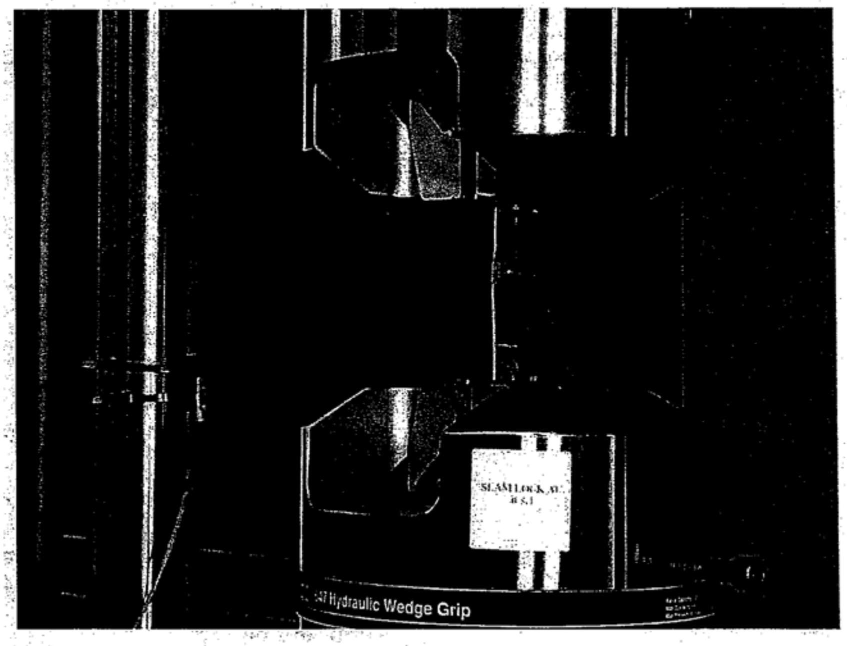

Fig. 10.12 - Aluminum Seam Specimen During Testing

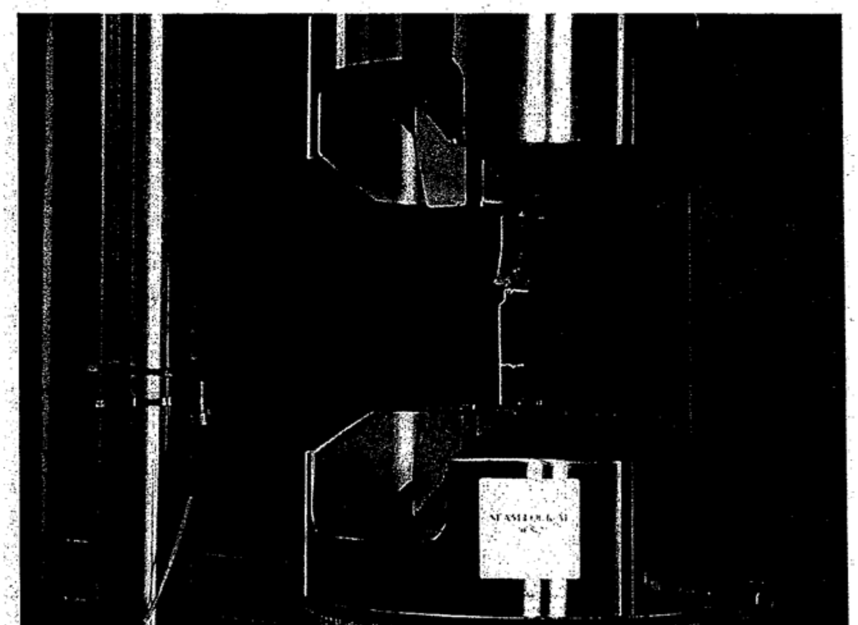

Fig. 10.13 - Aluminum Seam Specimen at Failure

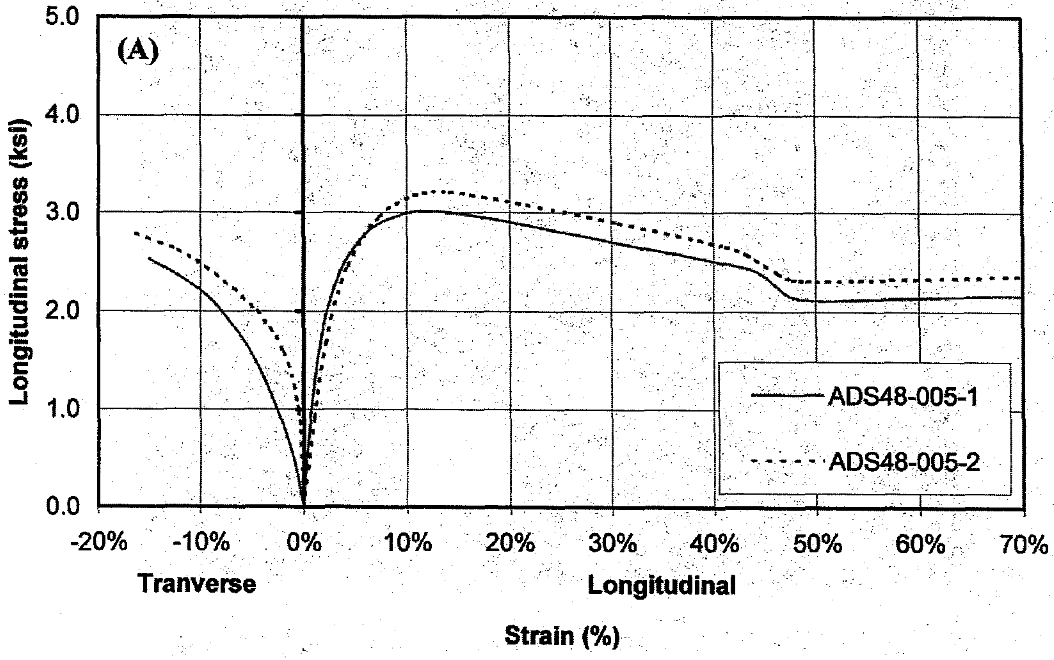

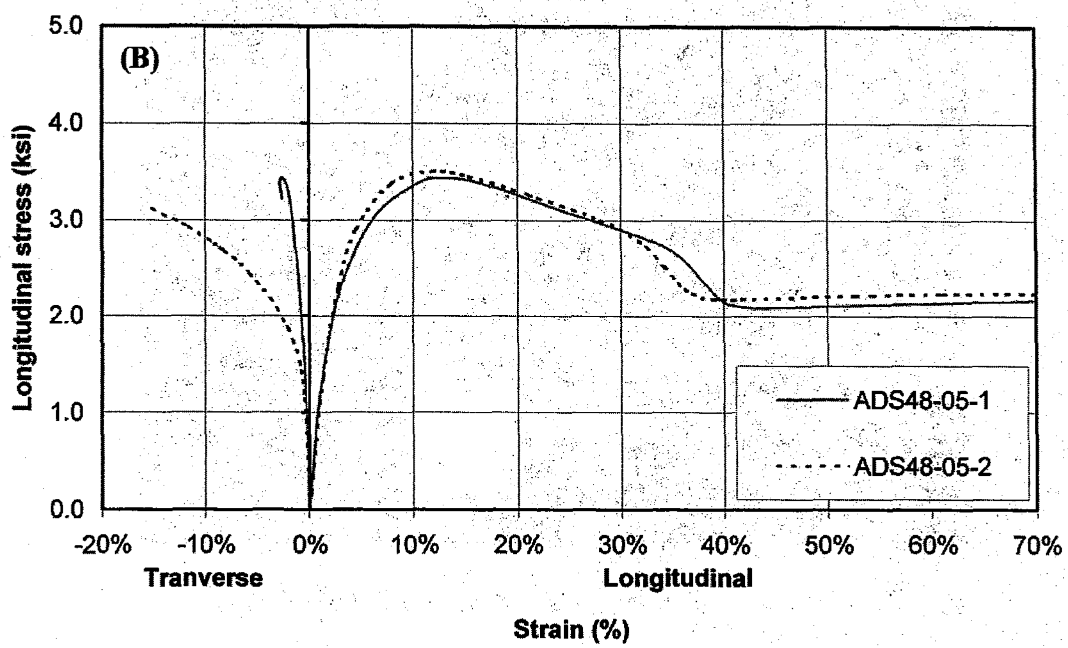

Fig.10.14a – Experimental Stress versus Strain Curves for ADS48 at a Loading Rate of : (A) 0.05 in./min. and (B) 0.5 in./min.

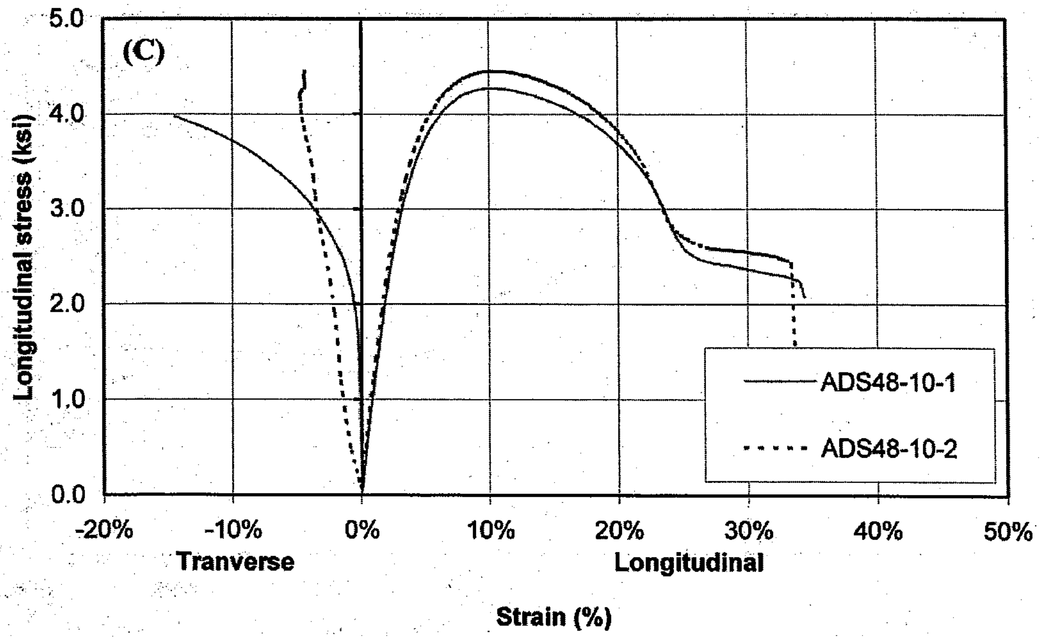

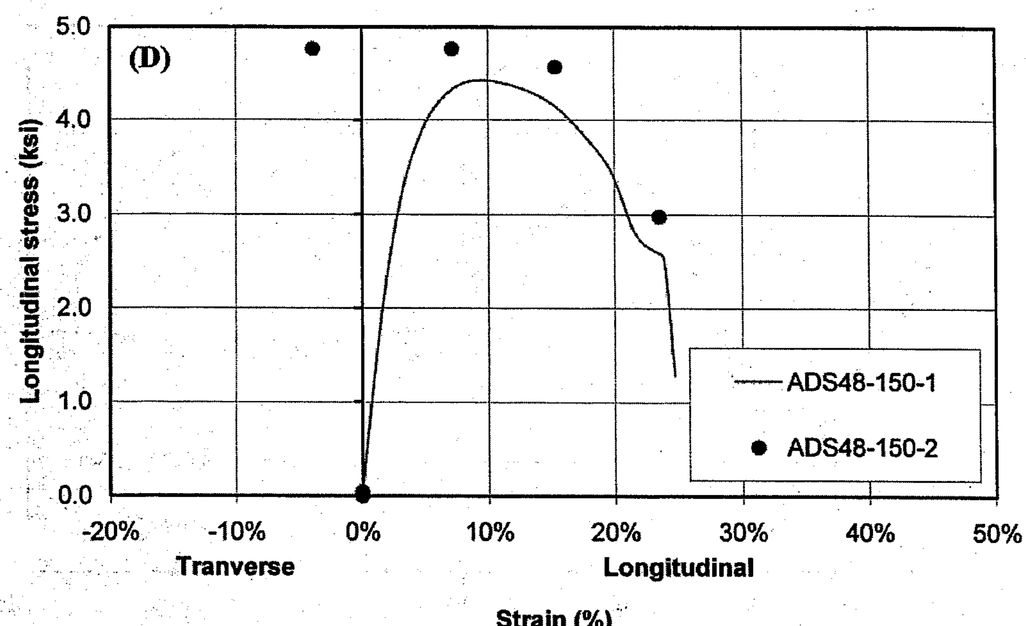

Fig.10.14b – Experimental Stress versus Strain Curves for ADS48 at a Loading Rate of : (C) 10 in./min. and (D) 150 in./min.

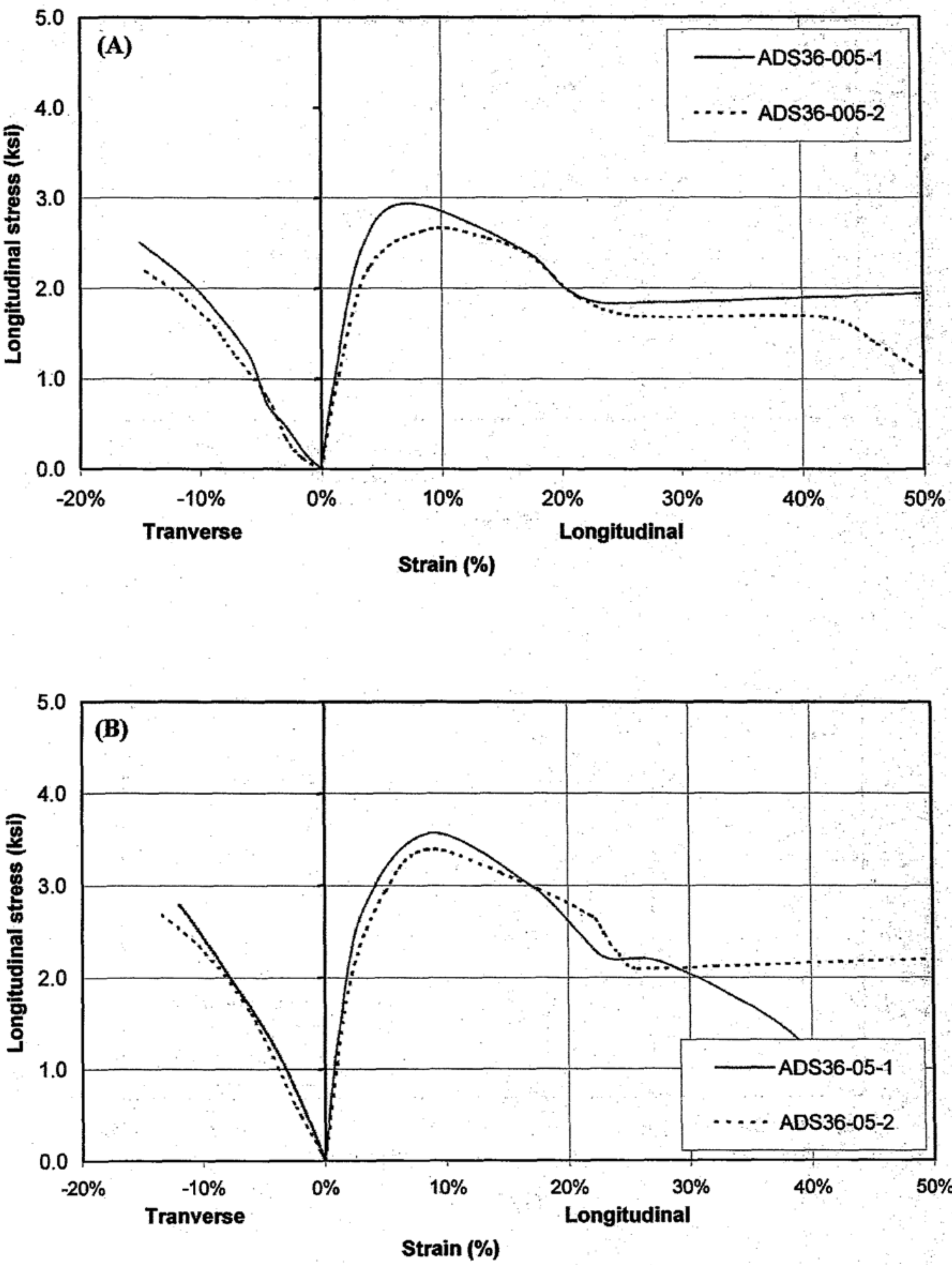

Fig.10.15a – Experimental Stress versus Strain Curves ADS36 and a Loading Rate of : (A) 0.05 in./min. and (B) 0.5 in./min.

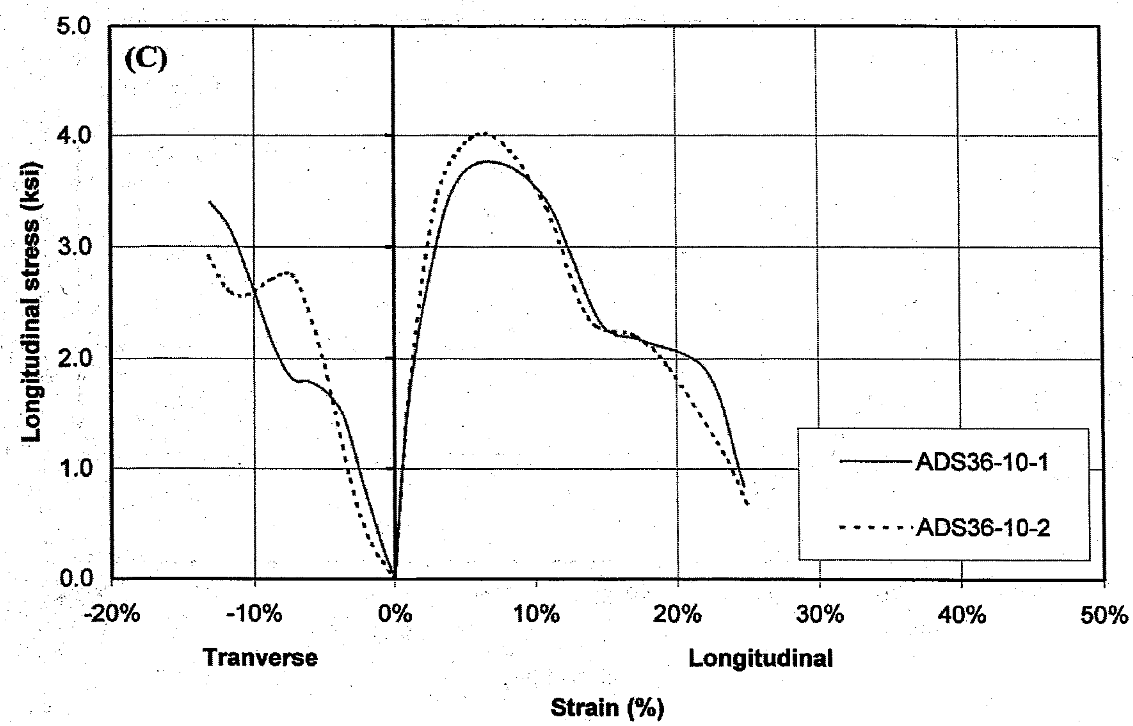

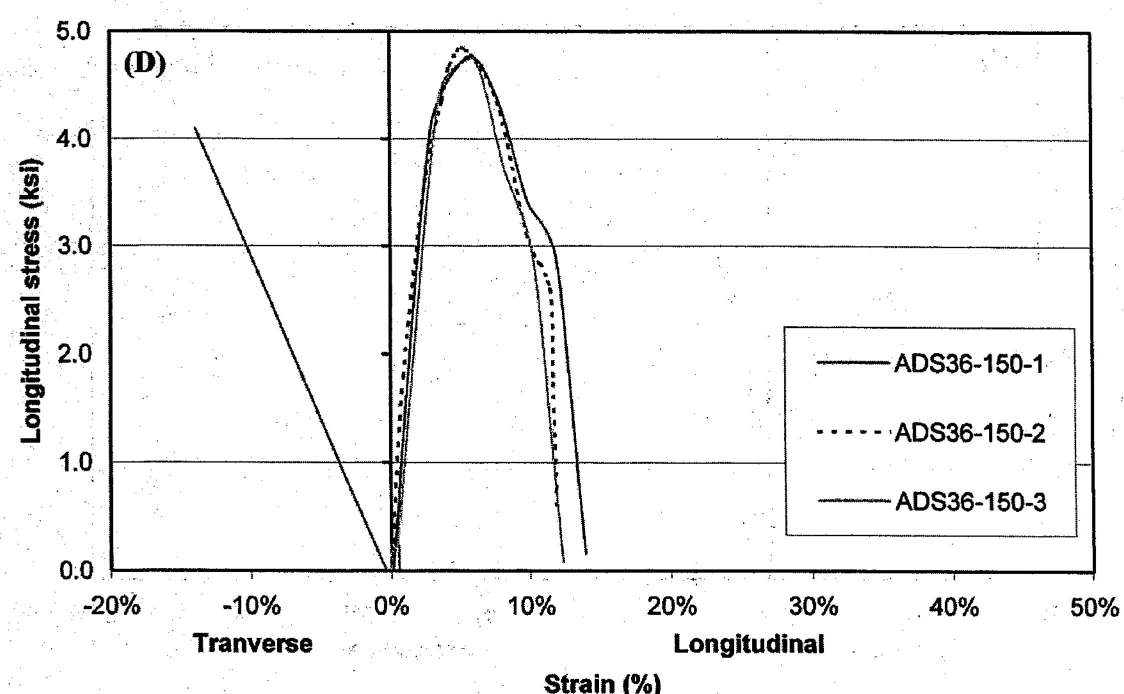

Fig.10-15b – Experimental Stress versus Strain Curves ADS36 at a Loading Rate of : (C) 10 in./min. and (D) 150 in./min.

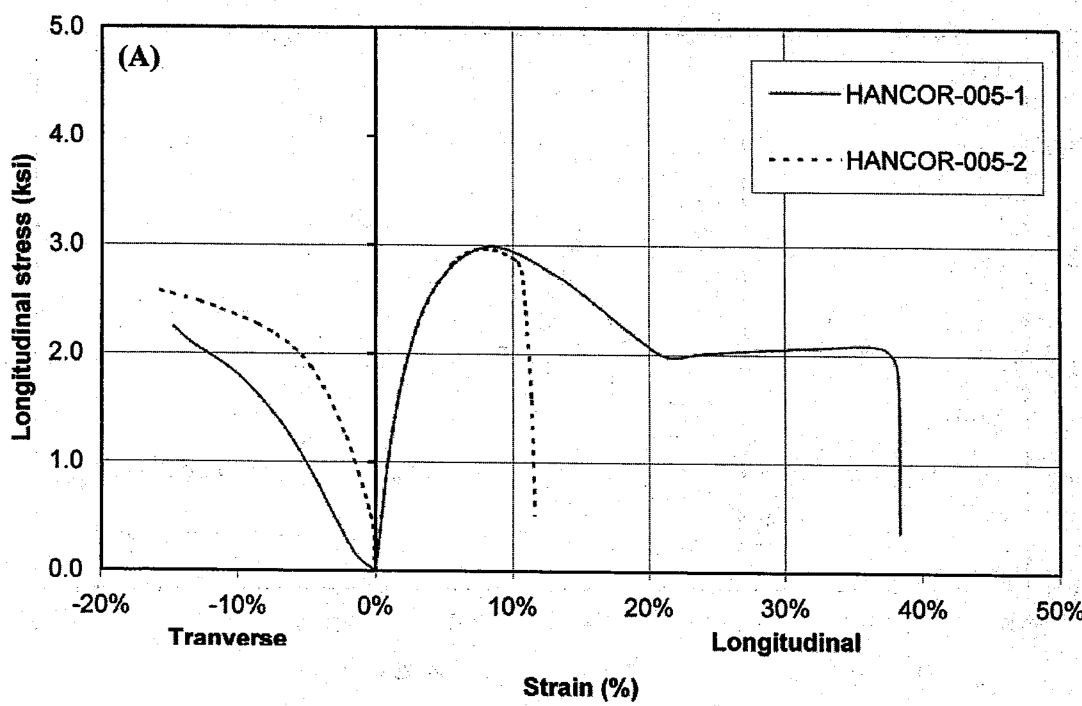

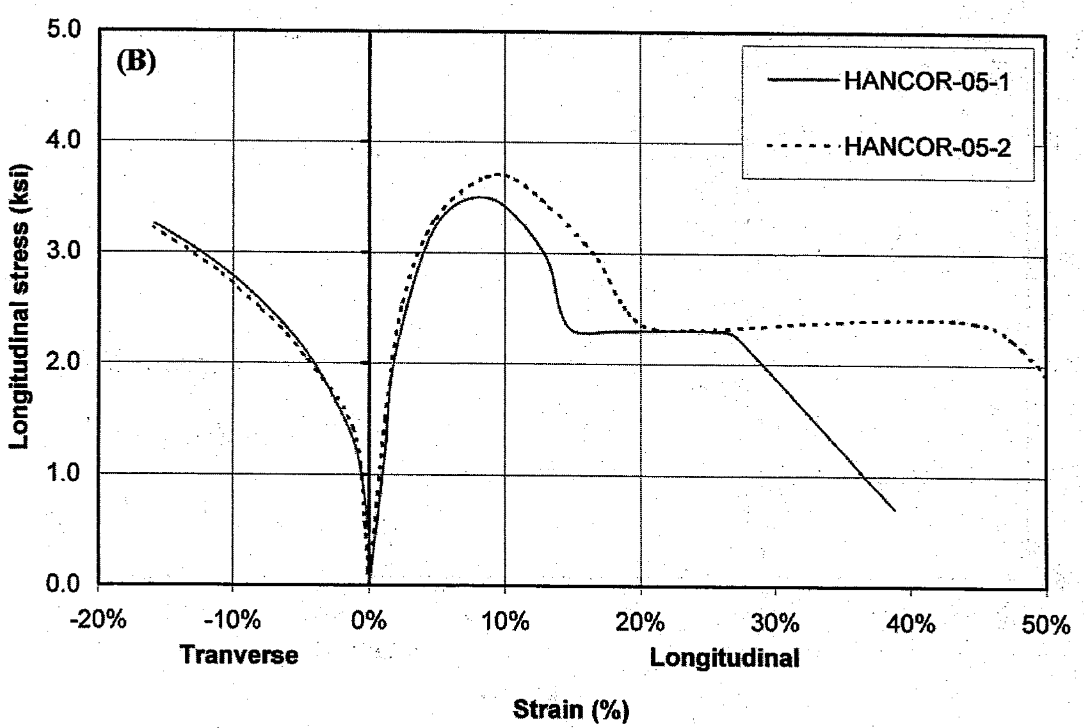

Fig.10-16a – Experimental Stress versus Strain Curves HANCOR 36 at a Loading Rate of : (A) 0.05 in./min. and (B) 0.5 in./min.

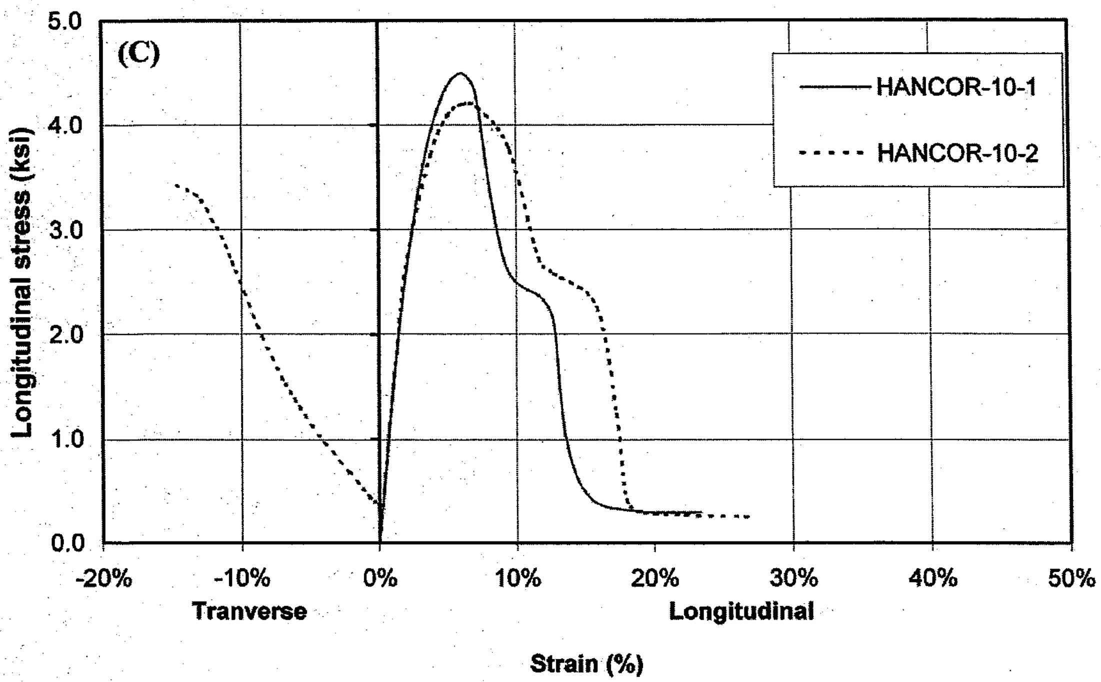

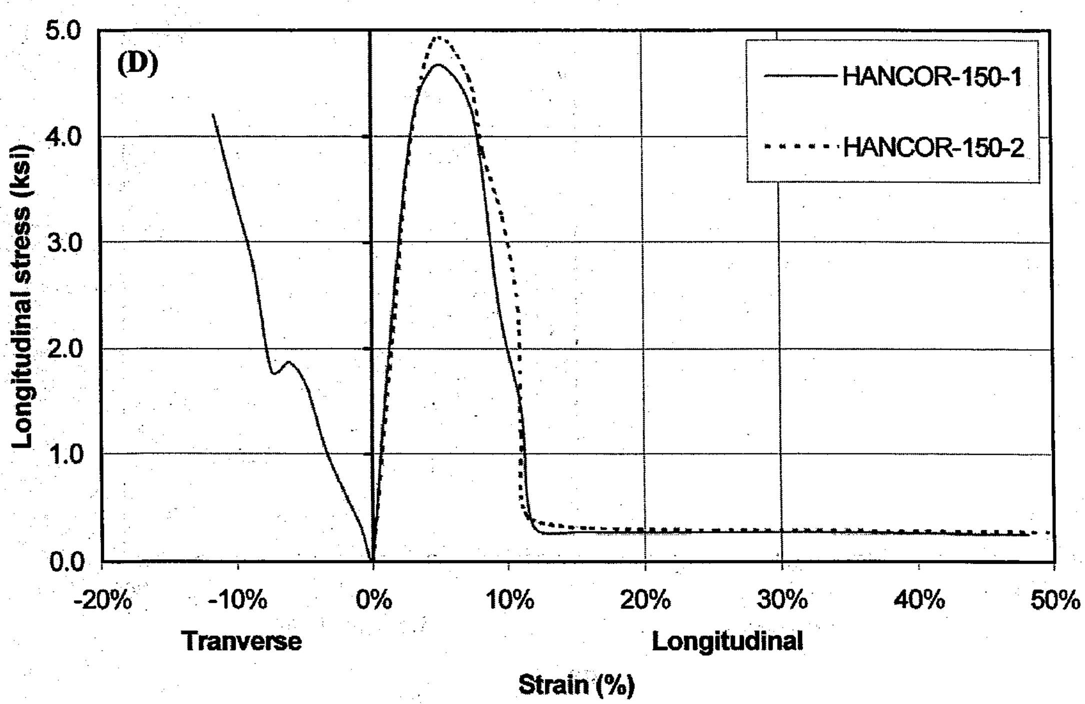

Fig.10-16b. – Experimental Stress versus Strain Curves HANCOR 36 at a Loading Rate of : (C) 10 in./min. and (D) 150 in./min.

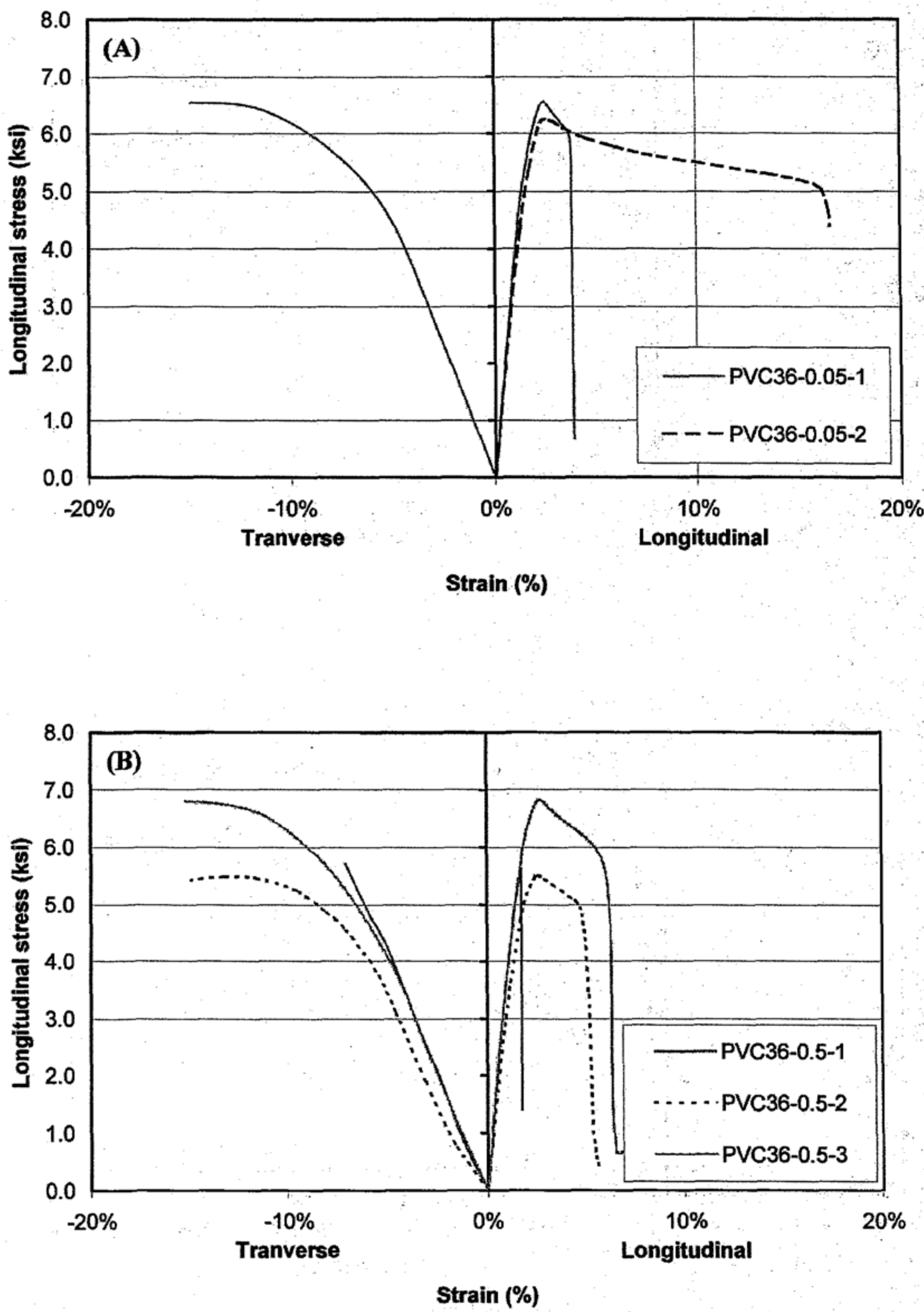

Fig.10-17a – Experimental Stress versus Strain Curves for PVC36 at a Loading Rate of : (A) 0.05 in./min. and (B) 0.5 in./min.

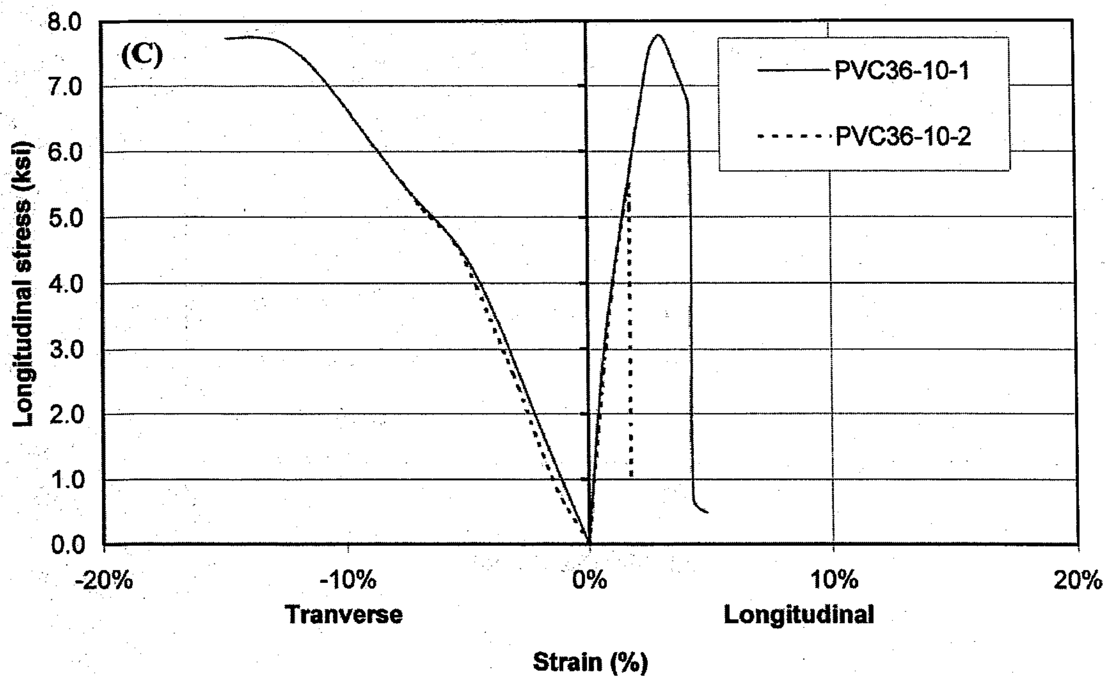

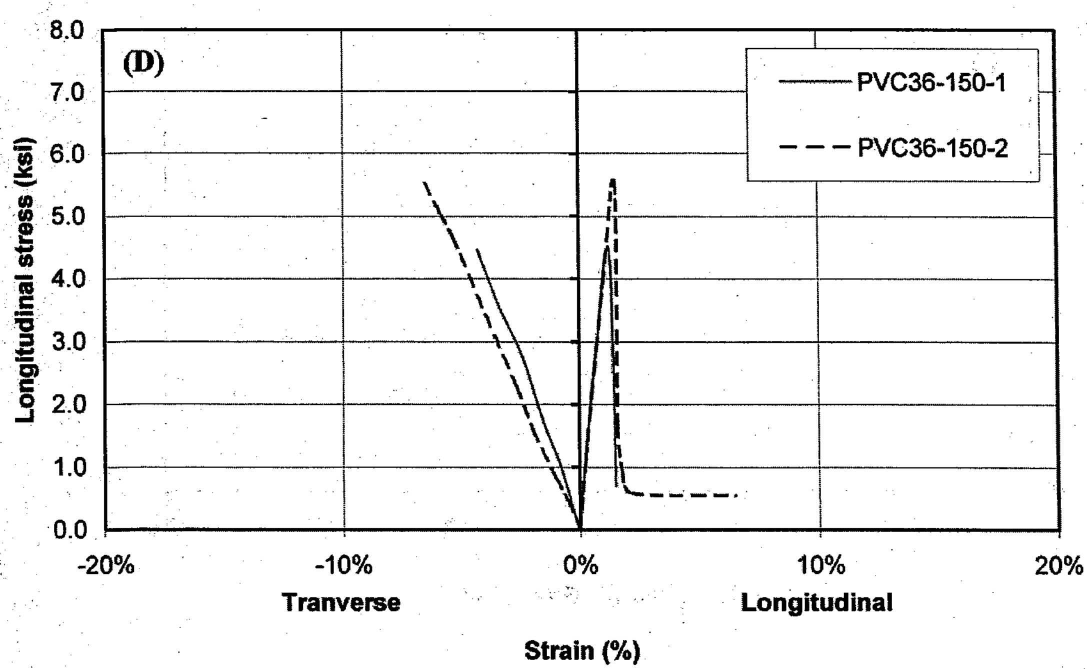

Fig.10-17b – Experimental Stress versus Strain Curves for PVC36 at a Loading Rate of : (C) 10 in./min. and (D) 150 in./min.

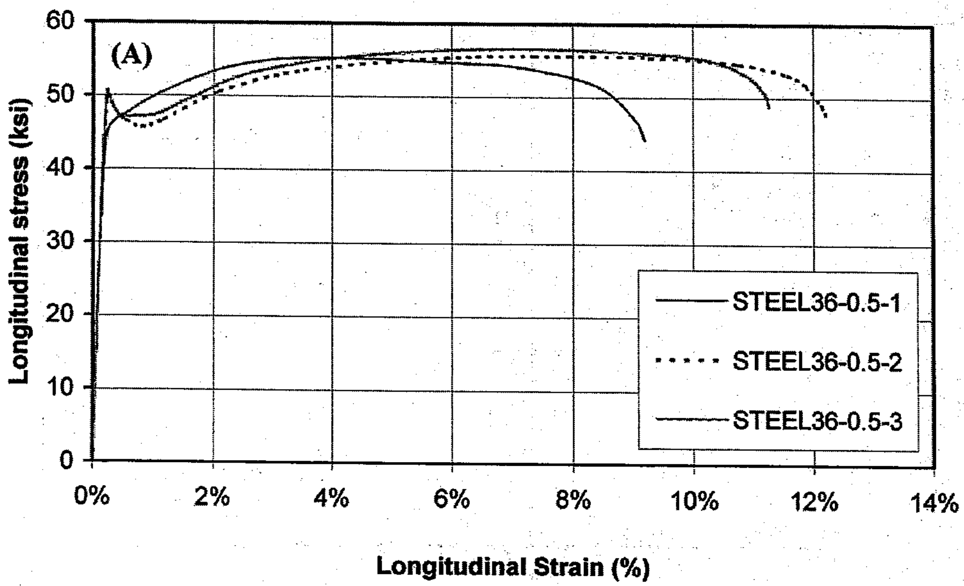

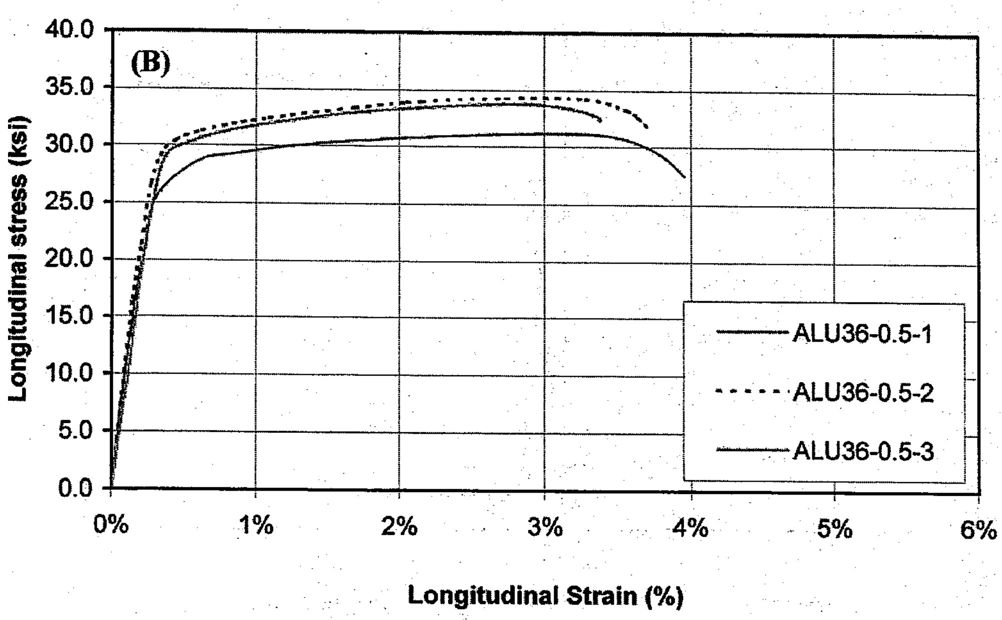

Fig.10-18 – Experimental Stress versus Strain Curves for a Loading Rate of 0.5 in./min. for : (A) STEEL36 and (B) ALU36

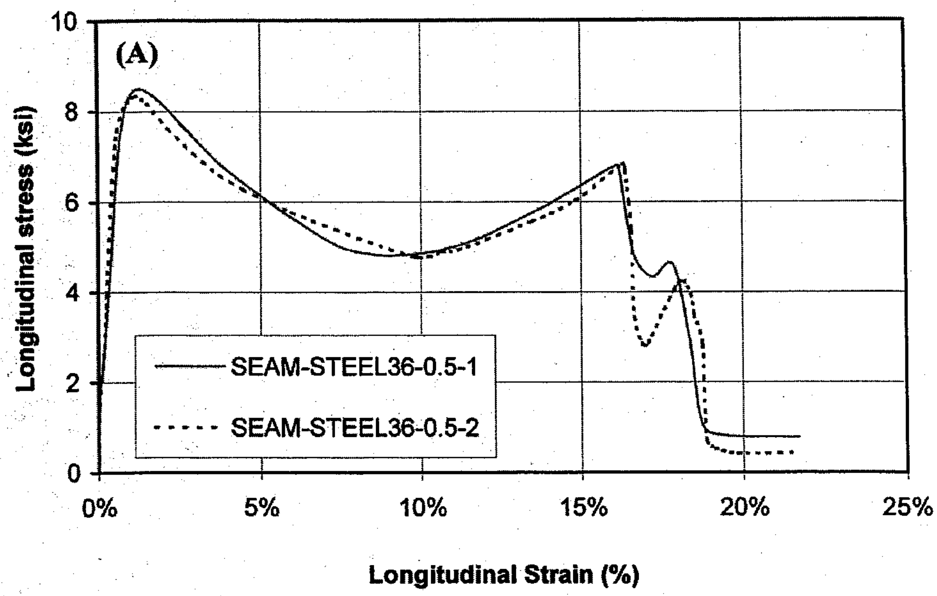

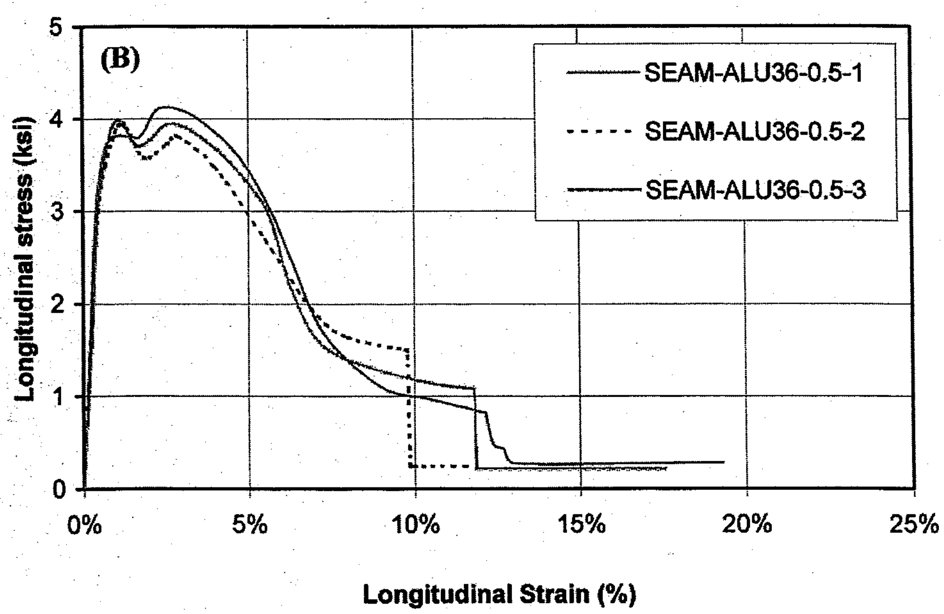

Fig. 10-19 – Experimental Stress versus Strain Curves for a Loading Rate of 0.5 in./min. for : (A) SEAM-STEEL36 and (B) SEAM-ALU36

Chapter 11: Environmental Stress Cracking Test

11.1 Scope and Objective

"Stress-crack" is defined in ASTM D 1693, Standard Test Method for Environmental Stress-Cracking of Ethylene Plastics, as an external and internal rupture in a plastic caused by tensile stresses smaller than its short-time mechanical strength. In the presence of an active environmental agent, cracking may occur under stresses that plastic resins might ordinarily resist indefinitely. This phenomenon is commonly referred to as "environmental stress cracking". Environmental stress cracking is a property that is highly dependent upon the .nature and level of the stresses applied and on the thermal history of the specimen (Decoste, 1951). Environmental stress cracking has been found to occur most readily under high local multi-axial stresses that are developed through the :introduction of a controlled imperfection (Hopkins, et al. 1950).

The objective of this test is to investigate the response of stressed and unstressed HDPE specimens with an imperfection on the specimen surface. The active agent, 100 percent Igepal, CO-630 preheated to 50 °C ± 2°C, is used as specified by AASHTO M 294, Section 9.4.4.

11.2. Experimental Program Apparatus

AASHTO M 294 requires that the specimen used must consist of a 90-degree arc length of pipe, that it is bent to shorten the inside chord length 20 ± 1 percent and retained in this position by a suitable holding device. The external force thus induced from this device is applied to both test conditions. Fig 11.1 shows the configuration of the holding device used to hold the specimen when it is bent. A controlled imperfection (notch) is made on the specimen with a specially designed jig.

Figure 11.2 shows the specimen, which has been exposed to the active agent. A digital caliper with an accuracy of 0.001 inches (0.02mm.) is used to measure the propagation of the notch. A measuring tab is used to measure the lengths of each of the specimens.

Test specimen

Fig. 11.3 shows the configuration of the specimen cut from the ADS 48" having a length of 20 inches. For the specimens of ADS 36, and Hancor 36" pipes, the length of the specimens was 15.5 inches. The imperfection made on the specimen surface was a notch of 1-in. long, and 1/8-in. deep. Fig. 11.4 shows the location of a notch.

Test Procedure

The specimens were tested under two conditions: in ambient air and under immersion in the active agent (100 percent Igepal CO-630). In ambient air, the notch size and chord lengths are measured prior to the application of the external force. The specimen was then subjected to the external force and the change in notch and chord lengths were recorded. The external force was maintained for 24 hours and the notch and chord lengths were then measured again at the end of the testing period. The external force was then released and both lengths were recorded immediately. In the second condition, a new specimen was used. Prior to the immersion in the active agent, measurements of the notch and chord lengths were taken before and after external load application. Then, the specimen was immersed completely in the bath of the preheated agent at 50°C ± 2°C. This temperature was maintained for 24 hours, then the specimen was removed and the notch and chord lengths were measured. The external force was then released and the measurements were taken again. Note that the measurements taken during the load application were recorded as a bound state; while in the case without load application, the measurements were recorded as an unbound state. Figs. 11.5 and 11.6 show the notch and chord lengths measurements. Figs. 11.7 to 11.19 show the preparation of the specimens, locations of notch, and measurements of the notch lengths.

Test Program

Table 11.1 gives details of the testing program for the environmental stress cracking test.

11.3 Calculations

Environmental stress cracking is evaluated by means of a "relative deformation," which is different from that of ASTM D-1693. "Relative deformation" is defined as the difference between the deformation of a length based on tests in ambient air and that based on tests under the active agent (100 percent Igepal CO-630).

i) Deformation

$$\text{Deformation (\%)} = \frac{\text{(Length after the test) - (Length before the test)} \times 100}{\text{(Length before the test)}} \qquad (11.1)$$

ii) Relative Deformation

$$\text{Relative deformation (\%)} = \text{(Deformation in active agent) - (Deformation in air)} \qquad (11.2)$$

11.4 Results and Observations

Any crack in the specimens visible to an observer with normal eyesight should be interpreted as the failure of the entire specimens. Tables 11.2 to 11.4 present the data obtained from the test for the ADS 48", ADS 36", and Hancor 36" series under both air and active conditions. Table 11.5 presents observations on the specimens during and after the tests.

The following observations are made:

(a) During the 24-hour exposure to air, the lengths of the notch and the chord of the bounded specimens did not vary (Tables 11.2 to 11.4).

(b) After 24 hours in Igepal solution, the notch length variation was negligible for ADS 36" and Hancor 36" under bound conditions. However, for ADS 48", the variation was in average 31.7%. This high percentage was due to test #1 where the notch length variation reached 56% (see Table 11.2).

(c) Comparing the notch length of specimens in a 24-hour Igepal solution after release of the load, with the original pristine specimen revealed that the change in length varied between 4.93% and 10.25% for ADS 36" and Hancor 36" (see Tables 11.3 and 11.4), whereas it reached 17.38% for ADS 48" (see Table 11.2).

(d) One of the two ADS 48" specimens showed major cracking after a 24-hour exposure in Igepal.

11.5 Conclusions

The following conclusions can be formulated:

(a) The 36- in. diameter HDPE pipes behaved satisfactorily under ESCR tests.

(b) One of the two specimens of the 48-in. diameter HDPE pipe failed the ESCR test under the conditions described in this study.

Table 11.1 - ESCR Test Program

Pipe Type	Environment	Temperature	Number of specimens
ADS 48	Air	Ambient	2
	Igepal	50%	2
ADS 36	Air	Ambient	2
	Igepal	50%	2
HANCOR 36	Air	Ambient	2
	Igepal	50%	2

Table 11.2 - Environmental Test Measurements for ADS 48

Environment - Specimen (Temp.)	Designation	Unbound Condition		Bound Condition	
		Notch (in.)	Chord (in.)	Notch (in.)	Chord (in.)
AIR-1 (22.8°C)	Before Test	1.031	33.82	1.0090	27.04
	After 24H	1.044[a]	30.71[a]	1.0235	26.97
	Deformation (%)	+1.26	-9.20	+1.44	-0.26
AIR-2 (22.8°C)	Before Test	0.9350	33.78	0.9425	27.01
	After 24H	0.9540[a]	30.51[a]	0.9260	27.05
	Deformation (%)	+2.03	-9.68	-1.75	+0.15
AIR- average	**Deformation (%)**	**+1.65**	**-9.44**	**-0.16**	**-0.05**
IGEPAL-1 (50.1°C)	Before Test	0.9470	34.13	0.941	27.32
	After 24H	1.2065[a]	31.06[a]	1.4680	27.32
	Deformation (%)	+27.40[b]	-9.00	+56.00[b]	0.00
IGEPAL-2 (51.6°C)	Before Test	1.0035	33.90	0.9815	27.01
	After 24H	1.0775[a]	30.43[a]	1.0545	26.73
	Deformation (%)	+7.37	-10.24	+7.44	-3.74
IGEPAL-average	**Deformation (%)**	**+17.38**	**-9.62**	**+31.72**	**-1.87**

Notes: (a) After release at end of test
(b) Crack along notch (see Figs. 11.11 and 11.12)

Table 11.3 - Environmental Test Length Measurements for ADS 36

Environment - Specimen # (Temp.)	Designation	Unbound Condition		Bound Condition	
		Notch (in.)	Chord (in.)	Notch (in.)	Chord (in.)
AIR-1 (22.5°C)	Before Test	1.0255	25.55	0.9415	20.470
	After 24H	0.9795	22.362	0.9570	20.394
	Deformation (%)	- 4.49	- 12.48	1.65	- 0.37
AIR-2 (25.2°C)	Before Test	0.9980	24.016	0.9580	19.134
	After 24H	0.9615	21.339	0.9425	19.173
	Deformation (%)	- 3.66	- 11.15	- 1.62	0.20
AIR- average	**Deformation (%)**	**- 4.08**	**- 11.81**	**0.015**	**- 0.09**
IGEPAL-1 (50.1°C)	Before Test	1.0005	25.470	0.9000	20.350
	After 24H	0.9470	22.165	0.8340	20.276
	Deformation (%)	- 5.35	- 12.98	- 7.33	- 0.36
IGEPAL-2 (51.6°C)	Before Test	0.9075	24.331	0.9510	19.488
	After 24H	1.0455	22.087	0.9760	19.450
	Deformation (%)	15.21	- 9.22	2.63	- 1.9
IGEPAL-average	**Deformation (%)**	**4.93**	**- 11.1**	**- 2.35**	**- 1.13**

Table 11.4 - Environmental Test Length Measurements for HANCOR 36

Environment - Specimen (Temp.)	Designation	Unbound Condition		Bound Condition	
		Notch (in.)	Chord (in.)	Notch (in.)	Chord (in.)
AIR-1 (-)	Before Test	0.3170	25.20	0.3245	20.31
	After 24H	0.3065[a]	22.36[a]	0.3100	20.27
	Deformation (%)	-3.31	-11.27	-4.47	-0.20
AIR-2 (-)	Before Test	0.2655	25.59	----	20.47
	After 24H	0.2935	22.72[a]	----	20.47
	Deformation (%)	+10.55	-11.22	----	0.00
AIR- Average	**Deformation (%)**	**+3.62**	**-11.24**	**-4.47**	**-0.10**
IGEPAL-1 (-)	Before Test	0.3410	25.47	0.2960	20.71
	After 24H	0.3150	22.60[a]	0.2940	20.63
	Deformation (%)	-7.62	-11.27	-0.68	-0.39
IGEPAL-2 (-)	Before Test	0.3225	25.20	0.2830	20.39
	After 24H	0.2810	22.13[a]	----	20.35
	Deformation (%)	-12.87	-12.18	----	-0.20
IGEPAL-average	**Deformation (%)**	**-10.25**	**-11.72**	**-0.68**	**-0.30**

Notes: [a] After release of load at end of test

Table 11.5 - Observations

Pipe Type	Environment	Observations	ASTM D1693
ADS 48	Air	No cracks or crazing	Pass
	Igepal	· Long cracks, extension of controlled notch · Depressions and cracks on the surface, and through wall open cracks in the 1st of the two tests (Fig. 11. 12)	Failure for 50% of tests Time = 24 hours
ADS 36	Air	No cracks or crazing	Pass
	Igepal	Cracks but extension of controlled imperfection	Pass
HANCOR 36	Air	No cracks or crazing	Pass
	Igepal	Cracks but extension of controlled imperfection	Pass

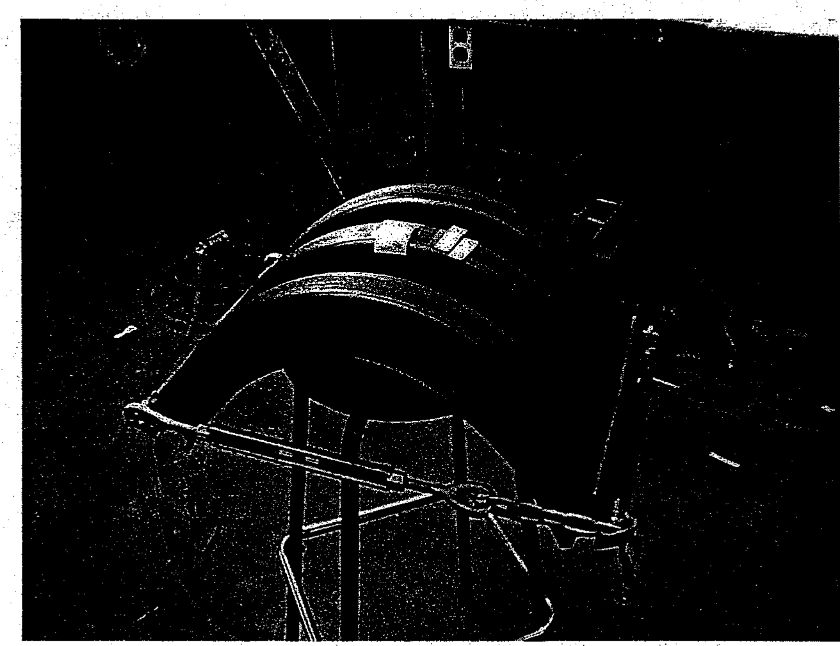

Fig. 11.1 - Configuration of the Holding Device.

Fig. 11.2 - Specimen After Exposure to the Active Agent

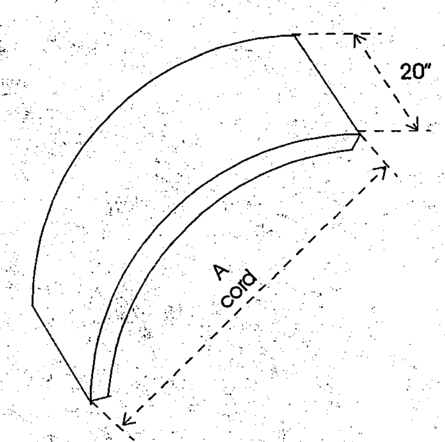

Fig. 11.3 - Specimen Configuration and Dimension for ADS 48 Pipe

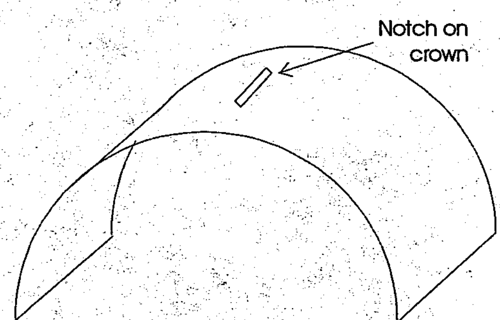

Fig. 11.4 - Location of the Notch on the Specimen Crown.

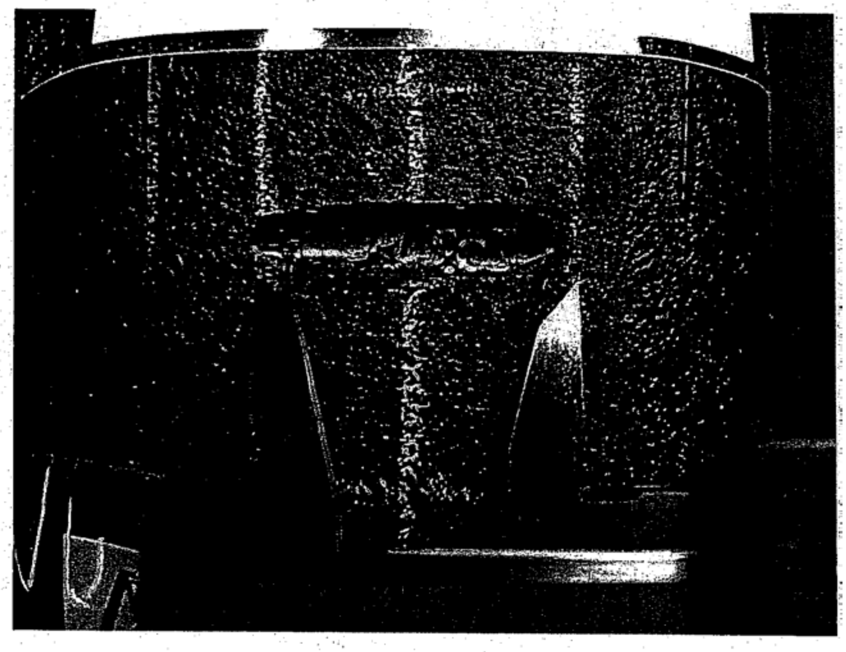

Fig. 11.5 - Measurement of a Notch Length by the Digital Caliper

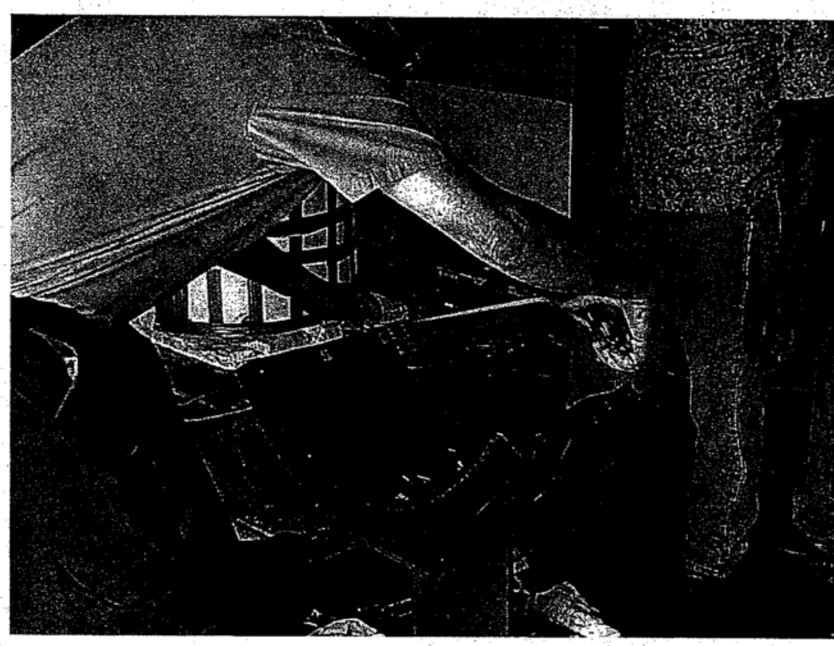

Fig. 11.6 - Measurement of Chord Length

Fig. 11.7 - Preparation of Notch for ADS 48 Specimen

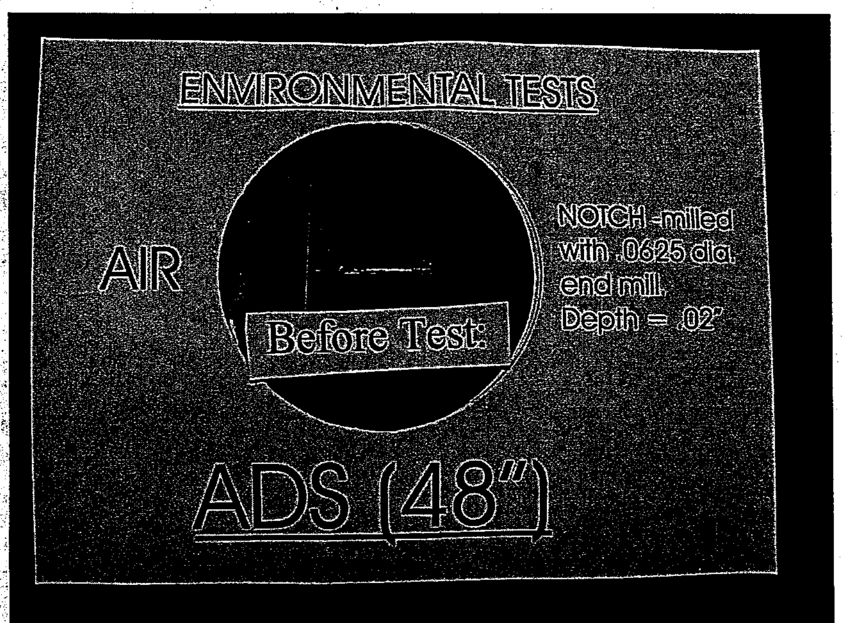

Fig. 11.8 - Close-up of Notch Before Test for ADS 48 Specimen

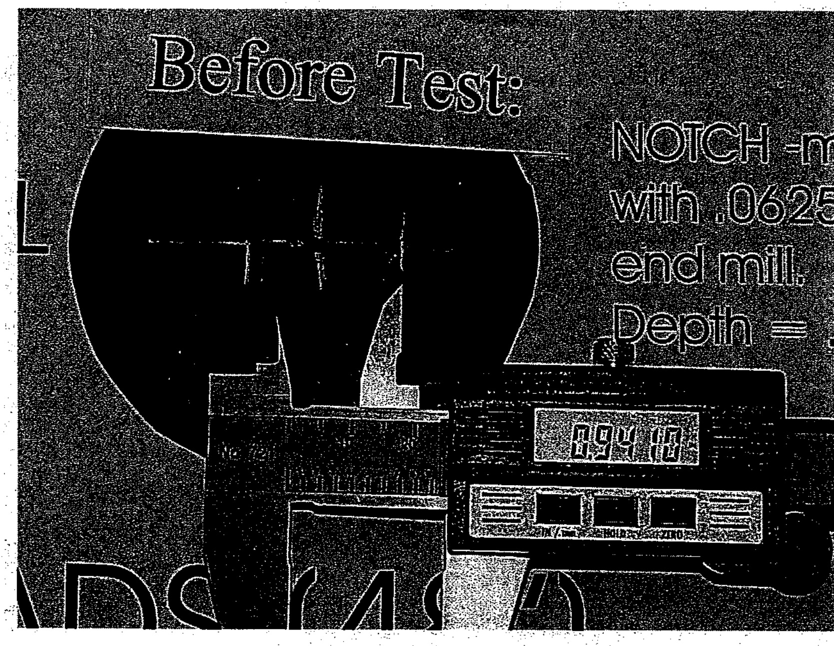

Fig. 11.9 - Measurement of Notch Length Before Test

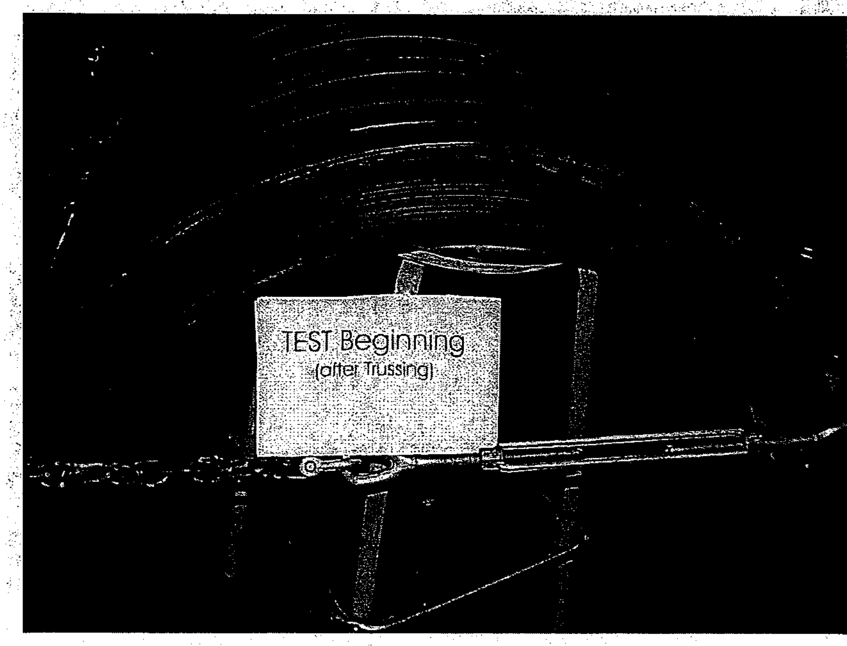

Fig. 11.10 - Preparation of Notch for ADS 48 Specimen

(a) Test #1

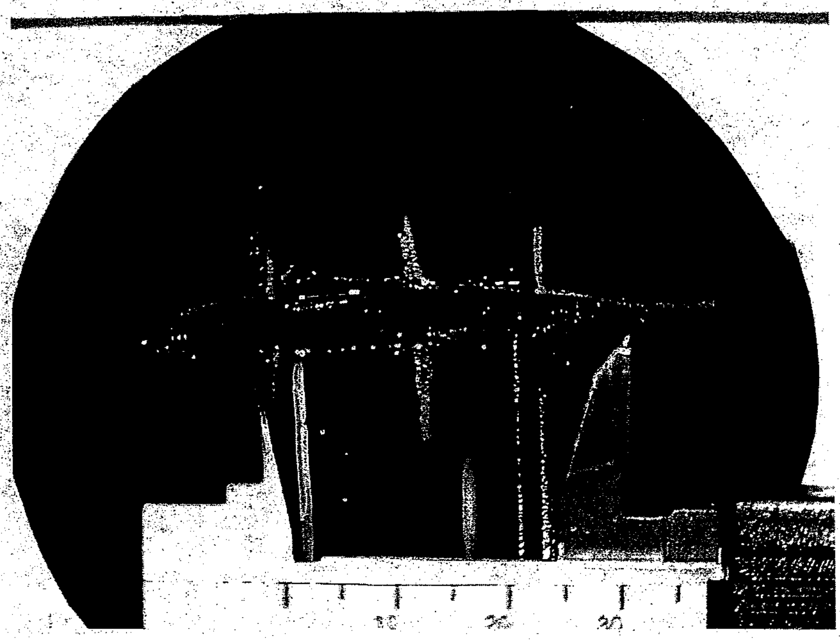

(b) Test #2

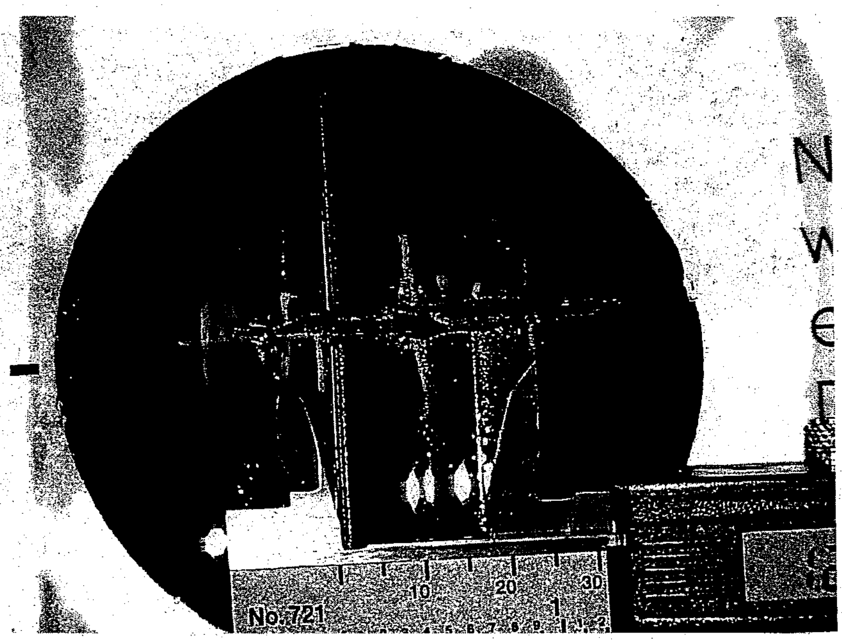

Fig. 11.11 - View of Notch after Test Under Igepal for Bound ADS 48 Specimen

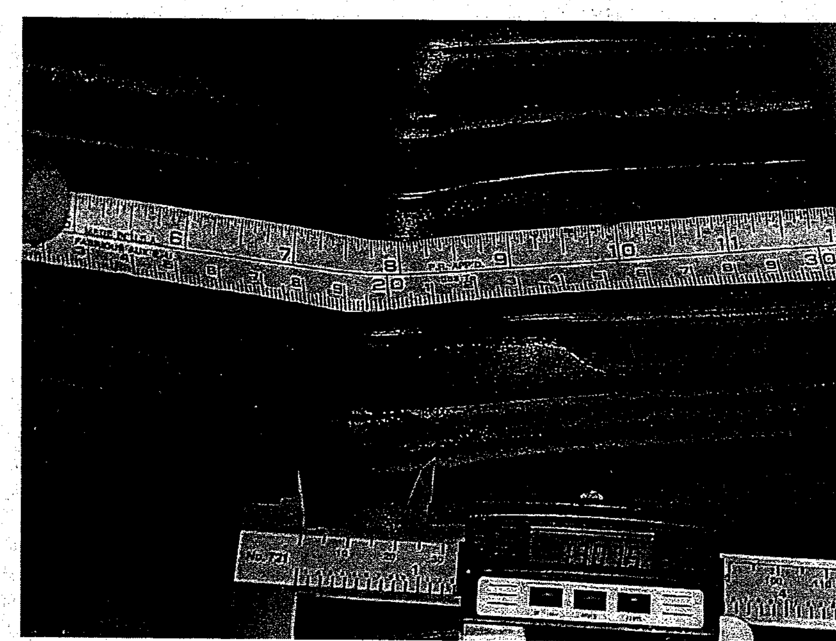

Fig. 11.12 - View of Notch after Test Under Igepal for Unbound ADS 48 Specimen

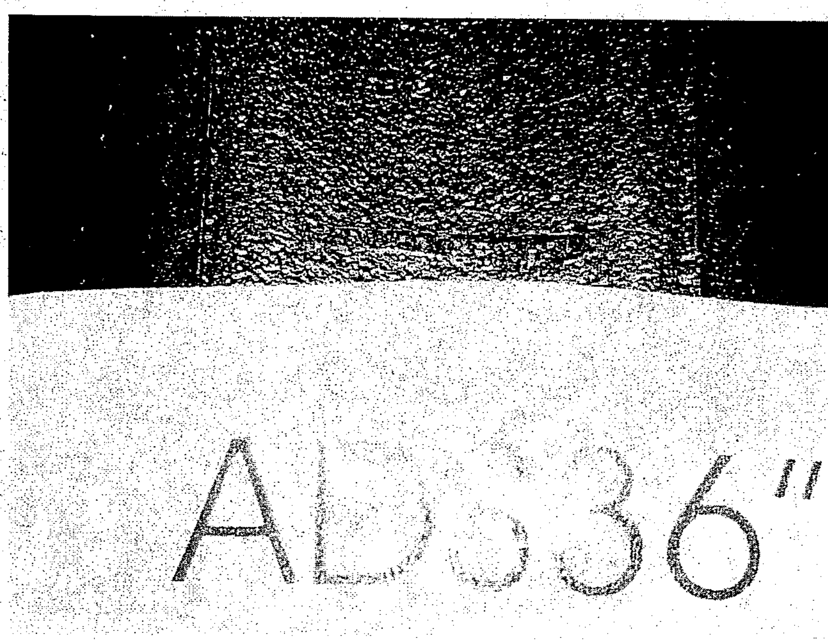

Fig. 11.13 - Close-up of Notch before Test for ADS 48 Specimen

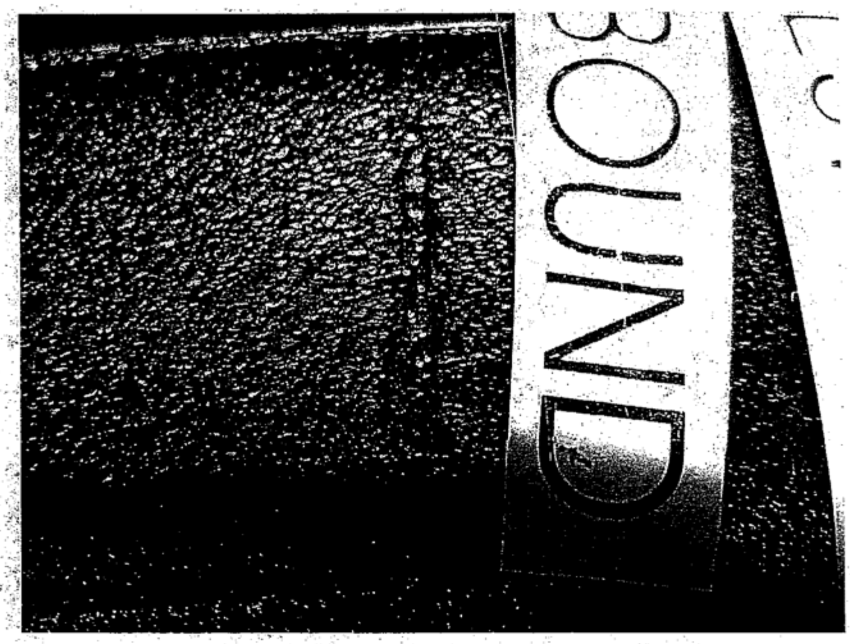

Fig. 11.14 - View of Notch after Test under 24 H Igepal for Bound ADS 36 Specimen

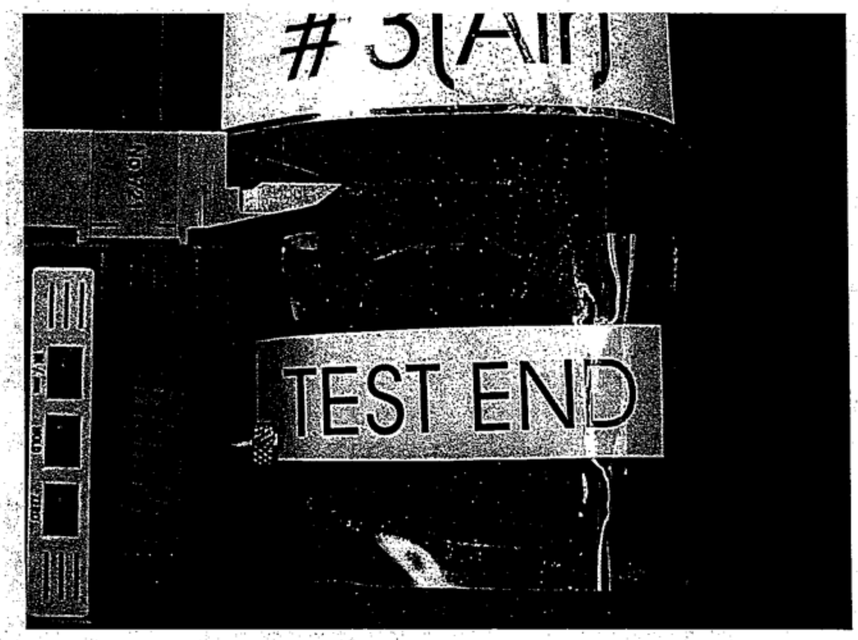

Fig. 11.15 - View of Notch after Test Under 24 H Air for Bound ADS 36 Specimen

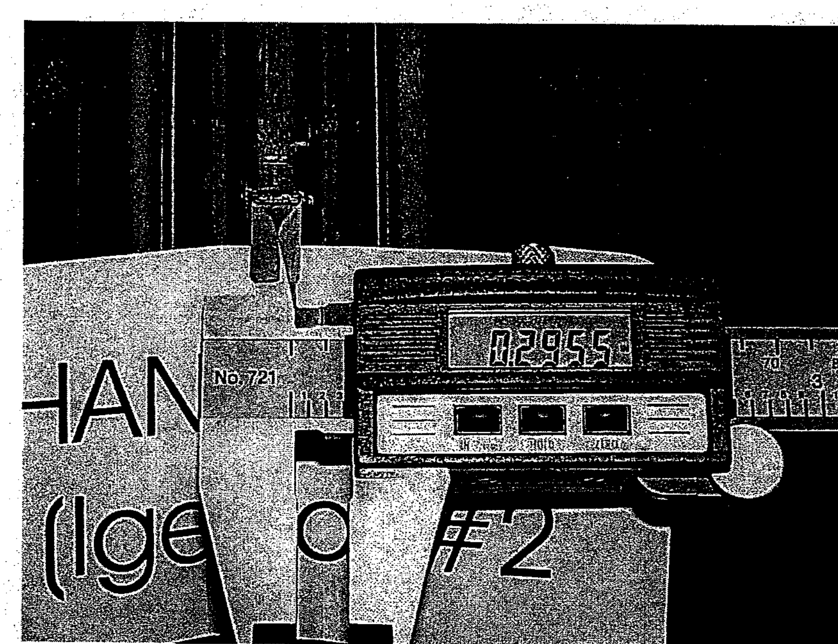

Fig. 11.16 - Close-up of Notch before Test for Hancor 36 Specimen

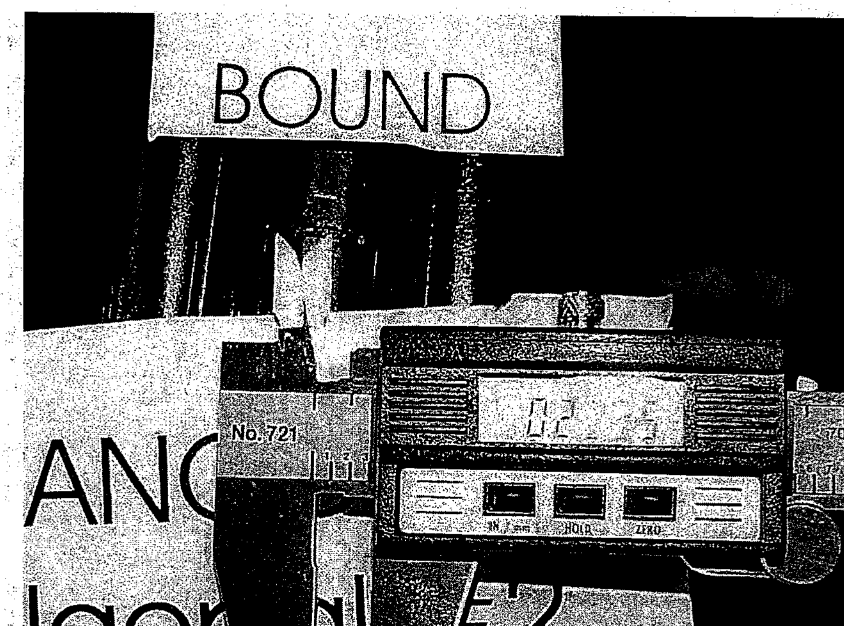

Fig. 11.17 - View of Notch after Test Under 24 H Igepal for Bound Hancor 36 Specimen 2

Fig. 11.18 - View of Notch after Test Under 24 H Igepal for Bound Hancor 36 Specimen 4

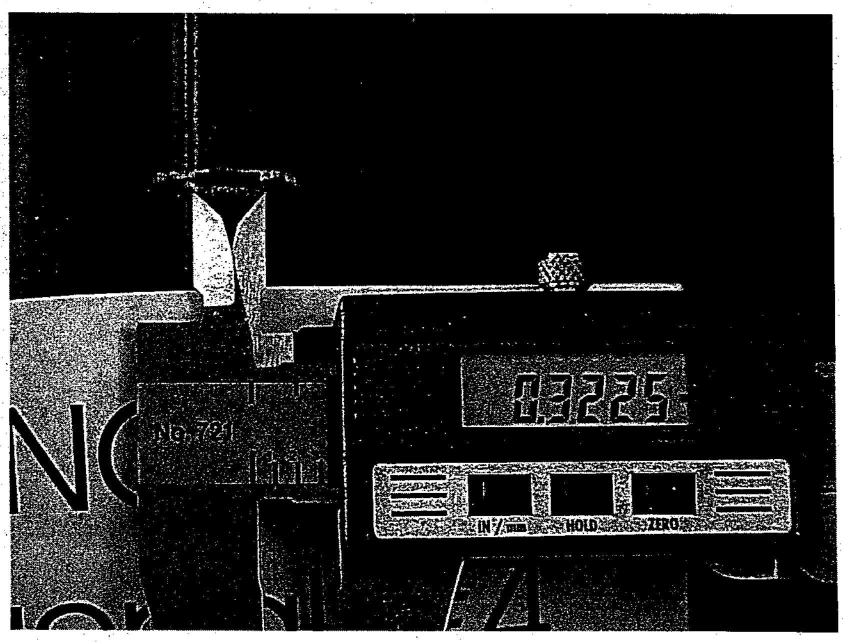

Fig. 11.19 - Close-up View of Notch after Test Under 24 H Igepal for Bound Hancor 36 Specimen 4

Chapter 12: Conclusions

This study describes the laboratory work performed and presents results for ten different tests carried out in this investigation. The main objective of the laboratory work was to evaluate and characterize, under laboratory conditions, the performance and properties of the different plastic and metal pipes considered in the study.

The following are the findings of `the laboratory investigation in this study:

(a) Visual Inspections of the different pipes indicated that HDPE, PVC, and metal pipes generally meet the requirements of AASHTO-M294, ASTM F949, and ASSHTO-T249. However, visible creasing at the surface of inside and outside walls, as well as irregular surface at certain locations around the circumference of the bell and spigot joint, were observed in ADS 48. Also the contact 1ength of the seam lap in the case of aluminum and its distance from the adjacent ribs for both types of metal pipes do not conform to AASHTO T249 requirements. These irregularities, even though they seem not to have an apparent incidence on structural performance, may require improvement.

(b) Beam Test results indicated that for the plastic pipes, the valley longitudinal bending strains were greater than the crown longitudinal bending strains. For the metal pipes, the longitudinal bending strains in the ribs were greater than the longitudinal bending strains in the wall (valley) between the ribs. For a vertical bottom deflection of 1% of the span length, the longitudinal bending strain ranged from 114με (i.e., 12.5 psi) to 1000με (i.e., 110 psi) for HDPE, it reached 600με (i.e., 240 psi) for PVC and 200με (i.e., 5800 psi for steel and 2000 psi for aluminum) for metal pipes.

(c) Parallel Plate Test results indicated that for 5% vertical deflection and a loading rate of 0.5in./min., all the pipes achieved a pipe stiffness, PS, greater than the minimum specified by the Standards. They also revealed no sign of distress or buckling in the pipes for vertical deflections less than 15%. Finally and as expected, the tests confirmed that for a given vertical deflection, the HDPE pipe stiffness (PS). substantially decreased as the loading rate decreased and vice-versa.

(d) **Flattening Test** results indicated that all the HDPE pipes passed this test, since no splitting, cracking, breaking, or separation of ribs or seams, or both, were observed under, normal light with unaided eyes. The PVC specimens that could be flattened up to 60% vertical deflection without failure also passed the flattening test. However, a number of PVC pipe specimens ruptured before reaching the 60% limit.

(e) Curved Beam Test results indicated that time-independent pipe stiffness K(0) is 2 to 3 times greater than the PS values determined by the parallel plate test for all the pipes and increase with the loading rate for HDPE pipes. For a vertical deflection of 5%diameter the tensile strain (stress) in the outer wall was approximately equal to 18,000 $\mu\varepsilon$ (i.e., 1,980 psi) for all HDPE, 17,000 $\mu\varepsilon$ (i.e., 6,800 psi) for PVC and 16,000 $\mu\varepsilon$ (L e., 60 ksi for steel and 21 ksi for aluminum) for metal pipes.

(f) Joint Integrity Test results indicated that all the pipes behaved satisfactorily with no sign of cracks or excessive gaps up to 10% vertical deflection. The radial gaps and longitudinal openings were small and reached 1.5 in. and 0.75 in., respectively, for 30% vertical deflection. The presence of a joint generally modified the PS of the pipe: it resulted in a 10% reduction of PS at 5% vertical deflection for HDPE ADS 48 and 36 inch diameter pipes, and in 23% and 37% increase of PS for 5% vertical deflection for Hancor 36 and PVC, respectively.

(g) Type C tension tests (Small Dog bone with no welds) indicated that the tensile properties of the pipes, the modulus of elasticity, and the tensile strength, are within the range of values specified by the AASHTO code. Type A tension tests (Double Wall Dumbbell Shape), performed on ADS 48 only, underestimated the tensile strength of the D-wall-type pipes, such as ADS 48. Type B tension tests (Single Wall Dumbbell Shape) indicated that the seam behavior of the D-wall-type pipe under tensile stresses is satisfactory given the maximum strength achieved. Type D tension tests (Split Disk. Test) performed on all the pipes indicated that the apparent tensile properties under split disk tests are lower than those under **Type C tension tests** on small dog bone specimen with no weld, but greater than those achieved on dumbbell shape specimens with welds for ADS 48.

(h) ESCR Tests performed on HDPE pipes indicated that the 36 inch-diameter HDPE pipes behaved satisfactorily under ESCR tests. For the 48 in-diameter HDPE pipe however, one of the two specimens failed the ESCR test under the conditions described in this study.

REFERENCES

AASHTO Standards

M249-93: Standard Method of Test for Helical Lock Seam Corrugated Pipe.

T249-98 : Standard Specifications for Corrugated Polyethylene Pipe, 300- to 1200-mm Diameter.

MP7-97 : Standard Specification for Corrugated Polyethylene Pipe, 1350 and 1500 mm Diameter.

M304-94: Standard Specification for Poly (Vinyl Chloride) (PVC) Profile Wall Drain Pipe and Fittings Based on Controlled Inside Diameter.

ASTM Standards

F949-00: Standard Specification for Poly (Vinyl Chloride) (PVC) Corrugated Sewer Pipe With a Smooth Interior and Fittings.

F679-00: Specification for Poly (Vinyl Chloride) (PVC) Large Diameter Plastic Gravity Sewer Pipe and Fittings.

D2412 : Test Method for Determination of External: Loading Characteristics of Plastic Pipe by Parallel-Plate Loading.

D618: Practice for Conditioning Plastics and Electrical Insulating Materials for Testing.

D883: Terminology Relating to Plastics.

D2122: Test Method for Determining Dimensions of Thermoplastic Pipe and Fittings.

D2290: Standard Test Method for Apparent Tensile Strength of Ring or Tubular Plastics and Reinforced Plastics by Split Disk Method.

D1693: Environmental Stress Cracking of Ethylene Plastic

D638: Standard Test Method for Tensile Properties of Plastic

Technical Papers

Decoste, J.B., Mahn, F.S., and Wallder, V.T., Cracking of Stressed Polyethylene Effect of Chemical Environment, Industrial and Engineering Chemistry, Vol. 43, 1951, pp. 117-121.

Gabriel Lester H., Ster III, James F., and Anthony. Brett, A Test Apparatus for Time-Independent Stiffness of Thermoplastic Pipe, Transportation Research Board (TRB) Congress, January 2002, Washington DC.

Goddard, James, B. and Gabriel, Lester H., Curved Beam Stiffness and Profile/Wall Stability, Transportation Research Board (TRB) Congress, Paper No. 99-0527, 10-14 January 1999, Washington, DC.

Havens, B.T., Klaider, F.W., Lohnes, R.A., and Zachary, L.W., Longitudinal Strength and Stiffness of Corrugated Steel Pipe, Transportation Research Record 1514, July 1995, pp. 1-9.

Hopkins, I.L., Baker, W.O., and Howard, J.B., Complex Stressing of Polyethylene, Journal of Applied Physics, Vol. 21, No. 3, pp. 206-213.

Powers, R.G., and Kasper, C.A., A Report of the Evaluation of Spiral Formed D-Wall, Corrugated High Density Polyethylene' Pipe Manufactured by Advanced Drainage: Systems, Inc., Columbus Ohio, Technical Report, FDOT, State Materials Office, Gainesville, Florida.

Watkins R.K., Longitudinal Stresses in Buried Pipes, Advances in Underground Pipeline Engineering: Proceedings of the International Conference, 1985, pp. 408-416.